Synthesis, Characterization and Application of Diphosphinoamine (PNP) Ligand

A thesis submitted in partial fulfillment of the requirements for the degree of

Doctor of Philosophy

By

Neha Vijay Kathewad

ID: 20133262

IISER PUNE

Indian Institute of Science Education and Research (IISER), Pune

2018

Dedicated to

Aai-Papa (My parents)

Indian Institute of Science Education and Research (IISER), Pune

Certificate

It is hereby certified that the work described in this thesis entitled "*Synthesis, Characterization and Application of Diphosphinoamine (PNP) Ligand*" submitted by Ms. Neha Vijay Kathewad was carried out by the candidate, under my supervision. The work presented here or any part of it has not been included in any other thesis submitted previously for the award of any degree or diploma from any other university or institution.

Date: 24.12.2018

Dr. Shabana Khan

Research Supervisor

Email: *shabana@iiserpune.ac.in*

Contact No.: *+91 (20) 2590-8137*

3

Declaration

I declare that this written submission represents my ideas in my own words and wherever other's ideas have been included; I have adequately cited and referenced the original sources. I also declare that I have adhered to all principles of academic honesty and integrity and have not misrepresented or fabricated or falsified any idea/data/fact/source in my submission. I understand that violation of the above will cause for disciplinary action by the Institute and can also evoke penal action from the sources which have thus not been properly cited or from whom proper permission has not been taken when needed.

Date: 24.12.2018   **Neha Vijay Kathewad**

                                                                         ID: 20133262

Acknowledgment

At the very outset, I would like to convey my deepest regards to my research supervisor Dr. Shabana Khan, who has continuously encouraged me in the last five years. I firmly believe that her inspiring guidance has been a key factor behind the wholesome learning process throughout my Ph.D. tenure. Her enthusiasm and energy inspire us every time. I acknowledge Indian Institute of Science Education and Research (IISER), Pune and its former director Prof. K. N. Ganesh for providing state-of-the-art research facilities, funding and an excellent interdisciplinary research atmosphere, facilitating thoroughly collaborative research endeavours. I also want to acknowledge the present director of IISER, Pune for providing the excellent facilities, research atmosphere. I would also like to thanks my colleague cum batch mate Mr. Shiv Pal for his support. Shiv Pal and I were the first Ph.D. students of the group, at a time where we did not have our lab, and we worked together as a team. So we were fortunate to get the unique opportunity to witness the setting up of a relatively new lab, almost from scratch. Our lab was developing from the nascent stage by taking tiny footsteps in the way of cumulatively achieving greater heights of the scientific establishment. I want to thank my collaborators Nanda Kumar and Subramanyam Sappatti. from IISER Pune and Sneha Parambath, Pattiyil Parameswaran from National Institute of Technology Calicut and Rameshwar L Kumawat, Md. Ehesan Ali from IISER Mohali. I will miss the scientific and non-scientific discussions with Mr. Rajarshi Dasgupta, Ms. Nasrina Parvin, Nilanjana Sen, Moushakhi Ghosh, Md. Jabed Hossain, Shweta Hiwse, Dharmika Guddey, Ashok Jadhav and Rahul. I also thank former lab members Angha M. C., Atanu Panda, Vikas Khade-Patil and Girish. I also want to thank my other batch-mates Yashwant Kumar, Manoharan R., Nilesh Deshpande, Himani Rawat, Shivashankar, Rakesh Pant and Debashish Saha for their support in extracurricular activities. I am grateful to my seniors Mandar Kulkarni, Madhuri Gade, Trimbak mete, Shahaji More, Prabhakar pawar, Jagadish Mettikotti, Sudeshana Manna, Reman Kumar and Plawan Kumar Jha for their guidance throughout my Ph. D tenure. I want to thank some people from other labs Rahul Nisal, Gulab Walke, Gayathri, Somendu and Nancy.

Contents

Synopsis

The thesis entitled "Synthesis, Characterization, and Application of Diphosphinoamine (DPPA) Ligand" is about the synthesis of the DPPA supported transition metal complexes and their applications in the various field of photoluminescence, catalysis, etc. This thesis is divided into five chapters starting with the brief introduction of DPPA ligand, and the application of ligand supported metal complexes. Each chapter contains the details of experimental as well as theoretical investigations of DPPA supported transition metal complexes (M = Cu, Ag, Au, and Pd) reported in this thesis.

Chapter 1: Introduction

This chapter explores the chemistry of diposphinoamine (DPPA) ligands. There are various types of DPPA ligands based on functional group present on the nitrogen and phosphorus, are discussed briefly. Various coordination modes of DPPA ligands are discussed in this chapter. The metal complexes based on such type of DPPA ligand have various applications to developed materials having unique photo-physical properties and homo- and hetero-geneous catalytic activity. So here, the applications of these ligands are discussed in brief. In the end, we discussed the ligand design employed in this thesis.

Chapter 2: Synthesis and Characterization of Diphosphinoamine Gold (I) Complexes

A series of N-functionalized DPPA ligand supported Au(I) complexes (**2.6-2.13**) are synthesized and characterized by X-ray crystallographic analysis and routine techniques (NMR and Mass spectroscopy). Most of the Au(I) complexes show aurophilic interaction with intramolecular Au⋯Au distance in the range of 2.78-3.00 Å. However, some of Au(I) complexes do not possess aurophilic interaction. The effect of the intramolecular aurophilic interaction on the photo-physical properties of these complexes discussed in chapter 3.

Chapter 3: Photophysical and Theoretical Studies of Diphosphinoamine Gold (I) Complexes

In this chapter, we studied the photo-physical properties of N-functionalized DPPA supported Au(I) complexes **2.6**, **2.7**, **2.9**, **2.11**, **2.12** and **2.13** which we synthesized and characterized in chapter 2. We observed that aurophillicity affects the emission properties of Au(I) complexes as those complexes which devoid of aurophilic interaction, do not display luminescence. Some of the Au(I) complexes show a high quantum yield. It is observed that a subtle change of substituent on ligand leads to the different colour of emission which could be very useful in designing new luminescent material of selective colour.
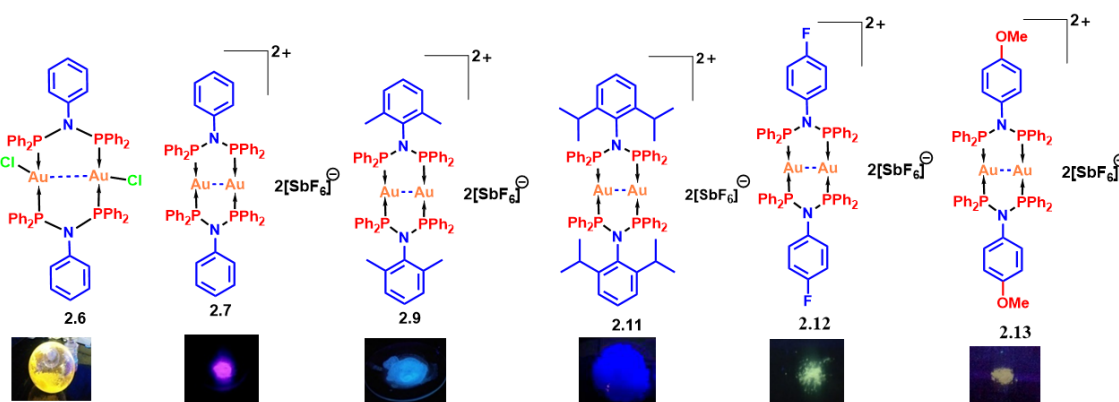
Chapter 4: Synthesis, characterization and photo-physical studies of Diphosphinoamine copper (I) and silver (I) complexes

In this chapter, we synthesized differently N-functionalized DPPA ligand supported copper (I) and silver(I) complexes, and studied their photo-physical properties. Cu···Cu interactions observed in these complexes ranging from 2.65 to 2.935 Å. The copper (I) complexes having Cu···Cu distance >2.8 Å were found to exhibit mechanochromic as well as thermochromic luminescent behaviour presumably stemming from a decrease in their Cu···Cu distances.

Chapter 5: Palladium Catalyzed C-N Cross-Coupling of Sterically Hindered Aryl Bromide Using Efficient Diphosphinoamine Ligands

In this chapter, we employed the easily accessible, cost effective diphosphinoamine ligands, for C-N cross-coupling of sterically demanding aryl bromides and aryl amines, by conventional as well as microwave-assisted organic synthesis (MAOS) technique. All the coupling products are obtained in multigram scale with good to excellent yields. MAOS method drastically reduces the reaction completion time up to 15-30 min when compared to the conventional heating and thereby rendering facile access to the C-N cross-coupled products, especially for the bulky substrates.

Reaction condition

I : Pd(dba)$_2$ (5mol%) **2.1** or **2.3** (5mol%) NaO*t*-Bu, toluene,reflux, 3d

II : Pd(dba)$_2$ (5mol%) **2.1** or **2.3** (5mol%) NaO*t*-Bu, toluene, MW, 15-30 min

2.1 R = H
2.3 R = 2,6-*ipr*
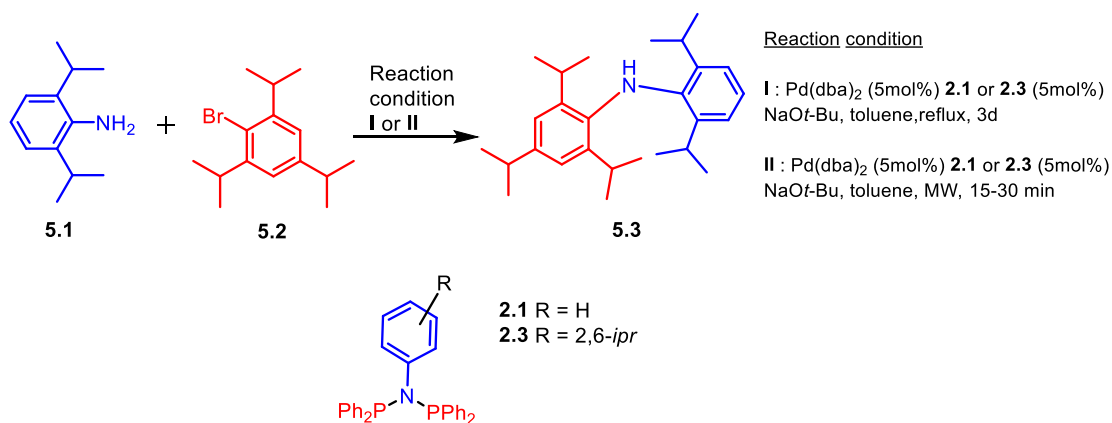
Abbreviations

Anal.	Analysis
Calcd.	Calculated
DPPA	Diphosphinoamine
CCDC	Cambridge Crystallographic Data Centre
CIF	Crystallographic Information file
DCM	Dichloromethane
DFT	Density Functional Theory
Dipp	Diisopropylaniline
CD_3CN	Deuterated acetonitrile
$CDCl_3$	Deuterated chloroform
HRMS	High-Resolution Mass Spectroscopy
hrs	Hours
*i*Pr	Isopropyl
MALDI	Matrix-Assisted Laser Desorption/Ionization
MAOS	microwave-assisted organic synthesis
min	Minutes
mmol	Millimoles
ppm	Parts per million
RT	Room Temperature
NMR	Nuclear Magnetic Resonance
XRD	X-ray Diffraction
Hz	Hertz
P-XRD	Powder X-ray diffraction

Publications

Publications included in Thesis

1. Synthesis, Characterization, and Luminescence Studies of Gold(I) Complexes with PNP- and PNB-Based Ligand Systems
   Shiv Pal, **Neha Kathewad**, Rakesh Pant, and Shabana Khan*
   Inorg. Chem. **2015**, 54, 10172-10183

2. Synthetic Diversity and Luminescence Properties of $ArN(PPh_2)_2$-Based Copper(I) Complexes
   Neha Kathewad, Shiv Pal, Rameshwar L. Kumawat, Md. Ehesan Ali,* Shabana Khan,*
   Eur. J. Inorg. Chem. **2018**, 2518-2523

3. Synthesis and Photophysical Properties of PNP Based Au(I) Complexes with Strong Intramolecular Au⋯Au Interaction,
   Neha Kathewad, Nanda Kumar, Rajarshi Dasgupta, Moushakhi Ghosh, Shiv Pal, and Shabana Khan,* *Dalton transaction, (just accepted) DOI: 10.1039/C8DT04471F*

4. Facile Buchwald-Hartwig coupling of sterically encumbered substrates effected by PNP as ligands,
   Neha Kathewad, Anagha M. C., Sneha Parambath, Pattiyil Parameswaran,* and Shabana Khan,* *Dalton Trans*., **2019**, 48, 2730-2734

Publications not included in Thesis

1. Stepwise isolation of an unprecedented silylene supported dinuclear gold(I) cation with aurophilic interaction
   Shabana Khan,* Shiv Pal, **Neha Kathewad**, Indu Purushothaman, Susmita Deb and Pattiyil Parameswaran,* *Chem. Commun*., **2016**, 52, 3880-3882

2. Silicon(II) Bis(trimethylsilyl)amide ($LSiN(SiMe_3)_2$, L = $PhC(NtBu)_2$) Supported Copper, Silver, and Gold Complexes
   Shabana Khan,* Saurabh K. Ahirwar, Shiv Pal, Nasrina Parvin, and **Neha Kathewad**
   Organometallics ***2015, 34, 5401-5406***

3. Synthesis of acyclic α-borylamido- germylene and stannylene and their catalytic application in hydroboration of aldehydes

   Shabana Khan[*], Shiv pal; Nilanjana Sen; Subhrashis Banerjee; **Neha Kathewad**; Kumar Vanka, *Manuscript under consideration*

Chapter 1

Introduction

Ligands are, atom or molecule, capable of functioning as the electron-pair donor in the electron-pair bond (a coordinate covalent bond) formed with the metal atom.[1] Various types of ligands are known, i.e., neutral, anionic, cationic, etc. depending upon the coordinating site of ligands.[2] Coordinating site of ligands possesses nitrogen, oxygen, phosphorus, carbene, sulphur, halides, etc. which have non-bonding or sigma bonding electron pair.[3] Phosphine ligands have been extensively used in inorganic and organometallic chemistry especially tertiary mono- and diphosphines.[4,5] The metal complxes of phosphine ligands are widely used for their catalytic application in various coupling reaction.[6]

1.1. Diphosphinoamine ligands and their various types

Over the past five decades, a considerable amount of work has been done in the area of synthesis and chemistry of metal complexes with bi- and polydentate short bite ligands containing group 15 donor atoms.[7] These ligands contain the donor sites (E = P, As) separated by X atom, where X= CH_2, NR (Chart 1.1).[7] Higher congeners (E = As) of these ligands have also been studied.[8] Here we are mainly focusing on Phosphorus (E = P) containing ligands.
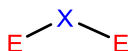
Chart 1.1. *General representation of short-bite ligands (X= CH_2, NR and E = P, As)*

Phosphine ligands (E = P, X= CH_2) with the P-C-P framework have been widely studied for their various applications,[9] whereas P-N bond containing aminophosphines (P-N framework),[10] Bis-diphosphinoamines (P-N-P framework)[11] and iminobiphosphines (P=N-P framework) (Chart 1.2) have also attracted considerable attention. P-N bond containing ligands evoked interest because of their different electronic properties.[12]
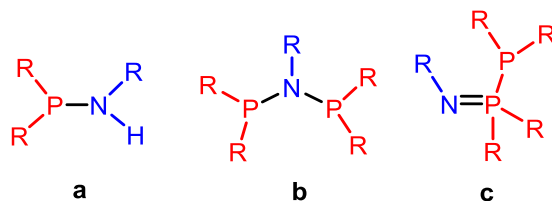
Chart 1.2. (**a**) *Aminophosphine* (**b**) *Diphosphinoamine* (**c**) *Iminobiphosphine*

In Bis-diphosphinoamine ligands, the substituent on both phosphorus and nitrogen can be varied resulting in the change of P-N-P bond angle and the conformation around the phosphorus atoms.[13] In these ligands, the phosphorus atoms are the chelating sites which generate a rather strained, four-membered chelate ring. Such ligands show a distinct tendency to coordinate in a bridging mode between metal atoms where the strain in the ligand backbone is largely absent. These ligands display different coordination mode (Chart 1.3). The tendency of bridging makes these short-bite ligands useful for the synthesis and stabilization of metal complexes with two or more metal atoms.[7]
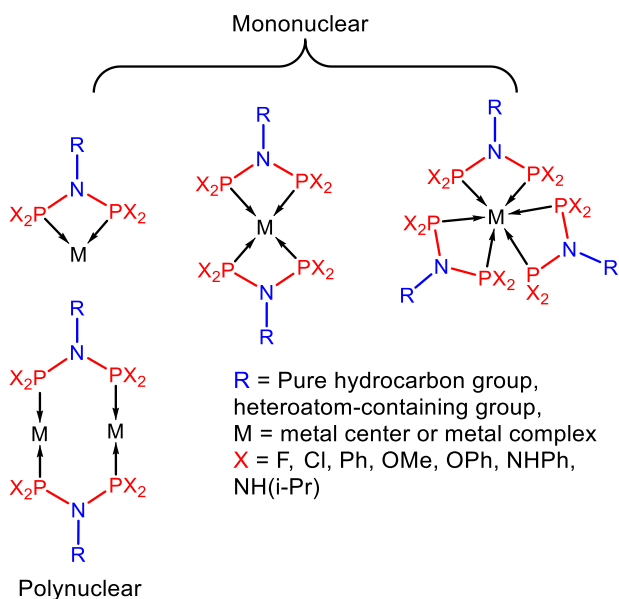
Chart 1.3. *Possible coordination mode of diphosphinoamine ligands*

A variety of substituted Bis-diphosphinoamine ligands has been synthesized and used in various applications.[10] Braunstein and coworkers elaborated all the different types of functionalized diphosphinoamine ligands, e.g., the various N-substituents include nitrogen-, oxygen-, phosphorus-, sulfur-, halogen-, and silicon-based functionalities and directly N-bound metals.[10e] This review also discusses about a diverse range of bis (diphosphino) amine-type ligands linked through an organic spacer and N-functionalized bis (dialkylphosphino) amine-type ligands, where the PPh2 substituents are replaced by PR2 (R = alkyl, benzyl) groups.

These DPPA-type ligands (**1-8**) bear an amino group as N-substituent, typically tertiary amino group, separated from DPPA moiety by aliphatic spacers. Such N-functionalization does not get involved during the complexation with metals. However this N-functionalization prompts these simple bidentate DPPA ligands to act as a hemilabile, [14-17] tridentate, mixed-donor ligand.
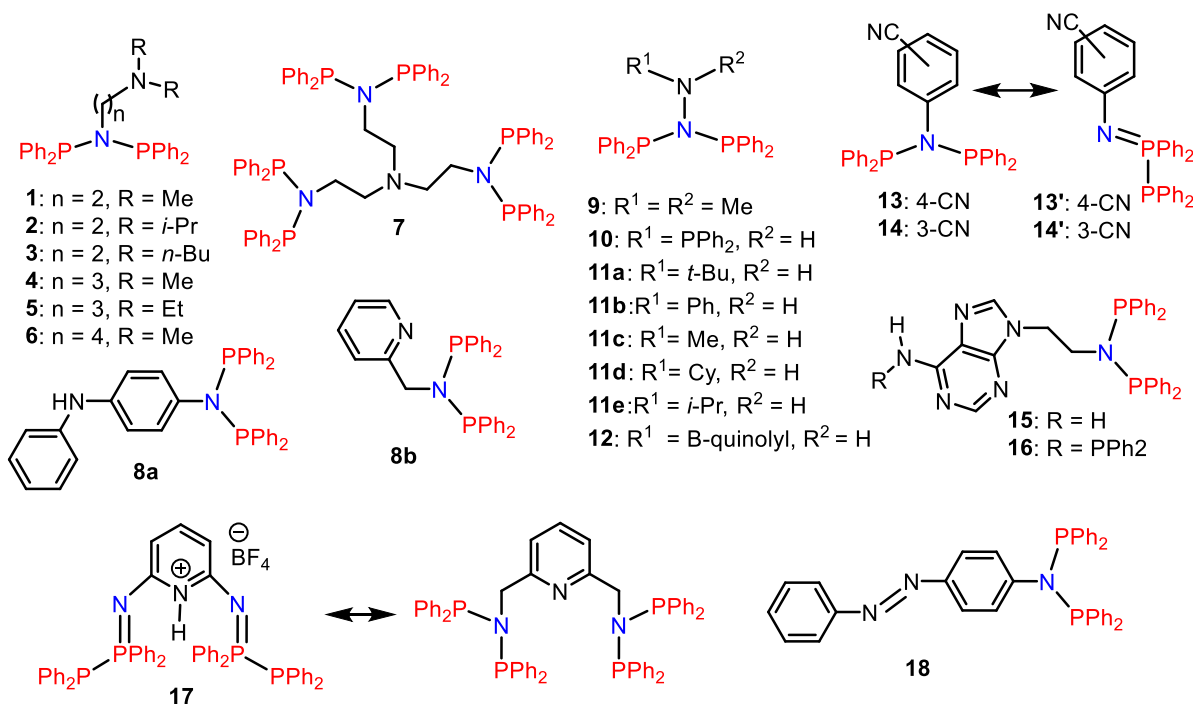
Chart 1.4. *Nitrogen-based functionalization*

Hydrazines-Derived DPPA-type Ligands **9-12** are also called as 'Diphosphinohydrazides' which display direct N-N single bond. These ligands are very much prone to migratory rearrangement.[18-21] When **10**, **11a** and **11b** are subjected for deprotonation with LiN(SiMe3)2, undergo molecular rearrangement and the migratory insertion of a PPh2 group into the N−N bond, give rise to a diphosphazenide products **10⁻**, **11a⁻**, and **11b⁻** (Scheme 1.1).[18] Similarly, ligand **12** also undergoes rearrangement on heating at 130°C in toluene solution or on reaction with LiN(SiMe3)2.[19] The reason behind such type of migration might be the nature of substituent on the nitrogen (NHR^1). The high electron density on nitrogen causes the elongation of N-N bond length which results in the subsequent cleavage and allows insertion of the PPh2 group.[18,19] There are some functionalized DPPA ligands which exist in the isomeric form of their corresponding iminobiphosphine ligands as they are not stable in the form of diphosphinoamine (chart 1.4, **13** and **14**)[20,21]. Zhaofu Fei et al. studied such type of ligands and the influence of functionalization of nitrogen atom on the corresponding diphosphinoamine ligand. Ligands RN=PPh2–PPh2, where R = C_6H_4(*p*-CN), C_6H_4(*m*-CN), C_6H_4(*o*-C_6H_5), C_6F_5 or C_6H_4(*o*-CF3), shows existence in two forms, diphosphinoamine, and their corresponding iminobiphosphine.[20]
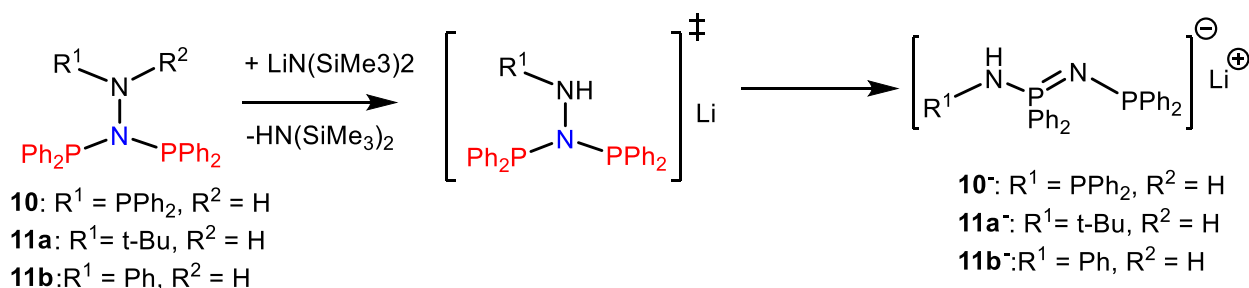
Scheme 1.1. *Rearrangement after Deprotonation Leading to the Diphosphazenide Group in* **10⁻**, **11a⁻**, *and* **11b⁻**

This type of isomeric transformation observed during coordination to transition metals, e.g., synthesis of the group 10 metal complexes (M = Pd, Pt) supported by *m*- or *p*-cyanoaryl-

functionalized DPPA-type ligands **13** and **14**, resulting from the rearrangement of the corresponding iminobisphosphine precursors **13′** and **14′** upon reaction with [MCl$_2$(COD)] (M = Pd, Pt).[20,21] Such type of rearrangements are giving a new approach for the synthesis of chelating and bis-chelating transition-metal complexes.

In biological systems, the metal complexes play a very important role, as they can form complementary hydrogen bonds which represent an important class of compounds for the development of biochemically active molecules. Woollins and colleagues reported N^9-(N$^{2'}$-diphenylphosphinoaminoethyl)-adenine functionalized DPPA-ligands **15** and **16**, as part of a mixture of compounds that resulted from the aminolysis of functionalized adenine derivative.[21] Synthesis of such adenine functionalized ligands has been tried to pursue an objective to prepare compounds with potential antiviral or anticancer activity. Ligand **17** is a pentadentate ligand based on the association of two DPPA-type units linked through a pyridine substituted in its 2 and 6 positions. Such ligands allow the synthesis of polynuclear metal complexes and macrocyclic ring systems since it has the presence of numerous donor groups, hence also known to be poly-DPPA ligands. [22,23] Similar to N-functionalized DPPA ligand **8**, N-furfuryl-functionalized DPPA ligand **19** also have an aliphatic spacer between the DPPA moiety and furfuryl ring.[15] Additional donor group functionality does not interact with the metal centre coordinated to DPPA fragment, because of the short spacer group between PNP moiety and the additional donor group in the 'scorpionate type' ligands. However, similar to DPPA ligand **1**-**8**, ligand **19** also plays a role during the catalytic cycle by stabilizing the active or low-valent species in intermolecular fashion. These ligands found to have application in catalyzing the ethylene oligomerization (Details discussed in section 1.2.2).[15]

Ligand **33** and **34** were reported by Wasserscheid, McGuinness, and colleagues for the purpose to access the corresponding alcohol.[24] Silyl ethers have often been employed as alcohol protecting groups as they are easily and selectively prepared in the presence of amines and can be readily cleaved either with tetrabutylammonium fluoride (TBAF) and a proton source or by hydrolysis. Since authors found out that the conventional methods failed to deprotect the silyl ether in order to generate alcohol, attempts were made for deprotection of silyl ether using TiCl$_4$.[25], but instead of deprotection, they isolated ligand-TiCl$_4$ (**34B**) adduct (scheme 2). Moreover, on refluxing ligand **34** with methanol solution leads to the

deprotection of silyl ether followed by intramolecular rearrangement to generate monocyclic hydrophosphorane (**34B**).
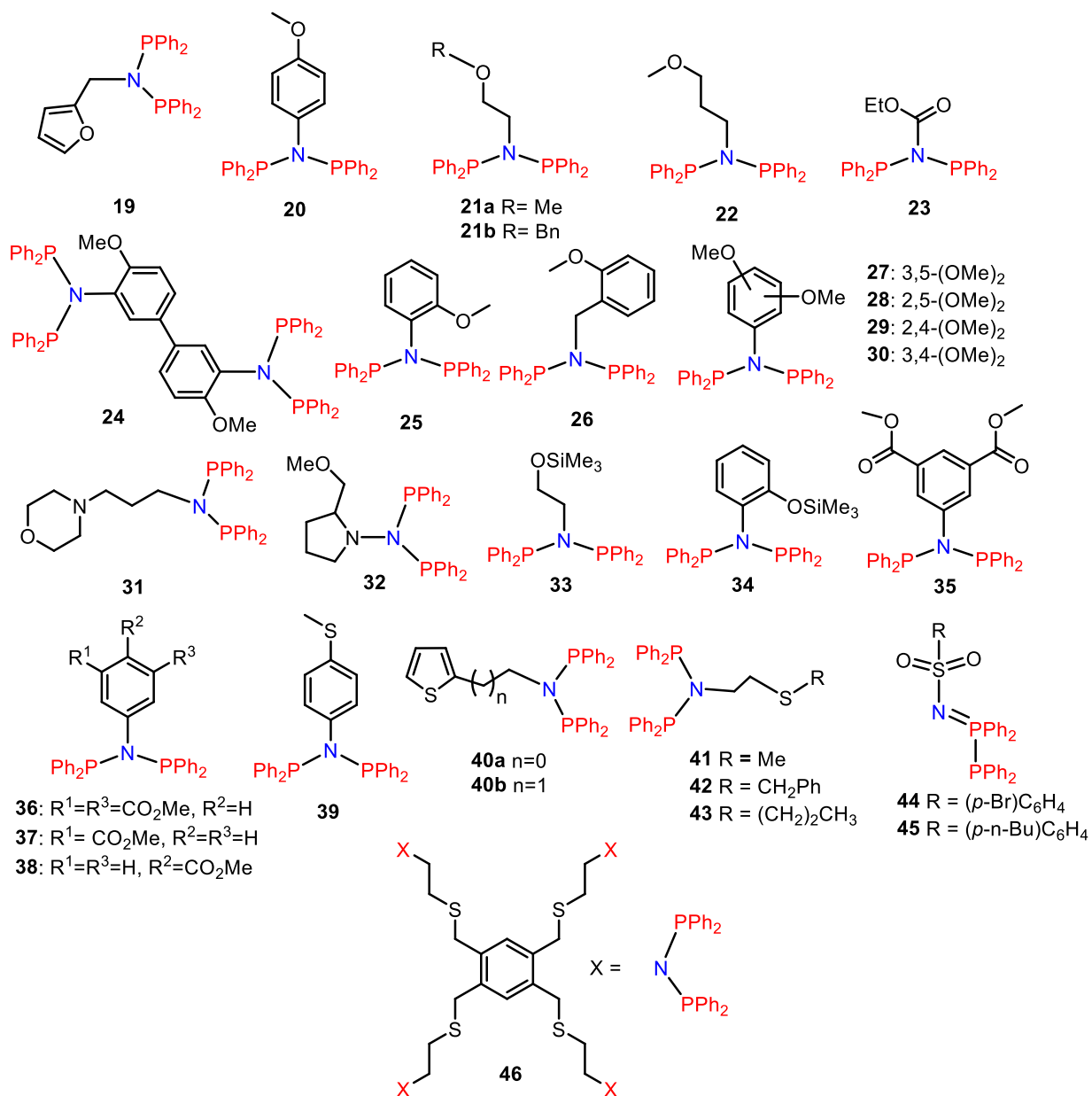
Chart 1.5. *Oxygen and Sulphur-based functionalization*
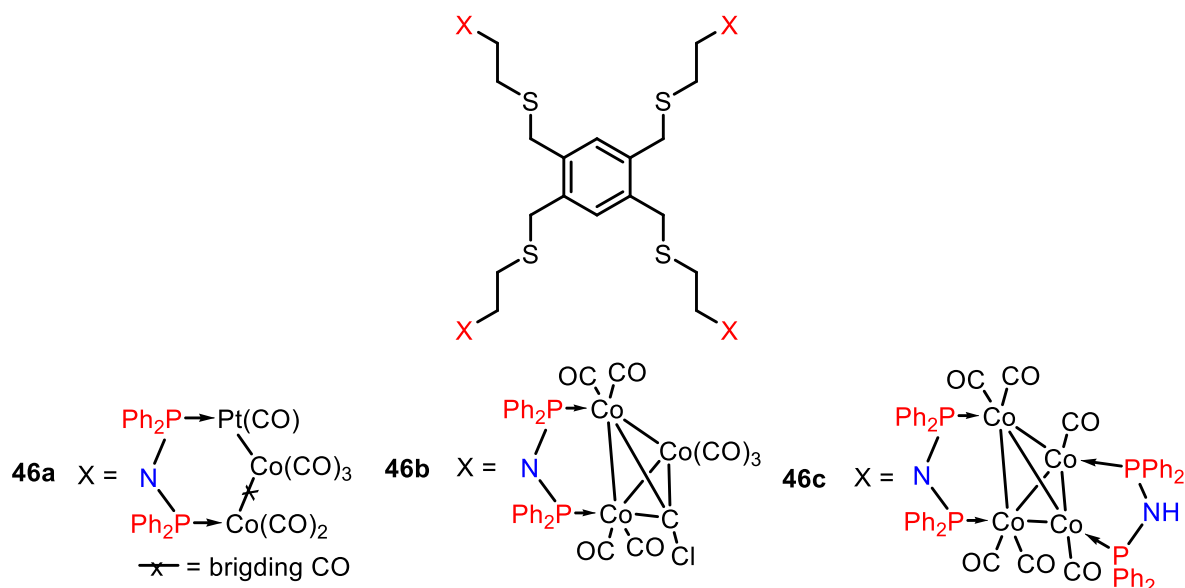
Chart 1.6. *Metal clusters stabilized by ligand 46*

N-[3-(methylthio)propyl]-substituted DPPA-type ligand **41** reported by Weng, Hor, and colleagues.[26] The in situ mixture of [Cr(acac)$_3$] with 2 equivalent of the PNP ligand (**41**) with 440 equiv. of MAO has been used to study their catalytic application in selective Cr-catalyzed ethylene teramerization.[26] Ni(II) coordination complex with ligand **41** was synthesized and employed for its catalytic application in selective ethylene oligomerization.[27] Series of iminobiphosphine type ligands directly functionalized on their N atom by a sulfonyl group (**44** and **45**) are the isomeric form of their corresponding bis-diphosphinoamine ligand, and undergo rearrangement during coordination with a metal center, e.g., nickel dibromide complexes.[28] Synthesis of the Novel octadentate ligand 1,2,4,5-{(Ph$_2$P)$_2$NCH$_2$CH$_2$SCH$_2$}$_4$C$_6$H$_2$ (**46**) (chart 1.5) was described by Smith and co-workers, which consists of four independent DPPA units, each connected to a phenyl ring by a thio-ether based spacer (CH$_2$CH$_2$SCH$_2$).[29a] This ligand has a very interesting role in stabilizing molecular metal clusters (**46a-c** chart 1.6).[29] Ellermann and colleagues reported tris(diphenylphosphino)amine ligand, **47** and examined its potential as assembling ligand for the formation of (hetero)polynuclear complexes.[30]
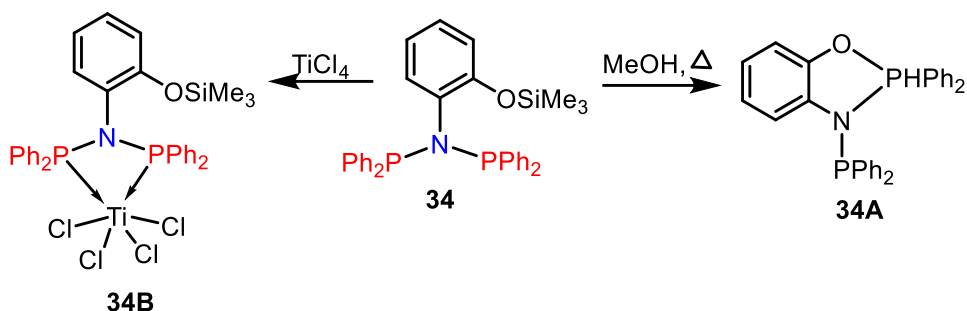
Scheme 1.2. *Reactivity of ligand 34 toward TiCl₄ (34B) and MeOH (34A)*

Phosphorus functionalized DPPA ligands **49**-**52** have multiple sites for coordinating the metals. 1,2-azaphophanolanes species **49**-**52** are easily synthesized by the one-pot reaction between the corresponding 3-halopropylamine hydro-halides and 2 equiv. of PPh₂Cl in the presence of an excess of NEt₃. The additional phosphorus donor site is not present; instead of that, it has P atom, i.e., PR₄⁺ moiety. [31]
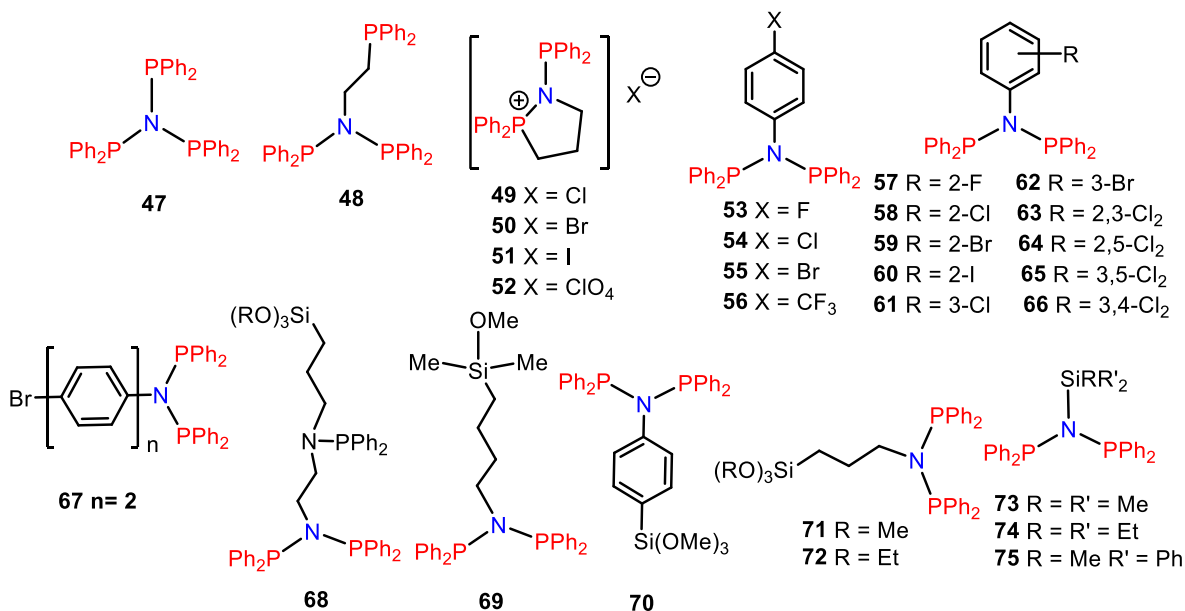
Chart 1.6. *Phosphorus, Halogen and Silicon-based functionalization*

Synthesis of halogen functionalized DPPA ligands **53-67** reported by Braunstein and co-workers. Lau and colleagues synthesized p-trifluoromethane substituted DPPA ligand (**56**) which has been employed to synthesize Ruthenium precatalyst [RuCl(Tp)(PPh$_3$)$_2$] and to study the reactivity of the precatalyst.[32] Ligands **55** and **67** have been used to study the coordination chemistry toward group 10 and 11 mononuclear metal precursors and Co(0) molecular clusters. The same group studied the possibility to stabilize low-valent cobalt carbonyl clusters with the ligand **55** and **67**.[33] A series of N-(halo) aryl functionalized mono- (**57-62**) and bis-halogenated (**63-66**) DPPA-type ligands are reported by Jiang and colleagues. In combination with [Cr(acac)$_3$] and MAO as co-catalyst, these ligands give a highly active system for catalytic selective tetra-merization of ethylene.[34]

Silicon functionalized DPPA-type ligands **68-75** were synthesized to serve a purpose of anchoring metal complexes or clusters into porous supports, for the formation of potential heterogeneous catalysts. (Details in section 1.2.2). Until now only five different types of this silicon functionalized DPPA ligands are known, which consist of connecting DPPA moiety to an alkoxy or mixed alkyl/alkoxy-silyl group separated by aliphatic (**69**, **71** and **72**) or rigid aromatic (**70**) spacer, or an additional donor spacer (**68**).[35]
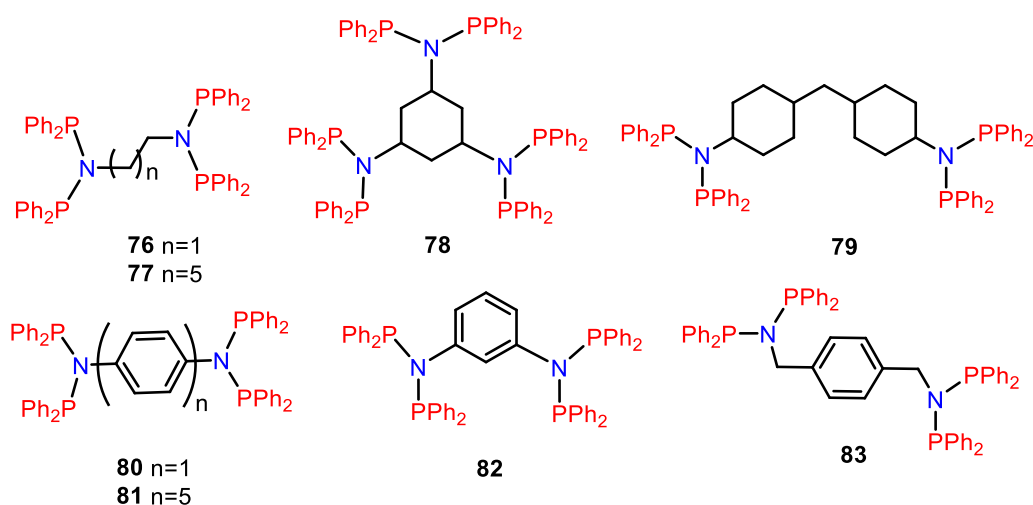
Chart 1.7. *Poly-bis(diarylphosphino)amine Derivatives*

DPPA-type ligands directly functionalized with the trimethylsilyl group (**73**-**75**) was first reported by Schmidbaur and colleagues in the late 1970s. The synthetic protocol involves two steps, deprotonation of acidic N-H proton of DPPA using *n*-BuLi followed by addition of SiClMe$_3$.[36]

Another important category is poly-bis(diarylphosphino) amine derivatives (**76**-**83**). They are multidentate ligands with two or more DPPA fragments assembled through an organic spacer.[35c,37] Ligand **76** was used to prepare Ni(II), Pd (II) and Pt(II) complexes and **76**-PdCl$_2$ complex was further evaluated in both Suzuki and Heck coupling reactions. [53] Ligand **77**, **78** and **79** were used in a ternary catalytic mixture of ligand/Cr(III)/MAO for selective ethylene tetra-merization.[60]

1.2. Applications

All above mentioned functionalized DPPA ligands have shown various applications from coordination to the metal center to catalysis using these metal complexes.[38-50] These pre-catalysts derived from these ligands and metals shows various applications as in homogeneous, heterogeneous catalysis. Some of the complexes have been (especially coinage metals, i.e., Cu, Ag, Au) found to displays photo-physical properties.

1.2.1 Coordination with Coinage Metal Complexes

The coinage metal (d^{10}) chemistry has attracted considerable attention in the last few decades due to their structural diversities, rich photo-physical properties,[38] and catalytic applications.[39] Our work focuses on photo-physical properties of DPPA coordinated coinage metal complexes. Some of the DPPA coordinated coinage metal complexes which are summarized in chart 1.8 studied for their photo-physical properties. Facile synthesis with tunable optical properties of these luminescent metal-organic complexes has attracted much interest over the past decades owing to their enormous potential application in optoelectronic devices.[38] Metallophilic interaction is an interesting type of bonding, i.e., the non-covalent interaction between the two closed shell d^{10} metal atoms which plays an

26

important role in influencing the structural as well as the photo-physical properties of coinage metal complexes.[40-42]

84

85

86 R = C_6H_4OMe-*p*, X= Cl
87 R = *i*-Pr, X = C≡CR',R'=Ph (**88a**), C_6H_4OMe-*p* (**87b**), C_6H_4Me-*p* (**87c**), C_6H_4Cl-*p* (**87d**), C6H4OMe-p (**87e**),
88 R = 3,5-$CO_2MeC_6H_3$, X = Cl

89 M= Au, R= 3,5-$CO_2MeC_6H_3$,Y= ClO_4
90 M= Au, R= 2,6-$iPrC_6H_3$,Y= SbF_6
91 M= Ag, R= $(CH_2)_3SMe$,Y= BF_4
92 M= Ag, R= *p*-$(SMe)C_6H_4$, Y= BF_4

93 M = Ag
94 M = Au

95

96a R = 4-$OMeC_6H_5$, R'= NHCONHPh
96b R = C_6H_{11}, R'= F

E **= S**, **97** R = ^nPr,
98 R =C_6H_5
99 R =$C_6H_4CH_3$-*p*
100 R = $C_6H_4OCH_3$-*p*
101 R = C_6H_4Cl-*p*
102 R = C_6H_4Br-*p*
103 R = C_6H_4F-*p*

E = Se, 104 R = ^nPr,
105 R =C_6H_5
106 R =$C_6H_4CH_3$-*p*
107 R = C_6H_4F-*p*

E = S, 108 R = ^nPr,
109 R =C_6H_5
110 R =$C_6H_4CH_3$-*p*
111 R = C_6H_4F-*p*
E = Se, 112 R = ^nPr,
113 R =C_6H_5
114 R =$C_6H_4CH_3$-*p*
115 R = C_6H_4F-*p*

116: 3,5-$(OMe)_2$
117: 2,5-$(OMe)_2$
118: 2,4-$(OMe)_2$
119: 3,4-$(OMe)_2$

120 X = Br, **R** =$OC_6H_4(OMe$-*o*$)(C_3H_5$-*p*$)$,
121 X = Br, R = $OC_6H_4C_3H_5$-*o*
122 X = I, R = $OC_6H_4(OMe$-*o*$)(C_3H_5$-*p*$)$
123 X= I, R = $OC_6H_4C_3H_5$-*o*

124 R = $OC_6H_4(OMe$-*o*$)(C_3H_5$-*p*$)$,
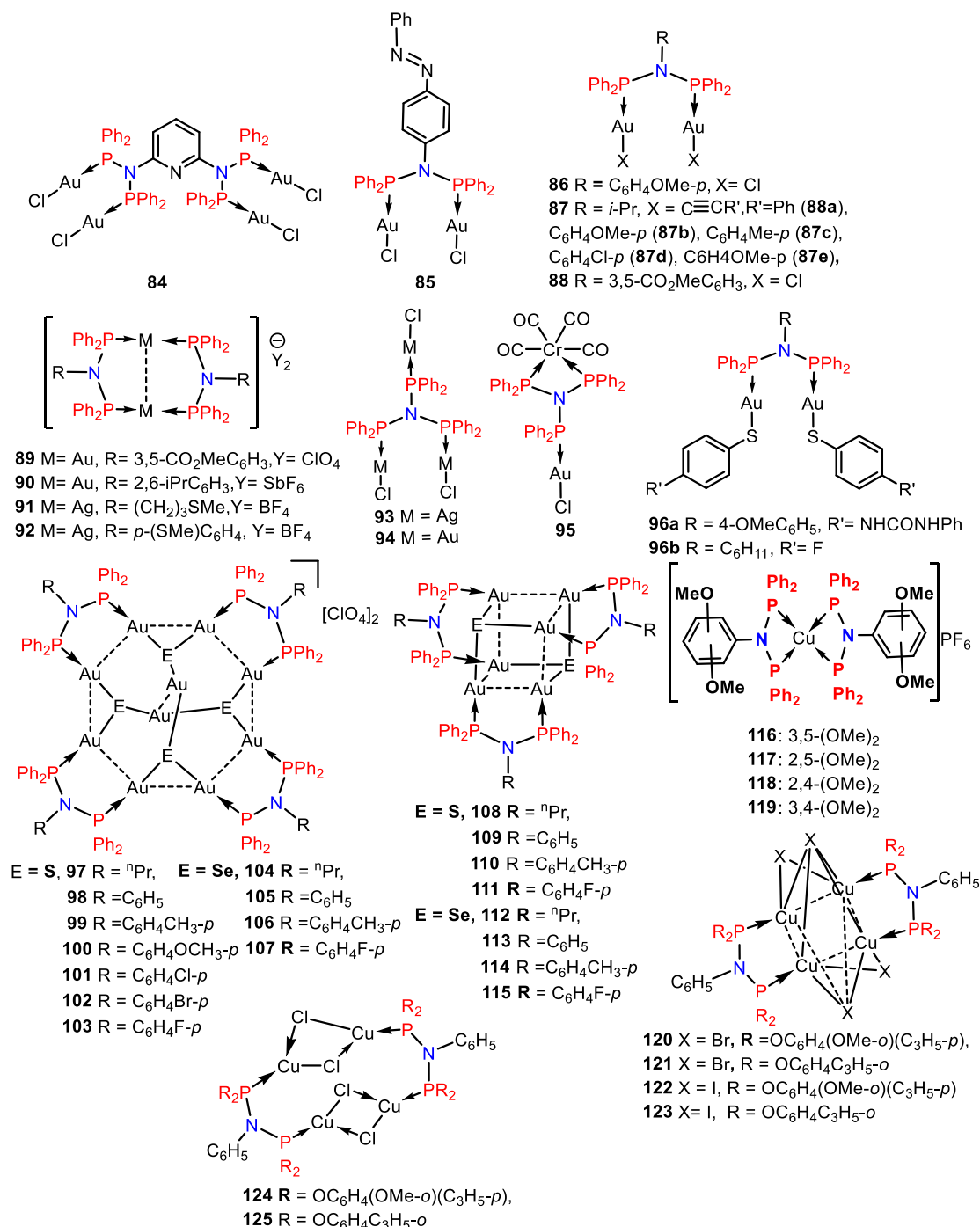**125** R = $OC_6H_4C_3H_5$-*o*

Chart 1.8. *DPPA Coinage metal complexes*

N-Functionalized DPPA ligands supported Au(I) complexes, **84** and **85** both are non-luminescent, and complex **85** shows Au-Au distance 3.0095(7)A°.[43,44] Ellermann and colleagues synthesized compounds **93**, **94** and **95.** Complexes **93** and **94** were synthesized by treating tris(tri-phenyl) diphosphinoamine ligand **47** with 3 equivalent of AgCl and [AuCl(CO)] respectively, whereas complex **95** was synthesized by treating chromium carbonyl complex of ligand **47** with 1 equivalent of [Au(CO)Cl].[30] Yam and co-workers synthesized a series of luminescent DPPA based Au(I) complexes (**86, 87**, **96, 97-115**) and studied their photo-physical properties. A series of alkynyl gold(I) bis(diphenylphosphino)alkyl-and aryl-amine complexes **87a-87e** have been prepared which show emission bands at room temperature as well as 77 K upon excitation at 350 nm. These complexes have short intermolecular distances in the range of 2.84-3.07 A°.[45]

Further studies on gold(I) thiolate complexes have shown that complexes with bridging DPPA ligands, [Au$_2$(PPh$_2$N(R)PPh$_2$)(SR')$_2$] (**96a** and **96b**), exhibits intense lower energy triplet thiolate-to-gold ^{3}LMCT (ligand-to-metal charge transfer) emissions analogous with methylene-linked diphosphine ligands, such as bis(dicyclohexylphosphino) methane (dcpm) and bis(diphenylphosphino)-methane (dppm) supported complexes display LMCT.[46] The reason for this can be attributed to the presence of the more electronegative N atom on the DPPA ligand, which would render the Au(I) centres less electron-rich and hence would lower the metal acceptor orbital energy. A series of DPPA supported Au(I) clusters (**97-115**) has also been synthesized and studied for their photo-physical properties. These are the high nuclearity chalcogenides (sulfido and selenido) Au(I) clusters (**97-115**) with bridging DPPA ligands showing phosphorescence upon photoexcitation in the solid as well as solution state at ambient and low temperature. Deca-nuclear clusters (**97-107**) have intermolecular Au···Au distance in the range of 3.0255-3.2783 Å and show intense dual luminescence in the green and orange-red region. Whereas the hexanuclear clusters (**108-115**) display intense emission in the orange-red region with Au···Au distance in the range of 2.9264(7) to 3.3508(10) Å.[47] Balakrishna and co-workers synthesized DPPA supported copper clusters **120-125**. DPPA supported tetrameric iodo cluster of Cu(I) **123** show photoluminescence with very short Cu-Cu distance of 2.568 A°.[48] Our group synthesized PNP based Au(I)

complex **90** and studied their photo-physical properties. (Discussed in brief chapter 2 and 3)[49]

1.2.2. Homogeneous Catalysis

The DPPA ligand supported metal complexes have been used for many catalytic applications, like catalytic Olefin Poly/Oligomerization, Oligomerization of ethylene, cross-coupling reactions, etc. Some of them has been discussed below.

1.2.2.1 Ethylene oligomerization

Researchers made an intensive effort to develop a catalytic system for selective oligomerization of ethylene, under the homogeneous condition, which remains an ongoing and attractive field of research. Combination of chromium metal and DPPA ligands have been used for ethylene oligomerization in two ways (i) as a part of the catalytic mixture, e.g., ligand/Cr(III)/MAO (MAO- methylaluminoxane) (ii) Chromium-DPPA ligand complex used as pre-catalyst.[51-53]

Jiang and colleagues studied the effect of different parameters, e.g. like temperature, pressure, chromium source, ligand structure, molar ratio of Cr/Al (MAO) on the catalytic activity and product selectivity of ethylene oligomerization. They used ligand **7**, **76**, **77**, **80** and **81** to study the effect of the ligands on ethylene oligomerization. Ligand **76**, **77** and **80** have been used with catalytic mixture ligand/Cr(III)/MAO under similar condition, **80** with rigid aromatic spacer exhibits 30% more yield compared to **77** which have long flexible aliphatic chain spacer, and four times higher than N-ethyl linked bis-DPPA ligand **76**.[54a] When catalysis was performed with the pre-catalyst of [(CrCl$_3$)$_3$] with triple-site DPPA ligand **7** both the activity and selectivity gets lowered.[54b]

Nitrogen-functionalized hydrazine-based ligands **13** and **15a-e** were recently investigated for the selective oligomerization of ethylene, where it was observed that selectivity gets induced from 1-octene to 1-hexene by **15c** to **15a**, **15b**, **15d** and **15e** respectively and the reason behind this is the increase in steric hindrance.[25] Ligand **15a** and **15c-e** give a large amount of polyethylene and a significant amount of higher oligomers, moreover, nitrogen-

functionalized DPPA ligand **2** and aromatic substituted hydrazine functionalized **15b** was found to be selective toward tri-merization and tetra-merization with overall 1-hexene product selectivity.[25] Bercaw and colleagues developed a series of chromium (pre)catalyst [CrCl$_3$(PNP)]$_2$ with oxygen functionalized ligands **21a**, **22**, **25** and **26** for the catalysis of ethylene oligomerization.[55] In contrast to the previous results for such systems, these catalyst found to be highly active, stable, and selective for tri- and tetra-merization under mild reaction conditions. Blann and co-workers synthesized chromium catalysts with N-SiMe$_3$ functionalized ligand **73** shows instability of the catalytic system due to a possible interaction between organo-aluminium co-catalyst and silicon functionalization of ligand and shows more selectivity toward tetra-merization.[35c]

Gao, Wu, and colleagues synthesized series of [NiBr$_2$(PNP)] complexes with N-pendent heterocycle (pyridine, fur-furyl, thio-phene, etc) DPPA ligands **8b**, **19**, **40a** and **40b** in order to incorporate these complexes for ethylene oligomerization.[15b] It was observed that all complexes were highly active and gave rise to butene and a small amount of hexane. Increased activity was observed in relation with the increase of basicity of the N-functionalized pendant group, i.e., N-benzyl < fur-furyl (**19**) < 2-methyl thio-phene (**40a**) < 2-picolyl (**8b**). Whereas in the case of Ni(II) catalyst of **40a** and **40b,** an increase of α-selectivity observed upon lengthening of the spacer between the PNP moiety and the additional S donor. This indicates that catalytic activity largely affected by subtle changes in the pendent group, and also the introduction of additional donor group has a beneficial effect by providing the additional binding site for the active species. Braunstein, and co-workers synthesized [NiCl$_2$(PNP)] complexes with N-alkyl- and N-aryl-thio-ether functionalized DPPA ligand **39** and **41** as a catalyst for ethylene polymerization.[28b] It was observed that N-aryl-thio-ether complex [NiCl$_2$(**41**)] shows better activity than the N-alkyl complex [NiCl$_2$(**39**)] at lower AlEtCl$_2$/Ni ratios (3-10 equiv), whereas at higher concentration of AlEtCl$_2$/Ni the later shows activity twice that of the former.

Poly-ketones which represents as low-cost thermoplastics has been synthesized by co-polymerizing CO and ethylene using a mixture of bis-DPPA type ligand **83** and 2 equivalents of [Pd(OAc)$_2$] with tri-fluoroacetic acid (4 equiv.) in excess of ethanol.[56]

1.2.2.2 Cross-coupling

Cross-coupling (C-X, X= C, N, O, S, etc) is a powerful tool for organic synthesis, and a number of ligands have been employed in catalytic system with transition metals.[57] However among them, phosphine are most widely used ligands.[6,58]

A series of $PdCl_2$ complexes of mono- and dimethoxyphenyl mono-DPPA- (**27-31**), dimethoxybiphenyl bis-DPPA-type (**24**.Pd) have been studied for their catalytic activity for Suzuki coupling. All these ligands gives excellent yields of coupling products, but found to be slightly less efficient with electron-rich or releasing groups (R =H, Me, OMe).[59,60] $(PdCl_2)_2$ and $(PdCl_2)_3$ complexes of tris-DPPA type **7** bis-DPPA type **77** have been synthesized and compared their catalytic performances, showed that the presence of more than one catalytic site does not lead to significant improvement in the activity of the Suzuki coupling. The $PdCl_2$ complex of ligand **19** was incorporated for Heck coupling and observed that this pre-catalyst only effectively work for aryl bromides with electron-withdrawing groups and gives poor yield in case of electron-releasing groups.[61]

### 1.2.3. Material Science and Heterogeneous Catalysis

Group of Braunstein reported complementary strategies for the anchoring of molecular palladium complexes, of cobalt or platinum clusters, or of gold colloids inside the nanopores of alumina membranes via N-functionalized DPPA-type ligands, as some of specific N-functionalized DPPA type ligands enable the anchoring of these metal complexes onto a mesoporous matrix or metal surface.[62,63]

Pure nanocrystalline Co_2P particles have been synthesized by anchoring the $[Co_4(CO)_{10}(\mu\text{-}DPPA)]$ onto the mesoporous silica matrix of type SBA-15, and that has been derivatized by DPPA ligand **72** $(Ph_2P)_2N(CH_2)_3Si(OMe)_3$.[62] Heating of such anchored clusters at higher temperature like 650-800°C gives rise to nanoparticles. Using the same strategy which was applied for the synthesis of the Co_2P nanoparticle, anchored cluster of $NiBr_2$ catalyst onto silica, which was synthesized by Braunstein, Schmid, and Wang colleagues (Scheme 1.4),[35b] was further evaluated in the Biginelli reaction (Scheme 1.4).[63] Good to excellent yields were

obtained for the reaction products with a series of aromatic aldehydes, ethyl acetoacetate, and (thio)urea. The silica-supported nickel catalysts could be recovered and recycled up to five times without significant loss of activity (yields 95–89%).
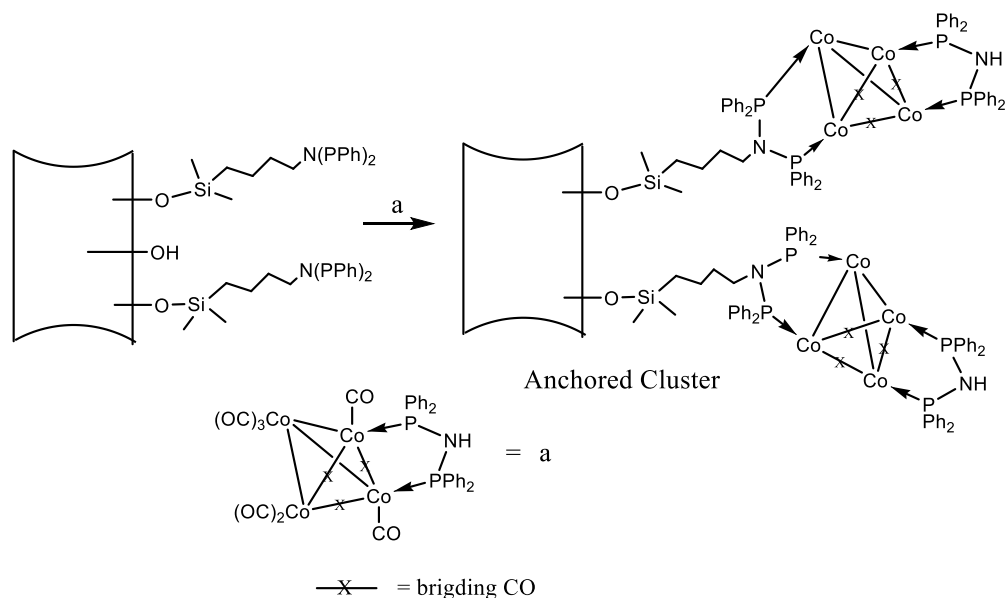
Scheme 1.3 *Synthetic strategy for Synthesis of CO₂P nanoparticles*
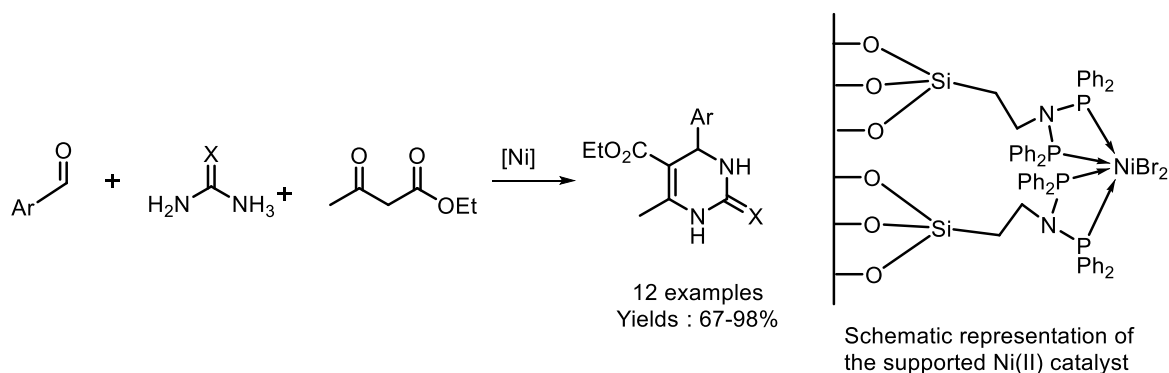
**Scheme 1.4**. *Biginelli Reaction Catalyzed by the Supported Ni Catalyst*

Recently in 2017, two palladium complexes has been synthesized using silicon functionalized DPPA ligand **72** *i.e.* [Pd{(Ph₂P)₂N(CH₂)₃Si(OCH₃)₃-kP,P'}X₂] (X= Cl and Br).

These palladium complexes are then immobilized with clay named as montmorillonite and then used as heterogeneous catalyst for Suzuki-Miyaura coupling. The immobilized complexes, used as heterogenized catalysts, displayed higher activity in the Suzuki-Miyaura coupling compared to that of the free complexes.[64]

1.3. Scope and objectives of the work

By taking inspiration from the fact that DPPA ligands can be utilized in various applications, e.g., DPPA-metal complexes show photoluminescence properties and can be employed in catalytic systems, we thought to use them for preparing fully supported coinage metal complexes (Cu, Ag, Au) as well as utilize them as an ancillary ligand in Buchwald-Hartwig coupling reactions. The effect of substitution on DPPA ligand on various factors like photoluminescence, catalytic application (using Palladium catalyst) is the main focus of this work. In order to do so we synthesize DPPA ligands with various N-functionalization (**L1-L6**).

DPPA ligands can be synthesized by using common aminolysis method by employing aliphatic or aromatic amine with PPh$_2$Cl and Et$_3$N. We slightly modified the procedure and used lithiation of amine followed by addition of PPh$_2$Cl (scheme 1.5) to synthesize our DPPA ligands (**2.1-2.5, 4.1** and **4.2**) (scheme 1.5).
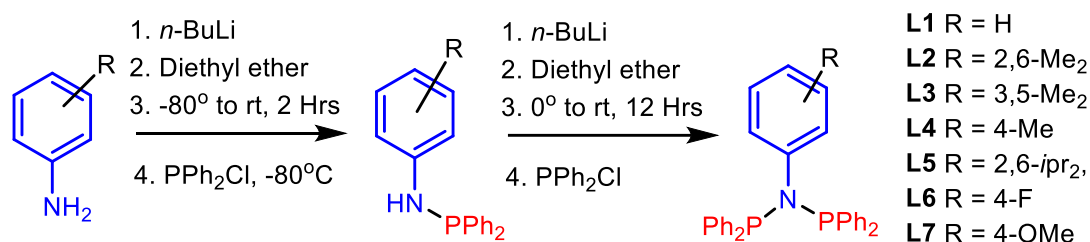
Scheme 1.5 *Synthesis of DPPA ligand*

[Ligands **L1-L7** denoted as (i) Chapter 2: **L1 = 2.1, L2 = 2.2, L5= 2.3, L6 = 2.4** and **L7 = 2.5**; (ii) Chapter 4 : **L3 = 4.1, L4 = 4.2**]

1.4. References

1. Cotton, F. A.; Geoffrey W.; Carlos A. M. *Advanced Inorganic Chemistry*. Wiley-Interscience, **1999**, 1355.

2. Bhatt, V.; Ram, S. *Chem. Sci. Rev. Lett.* **2015**, *4*, 414.

3. Lawrence, M. A. W.; Green, K.-A.; Nelson, P. N.; Lorraine, S. C. *Polyhedron, 143,* **2018**, 11.

4. (a) McAuliffe, C.A., *Comprehensive Coordination Chemistry*, vol. 2, Perganon Press, Oxford, **1987**, 989 (b) A. Pidcock, *Transition Metal Complexes of Phosphorus, Arsenic and Antimony Ligands*, MacMillan, London, **1973**, 3. (c) McAuliffe, C. A.; Levason, W.A., *Phosphine, Arsine and Stibine Complexes of the Transition Elements*, Elsevier, Amsterdam, **1979**.

5. (a) Tolman, C. A., *Chem. Rev.* **1977**, *77*, 313. (b) Appleby, T.; Woollins, J. D., Coord. Chem. Rev. 2002, 235, 121-140.

6. (a) Hartwig, J. F., *Acc. Chem. Res.*, **2008**, 41, 1534. (b) Surry, D. S.; Buchwald, S. L., *Chem. Sci.*, **2011**, *2*, 27.

7. Mague, J. T., *Journal of Cluster Science*, **1995**, *6*, 2.

8. (a) Mague, J. T. *Inorg. Chem.*, **1972**, *11*, 2558–2561. (b) Mague, J. T. *Inorg. Chem.*, **1969**, *8*, 1975.

9. (a) James M. Longmire, J. M.; Zhang, X *Tetrahedron Letters,* **1997**, *38*, 1725. (b) Chan, A. S. C.; Hu, W.; Pai, C.-C.; Lau, C.-P. *J. Am. Chem. Soc.* **1997,** *119,* 9570. (c) Hu, X.; Chen, H.; Zhang, X. *Angew. Chem. Int. Ed*. **1999**, *38*, 3518.

10. (a) Ly, T. Q.; Woollins, J. D., *Coord. Chem. Rev.* **1998**, *176*, 451. (b) Aucott, M. S.; Slawin, A. M. Z.; Woollins, J. D., *J. Chem. Soc.*, *Dalton Trans.*, **2000**, 2559. (c) Aucott, M. S.; Clarke, L.M.; Woollins, J. D., *J. Chem. Soc.*, *Dalton Trans.*, **2001**, 972. (d) Clarke, L.M.; Slawin, A. M. Z.; Wheatley, V.M.; Woollins, J. D. J. *J. Chem. Soc.*, *Dalton Trans.*, **2001**, 3421. (e) Gopalakrishnan, J. *Appl. Organomet. Chem.* **2009**, *23*, 291. (f) Fliedel, C.; Ghisolfi, A.; Pierre Braunstein, P.; *Chem. Rev.* **2016**, *116*, 9237.

11. (a) Bachert, I.; Braunstein, P.; Hasselbring, R. *New J. Chem.,* **1996**, *20*, 993. (b) Bachert, I.; Braunstein, P.; McCart, M. K.; Biani, F. F. de; Lashi, F.; Zanello, P.; Kickelbick, G.; Schubert, U. *J. Organomet. Chem.,* **1999**, *573*, 47. (c) Bachert, I.; Bartussek, I.; Braunstein, P.; Guillon, E.; Rose J. ; Kickelbick, G. *J. Organomet. Chem.,* **1999**, *580*, 257. (d) Gaw, K. G.; Smith, M. B.; Steed, J. W. *J. Organomet. Chem.,* **2002**, *664*, 294.

12. Fei, Z.; Scopelliti, R.; Dyson, P. J. *Dalton trans.,* **2003**, 2772.

13. Balakrishna, M. S.; Reddy, V. S.; Krishnamurthy, S. S.; Nixon, J. F.; Burckett St. Laurent, J. C. T. R.; *Coord. Chem. Rev.*, **1994**, *129*, 1.

14. (a) Biricik, N.; Durap, F.; Kayan, C.; Gümgüma, B.; Gürbüz, N.; Özdemir, I.; Ang, W. H.; Fei, Z; Scopelliti, R., *J. Organomet. Chem.*, **2008**, *693*, 2693. (b) Aydemir, M.; Baysal, A.; Gümgüm, B., *J. Organomet. Chem.*, **2008**, *693*, 3810. (b) Kayan,C.; Biricik, N.; Aydemir, M., *Transition Met Chem.*, **2011**, *36*, 513. (c) Gholivand, K.; Kahnouji, M.; Latifi, R.; Fadaei, F. T.; Gholami, A.; Schenk, K. J., *Inorg. Chim. Acta*, **2016**, *448*, 61.

15. (a) Mao, G.; Ning, Y.; Hu, W.; Li, S.; Song, X.; Niu, B.; Jiang, T., *Chin. Sci. Bull.* **2008**, *53*, 3511. (b) Song, K.; Gao, H.; Liu, F.; Pan, J.; Guo, L.; Zai, S.; Wu, Q., *Eur. J. Inorg. Chem.* **2009**, 3016. (c) Sa, S.; Lee, S. M.; Kim, S. Y., *J. Mol. Catal. A: Chem.* **2013**, *378*, 17.

16. Braunstein, P.; Naud, F. *Angew. Chem. Int. Ed.*, **2001**, *40*, 680.

17. Braunstein, P. *J. Organomet. Chem.*, **2004**, *689*, 3953.

18. Sushev, V. V.; Belina, N. V.; Fukin, G. K.; Kurskiy, Y. A.; Kornev, A. N.; Abakumov, G. A., *Inorg. Chem.* **2008**, *47*, 2608.

19. (a) Kornev, A. N.; Belina, N. V.; Sushev, V. V.; Panova, J. S.; Lukoyanova, O. V.; Ketkov, S. Y.; Fukin, G. K.; Lopatin, M. A.; Abakumov, G. A., *Inorg. Chem.* **2010**, *49*, 9677. (b) Panova, Y. S.; Kornev, A. N.; Sushchev, V. V.; Cherkasov, A. V.; Abakumov, G. A., *Dokl. Chem.* **2012**, *445*, 159.

20. (a) Fei, Z.; Scopelliti, R.; Dyson, P. J., *Dalton Trans.* **2003**, 2772. (b) Fei, Z.; Ang, W. H.; Zhao, D.; Scopelliti, R.; Dyson, P. J., *Inorg. Chim. Acta,* **2006** *359*, 2635.

21. Zhang, Q.; Hua, G.; Bhattacharyya, P.; Slawin, A. M. Z.; Woollins, J. D., *Dalton Trans.* **2003**, 3250.

22. (a) Biricik, N.; Fei, Z.; Scopelliti, R.; Dyson, P. J., *Helv. Chim. Acta* **2003**, *86*, 3281. (b) Biricik, N.; Fei, Z.; Scopelliti, R.; Dyson, P. J., *Eur. J. Inorg. Chem.* **2004**, 4232.

23. (a) Fei, Z.; Biricik, N.; Zhao, D.; Scopelliti, R.; Dyson, P. J., *Inorg. Chem.* **2004**, *43*, 2228. (b) Fei, Z.; Pa˘unescu, E.; Ang, W. H.; Scopelliti, R.; Dyson, P. J., *Eur. J. Inorg. Chem.* **2014**, 1745.

24. Suttil, J. A.; Wasserscheid, P.; McGuinness, D. S.; Gardiner, M. G.; Evans, S. J., *Catal. Sci. Technol.* **2014**, *4*, 2574.

25. Suttil, J. A.; McGuinness, D. S.; Pichler, M.; Gardiner, M. G.; Morgan, D. H.; Evans, S. J., *Dalton Trans.*, **2012**, *41*, 6625.

26. Weng, Z.; Teo, S.; Hor, T. S. A., *Dalton Trans.* **2007**, 3493.

27. (a) Ghisolfi, A.; Fliedel, C.; Rosa, V.; Pattacini, R.; Thibon, A.; Monakhov, K. Yu.; Braunstein, P., *Chem. - Asian J.* **2013**, *8*, 1795. (b) Ghisolfi, A.; Fliedel, C.; Rosa, V.; Monakhov, K. Yu.; Braunstein, P., *Organometallics,* **2014**, *33*, 2523.

28. Boulens, P.; Lutz, M.; Jeanneau, E.; Olivier-Bourbigou, H.; Reek, J. N. H.; Breuil, P.-A. R., *Eur. J. Inorg. Chem.* **2014**, *2014*, 3754.

29. (a) Gaw, K. G.; Smith, M. B.; Steed, J. W. *J. Organomet. Chem.* **2002**, *664*, 294. (b) Rodriguez-Zubiri, M.; Gallo, V.; Rosé, J.; Welter, R.; Braunstein, P., *Chem. Commun.* **2008**, 64.

30. (a) Ellermann, J.; Wend, W., *Z. Anorg. Allg. Chem.* **1986**, *543*, 169. (b) Ellermann, J.; Utz, J.; Knoch, F. A.; Moll, M., *Z. Anorg. Allg. Chem.* **1996**, *622*, 1871.

31. Aladzheva, I. M.; Lobanov, D. I.; Bykhovskaya, O. g. V.; Petrovskii, P. V.; Lyssenko, K. A.; Mastryukova, T. A. *Heteroat. Chem.* **2003**, *14*, 596.

32. Cheung, H. W.; So, C. M.; Pun, K. H.; Zhou, Z.; Lau, C. P., *Adv. Synth. Catal.* **2011**, *353*, 411.

33. Fliedel, C.; Pattacini, R.; Braunstein, P., *J Clust Sci.*, **2010**, *21*, 397.

34. Jiang, T.; Chen, H.; Cao, C.; Mao, G.; Ning, Y., *Chin. Sci. Bull.* **2010**, *55*, 3750.

35. (a) Posset, T.; Rominger, F.; Blümel, J., *Chem. Mater.* **2005**, *17*, 586. (b) Braunstein, P.; Kormann, H.-P.; Meyer-Zaika, W.; Pugin, R.; Schmid, G. *Chem. - Eur. J.* **2000**, *6*, 4637. (c) Blann, K.; Bollmann, A.; de Bod, H.; Dixon, J. T.; Killian, E.; Nongodlwana, P.; Maumela, M. C.; Maumela, H.; McConnell, A. E.; Morgan, D. H.; Overett, M. J.; Prétorius, M.; Kuhlmann, S.; Wasserscheid, P., *J. Catal.* **2007**, *249*, 244.

36. Schmidbaur, H.; Wagner, F. E.; Wohlleben-Hammer, A., *Chem. Ber.* **1979**, *112*, 496.

37. (a) Gümgüm, B.; Akba, O.; Durap, F.; Yıldırım, L. T.; Ülkü, D.; Özkar, S., *Polyhedron,* **2006**, *25*, 3133. (b) Jiang, T.; Tao, Y.; Gao, X.; Mao, G.; Chen, H.; Cao, C.; Ning, Y., *Chin. Sci. Bull.* **2012**, *57*, 1510.

38. (a) Xu, H.; Chen, R.; Sun, Q.; Lai, W.; Su, Q.; Huang, W.;Liu, X., *Chem. Soc. Rev.*, **2014**, *43*, 3259. (b) Volz, D.; Baumann, T.; Wallesch, M.; Bräse, S., *SPIE Newsroom*, 10.1117/2.1201409.005617, 2. (c) Liu, Z.; Qayyum, M. F.; Wu, C.; Whited, M. T.; Djurovich, P. I.; Hodgson, K. O.; Hedman, B.; Solomon, E. I.; Thompson, M. E., *J. Am. Chem. Soc.* **2011**, *133*, 3700. (d) Ma, Y.; Che, C.-M.; Chao, H.-Y.; Zhou, X.; Chan, W.-H.; Shen, J., *Adv. Mater.* **1999**, *11*, 852. (e) Ma, Y; Zhou, X; Shen, J; Chao, HY; Che, CM., *Applied Physics Letters*, **1999**, *74*, 1361. (f) Au, V. K.-M.; Wong, K. M.-C.; Tsang, D. P.-K.; Chan, M.-Y.; Zhu, N.; Yam, V. W.-W., *J. Am. Chem. Soc.*, **2010**, *132*, 14273.

39. (a) Li, Z.; Brouwer, C.; He, C. *Chem. Rev.* **2008**, *108*, 3239. (b) Liu, X.-Y.; Li, C.-H.; Che, C.-M. *Org. Lett.* **2006**, *8*, 2707.

40. (a) Schmidbaur, H.; Schier, *Chem. Soc. Rev.* **2012**, *41*, 370. (b) Schmidbaur, H.; Schier, A. *Chem.Soc. Rev.* **2008**, *37*, 1931.

41. Yam, V.W.-W.; Cheng, E.C.-C., *Chem. Soc. Rev.*, **2008**, *37*, 1806.

42. Pal, S.; Kathewad, N.; Pant, R.; Khan, S., *Inorg. Chem.* **2015**, *54*, 10172.

43. Biricik, N.; Fei, Z.; Scopelliti, R.; Dyson, P. J. *Eur. J. Inorg. Chem.* **2004**, 2004, 4232.

44. Sarcher, C.; Lebedkin, S.; Kappes, M. M.; Fuhr, O.; Roesky, P. W., *J. Organomet. Chem.* **2014**, *751*, 343.

45. Yip, S.-K.; Lam, W. H.; Zhu, N.; Yam, V. W.-W., *Inorg. Chim. Acta* **2006**, *359*, 3639.

46. (a) Yam, V. W.-W.; Chan C.-L., Li, C.-K.; Wong, K. M.-C., *Coord. Chem. Rev.*, **2001**, 216–217, 173. (b) Yam, V. W.-W.; Chan C.-L., Li, C.-K.; Wong, K. M.-C, *J. Chem. Soc .Dalton Trans.*, **1996**, 4019.

47. Cheng, E. C.-C.; Lo, W.-Y.; Lee, T. K.-M.; Zhu, N.; Yam, V. W.-W., *Inorg. Chem.* **2014**, *53*, 3854.

48. Naik, S.; Mague, J. T.; Balakrishna, M. S., *Inorg. Chem.* **2014**, *53*, 3864.

49. Pal, S.; Kathewad, N.; Pant, R.; Khan, S., *Inorg. Chem.* **2015**, *54*, 10172.

50. (a) Alessio Ghisolfi, A.; Fliedel, C.; Frémontc P. de; Braunstein, P., *Dalton Trans.*, **2017**, *46*, 5571-5586 (b) Kathewad, N.; Kumar, N.; Dasgupta, R.; Ghosh, M.; Pal S.; Khan, S., *Dalton Trans.*, **2019**, Advance Article just accepted DOI: 10.1039/C8DT04471F

51. Reviews: (a) Skupińska, J., *Chem. Rev.* **1991**, *91*, 613. (b) Dixon, J. T.; Green, M. J.; Hess, F. M.; Morgan, D. H., *J. Organomet. Chem.* **2004**, *689*, 3641. (c) Agapie, T. *Coord. Chem. Rev*. **2011**, *255*, 86. (d) Wass, D., *Dalton Trans.* **2007**, 816. (e) McGuinness, D. S., *Chem. Rev.* **2011**, 111, 2321-2341.(f) van Leeuwen, P. W. N. M.; Clément, N. D.; Tschan, M. J. L., *Coord. Chem. Rev.* **2011**, *255*, 1499. (g) Small, B. L., *Acc. Chem. Res*. **2015**, *48*, 2599.

52. (a) Zhou, Y.; Wu, H.; Xu, S.; Zhang, X.; Shi, M.; Zhang, J., *Dalton Trans*. **2015**, *44*, 9545. (b) Radcliffe, J. E.; Batsanov, A. S.; Smith, D. M.; Scott, J. A.; Dyer, P. W.; Hanton, M. J. *ACS Catal*. **2015**, *5*, 7095. (c) Jeon, J. Y.; Park, D. S.; Lee, D. H.; Eo, S. C.; Park, S. Y.; Jeong, M. S.; Kang, Y. Y.; Lee, J.; Lee, B. Y., *Dalton Trans.* **2015**, *44*, 11004. (d) Härzschel, S.; Kühn, F. E.; Wöhl, A.; Müller, W.; Al-Hazmi, M. H.; Alqahtani, A. M.; Müller, B. H.; Peulecke, N.; Rosenthal, U., *Catal. Sci. Technol*. **2015**, *5*, 1678. (e) Wang, T.; Gao, X.; Shi, P.; Pei, H.; Jiang, T., *Appl. Petrochem. Res.* **2015**, *5*, 143.

53. Nifant'ev, I. E.; Vinogradov, A. A.; Vinogradov, A. A.; Roznyatovsky, V. A.; Grishin, Y. K.; Ivanyuk, A. V.; Sedov, I. V.; Churakov, A. V.; Ivchenko, P. V., *Organometallics* **2018**, *37*, 2660-2664.

54. (a) Jiang, T.; Chen, H.; Ning, Y.; Chen, W., *Chin. Sci. Bull.* **2006**, *51*, 521. (b) Zhang, B.; Wang, Y.; Jiang, T.; Xing, L. *Chin. J. Catal.* **2006**, *27*, 416.

55. Elowe, P. R.; McCann, C.; Pringle, P. G.; Spitzmesser, S. K.; Bercaw, J. E., *Organometallics*, **2006**, *25*, 5255.

56. Majoumo-Mbe, F.; Lonnecke, P.; Novikova, E. V.; Belov, G. P.; Hey-Hawkins, E. *Dalton Trans.* **2005**, 3326.

57. (a) Marion, N.; Nolan, S. P., *Acc. Chem. Res.* **2008**, *41*, 1440. (b) Fliedel, C.; Braunstein, P., *J. Organomet. Chem.* **2014**, *751*, 286.

58. Gildner, P. G.; Colacot, T. J., *Organometallics* **2015**, *34*, 5497.

59. Biricik, N.; Kayan, C.; Gümgüm, B.; Fei, Z.; Scopelliti, R.; Dyson, P. J.; Gürbüz, N.; Özdemir, İ., *Inorg. Chim. Acta* **2010**, *363*, 1039.

60. Kayan, C.; Biricik, N.; Aydemir, M.; Scopelliti, R., *Inorg. Chim. Acta.* **2012**, *385*, 164.

61. Aydemir, M.; Baysal, A.; Sahin, E.; Gumguma, B.; Ozkar, S., *Inorg. Chim. Acta* **2011**, 378, 10.

62. Schweyer-Tihay, F.; Braunstein, P.; Estournès, C.; Guille, J. L.; Lebeau, B.; Paillaud, J.-L.; Richard-Plouet, M.; Rosé, *Chem. Mater*. **2003**, *15*, 57.

63. Zhang, L.; Wang, C.; Zhou, L.; Li, P.; Zhang, X.; Wang, L. *Sci. China: Chem*. **2011**, *54*, 74.

64. Stamatopoulos, I; Roulia, M.; Vallianatou, K. A.; Raptopoulou, C. P.; Psycharis, V.; Carravetta, M.; Papachristodoulou, C.; Hey-Hawkins, E.; Kostas, I. D.; Kyritsis, P., *Chemistry Select* **2017**, *2*, 12051‑12059.

Chapter 2

Synthesis and Characterization of Diphosphinoamine Gold (I) Complexes

2.1. Introduction

Aurophilic interaction, a noncovalent interaction between the two closed-shell Au atoms, has become the subject of intense current research. Such interaction between the two Au atoms often led to remarkable photo-physical properties displayed by a majority of multinuclear gold complexes and thereby reckoned as potential candidates for sensors and optical devices.[1–3] Aurophilic interaction ranges roughly from 2.5 to 3.5 Å and was thereby exploited as a tool for the synthesis of a number of unusual multinuclear gold complexes, which exhibit intriguing electronic absorption and luminescence properties.[4,5] Many gold(I) complexes are found to be luminescent at room temperature in the solution state, and some of them are emissive in the solid state. The luminescent properties of these complexes heavily rely on the nature and distance of Au⋯Au centers. Recent years have witnessed interesting developments starting from solvoluminescence to on-off switching of luminescence arising from the switching of intra- to intermolecular Au⋯Au interactions (Chart 1).[6] These Au(I) based luminescent materials, especially the blue luminescent materials, can be of great use for the development of certain organic light-emitting diodes.[7] To date, various P-, N-, S-, and C-based fully supported, semi-supported, and unsupported gold(I) systems have been used to study the luminescence properties.[1–4,6] In order to explore the influence of intramolecular aurophilic interaction on the color of the luminescence properties, we synthesized substituted diphosphinoamine ligand based Au(I) complexes (**2.6**-**2.13**), where these ligands are having different electron donating and withdrawing groups on the N-aromatic backbone, like $C_6H_5N(PPh_2)_2$ (**2.1**), $2,6\text{-}Me_2C_6H_3N(PPh_2)_2$ (**2.2**), $(2,6\text{-}iPr_2C_6H_3N)(PPh_2)_2$ (**2.3**), $4\text{-}FC_6H_4N(PPh_2)_2$ (**2.4**) and $4\text{-}OMeC_6H_4N(PPh_2)_2$ (**2.5**). In this chapter we have synthesized neutral and cationic Au(I) complexes such as $[ClAu(C_6H_5N)(PPh_2)_2]_2$ (**2.6**), $[Au(C_6H_5N)(PPh_2)_2]_2[SbF_6]_2$ (**2.7**), $[ClAu(2,6\text{-}Me_2C_6H_3N)(PPh_2)_2]$ (**2.8**), $[Au(2,6\text{-}Me_2C_6H_3N)(PPh_2)_2]_2[SbF_6]_2$ (**2.9**), $[AuCl\{(2,6\text{-}iPr_2C_6H_3N)(PPh_2)_2\}]$ (**2.10**), $[Au(2,6\text{-}iPr_2C_6H_3N)(PPh_2)_2]_2[SbF_6]_2$ (**2.11**) $[Au(4\text{-}FC_6H_4N)(PPh_2)_2]_2[SbF_6]_2$ (**2.12**) and $[Au(4\text{-}OMeC_6H_3N)(PPh_2)_2]_2[SbF_6]_2$ (**2.13**).

2.2. Experimental Section

2.2.1. General Remarks

All manipulations were performed under a dry and oxygen-free atmosphere (N_2) using standard Schlenk techniques and a glove box. All solvents were dried over activated molecular sieves after distillation. All the chemicals are purchased from Sigma Aldrich and alpha aesar. ^1H, ^{13}C, ^{31}P, and ^{19}F solution NMR spectra were recorded on a Jeol 400 and Bruker 400 MHz spectrometer.

2.2.2. Synthesis of *2.6-2.13*

Compound 2.6

A total of 20 mL of CH_2Cl_2 was added to the flask containing **2.1** [$C_6H_5N(PPh_2)_2$] (0.49 gm, 1 mmol) and [AuCl (Me$_2$S)] (0.294 gm, 1 mmol), and the solution was kept for overnight stirring. The reaction mixture become yellow, then filtered off and evaporated one third and 1:1 mixture of n-Pentane was added. Storing the solution at 0° C afford yellow crystals of **2.6** [$ClAu(C_6H_5N)(PPh_2)_2$]$_2$. Yield: 0.95 g (69.85 %); ^1H NMR (CDCl$_3$, 400 MHz, ppm): δ 7.31-7.34 (m, 22H, Ph), 7.44-7.48 (m, 13H, Ph), 7.53 (br, 15H, Ph) ; $^{31}P\{^1H\}$ NMR (CDCl$_3$, 161.976 MHz, ppm): δ 87.63 (s) ppm; $^{13}C\{^1H\}$ NMR (CDCl$_3$, 100.613 MHz, ppm): δ 129.06 (Ph), 129.36 (Ph), 130.82 (Ph), 131.74 (Ph), 132 (Ph), 132.68 (Ph), 132.98 (Ph), 134.08 (Ph) ppm; MS (ESI+). Calcd for $C_{60}H_{50}Au_2N_2P_4Cl_2$: m/z 1386.16. Found: m/z 1351.19 (M$^+$-Cl). Elemental analysis (%) calcd. C 51.93, H 3.63, N 2.02. Found. C 52.54, H 4.13, N 1.92.

Compound 2.7

A total of 20 mL of CH_2Cl_2 was added to the flask containing compound **2.6** [$ClAu(C_6H_5N)(PPh_2)_2$]$_2$ (0.693 gm, 0.5 mmol) and AgSbF$_6$ (0.172 gm, 0.5 mmol), and the solution was kept for overnight stirring. The reaction mixture become colourless, then filtered off and evaporated one third and 1:1 mixture of n-Pentane was added. Storing the solution at 0° C afford colourless crystals of **2.7** [$Au(C_6H_5N)(PPh_2)_2$]$_2$[SbF$_6$]$_2$. Yield: 0.7 g (78.29 %); ^1H NMR (CDCl$_3$, 400 MHz, ppm): δ 7.10-7.13 (m, 7H, Ph), 7.18 (s, 2H, Ph), 7.31 (s, 6H, Ph) 7.41-7.51 (m, 25H, Ph), 7.61-7.66 (m, 10H, Ph); $^{31}P\{^1H\}$ NMR (CDCl$_3$, 161.976 MHz,

ppm): δ 100 (s) ppm; ^{13}C{^{1}H} NMR (CDCl$_3$, 100.613 MHz, ppm): δ 125.80 (Ph), 129.23 (Ph), 129.31 (Ph), 130.67 (Ph), 132.17 (Ph), 136.56 (Ph), 135.49 (Ph) ppm; ^{19}F NMR (CDCl$_3$, 376.498 MHz, ppm): δ 166.0 ppm (br); MS (ESI+). Calcd for C$_{60}$H$_{50}$Au$_2$N$_2$P$_4$: m/z 658.11. Found: m/z 658.14 (M$^+$). Elemental analysis (%) calcd. C 40.30, H 2.82, N 1.57. Found C 40.78, H 3.12, N 1.39.

Compound 2.8

A total of 20 mL of CH$_2$Cl$_2$ was added to the flask containing compound **2.2** [2,6-Me$_2$C$_6$H$_3$N(PPh$_2$)$_2$] (0.49 gm, 1 mmol) and [AuCl (Me$_2$S)] (0.294 gm, 1 mmol), and the solution was kept for overnight stirring. The reaction mixture become pale yellow, then filtered off and evaporated one third and 1:1 mixture of *n*-pentane was added. Storing the solution at 0º C afford colourless crystals of **2.8** [ClAu(2,6-Me$_2$C$_6$H$_3$N)(PPh$_2$)$_2$]. Yield: 0.64 g (88.76 %); ^{1}H NMR (CDCl$_3$, 400 MHz, ppm): δ 2.15 (s, 6H, C*H$_3$*), 6.78 (br, 2H, Ph), 7.04 (s, 2H, Ph), 7.37 (t, J = 7.6 Hz, 8H, Ph) 7.49-7.55 (m, 6H, Ph), 7.79-7.84 (m, 7H, Ph); ^{31}P{^{1}H} NMR (CDCl$_3$, 161.976 MHz, ppm): δ 65.05, 84.88 ppm; ^{13}C{^{1}H} NMR (CDCl$_3$, 100.613 MHz, ppm): δ 20.51 (*C*H$_3$), 20.90 (*C*H$_3$), 126.23 (Ph), 128.22 (Ph), 128.66 (Ph), 128.85 (Ph), 129.63 (Ph), 130.65 (Ph), 130.76 (Ph), 132.37 (Ph), 132.6 (Ph), 135.05 (Ph) ppm; MS (ESI+). Calcd for C$_{32}$H$_{29}$AuClNP$_2$: m/z 723.11. Found: m/z 688.24 (M+-Cl); Elemental analysis (%) calcd. C 53.24, H 4.05, N 1.94. Found (%) C 52.90, H 4.02, N 1.85.

Compound 2.9

A total of 20 mL of CH$_2$Cl$_2$ was added to the flask containing compound **2.8** [ClAu(2,6-Me$_2$C$_6$H$_3$N)(PPh$_2$)$_2$] (0.537 gm, 0.74 mmol) and AgSbF$_6$ (0.128 gm, 0.74 mmol), and the solution was kept for overnight stirring. The reaction mixture become colourless, then filtered off and evaporated one third and 1:1 mixture of *n*-Pentane was added. Storing the solution at 0º C afford colourless crystals of **2.9** [Au(2,6-Me$_2$C$_6$H$_3$N)(PPh$_2$)$_2$]$_2$[SbF$_6$]$_2$. Yield: 0.92 g (67.64 %); ^{1}H NMR (CDCl$_3$, 400 MHz, ppm): δ 2.19 (s, 12H, CH$_3$), 7.10-7.13 (m, 7H, Ph), 7.18 (s, 2H, Ph), 7.31 (s, 6H, Ph) 7.41-7.51 (m, 25H, Ph), 7.61-7.66 (m, 10H, Ph); ^{31}P{^{1}H} NMR (CDCl$_3$, 161.976 MHz, ppm): δ 79.3 (s); ^{13}C{^{1}H} NMR (CDCl$_3$, 100.613 MHz, ppm): δ 21.53 (*C*H$_3$), 125.80 (Ph), 129.23 (Ph), 129.31 (Ph), 130.67 (Ph), 132.17 (Ph), 136.56 (Ph), 135.49 (Ph); ^{19}F NMR (CDCl$_3$, 376.498 MHz, ppm): δ 166.0 (br); MS (ESI+). Calcd for C$_{60}$H$_{50}$Au$_2$N$_2$P$_4$:

m/z 686.14. Found: m/z 686.14 (M^{2+}); Elemental analysis (%) calcd. C 56.29, H 4.36, N 2.02. Found (%) C 55.96, H 4.07, N 1.98.

Compound 2.10

A total of 20 mL of CH_2Cl_2 was added to the flask containing compound **2.3** [(2,6-iPr$_2$C$_6$H$_3$N)(PPh$_2$)$_2$] (0.272 g, 0.5 mmol) and [AuCl(Me$_2$S)] (0.197g, 0.5 mmol), and the solution was left stirring overnight. The solution became colorless from pale yellow, and then the solvent was evaporated under reduced pressure. The complex was extracted with CH_2Cl_2 and filtered off. The solvent was concentrated to one-third, and 5 mL of *n*-pentane was added. Storing the solution at 0°C afforded colorless crystals of **2.10** [AuCl{(2,6-iPr$_2$C$_6$H$_3$N)(PPh$_2$)$_2$}]. Yield: 0.304 g (78.5%). ^{1}H NMR (CD$_2$Cl$_2$, 400 MHz, ppm): δ 1.09-1.11 (d, 12H, J = 6.8 Hz, (C*H$_3$*)$_2$CH), 3.08-3.14 (m, 1H, (CH$_3$)$_2$C*H*), 7.06−7.84 (m, 23H, *Ph*). ^{31}P{^{1}H} NMR (CD$_2$Cl$_2$, 161.976 MHz, ppm): δ 20.09, 67.67. ^{13}C{^{1}H} NMR (CD$_2$Cl$_2$, 100.613 MHz, ppm): δ 23.97 (*C*H$_3$), 25.61 (*C*H$_3$), 122.62 (Ph), 123.56 (Ph), 127.79 (Ph), 128.43 (Ph), 128.87 (Ph), 129.16 (Ph) , 130.61 (Ph), 131.78 (Ph); MS (ESI+). Calcd for C$_{36}$H$_{37}$AuNP$_2$Cl: m/z 777.18. Found: m/z 775.39 [M]$^+$; Elemental analysis (%) calcd. C 41.68, H 3.17, N 1.52. Found (%) C 41.5, H 2.96, N 1.08.

Compound 2.11

CH_2Cl_2 (20 mL) was added to a mixture of compound **2.10** [AuCl{(2,6-iPr$_2$C$_6$H$_3$N)(PPh$_2$)$_2$}] (0.56 g, 0.7 mmol) and AgSbF$_6$ (0.24 g, 0.7 mmol) and stirred overnight. The solvent was evacuated under reduced pressure, and the residue was extracted with CH_2Cl_2 and filtered off. The solvent was concentrated to one-third, and 5 mL of n-pentane was added. Storing at 0 °C affords colorless crystals of **2.11** [Au(2,6-iPr$_2$C$_6$H$_3$N)(PPh$_2$)$_2$]$_2$[SbF$_6$]$_2$. Yield: 0.43 g (62%). ^{1}H NMR (CD$_2$Cl$_2$, 400 MHz, ppm): δ −0.05 to −0.07 (d, 24H, J = 6.5 Hz, (C*H$_3$*)$_2$CH), 2.64 (m, 4H, C*H*(CH$_3$)$_2$), 6.99 (d, 4H, J = 7.8 Hz, *Ph*), 7.33-7.40 (m, 18H, *Ph*), 7.58-7.63 (m, 24H, Ph). ^{31}P{^{1}H} NMR (CD$_2$Cl$_2$, 161.976 MHz, ppm): 100. ^{19}F NMR (CD$_2$Cl$_2$, 376.498 MHz, ppm): δ 150.85 (br). ^{13}C{^{1}H} NMR (CD$_2$Cl$_2$, 100.613 MHz, ppm): δ 23.54 (*C*H$_3$), 30.80 [*C*H(CH$_3$)$_2$], 126.99 (Ph), 129.93 (Ph), 130.89 (Ph), 134.68 (Ph), 135.23 (Ph), 148.87 (Ph); MS (ESI+). Calcd for [C$_{72}$H$_{74}$Au$_2$N$_2$P$_4$]$^{2+}$ (1484.41): m/z 742.20. Found: m/z 742.20[M]$^{2+}$. Elemental Analysis (%): calcd. C 58.48; H 5.11; N 1.87; P 8.26. Found C 58.02; H 5.10; N 1.80

Compound 2.12

CH_2Cl_2 (20 mL) was added to a mixture of **2.4** $[(4\text{-}FC_6H_4N)(PPh_2)_2]$ (0.48 g, 1 mmol), $Au(SMe_2)Cl$ (0.294 g, 1 mmol) and $AgSbF_6$ (0.324 g, 1 mmol) and stirred overnight. The solvent was evacuated under reduced pressure, and the residue was extracted with CH_2Cl_2 and filtered off. The solvent was concentrated to one-third, and 5 mL of *n*-pentane was added. Storing at 0 °C affords colorless crystals of **2.12** $[Au(4\text{-}FC_6H_4N)(PPh_2)_2]_2[SbF_6]_2$. Yield: 0.43 g (62%). ^{1}H NMR (CD_3CN, 400 MHz, ppm): δ 6.99 (m, 4H, Ph), 7.33-7.40 (m, 20H, Ph), 7.58–7.63 (m, 24H, Ph). ^{31}P{^{1}H} NMR (CD_3CN, 161.976 MHz, ppm): 99.67. ^{19}F NMR (CD_3CN, 376.498 MHz, ppm): δ -111.83 (s), 165.42 (br). ^{13}C{^{1}H} NMR (CD_3CN, 100.613 MHz, ppm): δ 133.96 (Ph), 130.14-129.27 (Ph), 117.26 (Ph); MS (ESI+). Calcd for $[C_{60}H_{48}Au_2N_2P_4F]^{2+}$: m/z 676.10. Found: m/z 676.10 $[M]^{2+}$. Elemental Analysis (%): Calcd. C 53.60; H 3.69; N 2.05. Found C 53.80; H 3.50; N, 2.01

Compound 2.13

CH_2Cl_2 (20 mL) was added to a mixture of **2.5** $[(4\text{-}OMeC_6H_3N)(PPh_2)_2]$ (0.48 g, 1 mmol), $Au(SMe_2)Cl$ (0.294 g, 1 mmol) and $AgSbF_6$ (0.324 g, 1 mmol) and stirred overnight. The solvent was evacuated under reduced pressure, and the residue was extracted with CH_2Cl_2 and filtered off. The solvent was concentrated to one-third, and 5 mL of n-pentane was added. Storing at 0 °C affords colorless crystals of **2.13** $[Au(4\text{-}OMeC_6H_3N)(PPh_2)_2]_2[SbF_6]_2$. Yield: 0.43 g (62%). ^{1}H NMR (DMSO-d_6, 400 MHz, ppm): δ 3.73 (s, 3H, CH_3), 6.01-6.31 (m, 4H, Ph), 7.01-7.58 (m, 50H, Ph); ^{31}P{^{1}H} NMR (DMSO-d_6, 161.976 MHz, ppm): 100. ^{19}F NMR (DMSO-d_6, 376.498 MHz, ppm): δ -102 to -132.44 (m). ^{13}C{^{1}H} NMR (DMSO-d_6, 100.613 MHz, ppm): δ 55.76 (OCH$_3$), 115.55 (Ph), 125.00 (Ph), 129.92 (Ph), 134.48 (Ph), 156.84 (Ph), 163.46 (Ph); MS (ESI+). Calcd for $[C_{61}H_{54}Au_2N_2P_4O]^{2+}$ (1846.41): m/z 688.12. Found: m/z 688.12 $[M]^{2+}$. Elemental Analysis (%): Calcd. C 54.40; H 4.06; N 2.01; O, 2.30. Found C 54.49; H 3.95; N 2.20; O, 2.35.

2.2.3. X-ray crystallographic Details

Crystallography reflections were collected on a Bruker Smart Apex Duo diffractometer at 150 K using Mo Kα radiation (λ = 0.71073 Å). The structures of **2.6-2.13** were solved by direct methods and refined by full-matrix least-squares methods against F2 (SHELXL-2014/6).[7]

2.3. Result and Discussion

Complexation of **2.1**, **2.2**, **2.3**, **2.4** and **2.5** with 1 equivalent of AuCl·Me$_2$S in DCM followed by addition of silver hexafluoroantimonate (AgSbF$_6$) led to the formation of mononuclear and dinuclear Au(I) complexes **2.6-2.13**, respectively (Scheme 2.1). The ^{31}P NMR of neutral dinuclear Au(I) **2.6** shows a single peak at δ 87.63 ppm, while mononuclear Au(I) compound **2.8** and **2.10** exhibits two peaks, for 2.8 at δ 84.78 and 64.94 and for 2.10 δ 20.09 and 67.67 which reflects the presence of two chemically non-equivalent phosphorus atoms. The formation of cationic complexes were accompanied by the shift in the ^{31}P NMR spectrum of **2.7** (δ 100.24 ppm), **2.9** (δ 78.81ppm), **2.11** (100 ppm), **2.12** (99.76 ppm) and **2.13** (100.24 ppm) which are in good agreement with previously reported cationic Au(I) complexes, such as [Au(2,6-iPr$_2$C$_6$H$_3$N)(PPh$_2$)$_2$]$_2$[SbF$_6$]$_2$ (δ 100 ppm),[11] [(Au)$_2$(dmbpaip)][ClO$_4$]$_2$ (δ 97.9 ppm).[12] The appearance of only one signal in the ^{31}P NMR of **2.7**, **2.8**, **2.9**, **2.11**, **2.12** and **2.13** indicates the presence of only one type of phosphorus atom in them. The single crystals suitable for X-ray diffraction studies for **2.6-2.13** were grown in DCM/n-pentane (1:1) mixture. Compound **2.6**, **2.8** and **2.10** crystallizes in P-1, P-1, and C2/c respectively. The molecular structure of **2.6** reveals a dinuclear trans-annular architecture with two tri-coordinated Au(I) atoms (Figure 2.1). The distance between the two Au(I) centers (3.0067(3) Å) is within the range of effective aurophilic interaction. Compound **2.6** shows the dimeric framework with Au···Au distance of 3.0056 (4) *Å*, which falls within the aurophilic interaction range (2.5 to 3.5 Å)*.* The P-Au-P bond angle (141.41(2)º) in **2.6** is deviating significantly from linearity and gives a slightly bent conformation to the structure.
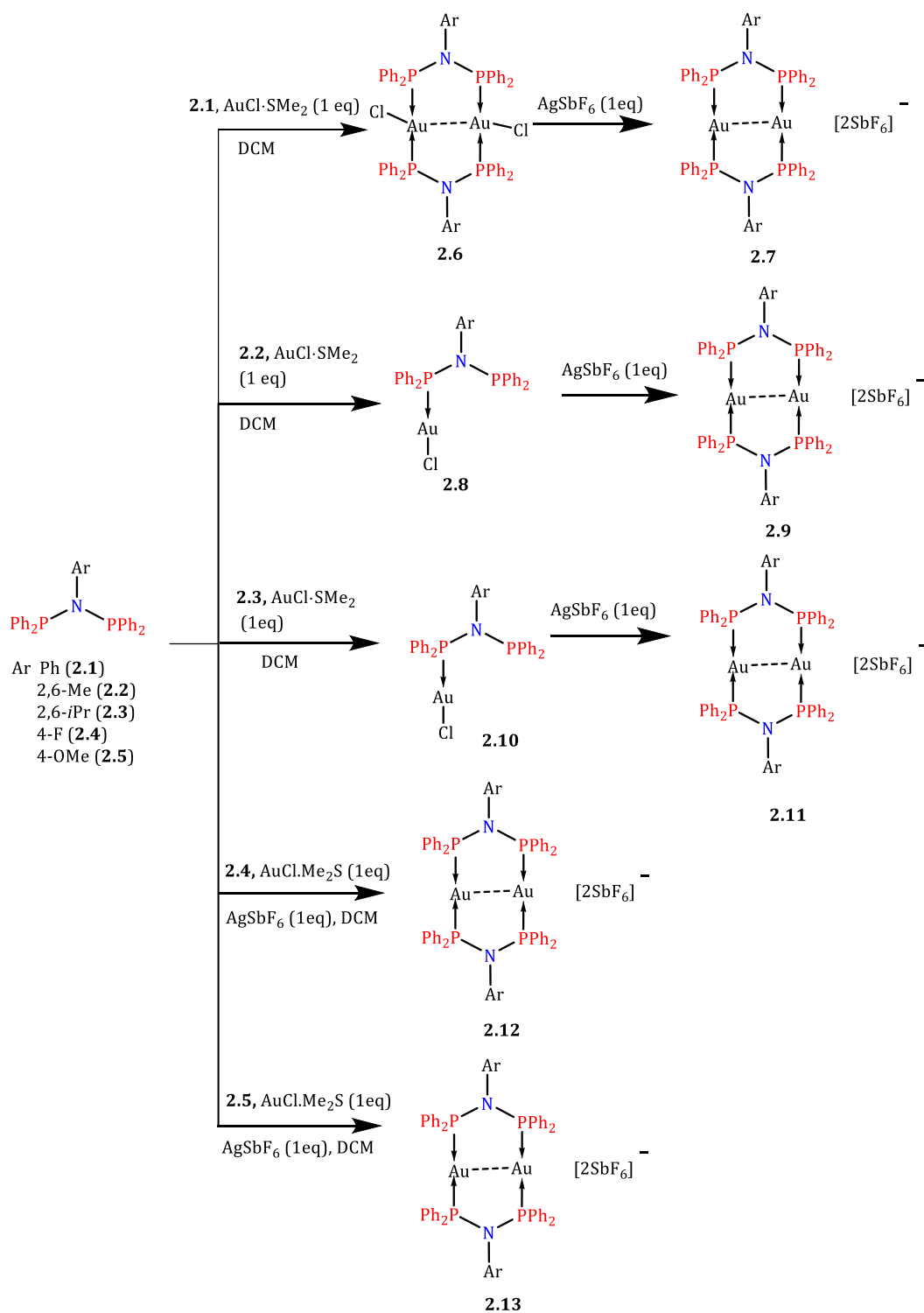
Scheme 2.1. *Synthesis of neutral (**2.6**, **2.8** and **2.10**) and cationic (**2.7**, **2.9**, **2.11**, **2.12** and **2.13**), Au(I) complexes.*

The molecular structures of **2.8** and **2.10** reveal a mononuclear complex with only one phosphorus atom coordinating to the Au center (P→Au 2.234 (1) Å) while the other phosphorus atom remains non-coordinated which is closely matching with the literature i.e. [(AuCl)₂Ph₂PN(p-BrC₆H₄)PPh₂] [Au–P = 2.233(2) Å and P–Au–Cl = 177.99(7)°] and [(AuCl)₂(dmbpaip)] [Au–P = 2.227(2) Å and P–Au–Cl = 174.07(10)°], respectively.[2-4,11,12,14]
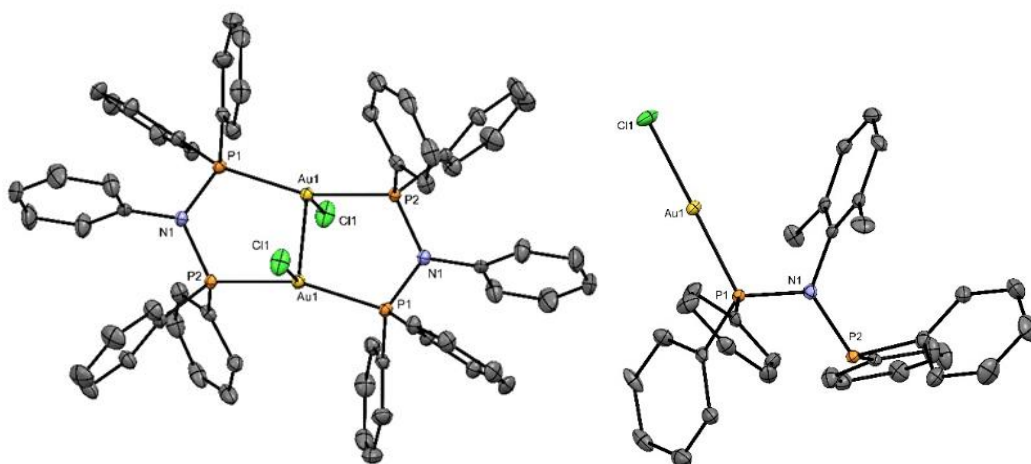
Figure 2.1*. Molecular structures of **2.6** (left) and **2.8** (right) with anisotropic displacement parameters depicted at the 50% probability level. Hydrogen atoms are omitted for clarity. Selected bond lengths (Å) for **2.6**: Au1-Au1 3.0056 (4), Au1-Cl 2.589 (1), P1-Au1 2.3062 (8), P2-Au1 2.3396 (7), P1-N1 1.708 (3), P2-N1 1.713 (3), bond angles (°) for **2.6**: P2-Au1-P1 141.39 (3), Cl1-Au1-Au1 123.84 (2), P1-Au1-Cl1 114.33 (3), P2-Au1-Cl1 102.43 (3).; Selected bond lengths (Å) for **2.8**: Au1-Cl1 2.278 (1), P1-Au1 2.234 (1), P1-N1 1.692 (4), P2-N1 1.748 (4), bond angles (°) for **2.8**: Cl1-Au1-P1 178.06 (4)*

There is no Au⋯Au interaction present in the crystal structure of **2.6** and **2.10**. This could be due to the presence of methyl and isopropyl groups on ortho-positions in ligand **2.2** and **2.3** rendering adequate electron density required to attenuate the dimerization. The linear geometry of the Au(I) center in **2.6** and **2.10** is confirmed by P-Au-Cl bond angle of 178.06(3)° and 175.57(4)° respectively, matching well with the previously reported Au(I) complexes.[11,13-19] Complexes **2.7** and **2.9** crystallize in *Pca21* and *P21/n* space group respectively, revealing a dinuclear dimeric framework

for both **2.7** and **2.9**. Molecular structures of **2.7** and **2.9** show dinuclear [Au(C$_6$H$_5$N)(PPh$_2$)$_2$]$_2^{2+}$ and [Au(2,6-Me$_2$C$_6$H$_3$N)(PPh$_2$)$_2$]$_2^{2+}$ cations with two non-coordinated SbF$_6^-$ anions. The most significant feature of **2.7** and **2.9** is the presence of strong intra-molecular aurophilic interaction with the Au···Au bond distances of 2.7988(4) Å and 2.8292(7) Å, respectively. The intramolecular Au···Au distances in **2.7** and **2.9** found to be shorter than those found in analogous Au(I) complexes reported previously for N, S-bridged Au$_2$ systems: 2.8797(4) Å in [Au$_2$(μ-TU)(μ-dppm)](CF$_3$CO$_2$), and 2.8617(7) and 2.8864 (6) Å in [Au$_2$(μ-Me-TU)(μ-dppm)](CF$_3$CO$_2$) and also the Au···Au distance in metallic gold (2.889(1) Å).[15]

Table 2.1 *^{31}P NMR data and Au-Au distance in Au(I) complexes 2.6, 2.7, 2.9, 2.11, 2.12 and 2.13.*

Compound	Ligand	^{31}P NMR (ppm)	^{31}P NMR of ligand (ppm)	Au-Au distance (Å)
2.6	**2.1**	87.63	70	3.00
2.7	**2.1**	100.24		2.79
2.8	**2.2**	84.78, 64.94	56	-
2.9	**2.2**	78.81		2.83
2.10	**2.3**	20.09, 67.67	-6.4	-
2.11	**2.3**	100		2.80
2.12	**2.4**	99.76	71	2.78
2.13	**2.5**	100.24	72	2.79

The P-Au-P bond angles in **2.7** (170.92(7)° and 173.26(7)°) deviate slightly from the linearity. **2.9** displays a significant deviation from the linearity in P-Au-P bond angle (164.61(3)°). The P→Au bonds for complexes **2.7** and **2.9** are slightly elongated [for **2.7**: 2.313 (2) and 2.308(2) Å; for **2.9**: 2.3183 (9) and 2.3202 (9) Å] than the P→Au bonds present in **2.6** and **2.8** [**2.6**: 2.3062 (8) and 2.3396 (7) Å; **2.8**: 2.234 Å].

The solid-state structure of **2.11** crystallized in *P21/n*, revealed formation of the anticipated [Au(2,6-*i*Pr$_2$C$_6$H$_3$N)(PPh$_2$)$_2$]$_2^{2+}$ along with two non-coordinated SbF$_6^-$ anions in the framework (Figure 2.3). The molecular structure of **2.11** discloses the presence of C$_2$ symmetry in the molecule. However, the most significant feature is the

Au···Au interaction of 2.7944(19) Å. The Au(1)···Au(2) distance falls within the range of aurophilic interaction, and to the best of our knowledge, this is one of the shortest distances (e.g., 2.798,[14] 2.858,[16] 2.862,[16] and 2.799 Å[17]) known for such aurophilic interactions.[15,16] The coordination geometry at the Au(I) atoms is distorted from linearity with P1−Au1−P1 bond angle of 170.9(2)° like [(Au)$_2$(dmbpaip)][ClO$_4$]$_2$ [P1−Au1−P2 169.0(2)°].[12] The backbone of **2.11** contains an eight-membered ring, bridging by an Au···Au interaction, and is folded by 57.14° with respect to the Au···Au axis (taking P1 → Au1···Au1 ← P1 into the account; Figure 2b). All four P → Au bond distances [Au1−P1 2.330(5) Å] are identical and in good agreement with the literature values.[12,14,15,16]
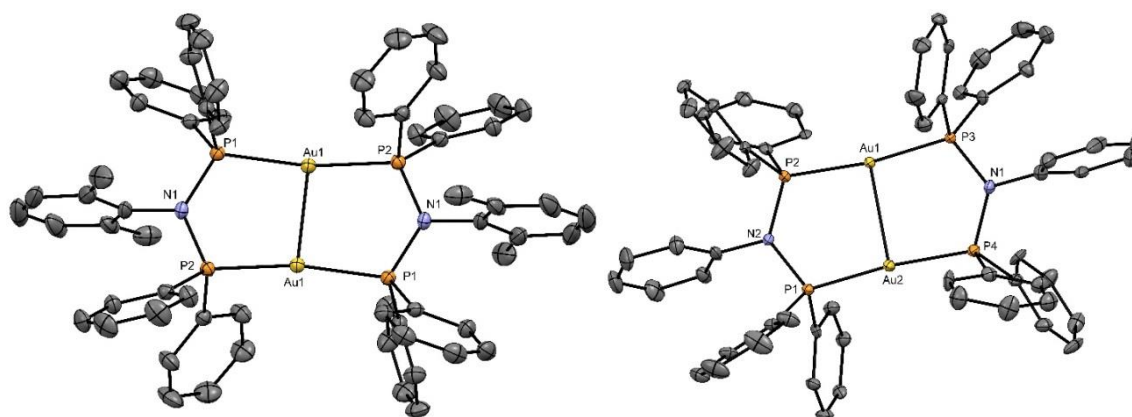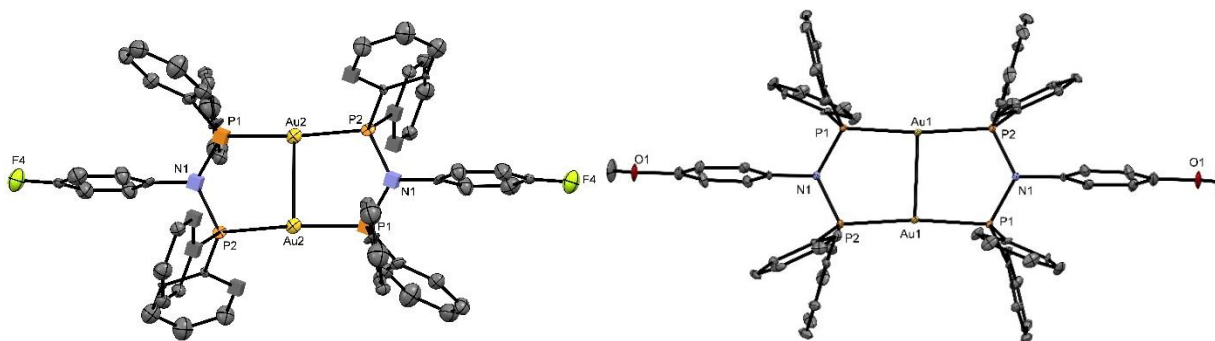

Figure 2.2. *Molecular structures of **2.7** (left) and **2.9** (right) with anisotropic displacement parameters depicted at the 50 % probability level. Hydrogen atoms and SbF$_6^-$ anion are not shown for clarity. Selected bond lengths (Å) for **2.7**: Au1-Au2 2.7987 (6), P1-Au2/P4-Au2 2.313 (2), P2-Au1/P3-Au1 2.308 (2), P1-N2 1.719 (7), P3-N1 1.700 (3), P2-N2 1.695 (6), P4-N1 1.705 (6), bond angles (°) for **2.7**: P1-Au2-P4 173.26 (7), P2-Au1-P3 170.92 (7) , P1-N2-P2 125.3 (4), P3-N1-P4 126.2 (4); Selected bond lengths (Å) for **2.9**: Au1-Au1 2.8293 (8), P1-Au1 2.317 (1), P2-Au1 2.3200 (9), P1-N1 1.715 (3), P2-N1 1.717 (3), bond angles (°) for **2.9**: P1-Au1-P2 164.61 (3), P1-N1-P2 124.4 (2).*
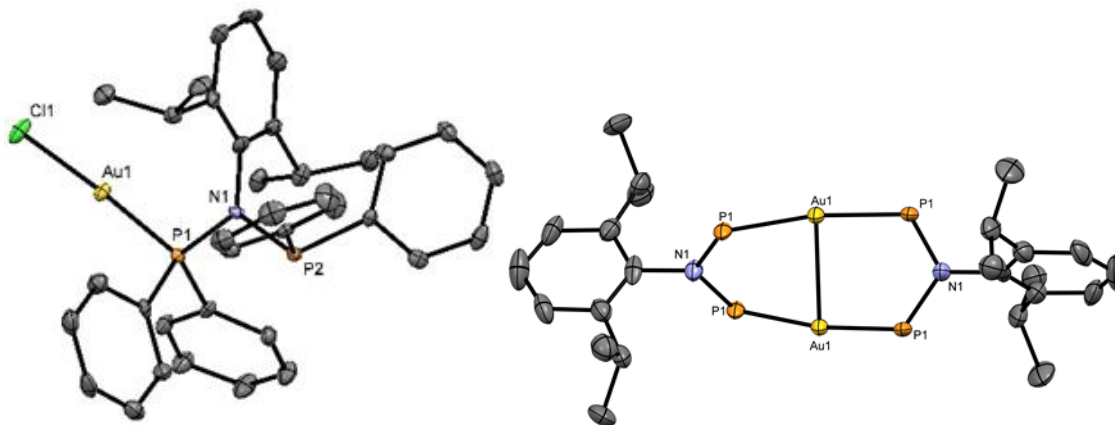
Figure 2.3 *Molecular structures of **2.10** (left) and **2.11** (right) with anisotropic displacement parameters depicted at the 50 % probability level. Hydrogen atoms and SbF_6^- anion are not shown for clarity. Selected bond lengths (Å) for **2.10**: Au1-Cl1 2.280 (12), P1-Au1 2.23134 (12), P1-N1 1.692 (4), P2-N1 1.748 (4), bond angles (º) for **2.10**: Cl1-Au1-P1 175.57 (4). bond lengths (Å) for **2.11** Au1-Au1 2.7944(19), P1-Au1 2.330, P1-N2 1.72, bond angles (º) for **2.11**: P1-Au1-P2 170.9, P1-N2-P2 119 (4).*

Figure 2.4 *Molecular structures of **2.12** (left) and **2.13** (right) with anisotropic displacement parameters depicted at the 30 % probability level. Hydrogen atoms and SbF_6^- anion are not shown for clarity. Selected bond lengths (Å) for **2.12**: Au1-Au2 2.783 (5), P1-Au2/P4-Au2 2.26 (2), P2-Au1/P3-Au1 2.28 (2), P1-N2 1.74 (4), P3-N1 1.69 (4); bond angles (º) for **2.12**: P1-Au2-P2 171.7 (5), P1-N2-P2 124 (2); Selected bond lengths (Å) for **2.13**: Au1-Au1 2.7927 (6), P1-Au1 2.301 (1), P2-Au1 2.299 (3), P1-N1 1.70 (1); bond angles (°) for **2.13**: P1-Au1-P2173.2 (1).*

Complexes **2.12** and **2.13** crystallize in *P-1* and *P21/n* space group respectively, and similar to that of compound **2.7**, **2.9** and **2.11** have a dimeric framework. Molecular structures of **2.12** and **2.13** show dinuclear $[Au(4-FC_6H_4N)(PPh_2)_2]_2^{2+}$ and $[Au(4-OMeC_6H_4N)(PPh_2)_2]_2^{2+}$ cations with each containing two non-coordinated SbF_6^- anions Strong intra-molecular aurophilic interaction is a significant feature of **2.12** and **2.13** where Au⋯Au distance is 2.783(5) Å and 2.7927(6) Å, respectively, shortest among all the above complexes. P-Au-P bond angle for both the compounds shows a slight deviation from linearity, [**2.12** (171.7°) and for **2.13** (173.2°)]

2.4 Conclusion

In conclusion, we synthesized differently N-functionalized DPPA ligand (**2.1**-**2.5**) supported Au(I) complexes. All the Au(I) complexes **2.6**-**2.13** characterized by X-Ray crystallographic studies and other routine techniques (NMR, Mass spectroscopy, etc). It was observed that compounds **2.6**, **2.7**, **2.9**, **2.11**, **2.12** and **2.13** show aurophilic interaction where Au⋯Au distance ranges from 2.794-3.005 Å. Compound **2.12** and **2.13** show short Au⋯Au distance of 2.794 and 2.783 Å among all other Au(I) complexes found in the literature.

2.5. References

(1) (a) Strasser, C. E.; Catalano, V. J. *J. Am. Chem. Soc.* **2010**, *132*, 10009. (b) Laguna, A.; Lasanta, T.; Lopez-de-Luzuriaga, J. M.; Monge, M.; Naumov, P.; Olmos, M. E. *J. Am. Chem. Soc.* **2010**, *132*, 456. (c) Fernández, E. J.; Lopez-de-Luzuriaga, J. M.; Monge, M.; Olmos, M. E.; Puelles, R. C.; Laguna, A.; Mohamed, A. A.; Fackler, J. P., Jr. *Inorg. Chem.* **2008**, *47*, 8069. (d) Sagara, Y.; Kato, T. *Nat. Chem.* **2009**, *1*, 605. (e) Au, V. K.-M.; Wong, K. M.-C.; Tsang, D. P.-K.; Chan, M.-Y.; Zhu, N.; Yam, V. W.-W. *J. Am. Chem. Soc.* **2010**, *132*, 14273. (f) Li, C.- K.; Lu, X.-X.; Wong, K. M.-C.; Chan, C.-L.; Zhu, N.; Yam, V. W.-W. *Inorg. Chem.* **2004**, *43*, 7421.

(2) Reviews and books: (a) Yam, V. W. W.; Chan, C.-L.; Li, C.-K.; Wong, K. M.-C. *Coord. Chem. Rev.* **2001**, *216*, 173. (b) Keefe, M. H.;Benkstein, K. D.; Hupp, J. T. *Coord. Chem. Rev.* **2000**,

205, 201. (c) Evans, R. C.; Douglas, P.; Winscom, C. J. *Coord. Chem. Rev.* **2006**, *250*, 2093. (d) He, X.; Yam, V. W.-W. *Coord. Chem. Rev.* **2011**, *255*, 2111. (e) Yam, V. W. W.; Cheng, E. C. C. *Chem. Soc. Rev.* **2008**, *37*, 1806. (f) Tiekink, E. R.T.; Kang, J.-G. *Coord. Chem. Rev.* **2009**, *253*, 1627. (g) López-de-Luzuriaga, J. M. *In Modern Supramolecular Gold Chemistry*; Laguna, A., Ed.; Wiley-VCH: Weinheim, Germany, 2008. (h) Katz, M. J.; Sakai, K.; Leznoff, D. B. *Chem. Soc. Rev.* **2008**, *37*, 1884. (i) Balch, A. L. *Angew. Chem., Int. Ed.* **2009**, *48*, 2641. (j) Yam, V. W.-W.; Cheng, E. C.-C. *Top. Curr. Chem.* **2007**, *281*, 269. (k) Gimeno, M. C.; Laguna, A. *Chem. Soc. Rev.* **2008**, *37*, 1952. (l) Fung, E. Y.; Olmstead, M. M.; Vickery, J. C.; Balch, A. L. *Coord. Chem. Rev.* **1998**, *171*, 151.

(3) For theoretical aspects, see: (a) Pyykkö, P. *Angew. Chem., Int. Ed*. **2004**, *43*, 4412. (b) Pyykkö, P. *Chem. Soc. Rev.* **2008**, *37*, 1967. (c) Pyykkö, P. *Chem. Rev.* **1997**, *97*, 597. (d) Pathaneni, S. S.; Desiraju, G. R. *J. Chem. Soc., Dalton Trans*. **1993**, 319. (e) Pyykkö, P.; Li, J.; Runeberg, N. *Chem. Phys. Lett.* **1994**, *218*, 133. (f) Pyykkö, P.; Zaleski- Ejgierd, P. *J. Chem. Phys.* **2008**, *128*, 124309. (g) Pyykkö, P.; Runeberg, N. *Angew. Chem., Int. Ed.* 2002, *41*, 2174. (h) Pyykkö, P. *Inorg. Chim. Acta* **2005**, *358*, 4113. (i) Fernández, E. J.; Laguna, A.; López-de-Luzuriaga, J. M.; Monge, M.; Montiel, M.; Olmos, M. E.; Rodríguez-Castillo, M. *Organometallics* **2006**, *25*, 3639. (j) Pyykkö, P. *Angew. Chem., Int. Ed*. **2002**, *41*, 3573. (k) Pyykkö, P. *Relativistic Theory of Atoms and Molecules;* Springer: Berlin, **2000**; Vol. III, p 108. (l) Schmidbaur, H.; Schier, *A. Chem. Soc. Rev.* **2008**, *37*, 1931.

(4) For selected reports on the correlation between the aurophilic interactions and emission properties of gold complexes, see: (a) Lu, W.; Zhu, N.; Che, C. M. *J. Am. Chem. Soc.* **2003**, *125*, 16081. (b) Rodríguez, L.; Ferrer, M.; Crehuet, R.; Anglada, J.; Lima, J. C. *Inorg. Chem.* **2012**, *51*, 7636. (c) Lim, S. H.; Schmitt, J. C.; Shearer, J.; Jia, J.; Olmstead, M. M.; Fettinger, J. C.; Balch, A. L. *Inorg. Chem.* **2013**, *52*, 823. (d) Lee, T. K.-M.; Zhu, N.; Yam, V.W.-W. *J. Am. Chem. Soc.* **2010**, *132*, 17646. (e) Saitoh, M.; Balch, A. L.; Yuasa, J.; Kawai, T. *Inorg. Chem.* **2010**, *49*, 7129. (f) Rios, D.; Pham, D. M.; Fettinger, J. C.; Olmstead, M. M.; Balch, A. L. *Inorg. Chem.* **2008**, *47*, 3442.

(5) White-Morris, R. L.; Olmstead, M. M.; Balch, A. L.. *Inorg. Chem.* **2003**, *42*, 6741.

(6) (a) Vickery, J. C.; Olmstead, M. M.; Fung, E. Y.; Balch, A. L. *Angew. Chem., Int. Ed. Engl.* **1997**, *36*, 1179. (b) Yam, V. W. W.; Li, C. K.; Chan, C. L. *Angew. Chem., Int. Ed.* **1998**, *37*, 2857. (c) White-Morris, R. L.; Olmstead, M. M.; Jiang, F.; Tinti, D. S.; Balch, A. L. *J. Am. Chem. Soc.*

2002, *124*, 2327. (d) Lee, A. Y.; Eisenberg, R. *J. Am. Chem. Soc.* **2003**, *125*, 7778. (e) Catalano, V. J.; Horner, S. J. *Inorg. Chem.* **2003**, *42*, 8430. (f) Mohamed, A. A.; Kani, I.; Ramirez, A. O.; Fackler, J. P., Jr. *Inorg. Chem.* **2004**, *43*, 3833. (g) Barnard, P. J.; Wedlock, L. E.; Baker, M. V.; Berners-Price, S. J.; Joyce, D. A.; Skelton, B. W.; Steer, J. H. *Angew. Chem., Int. Ed.* **2006**, *45*, 5966. (h) Ito, H.; Saito, T.; Oshima, N.; Kitamura, N.; Ishizaka, S.; Hinatsu, Y.; Wakeshima, M.; Kato, M.; Tsuge, K.; Sawamura, M. *J. Am. Chem. Soc.* **2008**, *130*, 10044. (i) Han, S.; Yoon, Y. Y.; Jung, O.-S.; Lee, Y.-A *Chem. Commun.* **2011**, *47*, 10689. (j) Liang, J.; Chen, Z.; Yin, J.; Yu, G.-Ao; Liu, S. H. *Chem. Commun.* **2013**, *49*, 3567. (k) Lim, S. H.; Schmitt, J. C.; Shearer, J.; Jia, J.; Olmstead, M. M.; Fettinger, J. C.; Balch, A. L. *Inorg. Chem.* **2013**, *52*, 823. (l) Seki, T.; Sakurada, K.; Muromoto, M.; Ito, H. *Chem. Sci.* **2015**, *6*, 1491.

(7) Wen, S.-W.; Lee, M.-T.; Chen, C. H. *J. Disp. Technol.* **2005**, *1*, 90.

(8) Kottke, T.; Stalke, D. J. *Appl. Crystallogr.* **1993**, *26*, 615. (b) Stalke, D. J. *Chem. Soc. Rev.* **1998**, *27*, 171. (c) Sheldrick, G. M. *Acta Crystallogr., Sect. A: Found. Crystallogr.* **2008**, *64*, 112. (d) Schulz, T.; Meindl, K.; Leusser, D.; Stern, D.; Graf, J.; Michaelsen, C.; Ruf, M.; Sheldrick, G. M.; Stalke, D. J. *Appl. Crystallogr.* **2009**, *42*, 885.

(9) Frisch, M. J. *Gaussian 09, Revision D.01*, Gaussian, Inc., Wallingford, CT, **2009**.

(10)   (a) Becke, A. D. *Journal of Chemical Physics* **1993**, *98*, 5648. (b) Lee, C.; Yang, W.; Parr, R. G. *Phys. Rev. B* **1988**, *37*, 785. (c) Hay, P. J.; Wadt, W. R. *Journal of Chemical Physics* **1985**, *82*, 270. (d) Hay, P. J.; Wadt, W. R. *Journal of Chemical Physics* **1985**, *82*, 299.

(11)   Pal, S.; Kathewad, N.; Pant, R.; Khan, S. *Inorg. Chem.*, **2015**, *54*, 10172.

(12)   Fliedel, C.; Pattacini, R.; Braunstein, P. *J. Cluster Sci.*, **2010**, *21*, 397.

(13)   Schmidbaur, H.; Wohlleben, A.; Schubert, U.; Frank, A.; Huttner, G. *Chem. Ber.*, **1977**, *110*, 2751.

(14)   Wiedemann, D.; Gamer, M. T.; Roesky, P. W. *Z. Anorg. Allg. Chem.* **2009**, *635*, 125.

(15)   Deaìk, A.; Megyes, T.; Taìrkaìnyi, G.; Kiraìly, P.; Biczoìk, L.; Paìlinkaìs G. and Stang, P. J. *J. Am. Chem. Soc.*, **2006**, *128*, 12668.

(16)   Tunyogi, T.; Deaìk, A.; Taìrkaìnyi, G.; Kiraìly, P.; Paìlinkaìs, G. *Inorg. Chem.*, **2008**, *47*, 2049.

(17)   Vicente, J.; Chicote, M. T.; Gonzalez- Herrero, P.; Jones, P. G. *J. Chem. Soc., Chem. Commun.*, **1995**, 745.

(18)   Schmidbaur, H.; Schier, A. *Chem. Soc. Rev.*, **2012**, *41*, 370.

(19)   Balch, A. L. *Gold Bull.* **2004**, *37*, 45.

Chapter 3

Photophysical and Theoretical Studies of Diphosphinoamine Gold (I) Complexes

3.1 Introduction

The study of photo physical property e. g. photoluminescence, chemiluminescence, thermoluminescence, electroluminiscence etc. of luminescent materials has been attracted lot of attention[1] in the last few decades for their potential use in light-emitting[2] diodes, chemosensing,[3] thermoluminescence dating etc.[4] Among the coinage metal (d^{10} system) complexes, gold (I) complexes have been well documented for their luminescence property.[5] As it has been discussed in the previous chapter, the short Au⋯Au distance which is known as Aurophilic interaction originate as a result of the relativistic effects and correlation effects, is solely responsible for luminescent behaviour of gold(I) complexes.[6] The Au(I), being a soft center, have a strong affinity towards phosphorus and therefore a large number of P→Au luminescent complexes have been reported till date utilizing the diphosphine or aminodiphosphine ligands.[7] It was observed that gold complexes show photoluminescence properties and they are luminescent at room temperature in solid as well as solution state. Some of the gold (I) complexes are found highly emissive in solid state and have high quantum yields, e.g. $[Au_2(dcpm)_2](ClO_4)_2$ (0.37), $[Au_2(dcpm)_2](PF_6)_2$ (0.74), $[Au_2(dcpm)_2](SO_3CF_3)_2$ (0.53), $[Au_2(dcpm)_2][Au(CN)_2]_2$ (0.12). Since compounds with Au(I) centres have Au⋯Au interaction which display luminescent behaviour are well documented. So we thought to study differently functionalized DPPA supported Au(I) complexes for their photophysical properties. We utilized complexes **2.6**-**2.13** (prepared in Chapter 2) for further photophysical studies. Among them, mononuclear Au(I) complexes **2.8** and **2.10** were found to be non-luminescent due to absence of Au⋯Au interaction. However, rest of the Au(I) complexes display emission properties in the solid state. **2.7** displays a remarkably high quantum yield of 0.59 with a decay lifetime of 50 ns. Other complexes **2.6**, **2.7**, **2.9**, **2.11** **2.12** and **2.13** also shows luminescence. Our results are reported herein. It was observed that aurophilic interaction also plays an important role, which is discussed in section 3.2.3

3.2 Result and Discussion

3.2.1. General Remarks

UV-visible absorption spectra were recorded using a Perkin-Elmer UV- visible spectrometer. Steady-state PL and PL decay dynamics (time-correlated single photon counting) were measured using a Horiba Jobin-Yvon Fluorolog 3 spectrometer and FLS 980 instrument (Edinburg Instruments).

3.2.2. Photophysical Studies of 2.6, 2.7, 2.9, 2.11, 2.12 and 2.13

Since compound **2.6**, **2.7, 2.9, 2.11, 2.12** and **2.13** possess strong Au···Au interactions, we probed them further for their photo-physical properties. Interestingly all of these complexes were found to display emission, under UV-light in the solid state (Figure 3.1) and in good agreement with the CIE plots, but weakly emissive in solution state. On account of having no aurophilic interaction, **2.8** and **2.10** do not show photoluminescence either in solid or in solution state. Among these luminescent complexes, **2.9** shows a significant quantum yield of 60%. All these complexes show a variety of colour of emission, e.g., **2.6**, **2.7**, **2.9**, **2.11**, **2.12** and **2.13** show yellow, lilac, cyan blue, blue, greenish-yellow and yellowish-orange respectively. It is interesting to observe that by changing the substituent on DPPA ligand from electron-donating (-Me, -ipr, -OMe) to electron-withdrawing (-F) the colour of emission can be tuned. This might be helpful in developing fluorescent compound of choice of colour.

The absorption and emission spectra for all the luminescent complexes is recorded in solid state and are shown in Figure 3.1 and 3.2. **2.6** exhibits absorption bands around 224 nm, 280-290 nm, and 390-450 nm. The absorption band around 224 and 280-290 nm corresponds to the intra-ligand transitions (ILCT),[1-6] while the low energy absorption maximum band in the range of 390-450 nm can be tentatively assigned as a mixture of ^{1}XLCT and ^{1}MLCT charge transfer transitions,[7,8] which also supported by theoretical calculation. Compounds **2.7**, **2.9**, **2.11**, **2.12** and **2.13** display very similar pattern of absorption with high energy and low energy band.

Table 3.1 *Photo physical data of 2.6, 2.7, 2.9, 2.11, 2.12 and 2.13 with their respective Au···Au distances*

Compound	2.6	2.7	2.9	2.11	2.12	2.13
Au-Au distance	3.00	2.79	2.83	2.80	2.78	2.79
Absorbance wavelength (nm)	224, 280, 415	273, 319, 365	260, 315, 347	275, 330	270, 327, 345	260, 300, 328
Excitation wavelength (nm)	400	365	383	330	327	300
Emission wavelength (nm)	520, 625	425	422, 497	417	420, 520	591
Lifetime (µs)	0.169	0.050	0.050	0.049	701	11
Quantum yield (ϕ) (%)	20.83	59	37	15 (CH$_2$Cl$_2$)	-	-

Compound **2.7** and **2.9** three bands, one band ranging from 250-300 nm, the second band around 322 nm and third low energy band around 370-380 nm. Absorption peaks observed in the range of 225-280 nm can be attributed to the intra-ligand charge transfer (ILCT) transitions involving the aromatic backbone of the DPPA ligand, whereas the low energy peaks can be assigned for the mixture of ligand to metal charge transfer (P→Au) (LMCT) and intra-ligand charge transfer (ILCT) transitions perturbed by intra-molecular Au···Au interactions.[1-6] The absorption spectrum of **2.11** shows similar pattern to that of the compound **2.7** and **2.9.** The spectral features for the gold complexes **2.11** include an absorption band around 260-280 nm which is related to the aromatic rings of the phosphine ligands and a low-energy band at 330 nm, which is tentatively related to the mixture of ligand-to-metal charge-transfer (LMCT) and intraligand charge-transfer (ILCT) transitions.[1-6]

UV-visible absorption spectra of Au(I) cationic compound **2.12** and **2.13** display the similar kind of pattern for absorption peaks as that of other Au(I) cationic complexes.

Steady state measurement of yellow luminescent compound **2.6** in the solid state at room temperature shows a peak at 520 nm and a broad shoulder ranging from 630-660 nm on excitation at 400 nm (Figure 3.2) with large Stoke shift (120 nm) and long lifetime of 169 *ns*. Cationic complexes **2.7** and **2.9** show a sharp, intense peak at 425 and 422 nm which shows lilac and cyan blue colour of fluorescence under UV light respectively. Compound **2.9** show one more additional less intense low energy peak at 497 nm on excitation at 322 nm.
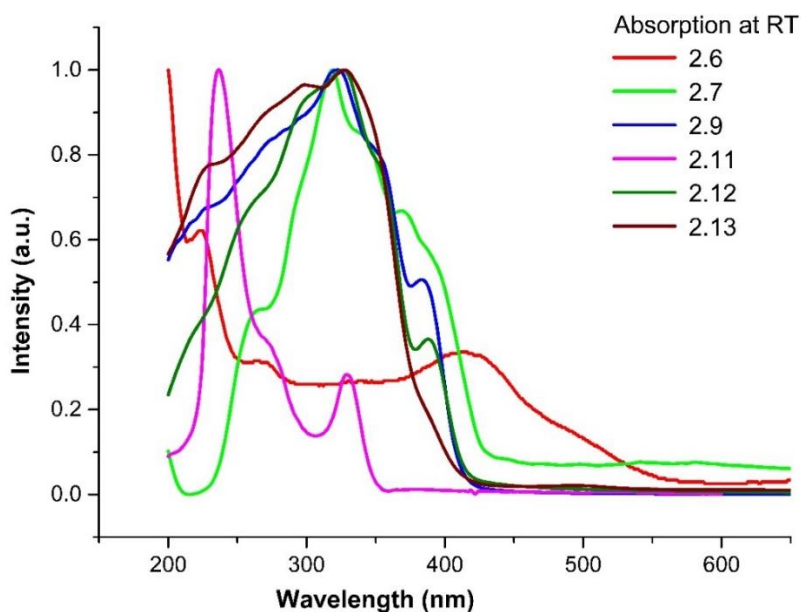
Figure 3.1 *UV-Visible spectra of **2.6**, **2.7**, **2.9**, **2.11**, **2.12** and **2.13***

The lifetime values of **2.7** (201 *ns*) and **2.9** (49.3 *ns*) indicate the fluorescent nature of emission.[1,12-18] The most remarkable feature of compound **2.6**, **2.7** and **2.9** is their high quantum yields (ϕ) [0.21 (**2.6**), 0.59 (**2.7**) and 0.37 (**2.9**)], and value of quantum yield for **2.7** i.e. 0.59 is the second largest one compared to the literature {$[Au_2(dcpm)_2](ClO_4)_2$ (0.37), $[Au_2(dcpm)_2](PF_6)_2$ (0.74), $[Au_2(dcpm)_2](SO_3CF_3)_2$ (0.53), $[Au_2(dcpm)_2][Au(CN)_2]_2$ (0.12)}.[9-11]

Blue luminescence was observed from colorless crystals of **2.11** under irradiation of UV light. The emission spectrum of **2.11** is recorded in solid as well as solution state

display the appearance of a band at 417 nm on excitation at 330 nm. This complex exhibits quantum yield of 0.15 in solution state (DCM).

Table 3.2 Photophysical data for reported luminescent Au(I) complexes of same type.

Compound	Emission (nm)		Quantum yield	
	Solid (nm)	Solution (nm)	Solution	solid
$[Au_2(dcpm)_2]Cl_2$ [16,18c]	366, 505	513	0.065 ± 0.002	0.23
$[Au_2(dcpm)_2][(ClO_4)_2]$ [16,18c]	368, 564 (w)	370, 510 (CH_3CN)	0.048 ± 0.007	0.37
$[Au_2(dcpm)_2][PF_6]$ [16,18c]	368, 505 (w)	370, 490 (CH_3CN)	0.025 ± 0.001	0.74
$[Au_2(dcpm)_2][(SO_3CF_3)_2]$ [16,18c]	368	370, 500 (CH_3CN)	0.027 ± 0.002	0.53
$[Au_2(dcpm)_2]I_2$ [16,18c]	473, 486	530 (CH_3CN)	0.085 ± 0.002	0.17
$[Au_2(dcpm)_2][Au(CN)_2]_2$ [16,18c]	368	370, 495 (CH_3CN)	0.013 ± 0.001	0.12
$[Au_2(dcpm)_2][SCN]$ [18c]	465	-	-	0.09

The short luminescence lifetimes (*Table 3.1*) and the relatively small Stokes shift between the absorption and emission bands suggest that the emission is fluorescent between singlet states. Compound **2.12** which displays intense greenish-yellow emission under a UV lamp, shows emission maximum at 420 and 520 nm on excitation at 327 nm, with a longer lifetime of 700 μs. Longer lifetime and stock shift of around 90 nm indicate that it might be a phosphorescence. Whereas compound **2.13** displays an emission maximum at 591 nm, and have longer decay lifetime of 11μs. Longer lifetime of **2.13** indicates it might be phosphorescence or delayed fluorescence. Similar kind of systems from the literature found to have higher lifetimes and are phosphorescent, [12-18] while some of our systems (**2.6**, **2.12** and **2.13**) also have longer decay lifetime and might have phosphorescence (Table 3.1). This observation of change in emission properties by changing substituents on ligand backbone reveals

that Au···Au interaction is sensitive to the subtle change in ligand fragment and can be tuned to get the desired colour of emission.
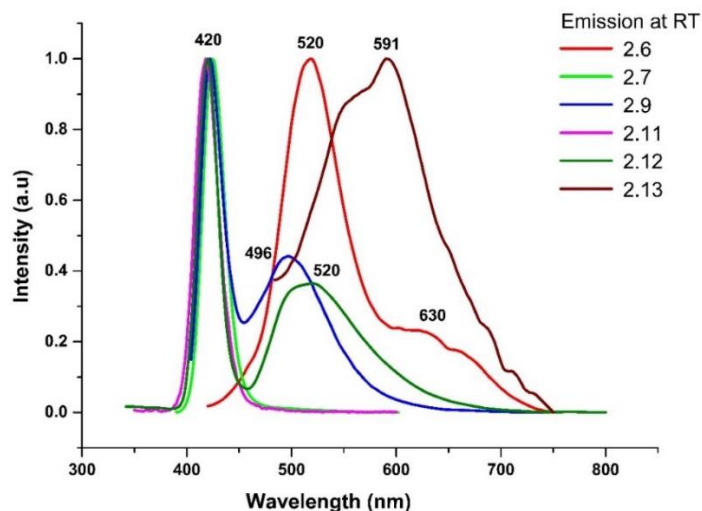
*Figure 3.1 Emission spectra of **2.6**, **2.7**, **2.9**, **2.11**, **2.12** and **2.13***

*3.2.3.   Theoretical investigation of **2.6, 2.7, 2.9, 2.11-2.13***
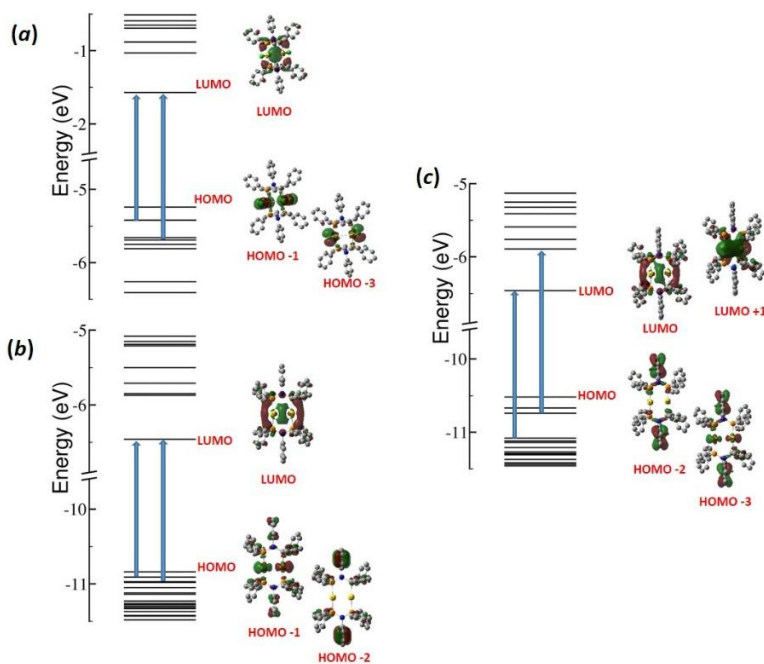
*Figure 3.3. Molecular orbitals of complexes (a) **2.6**; (b) **2.7**; (c) **2.9***

LUMO   LUMO +4   LUMO   LUMO   LUMO

HOMO -3   HOMO -3   HOMO   HOMO -1   HOMO -16

(a)   *(b)*

LUMO   LUMO +2   LUMO +4

HOMO -2   HOMO -9   HOMO -7   HOMO -2
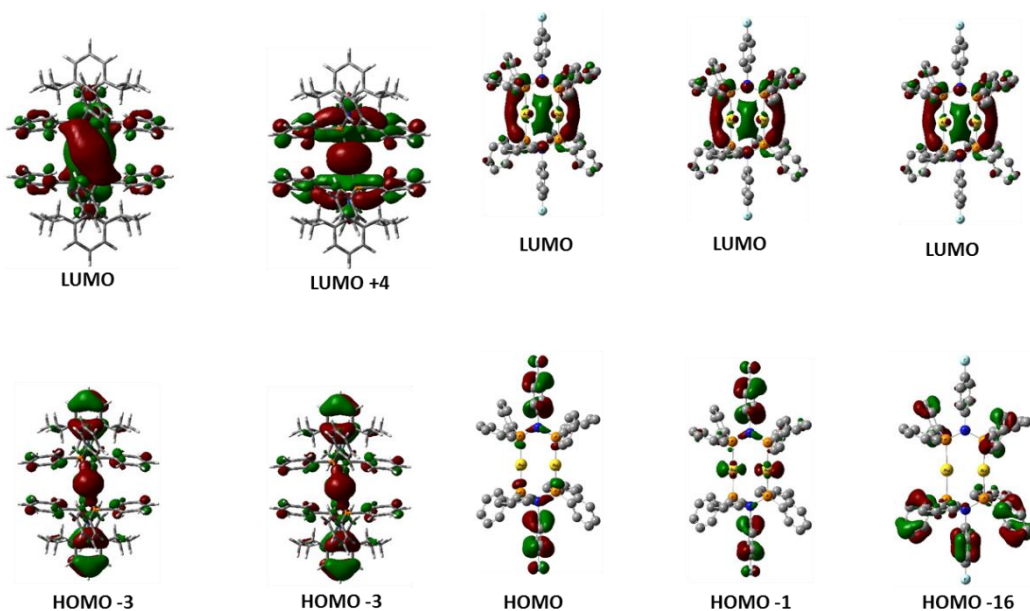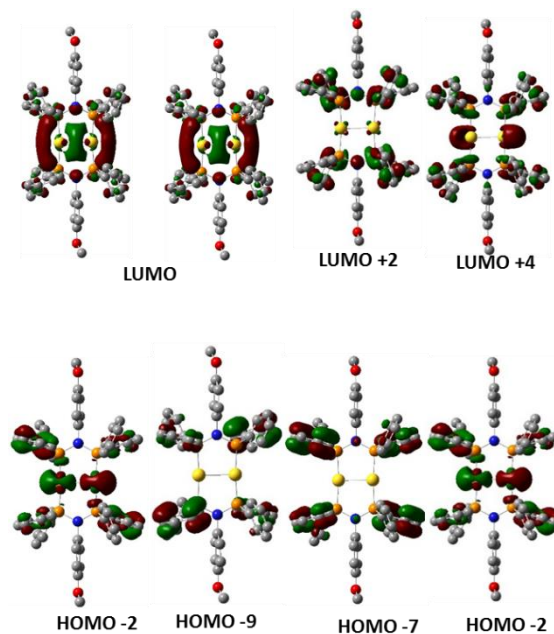
(c)

Figure 3.4*. Molecular orbitals of complexes (a)* ***2.11****; (b)* ***2.12****; (c)* ***2.13***

To understand the origin of the observed photo-physical properties of **2.6**, **2.7**, **2.9**, **2.11**, **2.12** and **2.13** TD-DFT calculations were performed (see Appendix section for details).[19-23]

Computed values of bond distances are in fair agreement with a slight over estimation to the experimentally measured values. The simplified MO diagrams corresponding to the optimized structures of **2.6, 2.7, 2.9, 2.11, 2.12** and **2.13** are shown in *Figure 3.3* and *3.4.* A detailed analysis of the frontier molecular orbitals reveals that the HOMOs of compound **2.6** are mainly composed of *d*-orbitals of metal and *p*-orbitals of chloride, while the LUMO is spread over the cluster core with small contribution coming from the ligand orbitals. The high energy orbitals (from LUMO+1 to LUMO+4) are mainly localized on the DPPA ligand (Figure 3.3a). Molecular orbitals of **2**, **4**, **6**, **7** and **8** show a similar kind of transition pattern. The HOMOs of **2.7**, **2.9**, **2.11**, **2.12** and **2.13** are mainly located on the phenyl rings of the ligand, while most of the LUMOs are located on the cluster core. The energy separation between the HOMO and LUMO orbitals of **2.6** (3.67 eV) is relatively smaller than the complexes **2.7** (4.38 eV), **2.9** (4.06 eV), **2.11** (3.03 eV), **2.12** (4.26 eV) and **2.13** (4.06 eV).

Moreover, the smaller gap of **2.6** can be attributed to the observed low energy emission as compared to **2.7**, **2.9**, **2.11**, **2.12** and **2.13**. The computed lowest energy electronic transitions are in accordance with the HOMO-LUMO gaps. Further analyses of the orbitals involved in the lowest energy transitions suggest that the peak around 410 nm for **2.6** is primarily due to a mixture of ^{1}XLCT and ^{1}MLCT charge transfer transitions which correspond to HOMO→LUMO. In contrast to **2.6** The low energy peak at 322 nm for **2.7** corresponds to HOMO-1→LUMO, peak at 328 nm for **2.9** corresponds to HOMO→LUMO. Similar to **2.7** and **2.9** results were obtained for **2.11**-**2.13**. HOMO's are localized on the ligands and LUMO present on metal centres. Peak 330 nm for **2.11** corresponds to HOMO-1→LUMO, peak at 325 nm for **2.12** corresponds to HOMO-1→LUMO and peak at 329 nm for **2.13** corresponds to HOMO-2→LUMO are primarily from the ^{1}LMCT.

3.3   Conclusion

In summary we have studied the photophysical properties of DPPA supported Au(I) complexes (**2.6-2.13**). Complexes **2.6**, **2.7**, **2.9**, **2.11**, **2.12** and **2.13** are emissive and show

yellow, lilac, cyan blue, blue, greenish yellow and orangish yellow emission respectively when exposed to UV light. Mononuclear Au(I) complexes **2.8** and **2.10** are non-luminescent, which could be attributed to the absence of aurophilic interaction, in their crystal packing. It is observed that subtle change of substituent leads to the different colour of emission which could be very useful in designing new luminescent material of selective colour.

3.4 References

1. (a) Tang, C. W.; Slyke, S. A. V. *Appl. Phys. Lett.*, **1987**, *51*, 913. (b) Baldo, M. A.; O'Brien, D. F.; You, Y.; Shoustikov, A.; Sibley, S.; Thompson, M. E.; Forrest, S. R. *Nature*, **1998**, *395*, 151. (c) Tang, C. W. *Appl. Phys. Lett.*, **1986**, *48*, 183. (d) Shirk, J. S.; Lindle, J. R.; Bartoli, F. J.; Boyle, M. E. *J. Phys. Chem.,* **1992**, *96*, 5847. (e) Reineke, S.; Lindner, F.; Schwartz, G.; Seidler, N.; Walzer, K.; Lussem , B.; Leo, K. *Nature*, **2009**, *459*, 234. (f) McCarthy, M. A.; Liu, B.; Donoghue, E. P.; Kravchenko, I.; Kim, D. Y.; So, F.; Rinzler, A. G. *Science*, **2011**, *332*, 570. (g) Liu, Q.; Yang, T.; Feng, W.; Li, F. *J. Am. Chem. Soc.,* **2012**, *134*, 5390.

2. Xu, H.; Chen, R.; Sun, Q.; Lai, W.; Su, Q.; Huang, W. ; Liu, X. *Chem. Soc. Rev.*, **2014**, *43*, 3259.

3. He, X.; Yam, V. W.-W. *Coord. Chem. Rev.* **2011**, *255*, 2111.

4. (a) Murthy, K.V.R. *Defect and Diffusion Forum* **2014***, 347,* 35. (b) Omanwar, S. K.; Koparkar, K. A.; Virk, H.S. *Defect and Diffusion Forum* **2014***, 347,* 75.

5. (a) Strasser, C. E.; Catalano, V. J. *J. Am. Chem. Soc.* **2010**, *132*, 10009. (b) Laguna, A.; Lasanta, T.; Lopez-de-Luzuriaga, J. M.; Monge, M.; Naumov, P.; Olmos, M. E. *J. Am. Chem. Soc.* **2010**, *132*, 456. (c) Fernández, E. J.; Lopez-de-Luzuriaga, J. M.; Monge, M.; Olmos, M. E.; Puelles, R. C.; Laguna, A.; Mohamed, A. A.; Fackler, J. P., Jr. *Inorg. Chem.* **2008**, *47*, 8069. (d) Sagara, Y.; Kato, T. *Nat. Chem.* **2009**, *1*, 605. (e) Au, V. K.-M.; Wong, K. M.-C.; Tsang, D. P.-K.; Chan, M.-Y.; Zhu, N.; Yam, V. W.-W. *J. Am. Chem. Soc.* **2010**, *132*, 14273. (f) Li, C.- K.; Lu, X.-X.; Wong, K. M.-C.; Chan, C.-L.; Zhu, N.; Yam, V. W.-W. *Inorg. Chem.* **2004**, *43*, 7421.

6. (a) Lu, W.; Zhu, N.; Che, C. M. *J. Am. Chem. Soc.* **2003**, *125*, 16081. (b) Rodríguez, L.; Ferrer, M.; Crehuet, R.; Anglada, J.; Lima, J. C. *Inorg. Chem.* **2012**, *51*, 7636. (c) Lim, S. H.; Schmitt, J. C.; Shearer, J.; Jia, J.; Olmstead, M. M.; Fettinger, J. C.; Balch, A. L. *Inorg. Chem.* **2013**, *52*, 823. (d) White-Morris, R. L.; Olmstead, M. M.; Balch, A. L.; Elbjeirami, O.; Omary, M. A. *Inorg. Chem.* **2003**, *42*, 6741. (e) Lee, T. K.-M.; Zhu, N.; Yam, V.W.-W. *J. Am. Chem. Soc.*

2010, *132*, 17646. (f) Saitoh, M.; Balch, A. L.; Yuasa, J.; Kawai, T. Inorg. Chem. **2010**, *49*, 7129. (g) Rios, D.; Pham, D. M.; Fettinger, J. C.; Olmstead, M. M.; Balch, A. L. *Inorg. Chem.* **2008**, *47*, 3442.

7. R.F. Ziolo, S. Lipton, Z. Dori, *Chem. Commun.,* **1970**, 1124.

8. Pal, S.; Kathewad, N.; Pant, R.; Khan, S. *Inorg. Chem.*, **2015**, *54*, 10172.

9. Narayanaswamy, R.; Young, M. A.; Parkhurst, E.; Ouellette, M.; Kerr, M. E; Ho, D. M.; Elder, R. C.; Bruce, A. E.; Bruce, M. R. M. *Inorg. Chem.*, **1993**, *32*, 2506.

10. Forward, J. M.; Bohmann, D.; Fackler, J. P.; Staples, R. J. *Inorg. Chem.*, **1995**, *34*, 6330.

11. B.-C. Tzeng, J.-H. Liao, G.-H. Lee and S.-M. Peng, *Inorg. Chim. Acta*, **2004**, *357*, 1405.

12. Ferle, A.; Pizzuti, L.; Inglez, S. D.; Caires, A. R. L.; Lang, E. S.; Back, D. F.; Flores, A. F. C.; Júnior, A. M.; Deflon, V. M.; Casagrande, G. A. *Polyhedron*, **2013**, *63*, 9.

13. Mohamed, A. A.; Kani, I.; Ramirez, A. O.; Fackler, J. P. Jr., *Inorg. Chem.*, **2004**, *43*, 3833.

14. Pintado-Alba, A.; De la Riva, H.; Nieuwhuyzen, M.; Bautista, D.; Raithby, P. R.; Sparkes, H. A.; Teat, S. J.; López-de-Luzuriagae, J. M.; Lagunas, M. C. *Dalton Trans.*, **2004**, 3459.

15. Karimi M. J.; Jamali, S. *J. Organometal. Chem.*, **2015**, 786, 14.

16. Fu, W.-F.; Chan, K.-C.; Cheung, K.-K.; Che, C.-M. *Chem. Eur. J.*, **2001**, *7*, 4656.

17. Yam, V. W.-W.; Choi, S. W.-K. *J. Chem. Soc. Dalton Trans.*, **1994**, 2057.

18. (a) Cheng, E. C.-C.; Lo, W.-Y.; Lee, T. K.-M.; Zhu, N.; Yam, V. W.-W. *Inorg. Chem.*, **2014**, *53*, 3854. (b) Yam, Y. W.; Lee, W.-K. *J. Chem. Soc., Dalton Trans.* **1993,** 2097. (c) Fu, W.-F.; Chan, K.-C; Miskowski, V. M.; Che, C.-M. *Angew. Chem., Int. Ed.* **1999**, *38*, 2783. (d) Ma, Y.; Che, C.-M; Chao, H.-Y.; Zhou, X.; Chan, W.-H.; Shen, *J. Adv. Mater*. **1999**, *11*, 852. (e) Lee, Y.-A; McGarrah, J. E.; Lachicotte, R. J.; Eisenberg, R. *J. Am. Chem. Soc.* **2002**, *124*, 10662. (f) Tzeng, B.-C.; Liao, J.-H.; Lee, G.-H.; Peng, S.-M. *Inorg. Chim. Acta* **2004**, *357*, 1405. (g) Monzittu, F. M.; Fernández-Moreira, V.; Lippolis, V.; Arca, M.; Laguna, A.; Gimeno, M. C. *Dalton Trans*. **2014**, *43*, 6212. (h) He, X.; Lam, W. H.; Cheng, E. C.-C.; Yam, V. W.-W. *Chem. Eur. J.* **2015**, *21*, 8447.

19. Frisch, M. J. et al. *Gaussian09, revision C.01; Gaussian, Inc.: Wallingford, CT*, **2013**

20. Becke, A. D. *J. Chem. Phys.* **1993**, *98*, 5648.

21. Lee, C.; Yang, W.; Parr, R. G. *Phys. Rev. B* **1988**, *37*, 785.

22. Hay, P. J.; Wadt, W. R. *J. Chem. Phys.*, **1985**, *82*, 270.

23. Hay, P. J.; Wadt, W. R.; *J. Chem. Phys.*, **1985**, *82*, 299.

Chapter 4

Synthesis, Characterization and Photophysical studies of copper (I) and silver (I) complexes

4.1. Introduction

The copper(I) complexes have been studied recently with great interest as they exhibit structural diversities,[1] metallophilicity,[2] rich photophysical properties,[3] and they have been found application in catalysis,[4] as well as in organic light emitting diodes (OLEDs) as dopants.[5] Previous studies showed that a wide range of structure motifs could be accessible by combining copper halides and a variety of N, P, O, and S based ligand systems leading to di-, tri-, and tetra-nuclear copper (I) complexes that show strikingly different luminescent behavior.[6-9] Recently, we reported the synthesis and luminescence studies of gold(I) complexes with PNP-based ligand systems.[10] As copper is a more appealing element as luminescent dopant due to low cost and non-toxicity, we decided to prepare analogous copper(I) complexes with PNP-ligands and compare their structural and photophysical properties. The reaction of $Ph_2PN(2,6-Me_2C_6H_3)PPh_2$ (**2.2**) with copper bromide/chloride led to dimeric copper(I) complexes analogous to our recent report on silylene supported dimeric copper(I) complexes.[11,12] It has to be noted here that the reactions of simple $(PPh_2)_2NPh$ (**2.1**) ligand with copper(I) halides led to tetrameric structures.[13a] These findings indicate that the ligand/substituent has a vital role in the structural arrangement as well as on the resulting photophysical properties of the complexes.[14] Therefore, we sought to alter the position of the methyl substituents in the N-phenyl ring and isolate the resulting copper complexes. Interestingly, these complexes show significant structural diversities as the methyl groups in ortho, meta, and para position of the N-phenyl ring afforded three entirely different structural motifs. Apart from structural diversities, the resulting complexes (**4.3**-**4.8**) show different photophysical behavior. For example, complex **4.3** and **4.4** are non-luminescent while **4.5**-**4.8** exhibit mechanochromic and thermochromic behaviour.

Among coinage metal complexes gold and copper are most widely used complexes for their photophysical properties. However, silver also shows metallophilic interaction, i.e. Ag...Ag distance in the range of 2.7-3.4 A^o and termed as argentophilic interaction, but examples of their photophysical properties are limited.[15] Therefore we planned to prepare DPPA supported silver complexes and studied them for their emission properties.
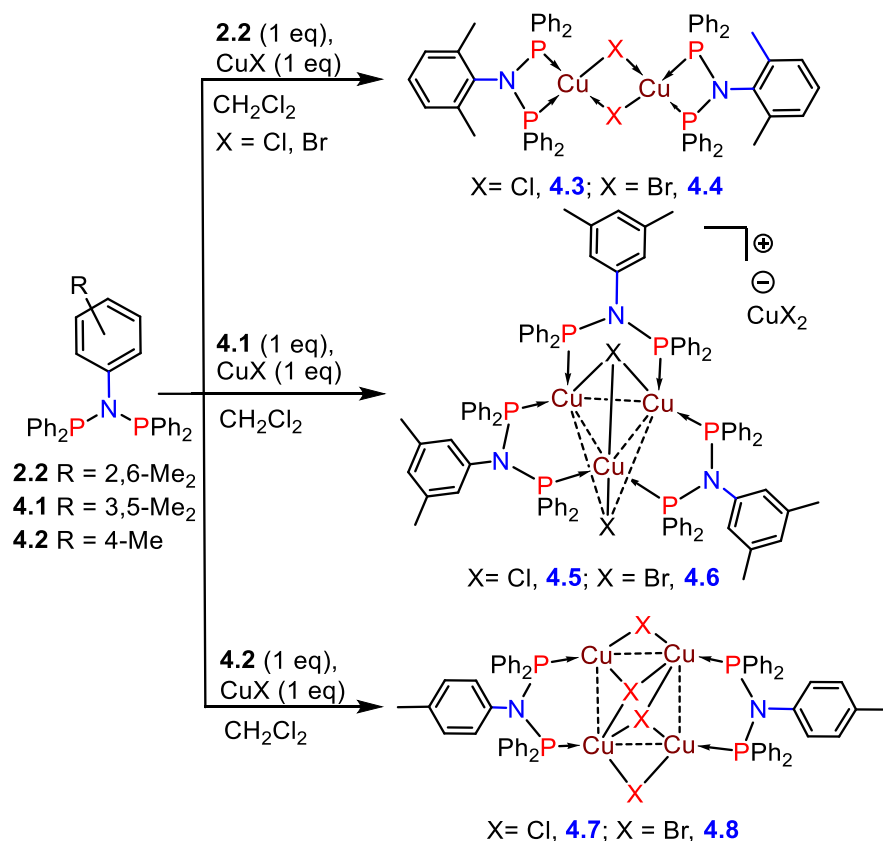
Scheme 4.1. *Syntheses of differently substituted diphosphinoamine ligand based copper (I) complexes* **4.3-4.8**.

4.2 Experimental section

4.2.1. General Remarks

All manipulations were performed under a dry and oxygen-free atmosphere (N_2) using standard Schlenk techniques and glove box. All solvents were dried over activated molecular sieves after distillation. All the chemicals are purchased from Sigma Aldrich and alpha aesar. [1]H, ^{13}C, ^{31}P, and ^{19}F solution NMR spectra were recorded on a Jeol 400 and Bruker 400 MHz spectrometer. Fourier transform infrared (FT-IR) spectra were taken on a PerkinElmer spectrophotometer. UV-visible absorption spectra were recorded using a Perkin-Elmer UV-visible spectrometer. Steady-state PL and PL decay dynamics (time-correlated single photon

counting) were measured using a Horiba Jobin-Yvon Fluorolog 3 spectrometer and FLS 980 instrument (Edinburg Instruments).
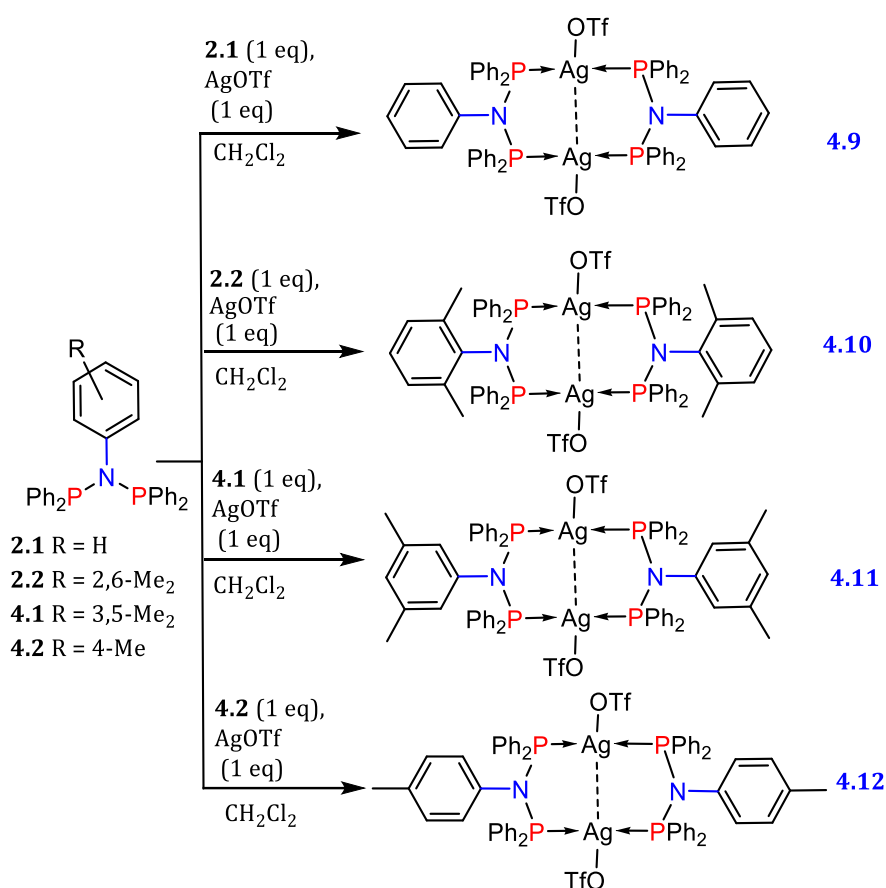
Scheme 4.2. *Syntheses of differently substituted diphosphinoamine ligand based Silver (I) complexes* ***4.9-4.12***

4.2.2 Synthesis of complexes *4.3-4.12*

Compound 4.3

CH_2Cl_2 (20 mL) was added to a flask containing **2.2** (0.490 g, 1 mmol) and CuCl (0.099 g, 1 mmol), and the solution was stirred overnight. The reaction mixture was filtered off and reduced to 5 mL. Subsequently *n*-pentane (5 mL) was added to the flask and the solution was stored at 0 °C to afford pale yellow crystals of **4.3**. Yield: 0.82 g (74.54 %). ^{1}H NMR (CDCl$_3$, 400 MHz): δ = 2.03 (s, 12 H, CH3-*p*Ph), 6.65 (s, 2 H, Ph), 7.29–7.44 (m, 44 H, Ph) ppm; ^{31}P{^{1}H}

NMR (CDCl$_3$, 161.976 MHz): δ = 68.50 (s) ppm. ^{13}C{^{1}H} NMR (CDCl^3, 100.613 MHz): δ = 19.75 (o-CH$_3$), 127.73 (Ph), 128.70 (Ph), 130.43 (Ph), 134.59 (Ph), 135.94 (Ph) ppm. IR: $\tilde{\nu}$ = 689.26, 813.87, 1031.45, 1101.04, 1266.88, 1431.11, 1574.53 cm^{-1}. MS (ESI+) Cu$_2$(μ$_2$-Cl)$_2${C$_8$H$_9$N(PPh$_2$)$_2$}$_2$ (1174): m/z = 1175.32 [M$^+$]. Elemental Analysis (%): Calcd. C 65.31; H 4.97; N 2.38. Found C 65.25; H 4.90; N 2.29

Compound 4.4

The same procedure used for **2.2** was followed with CuBr instead of CuCl. Pale yellow colored crystals of **4.4** were obtained. Yield: 0.88 g (75.21 %). ^{1}H NMR (CDCl$_3$, 400 MHz): δ = 2.01 (s, 12 H, CH3-pPh), 6.75–6.84 (s, 7 H, Ph), 7.15–7.58 (m, 39 H, Ph) ppm. ^{31}P{^{1}H} NMR (CDCl$_3$, 161.976 MHz): δ = 73.65 (s) ppm. ^{13}C{^{1}H} NMR (CDCl$_3$, 100.613 MHz): δ = 22.34 (o-CH$_3$), 127.9 (Ph), 128.81 (Ph), 129.34 (Ph), 130.36 (Ph), 134.48 (Ph) ppm; IR: $\tilde{\nu}$ = 689.26, 813.87, 1031.45, 1101.04, 1266.88, 1431.11, 1574.53 cm^{-1}. MS (ESI+) Cu$_2$(μ$_2$-Br)$_2$-{C$_8$H$_9$N(PPh$_2$)$_2$}$_2$ (1264): m/z = 1185.14 [M$^+$ – Br]. Elemental Analysis (%): Calcd. C 60.72; H 4.62; N 2.21. Found C 60.65; H 4.70; N 2.00

Compound 4.5

CH$_2$Cl$_2$/toluene mixture (1:1) (20 mL) was added to the flask containing **4.1** (0.490 g, 1 mmol) and CuCl (0.099 g, 1 mmol) and the solution was stirred overnight. The reaction mixture was filtered off and concentrated to 5–6 mL and kept at room temperature to obtain colorless crystals of **4.5**. Yield: 0.67 g (71.05 %); ^{1}H NMR (CDCl$_3$, 400 MHz): δ = 2.38 (s, 6 H, CH3-oPh), 6.41 (s, 3 H, Ph), 6.95–6.99 (m, 32 H, Ph), 7.05–7.06 (br, 32 H, Ph), 7.19–7.28 (m, 27 H, Ph) ppm. ^{31}P{^{1}H} NMR (CDCl$_3$, 161.976 MHz): δ = 59.11 (s) ppm. ^{13}C{^{1}H} NMR (CDCl$_3$, 100.613 MHz) δ = 20.62 (m-CH$_3$), 125.22 (Ph), 127.82 (Ph), 128.15 (Ph), 128.90 (Ph), 136.50 (Ph), 130.47 (Ph), 133.04 (Ph) ppm. IR: $\tilde{\nu}$ = 689.26, 813.87, 1031.45, 1101.04, 1266.88, 1431.11, 1574.53 cm^{-1}. Elemental Analysis (%): Calcd. C 66.64; H 5.07; N, 2.43. Found C 66.55; H 5.25; N, 2.20.

Compound 4.6

The same procedure used for **4.5** was followed with CuBr instead of CuCl. Yield: 0.67 g (73 %). ^{1}H NMR (CDCl$_3$, 400 MHz) δ = 2.37 (s, 6 H, CH3-oPh), 6.41 (s, 3 H, Ph), 6.95–6.99 (m, 32

H, Ph), 7.05–7.06 (br., 32 H, Ph), 7.19–7.28 (m, 27 H, Ph) ppm. ^{31}P{^{1}H} NMR (CDCl$_3$, 161.976 MHz): δ = 55.86 (s) ppm. ^{13}C{^{1}H} NMR (CDCl$_3$, 100.613 MHz): δ = 136.50 (Ph), 133.04 (Ph), 130.47 (Ph), 128.90 (Ph), 128.15 (Ph), 127.82 (Ph), 125.22 (Ph), 20.62 (m-CH$_3$) ppm; IR: ṽ = 689.96, 811.65, 1029.50, 1096.72, 1266.30, 1478.57, 2376.39 cm^{-1}. Elemental Analysis (%): Calcd. C 63.39; H 4.82; N, 2.31. Found: C 63.39; H 4.81; N, 2.25.

Compound 4.7

CH$_2$Cl$_2$ (20 mL) was added to the flask containing **4.2** (0.475 g, 1 mmol) and CuCl (0.099 g, 1 mmol), and the solution was stirred overnight. The reaction mixture was then filtered off and concentrated to 5 mL and equal amounts of n-pentane were added. Storing the solution at 0 °C afforded colorless crystals of **4.7**. Yield: 0.74 g (73.03 %). ^{1}H NMR (CDCl$_3$, 400 MHz): δ = 2.07 (s, 6 H, CH3-oPh), 5.80 (d, J = 8.1 Hz, 4 H, Ph), 6.46 (d, J = 8.2 Hz, 4 H, Ph),7.25–7.50 (m, 40 H, Ph) ppm. ^{31}P{^{1}H} NMR (CDCl$_3$, 161.976 MHz): δ = 60.20 (s) ppm. ^{13}C{^{1}H} NMR (CDCl$_3$, 100.613 MHz): δ = 20.80 (p-CH$_3$), 128.43 (Ph), 128.63 (Ph), 130.47 (Ph), 131.39 (Ph), 132.82 (Ph), 134.08 (Ph), 136.87 (Ph) ppm. IR: ṽ = 689.26, 811.65, 1029.50, 1096.72, 1266.30, 1430.28, 1478.57 cm^{-1}. MS (ESI+) Cu$_2$(μ$_2$-Cl)$_2${C$_8$H$_9$N(PPh$_2$)$_2$}$_2$ (1341): m/z = 1306.42 [M$^+$– Cl]. Elemental Analysis (%): Calcd. C 55.28; H, 4.04; N, 2.08. Found: C 54.98; H 3.95; N 2.01.

Compound 4.8

The same procedure used for **4.7** was followed with CuBr instead of CuCl. Yield: 0.60 g (80 %). ^{1}H NMR (CDCl$_3$, 400 MHz): δ = 1.98 (s, 6 H, CH3-oPh), 5.32 (d, J = 8.1 Hz, 4 H, NPh), 6.26 (d, J = 8.2 Hz, 4 H, NPh), 6.94–7.29 (m, 40 H, Ph) ppm; ^{31}P{^{1}H} NMR (CDCl$_3$, 161.976 MHz): δ = 57.04 (s) ppm; ^{13}C{^{1}H} NMR (CDCl$_3$, 100.613 MHz): δ = 20.76 (p-CH$_3$), 127.98 (Ph), 130.29 (Ph), 132.15 (Ph), 132.96 (Ph), 136.95 (Ph) ppm; IR: ṽ = 687.33, 739.09, 864.80, 1008.89, 1079.77, 1258.06, 1433.41, 2963.06 cm^{-1}. MS (ESI+) Cu$_2$(μ$_2$-Br)$_2${C$_8$H$_9$N(PPh$_2$)$_2$}$_2$ (1527): m/z = 1447.02 [M$^+$ –Br]. Elemental Analysis (%): Calcd. C 48.84; H 3.57; N, 1.84. Found: C 48.84; H 3.794; N, 1.70.

Compound 4.9

CH$_2$Cl$_2$ (20 mL) was added to a flask containing **2.1** (0.460 g, 1 mmol) and AgOTf (0.256 g, 1 mmol), and the solution was stirred overnight. The reaction mixture was filtered off and

reduced to 5 mL. Subsequently *n*-pentane (5 mL) was added to the flask and the solution was stored at 0 °C to afford colourless crystals of **4.9**. Yield: 0.57 g (80 %). ^{1}H NMR (CDCl$_3$, 400 MHz): δ = 6.17 (d, 4H, J = 7.8 Hz, Ph), 6.69 (t, 4H, J = 7.9 Hz, Ph), 6.9 (s, 2H, Ph), 7.33-7.49 (m, 29 H, Ph) ppm; ^{31}P{^{1}H} NMR (CDCl$_3$, 161.976 MHz): δ = 83.15 (dt, $J_{\text{P-Ag}}$ = 553.4, 19.8 Hz) ppm. ^{13}C{^{1}H} NMR (CDCl^3, 100.613 MHz): δ 133.49 (Ph), 132.17 (Ph), 131.31 (Ph), 129.21 (Ph), 128.56 (Ph) ppm. ^{19}F NMR -77.61(s) ppm. MS (ESI+) {(C$_6$H$_5$N(PPh$_2$)$_2$AgOTf}$_2$ (1436.01): m/z = 1436.83 [M$^+$]; Elemental Analysis (%): Calcd. C 51.83; H 3.51; N 1.95; O 6.68; S, 4.46. Found C 51.50; H 2.86; N, 2.20; O 6.60; S, 4.45.

Compound 4.10

CH$_2$Cl$_2$ (20 mL) was added to a flask containing **2.2** (0.490 g, 1 mmol) and AgOTf (0.256 g, 1 mmol), and the solution was stirred overnight. The reaction mixture was filtered off and reduced to 5 mL. Subsequently n-pentane (5 mL) was added to the flask and the solution was stored at 0 °C to afford pale yellow crystals of **4.10**. Yield: 0.55 g (70 %). ^{1}H NMR (CD$_3$CN, 400 MHz): δ = 1.99 (s, 12H, CH$_3$-*o*Ph), 7.35-7.39 (m, 30 H, Ph), 7.56-7.6 (m, 16 H, Ph) ppm. ^{31}P{^{1}H} NMR (CD$_3$CN, 161.976 MHz): δ = 85.61 (br) ppm. ^{13}C{^{1}H} NMR (CD$_3$CN, 100.613 MHz): δ = 138.98 (Ph), 134.96 (Ph), 132.42 (Ph), 129.48 (Ph), 128.74 (Ph), 20.32 (*o-C*H$_3$) ppm. ^{19}F NMR δ = -79.27 (s) ppm. MS (ESI+) {(C$_8$H$_9$N(PPh$_2$)$_2$AgOTf}$_2$ (1492.07): m/z = 1004 (M$^+$-C$_8$H$_9$N(PPh$_2$)$_2$). Elemental Analysis (%): Calcd. C 53.10; H 3.92; N 1.88; O 6.43; S 4.29. Found C 52.68; H 2.844; N, 2.50; O 6.55; S, 4.25.

Compound 4.11

CH$_2$Cl$_2$ (20 mL) was added to a flask containing **4.1** (0.490 g, 1 mmol) and AgOTf (0.256 g, 1 mmol), and the solution was stirred overnight. The reaction mixture was filtered off and reduced to 5 mL. Subsequently n-pentane (5 mL) was added to the flask and the solution was stored at 0 °C to afford pale yellow crystals of **4.11**. Yield: 0.57 g (77 %). ^{1}H NMR (CD$_3$CN, 400 MHz): δ = 2.2 (s, 12 H, CH3-*m*Ph), 7.35-7.39 (m, 30 H, Ph), 7.56-7.76 (m, 16H, Ph) ppm; ^{31}P{^{1}H} NMR (CDCl$_3$, 161.976 MHz): δ = 85.97 (br) ppm. ^{13}C{^{1}H} NMR (CDCl^3, 100.613 MHz): δ = 138.98 (Ph), 134.96 (Ph), 132.42 (Ph), 129.48 (Ph), 128.74 (Ph), 20.32 (*m-C*H3)ppm. ^{19}F NMR -79.24 (s) ppm. MS (ESI+) {(C$_8$H$_9$N(PPh$_2$)$_2$AgOTf}$_2$ (1286.15): m/z = 986 (M$^+$-

$C_8H_9N(PPh_2)_2$). Elemental Analysis (%): Calcd. C 53.10; H 3.92; N 1.88; O 6.43; S 4.29. Found C 53.07; H, 3.99; N, 1.79; O, 6.41; S, 4.23.

Compound 4.12

CH_2Cl_2 (20 mL) was added to a flask containing **4.2** (0.475 g, 1 mmol) and AgOTf (0.256 g, 1 mmol), and the solution was stirred overnight. The reaction mixture was filtered off and reduced to 5 mL. Subsequently n-pentane (5 mL) was added to the flask and the solution was stored at 0 °C to afford pale yellow crystals of **4.12**..Yield: 0.51 g (70 %). ^1H NMR ($CDCl_3$, 400 MHz): δ = 2.07 (s, 6H, CH_3-pPh), 5.98-6.0 (d, 4H, J = 8.3 Hz, Ph), 6.5-6.52 (d, 4H, J = 8.3 Hz, Ph) 7.34-7.52 (m, 42H, Ph) ppm. $^{31}P\{^1H\}$ NMR ($CDCl_3$, 161.976 MHz): δ = δ 84.32 (dt, J_{P-Ag}= 550.1, 19.5 Hz) ppm. $^{13}C\{^1H\}$ NMR (CD_3CN, 100.613 MHz): δ = 138.36 (Ph), 133.57 (Ph), 132.06 (Ph), 130.90 (Ph), 128.95 (Ph), 19.82 (p-CH$_3$) ppm. ^{19}F NMR -77.49 (s) ppm. Elemental Analysis (%): Calcd. C 52.48; H 3.72; N 1.91; O 6.55; S 4.38. Found C 52.30; H 3.25; N 1.67; O 6.40; S 4.26.

4.2.3. X-ray Crystallographic Details

Single crystals of suitable size were coated with paraffin oil was mounted for all the complexes. Crystal data for all the complexes were collected on a Bruker Smart Apex Duo diffractometer at 100 K using Mo Kα radiation (λ = 0.71073 Å) and Cu Kα radiation (λ = 1.5418 Å). [16] A multi-scan absorption correction was applied to the collected reflections. The structures were solved by the direct method using SHELXTL[17] and were refined on F^2 by full-matrix least-squares technique using the SHELXL-97[17] program. All non-hydrogen atoms were refined anisotropically. All hydrogen atoms were located in successive difference Fourier maps, and they were treated as riding atoms using SHELXL default parameters. Appendix tables 4A.1-4A.4 contain crystallographic data for **4.3**-**4.12**. 1568543 (**4.3**), 1568544 (**4.4**), 1568545 (**4.5**), 1568546 (**4.6**), 1568547 (**4.7**), and 1568548 (**4.8**). These data can be obtained free of charge from Cambridge Crystallographic Data Centre via www.ccdc.cam.ac.uk/data_request/cif.

4.2.4. Computational Methods

The molecular geometries of all the Cu(I) complexes were fully optimized applying density functional theory (DFT) based full-potential VASP code.[18] The projector-augmented wave (PAW) method was employed to take into account the full nodal character of the all-electron charge density in the core region.[19] In order to obtain an accurate description of the electronic states the energy cut off of 450 eV for the pseudopotentials along with Perdew-Burke-Ernzenhof (PBE) prescription for the exchange-correlation energy in the generalized gradient approximation (GGA) was used.[20] The electronic structures and the optical properties of all the complexes were investigated applying density functional theory (DFT) using Becke's three-parameter, Lee-Yang-Parr exchange correlation hybrid functional B3LYP along with Ahlrich's def2-TZVP(P) polarized basis set of triple ζ quality on all atoms. We also employed the RIJCOSX approximation combining the RI-J method and the COSX approximation with ORCA 3.0.3 chemical code. The electronic spectra were obtained applying TD-DFT approach within the framework of Tamm-Dancoff approximations.[21,22] The ground state molecular geometries were optimized applying PBE exchange correlation functionals in the DFT.

4.3.   Result and Discussion

4.3.1. Synthesis and characterization of DPPA supported Copper(I) complexes (4.3-4.8)

DPPA ligands (**2.2**, **4.1**, and **4.2**) were synthesized adopting the same synthetic protocol that has been used to prepare $Ph_2PN(2,6-iPr_2C_6H_3)PPh_2$.[10] The purpose of synthesizing these ligands is to study the modulation of the structural and Photophysical properties of the copper(I) complexes. Complexation of copper(I) chloride and bromide with these DPPA ligands, **2.2**, **4.1**, and **4.2**, affords structurally different copper(I) complexes **4.3-4.8** (Scheme 4.1).
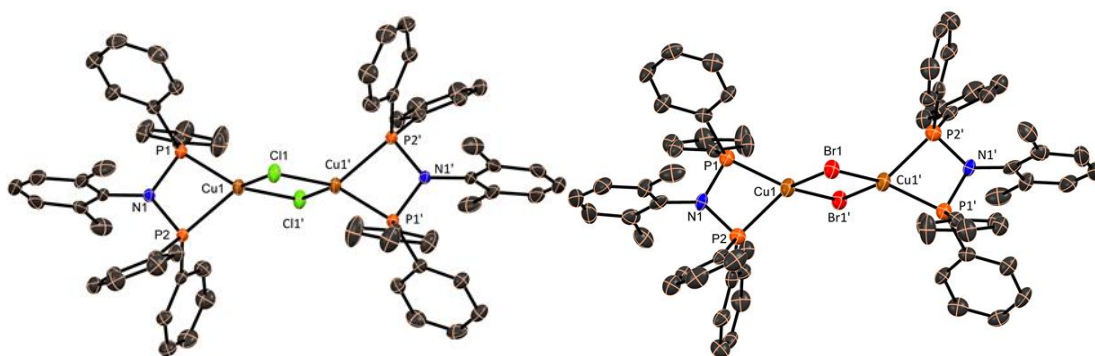
Figure 4.1*. The molecular structure of **4.3** and **4.4**, with anisotropic displacement parameters depicted at the 50% probability level. All hydrogen atoms and lattice solvent have been omitted for clarity. Selected bond lengths (Å) and bond angles (o) for **4.3** Cu1-Cl1/Cu1'-Cl1' 2.301(1), Cu1-Cl1'/Cu1'-Cl1 2.3513(9), P1-Cu1/P1'-Cu1' 2.288(1), P2-Cu1/P2'-Cu1' 2.320(1), P1-N1/P1'-N1' 1.725(2), P2-N1/P2'-N1'1.723(2); Cl1-Cu1-Cl1'/Cl1-Cu1'-Cl1' 96.46(3), Cu1-Cl1-Cu1'/Cu1-Cl1'-Cu1' 83.54 (3), P1-Cu1-P2/P1'-Cu1'-P2' 73.87(3); for **4.4** Cu1-Br1/Cu1'-Br1' 2.473(2), Cu1-Br1'/Cu1'-Br1 2.434(2), P1-Cu1/P1'-Cu1' 2.338(3), P2-Cu1/P2'-Cu1' 2.292(3), P1-N1/P1'-N1' 1.693(8), P2-N1/P2'-N1' 1.748(7); Br1-Cu1-Br1'/Br1-Cu1'-Br1' 100.15(6), Cu1-Br1-Cu1'/Cu1-Br1'-Cu1' 79.85(5), P1-Cu1-P2/P1'-Cu1'- P2' 73.31(9).*

The reactions of CuCl and CuBr with **2.2** in CH_2Cl_2 resulted in dinuclear dimeric copper(I) complexes **4.3** and **4.4**. Analogous reactions of CuBr and CuCl with ligand **4.1** in a 1:1 ratio led to trinuclear structures with μ_3-bridging halide atoms (complexes **4.5** and **4.6**). Tetranuclear clusters **4.7** and **4.8** were obtained on treatment of **4.2** [4-MeC$_6$H$_4$N(PPh$_2$)$_2$] with CuCl and CuBr in CH_2Cl_2 in a 1:1 ratio. Complexes **4.7** and **4.8** display bi-capped "octahedron"-type arrangements in which two of the halide atoms are μ_2-bridged, and the other two halides have μ_3- or μ_4-coordination. The crystals of all of these copper(I) complexes were grown from a CH_2Cl_2/n-pentane (1:1) and CH_2Cl_2/toluene (1:1) mixture and are moderately stable upon exposure to air and moisture.

The complexation of the ligand **2.2** is accompanied by the downfield shift in the ^{31}P NMR spectra of **4.3** (δ = 61.0 ppm) and **4.4** (δ = 72.8 ppm) compared with **2.2** (δ = 55.9 ppm).
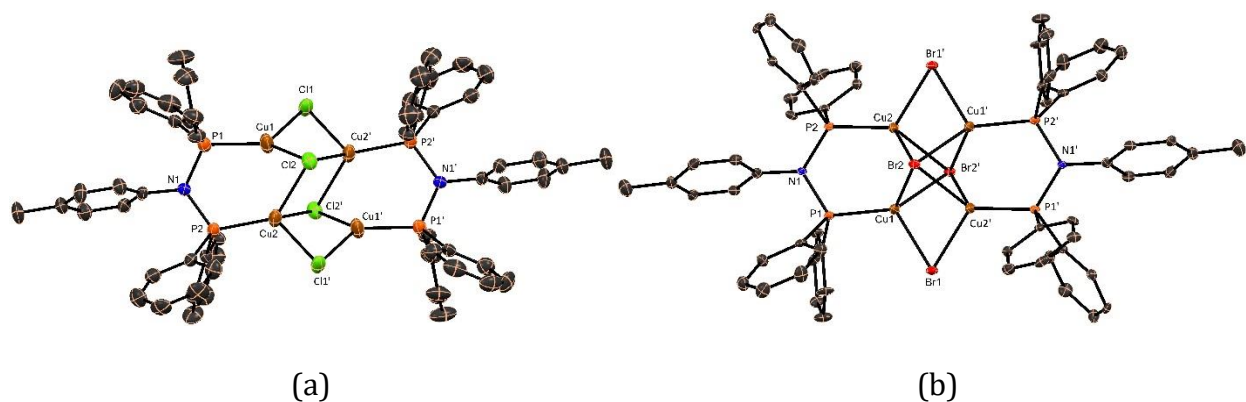
(a)	(b)
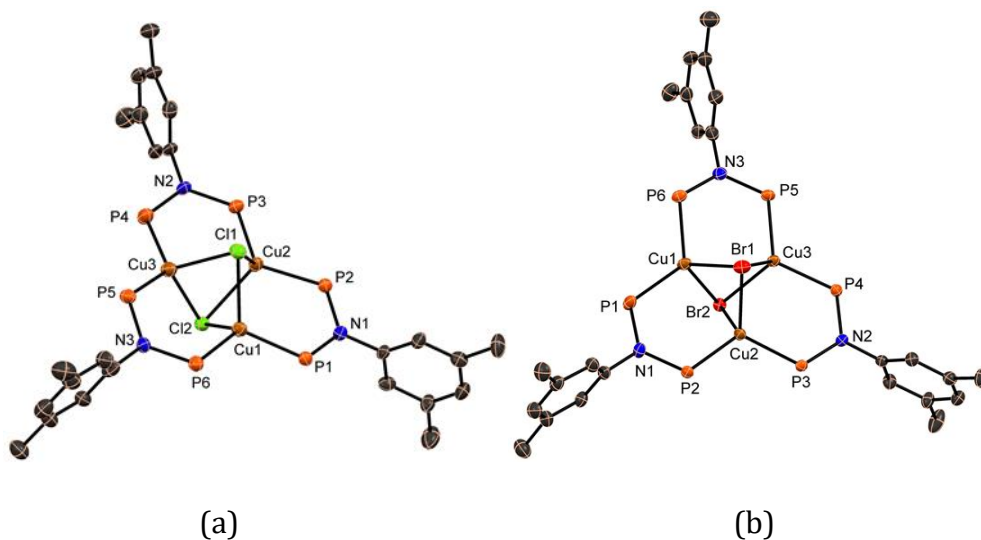
Figure 4.2. *Molecular structure of (a)* **4.4** *and (b)* **4.5** *with anisotropic displacement parameters depicted at the 50% probability level. All hydrogen atoms and lattice solvent have been omitted for clarity. Selected bond lengths (Å) and bond angles (°) for* **4.4***: Cu1-Cu2 2.808(2), Cu2-Cu3 2.925(1), Cu3-Cu1 2.934(2), Cu1-Cl1 2.434 (2), Cu1-Cl2 2.465(2), Cu2-Cl1 2.415(2), Cu2-Cl2 2.472(2), Cu3-Cl1 2.469(2), Cu3-Cl2 2.430(2), Cl3-Cu4 2.087(5), Cl4-Cu4 2.077(5), P1-Cu1 2.244(2), P2-Cu2 2.238(2), P3-Cu2 2.233(2), P4-Cu3 2.240(2), P5-Cu3 2.238(2), P6-Cu1 2.240(2); Cu1-Cu2-Cu3 61.57(4), Cu2-Cu3-Cu1 57.29(4), Cu3-Cu1-Cu2 61.14 (4), Cu1-P1-N1 117.7(2), Cu2-P2-N1 117.1(2), Cu2-P3-N2 118.2(2), Cu1-P6-N3/ Cu3-P4-N2 117.5(2), Cu3-P5-N3 117.5(2), Cl3-Cu4-Cl4 176.6(2), P1-N1-P2 120.5(3), P3-N2-P4 121.54(3), P5-N3-P6 121.0(4); For* **4.5***: Cu1-Cu2 2.923(1), Cu2-Cu3 2.801(1), Cu3-Cu1 2.934(1), Cu1-Br1 2.565(1), Cu1-Br2 2.546(1), Cu2-Br1 2.534(1), Cu2-Br2 2.590(1), Cu3-Br1 2.553(1), Cu3-Br2 2.585(1), Cu4-Br3/ Cu4-Br4 2.210(2), P1-Cu1/ P2-Cu2 2.240(2), P3-Cu2/ P6-Cu1 2.241(2), P4-Cu3 2.252(2), P5-Cu3 2.244(2); Cu1-Cu2-Cu3 61.62(3), Cu2-Cu3-Cu1 61.23(3), Cu3-Cu1-Cu2 57.15(3), Cu1-P1-N1 117.2(2), Cu2-P2-N1 118.0(2), Cu2-P3-N2 117.5(2), Cu1-P6-N3 117.0 (2) Cu3-P4-N2/Cu3-P5-N3 117.4(2), Br3-Cu3-Br4 178.23(9), P1-N1-P2 121.8 (3), P3-N2-P4 120.4(3), P5-N3-P6 121.4(3).*

Molecular structures of complexes **4.3** and **4.4** are shown in *Figure 4.1*. Complexes **4.3** and **4.4** crystallize in the monoclinic space group *P21/c*, and each consists of a planar four-membered Cu_2X_2 ring. Each copper atom in complexes **4.3** and **4.4** is coordinated with one ligand **2.2** through two phosphorus atoms and thereby exhibit distorted tetrahedral geometries. There is no Cu⋯Cu interaction present in complexes **4.3** and **4.4**, as the two copper atoms in **4.3** and **4.4** are separated by a distance of 3.098(4) and 3.149(2) A,

respectively, which is greater than the sum of van der Waals radii of copper (2.8 A). The resonances in the ^{31}P NMR spectra of complexes **4.5** and **4.6** appear at δ = 58.9 and 55.7 ppm, respectively, which is upfield shifted compared with the corresponding ligand **4.1** (δ = 66.2 ppm). Molecular structures of **4.5** and **4.6** comprise of linear dihalocuprate(I) anions, $[CuX_2]$, and $[Cu_3(\mu_3-X)_2\{C_8H_9N(PPh)_2\}_3]^+$ complex cations [X = Cl and Br]. The molecular structures of complexes **4.5** and **4.6** (*Figure 4.2*) possess three copper atoms in the cationic segment with a discrete CuX_2 anion.

Each copper atom is tetra-coordinated, connected to two ligands (**4.1**) through phosphorus atoms and with bridging halogen atoms above and below the Cu_3-plane, and thereby exhibit tetrahedral geometries. The Cu–Cu distances in both the complexes are found to be in the range of 2.8–2.9 A.[23] The copper-phosphorus bond lengths range from 2.23 to 2.24 A, which are in accordance with those in $[Cu_4(\mu_3-Cl)_4(\mu-dtbpf)_2]$[24] [2.1950(17) A] [dtbpf = 1,1′-bis(di-tert-butylphosphanyl)ferrocene] and $[Cu_3-(dppm)_3(\mu_3-Br)_2]^+$ [dppm = bis(diphenylphosphanyl) methane] [2.241(5)–2.259(4) A].[23b] For both complexes **4.5** and **4.6,** the halide atoms above and below the triangular plane are found to be almost equidistant from the copper atoms, varying with a very small difference of 2.415(2)–2.470(2) and 2.534(1)-2.587(1) Å, respectively. The presence of a dihalocuprate anion in both complexes 4.5 and 4.6 is confirmed by single-crystal X-ray studies. The Cu–Cl bond lengths in the $[CuCl_2]^-$ anions are 2.077(5) and 2.081(5) Å with a bond angle of 176.6(2)° for Cl3–Cu4–Cl4 indicating a linear structure. Similarly, the Cu–Br distance is 2.210(4) Å for the $[CuBr_2]^-$ anion in complex 4.6 (Figure 4.2) and the linearity is confirmed by the bond angle of Br3–Cu4–Br4 [178.23(9)°].

To the best of our knowledge, there is no report on such a type of dihalocuprate anion generated with a halogen bridged trinuclear copper (I) complex. A singlet resonance at δ = 59.9 and 56.9 ppm was observed in the ^{31}P NMR spectra of complexes **4.7** and **4.8**, respectively, and it seems to be slightly upfield compared with that of ligand **4.2** (δ = 68.5 ppm), but in agreement with those reported for $Cu_4(dppan)_2Cl_4$ (59.1 ppm), $Cu_4(dppan)_2Br_4$ (59.0 ppm) [dppan = bis(diphenylphosphanyl) aniline].[13a]
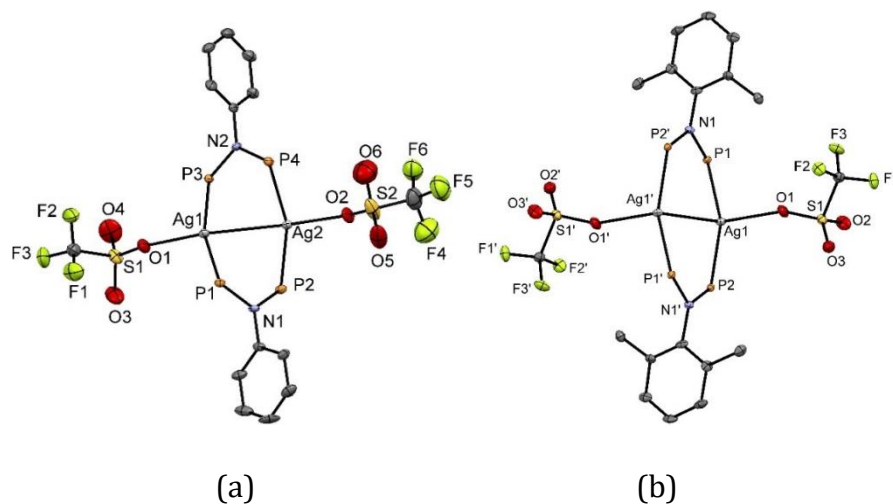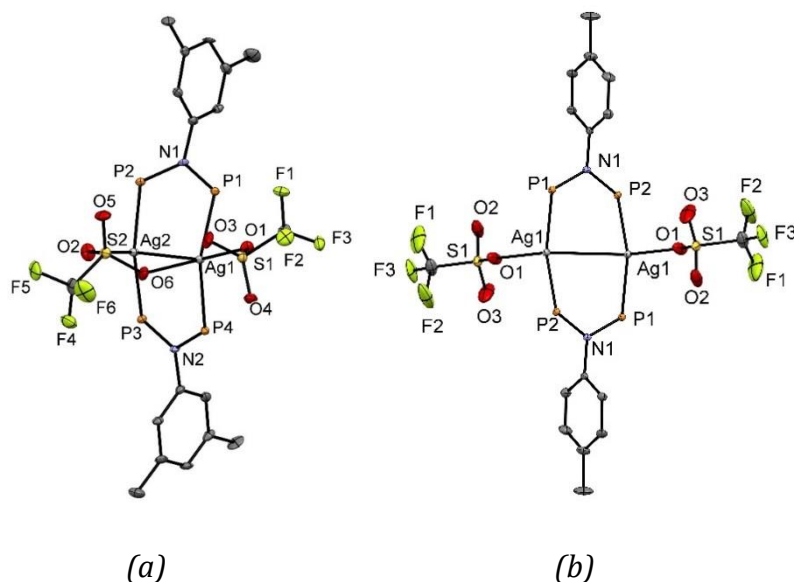
Figure 4.3. *Molecular structure of (a)* **4.7** *and (b)* **4.8** *with anisotropic displacement parameters depicted at the 30% probability level. All hydrogen atoms and lattice solvent have been omitted for clarity. Selected Bond lengths (Å) and Selected Bond angles (o) For* **4.7**: *Cu2-Cu1/ Cu2'-Cu1' 2.748(4), Cu1-Cu2'/ Cu1'-Cu2 2.858(5), Cu2'-Cl1/ Cl1'-Cu2 2.344(4), Cu1-Cl1/ Cu1'-Cl1' 2.235(4), Cu1-Cl2/ Cl2'-Cu1' 2.381(4), Cu2-Cl2/ Cu2'-Cl2' 2.411(4), Cl2-Cu2'/ Cl2'-Cu2 2.569(4), P2-Cu2/ P2'-Cu2' 2.185(4), P1-Cu1/ P1'-Cu1' 2.163(4); Cu1-Cu2-Cu1'/Cu1-Cu2'-Cu1' 99.60(5), Cu2-Cu1-Cu2'/Cu2-Cu1'-Cu2' 80.40(5), P1-Cu1-Cu2/ P1-Cu1-Cu2 92.02(8), P2-Cu2-Cu1/ P2'-Cu2'-Cu1' 90.92(7), Cu2-Cl1'-Cu1'/Cu1-Cl1-Cu2' 77.20(9), Cu1-Cl2-Cu2/ Cu1'-Cl2'-Cu2' 69.97(7), Cu1-Cl2-Cu2'/ Cu1'-Cl2'-Cu2 70.42(7); For* **4.8**: *Cu2-Cu1/ Cu2'-Cu1' 2.650(1), Cu1-Cu2'/ Cu1'-Cu2 2.702(1), Cu2-Br1/' Br1-Cu2' 2.424(1), Cu1-Br1/ Cu1'-Br1' 2.4174(8), Cu1-Br2/ Br2'-Cu1' 2.736(1), Cu2-Br2/ Cu2'-Br2' 2.8641(1), Cu2-Br2'/ Cu2'-Br2 2.5598(9), Cu1-Br2'/ Cu1'-Br2 2.580(1), P2-Cu2/ P2'-Cu2' 2.192(2), P1-Cu1/ P1'-Cu1' 2.185(2); Cu1-Cu2-Cu1'/Cu1'-Cu2'-Cu1 87.53(3), Cu2-Cu1-Cu2'/Cu2'-Cu1'-Cu2 92.47(3), P1-Cu1-Cu2/ P1'-Cu1'-Cu2' 93.67(5), P2-Cu2-Cu1/ P2'-Cu2'-Cu1' 93.63(5), P1-N1-P2/ P1'-N1'-P2' 117.3(2), Cu2-Br1'-Cu1'/Cu1-Br1-Cu2' 67.83(3), Cu1-Br2-Cu2/ Cu1'-Br2'-Cu2' 56.43(2), Cu1-Br2-Cu2'/ Cu1'-Br2'-Cu2 59.23(2), Cu1-Br2'-Cu2/Cu1'-Br2-Cu2' 62.07(3), Cu1-Br2'-Cu2'/ Cu2-Br2-Cu1' 61.24(2).*

The molecular structures of complexes **4.7** and **4.8** with atom-numbering schemes are shown in *Figure 4.3(a)* and *(b)* respectively. The molecular structure of **4.7** consists of a [{Cu$_4$(μ_2-Cl)$_2$(μ_3-Cl)$_2$}] core [*Figure 4.3a)*, while the molecular structure of **4.8** contains a [{Cu$_4$(μ_2-Br)$_2$(μ_4-Br)$_2$}] core (*Figure 4.3b*). In complex **4.7** two of the four copper atoms are tetra-coordinated while the other two are tri-coordinated. Four copper atoms are arranged in a distorted rectangular shape. Two halide atoms are situated at apical positions above and below the plane and coordinated to the three copper atoms. These two halide atoms are

connected to three copper atoms, while there is no significant bonding interaction with the fourth copper atom [3.060(5) Å]. The other two halide atoms are connected in a μ_2-fashion with the copper atoms. In complex **4.8** capping halides are bonded to four copper atoms in a μ_4-fashion and are placed in axial positions above and below the Cu_4-plane, whereas both the bromine atoms above and below the core plane are not exactly equidistant from each of the copper atoms. One of the copper atoms is at a longer distance of 2.861(1) Å, while the other three copper atoms are at a distance of 2.580(1), 2.560(1), and 2.736(1) Å, from the bromine atom. The Cu–Cu distances in complexes **4.7** and **4.8** range from 2.65-2.87 Å.

4.3.2. *Synthesis and characterization of DPPA supported silver(I) complexes (4.9-4.12)*

Complexation of silver (I) triflate with DPPA ligands, **2.1**, **2.2**, **4.1**, and **4.2** affords silver(I) complexes **4.9-4.12** (*Scheme 4.2*). The reactions of AgOTf with DPPA ligands **2.1**, **2.2**, **4.1**, and **4.2** in 1:1 ratio in CH_2Cl_2 resulted in dinuclear dimeric silver(I) complexes. The purpose of synthesizing these complexes is to study the structural and Photo-physical properties of the silver (I) complexes. Silver complexes also shows cluster structure as like copper complexes.[25] But in this case we got only dimeric structure of silver complexes, the reason behind this might be the size of anion in silver salt which has been used for complexation and nature of ligand where there is phosphine group of DPPA ligand situated near to each other.[26] Whereas in case of copper complexes the copper salt (CuCl, and CuBr) which we used for complexation is small in size. All of these compounds are characterized by routine techniques (NMR, Mass, etc). Single crystals suitable for X-Ray diffraction studies were grown in CH_2Cl_2/*n*-pentane mixture. Phosphorus NMR of these complexes has been recorded. Complexes **4.9** and **4.12** show doublet of triplet in ^{31}P NMR spectrum with coupling constant (*J*) of 550 and 119 Hz, indicating coupling of Ag-P (figure 4A.7- 4A.10).[27] Whereas ^{31}P NMR spectra of **4.10** and **4.11** show a broad signal at 85.97 and 85.61 ppm, respectively. A sharp singlet in ^{19}F NMR was observed for all the silver complexes in the range of -77 to -79 ppm which matches well with the OTf group reported in the literature.[27] Molecular structures of all of the silver complexes show dimeric dinuclear framework with Ag...Ag distance in the range of 2.80-3.05 Ao which falls within the range of argentophilic

interaction (2.7-3.4 Ao). The P-Ag-P bond angles of **4.9-4.12** are in the range of 142-161o which are deviated from the linearity. **4.11** shows Ag…Ag distance 2.864 Ao which is the shortest among all other silver complexes.

(a)   (b)

*Figure 4.4. Molecular structure of **4.9** (a) and **4.10** (b) with anisotropic displacement parameters depicted at the 50% probability level. All hydrogen atoms, phenyl rings, and lattice solvent have been omitted for clarity. Selected Bond lengths (Å) and Selected Bond angles (o) for **4.9**: Ag1-Ag2 3.0202(8), Ag1-O1 2.508; Bond angles(o) P1-Ag1-P3 161.24(6)/158.64(6), P1-N1-P2 119.7(4); Selected Bond lengths (Å) and Selected Bond angles (o) for **4.10** Ag1-Ag2 3.0202(8), Ag1-O1 2.631(2); Bond angles(o) P1-Ag1-P3 152.00(2), P1-N1-P2 119.5(1)*

Unlike copper complexes (**4.3-4.8**) silver complexes (**4.9-4.12**) are found to be non-luminescent or weakly luminescent. To confirm the presence of Ag-Ag interaction we studied the Raman spectra of these complexes. But we able to record the spectra only for **4.9** and **4.10** (Appendix Figure 4A.11 and 4A.12). Other two complexes could not be characterized using Raman spectroscopy might be because of competent phenomena of fluorescence. In case of **4.9** and **4.10** we observed peaks at 88 and 90 cm^{-1} this peak corresponds to the Ag-Ag stretch fundamental and overtone bands.

(a)   *(b)*

Figure 4.6. *Molecular structure of **4.11** (a) and **4.12** (b) with anisotropic displacement parameters depicted at the 50% probability level. All hydrogen atoms and lattice solvent have been omitted for clarity. Selected Bond lengths (Å) and Selected Bond angles (°) for **4.11**: Ag1-Ag2 2.864(3), Ag1-O1 2.438(7) Ag1-O6 2.468(8); Bond angles(°) P1-Ag1-P3 144.84(7)/144.67(7), P1-N1-P2 122.4(4)/121.7(4); Selected Bond lengths (Å) and Selected Bond angles (°) for **4.12** Ag1-Ag2 3.054(1), Ag1-O1 2.425(3); Bond angles (°) P1-Ag1-P3 142.02(3), P1-N1-P2 120.2(2).*

4.3.3. *Photophysical studies of copper complexes **4.5-4.8***

Copper (I) halide complexes, especially the iodide derivatives, have been investigated extensively due to their intriguing photoluminescence properties. Hence, we have also studied the luminescence properties of complexes **4.5-4.8**. It has been observed that complexes **4.5-4.8** show mechanochromism as well as thermochromism.

We have investigated the frontier molecular orbitals for all the complexes to understand the difference in their properties. The stimuli-responsive properties of complexes **4.5-4.8** are explored in the solid state by studying their steady-state measurements (absorption-emission profile) and lifetimes.
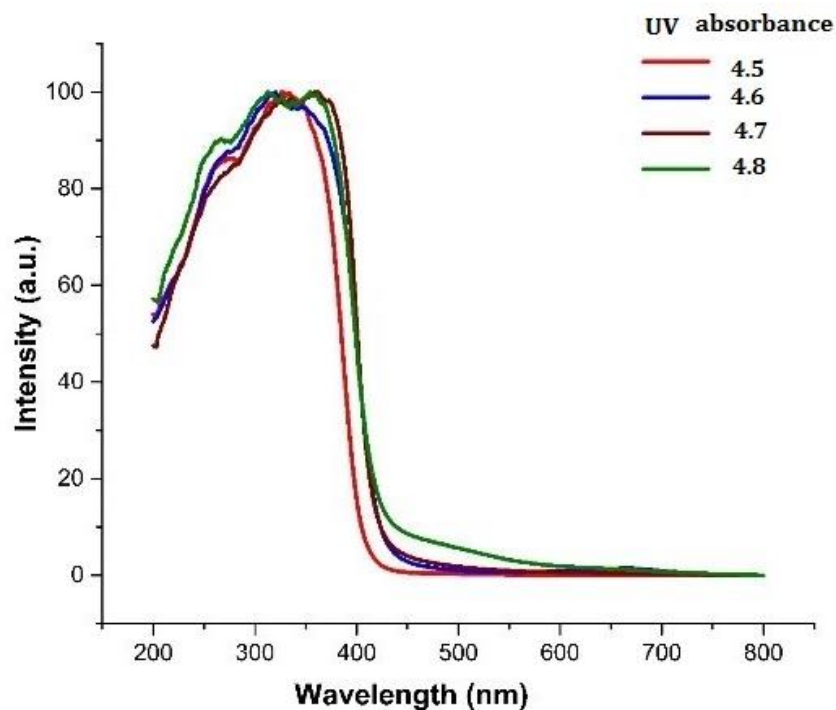
Figure 4.4. UV-visible absorbance spectra of 4.5-4.8 at room temperature in the solid state.

Complexes *4.5-4.8* are luminescent in the solid state and show orange to orangish-yellow luminescence under UV light, whereas they are very weakly emissive in solution. The absorption spectra of complexes *4.5-4.8* were recorded in the solid state at 298 K. UV/Visible absorption spectra of complexes *4.5-4.8* (*Figure 4.4*) show ligand-centered characteristic bands, n→π* and π→π* over the range 250–300 nm. The peaks from 330 to 370 nm indicate the halide-to-ligand charge transfer (XLCT) transition.[13b] Mechanochromism is the change of the color of emission upon addition of a mechanical stimulus, typically grinding of the samples. The unground and ground forms have a propensity to exhibit different molecular arrangements and intermolecular interactions, leading to different photophysical properties.[28] Upon grinding the solid samples of complexes **4.5–4.8** using a pestle and mortar, mechanochromic luminescence properties are observed. The otherwise non-luminescent complexes **4.5–4.8** become luminescent after grinding and show yellowish to orangish-yellow colors of emission upon irradiation of UV light [*Figure 4.5(b)*].
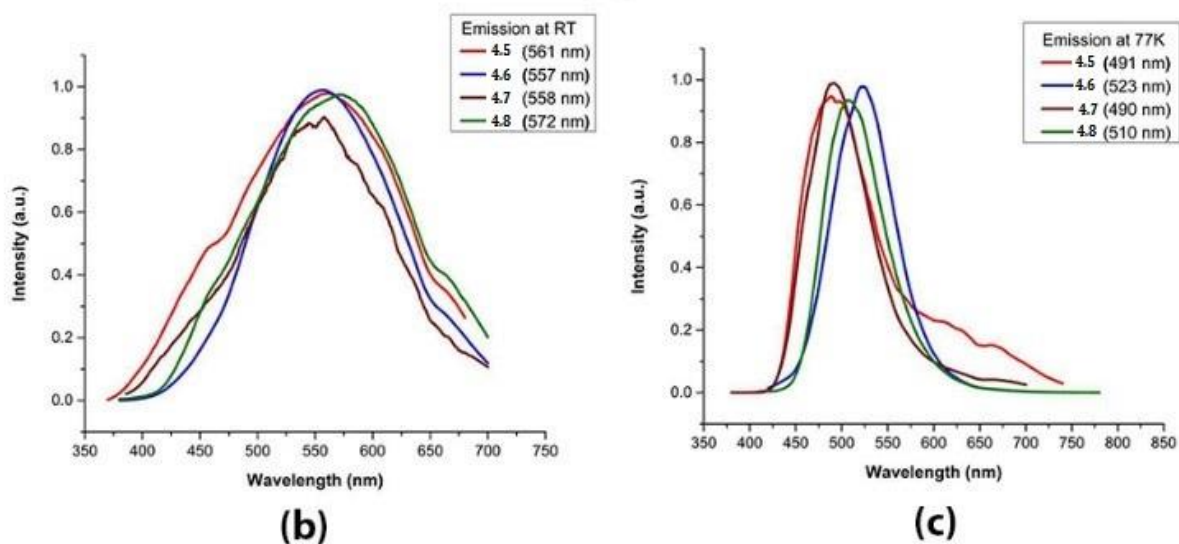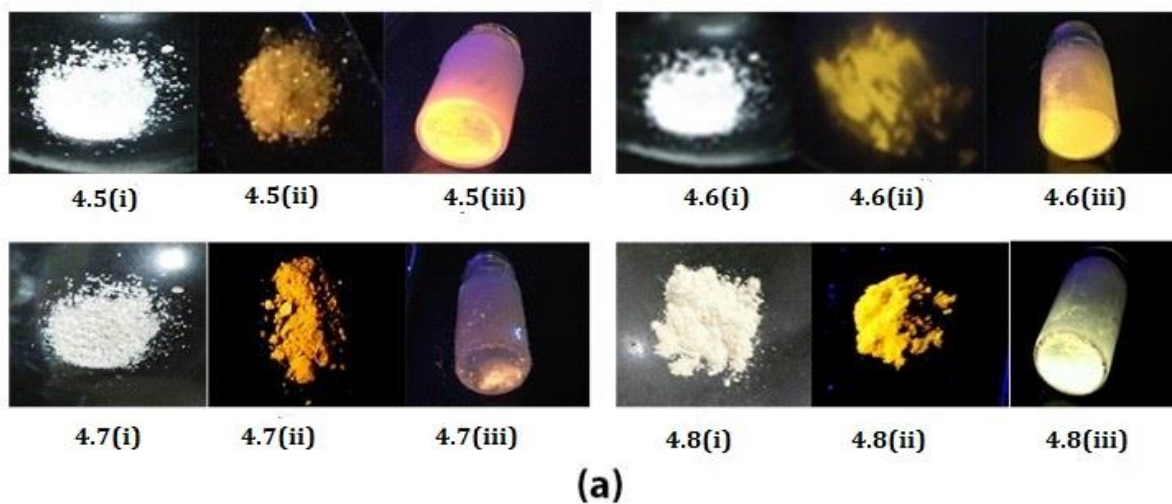
Figure 4.5*. (a) Images of ground samples of complexes **4.5**-**4.8** (i) under normal light, (ii) under UV light at room temperature, and (iii) under UV light at 77K; (b) Emission spectra of **4.5**-**4.8** (after grinding, solid state) at room temperature; (°c) at 77 K. [λex = 350 nm (**4.5**), 351 nm (**4.6**), 360 nm (**4.7**) and 360 nm (**4.8**)].*

Solid-state photoluminescence measurements of the ground samples of **4.5**–**4.8** reveal broad emission bands ranging from ca. 557–572 nm, thereby confirming the mechanochromism in these complexes. The emission bands observed at room temperature for complexes **4.5**–**4.8** (*Figure 4.5*) most likely originate from the cluster centered (^{3}CC) triplet excited state, which is a combination of halide-to-metal charge transfer (XMCT) and

copper-centered 3d→4s, 4p transitions.[29] The lifetime values for these complexes (**4.5–4.8**) are detected in *μs* (Table 1), reflecting that these emissions are from triplet excited states.[13b]

In addition to the mechanochromism compounds **4.5–4.8** also show thermochromism (*Figure 4.5*). Complexes **4.5**-**4.8** exhibit chromism when the ground solids are cooled (they return to their original emissions at r.t.) as shown in *Figure 4.5(c)*. The blue shift upon cooling at 77 K for complexes **4.5**-**4.8** can be attributed either to the structural changes of the multiplex excimer or lattice contraction.[30] Emission spectra of complexes **4.5**-**4.8** at 77 K show peaks at around the 490–520 nm region. It is assumed that at 77 K, the singlet state is more populated in comparison with the triplet state. Hence, a cluster-centered transition (^{1}CC) from the excited singlet state (S^1) to the singlet ground state (S^0) could be responsible for the emission at shorter wavelengths (high energy) upon cooling.[24]

4.3.4. *Powder-XRD studies of copper complexes* **4.5-4.8**

To understand whether mechanical grinding has caused any structural changes, powder X-ray diffraction (PXRD) analyses were performed with complexes 4.5-4.8 (Figure 4.6). All the complexes show weak diffractions in the ground PXRD pattern (4.5G-4.8G) as compared with those of the unground samples. The decrease in intensity and the presence of some ambiguous peaks in the PXRD spectra of the ground samples (4.5G-4.8G) suggest a change of the crystalline phase toward a microcrystalline and amorphous phase.[30]

To confirm our hypothesis, we dissolved the complexes in DCM and dried the solution quickly so that they could form only microcrystalline and amorphous solids instead of crystals. The quickly dried samples showed luminescence that was comparable to those obtained from ground samples. The PXRD patterns (4.5R-4.8R) of the dried samples showed lower 2θ peaks. However, higher 2θ peaks were diminished, thus confirming their microcrystalline and amorphous nature.[29-31] The mechanochromic luminescence is found to be reversible as after recrystallization the luminescence is not seen. The reason behind such mechanochromic behaviour might be the change in molecular arrangement and intermolecular interactions, leading to different photo-physical properties.
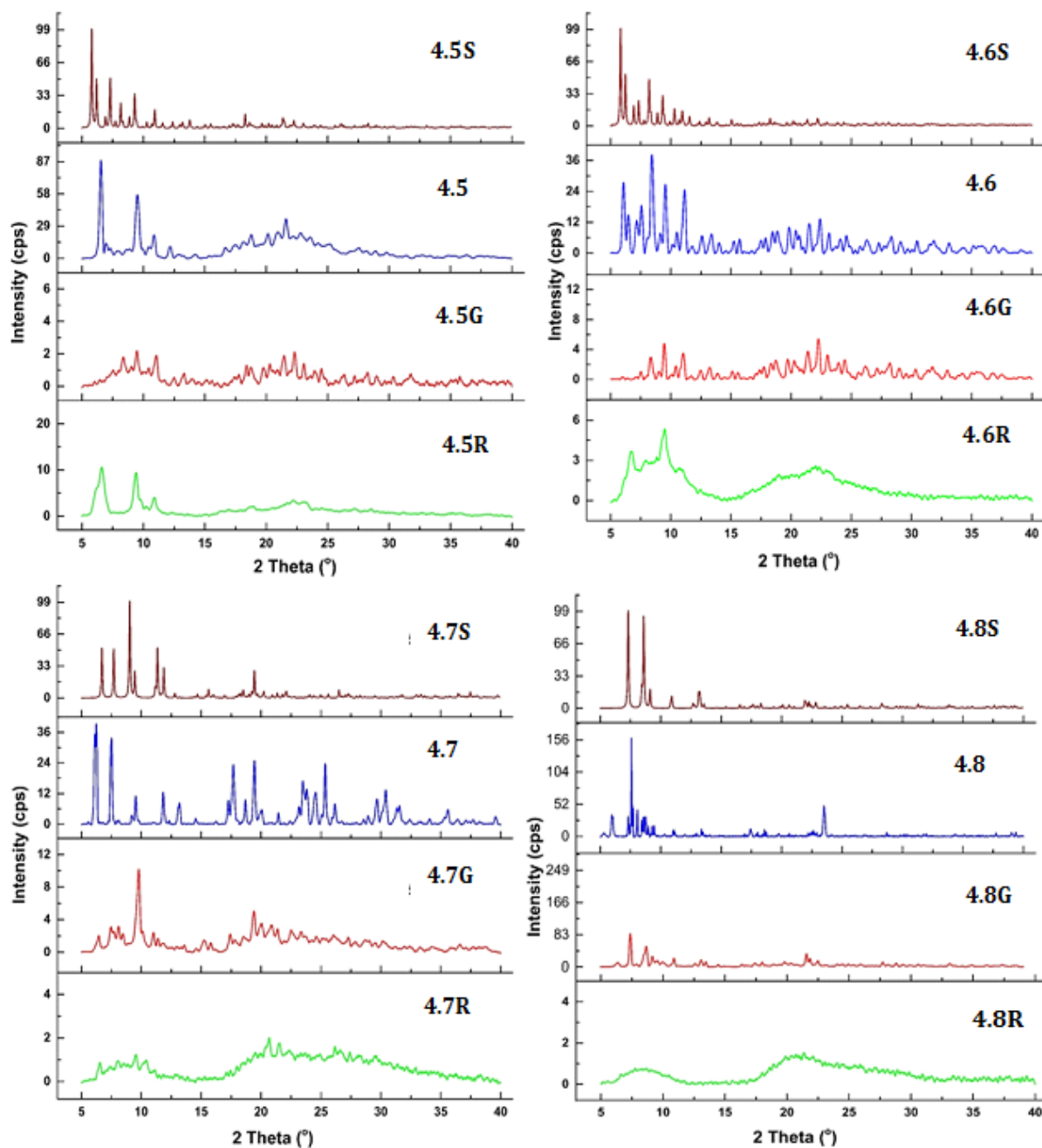
*Figure 4.6. The powder X-ray diffraction patterns of **4.5-4.8** in different states (S-simulated, unground, G-ground and R-recovered).*

Peaks with decreased intensity are observed in unground samples. Broadening of the overall pxrd pattern is observed this might be because of the phase change from crystalline to amorphous state of the complexes. The reason behind such broadening of peak might be

because of size confinement of the crystalline material which might be converting to nanoparticles.

4.3.5. *Theoretical investigation of 4.3-4.8*

The optimized structures are shown in *Figure 4.7*, and the computed structural parameters, i.e. bond lengths (Å) and angles (°) are also tabulated and compared in Table 4A.1 for **I** & **II** (previously reported), Table 4A.2 for **4.3** & **4.4,** Table 4A.3 for **4.5** & **4.6** and Table 4A.4 for **4.7** & **4.8**. In general, we observed a fair agreement between the computed structures and the structures obtained in the x-ray crystallographic studies.

To understand the luminescent properties and electronic structures, we have investigated the frontier molecular orbitals for all the complexes. The orbital energies are plotted in *Figure 4.7,* and we indeed observe a correlation between the luminescent properties and HOMO-LUMO energy gaps (ΔE) apart from the Cu····Cu interactions. The HOMO-LUMO gap for the luminescent complexes, i.e. **II** (Chart 4.1) and **4.8** are smaller by 45 meV and 245 meV than the corresponding copper (I) chloride complexes, i.e. **I** and **4.7**, respectively**.** In all other non-luminescent complexes (unground state), the HOMO-LUMO gap for the bromide complexes is higher than its chloride counterparts (*Figure 4.7*). The luminescence is an excited state phenomenon and controlled by the electronic structure of the excited states, the lifetime of the excited states and the mechanisms involved in the de-excitation processes. The electron-phonon couplings and the intersystem crossings also play the major role for the lifetimes of the excited state. The *ab initio* calculation of luminescence spectra is not straight forward as the excited states geometries, and wave functions optimizations are involved This is beyond the scope of the current work, however we have performed the TD-DFT calculations for complexes **I** & **II** and complexes **4.7** and **4.8** that provides the excitation spectra and their oscillator strengths that eventually provide an idea for the electronic transition from the ground state to the excited states.

The orbitals involved in these electronic excitations, i.e., HOMO to LUMO+3, HOMO-2 to LUMO and HOMO-1 to LUMO (*Figure 4.8*). Considering the fact that the electrons fall back from the excited state to the HOMO in the de-excitation process, we observed that the

LUMO+3 to HOMO transitions [i.e., halide (equatorial) to ligands transitions] are responsible for the luminescent spectra for complex **II** and **4.8**.
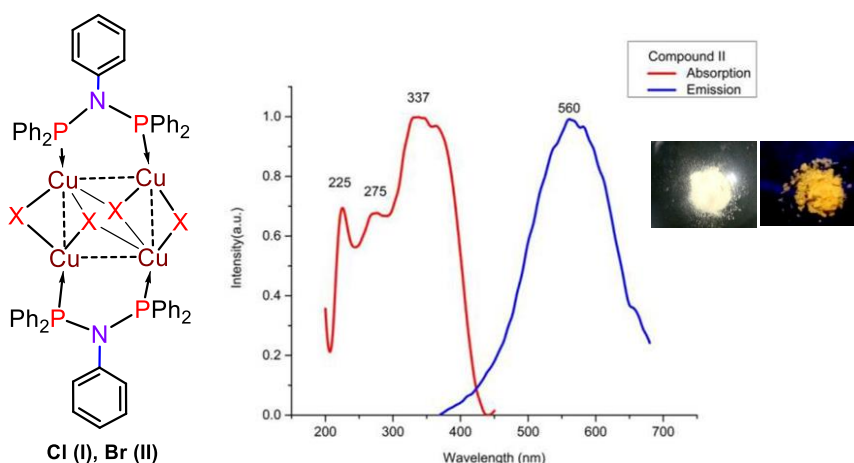
Chart 4.1. *UV-visible absorption and emission spectra of **II** in the solid state (λex = 337 nm).*

The dx^2-y^2 orbitals of Cu(I) atom significantly contributes to the HOMOs of all the complexes associated in this work. The planer arrangements of the Cu(I) atom assists the Cu···Cu interactions that originate from the bonding interactions between the dx^2-y^2 orbitals of the Cu(I). The square planner symmetric interaction for the bromide complexes (**II** & **4.8**) breaks down for complex **I** and **4.7.** This could be attributed to the additional bonding interactions between the P and Cu atomic orbitals. The utilization of the dx^2-y^2 atomic orbitals of the Cu-atoms for the additional Cu-P bonding (that decrease the Cu-P bond lengths) makes it unavailable for the Cu···Cu interactions. The Cu····Cu interactions are mainly driven by the dx^2-y^2 atomic orbitals of all the four Cu-atoms. In the case of luminescent molecules, all the four dx^2-y^2 orbitals of the Cu(I) atoms contributes equally that eventually reduces the intra copper distances in complex **6**. HOMO LUMO+3 **II 4.8** HOMO LUMO+3. In complex [Cu$_4$(μ_2-Cl)$_2$(μ_3-Cl)$_2$]{C$_7$H$_7$N(PPh$_2$)$_2$}$_2$] **4.7**, two chloride atoms were found to form μ_2-bridges and two in μ_3-bridges fashion. While in the case of [Cu$_4$(μ_2-Br)$_2$(μ_4-Br)$_2${C$_7$H$_7$N(PPh$_2$)$_2$}$_2$], i.e., complex **4.8**, two of bromide atoms are in μ_2-bridges with copper, and the other two were found in μ_4- fashion.
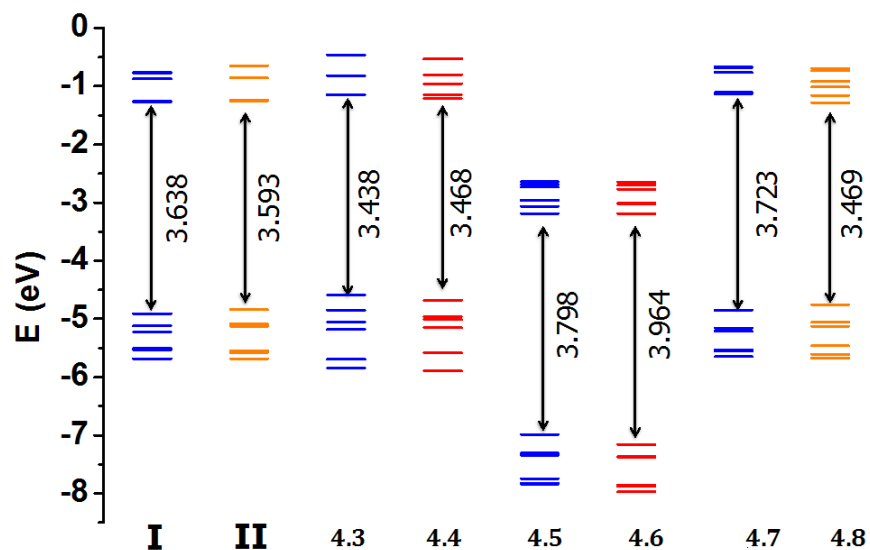
Figure 4.7. *The energy level diagrams correspondence to the frontier molecular orbitals (FMOs) calculated using the B3LYP/def2-TZVP(P) method. The HOMO-LUMO energy gaps for the luminescent complexes, i.e. **II** and **4.8** are smaller than the corresponding copper (I) chloride complexes, while higher for the non-luminescent complexes.*
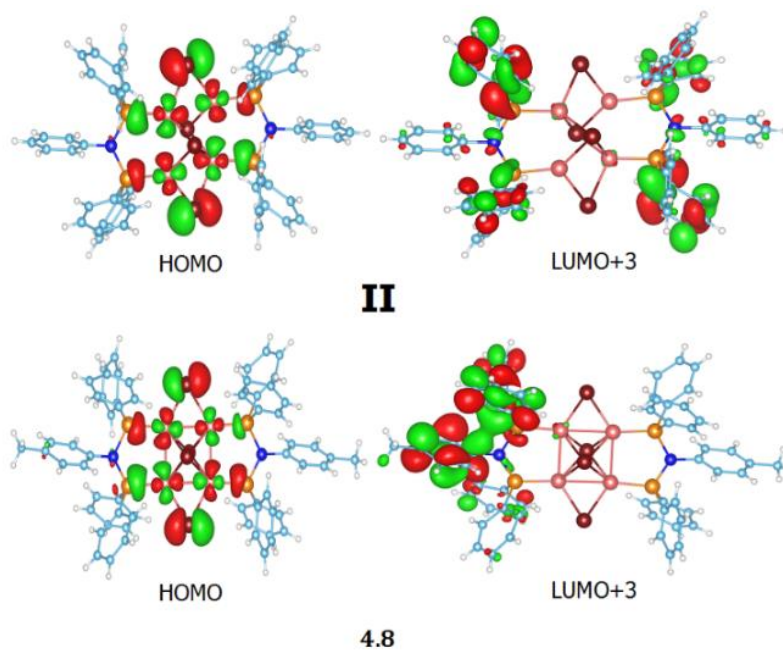
Figure 4.8. *Molecular orbitals involved in the emission properties of **II** and **4.8**.*
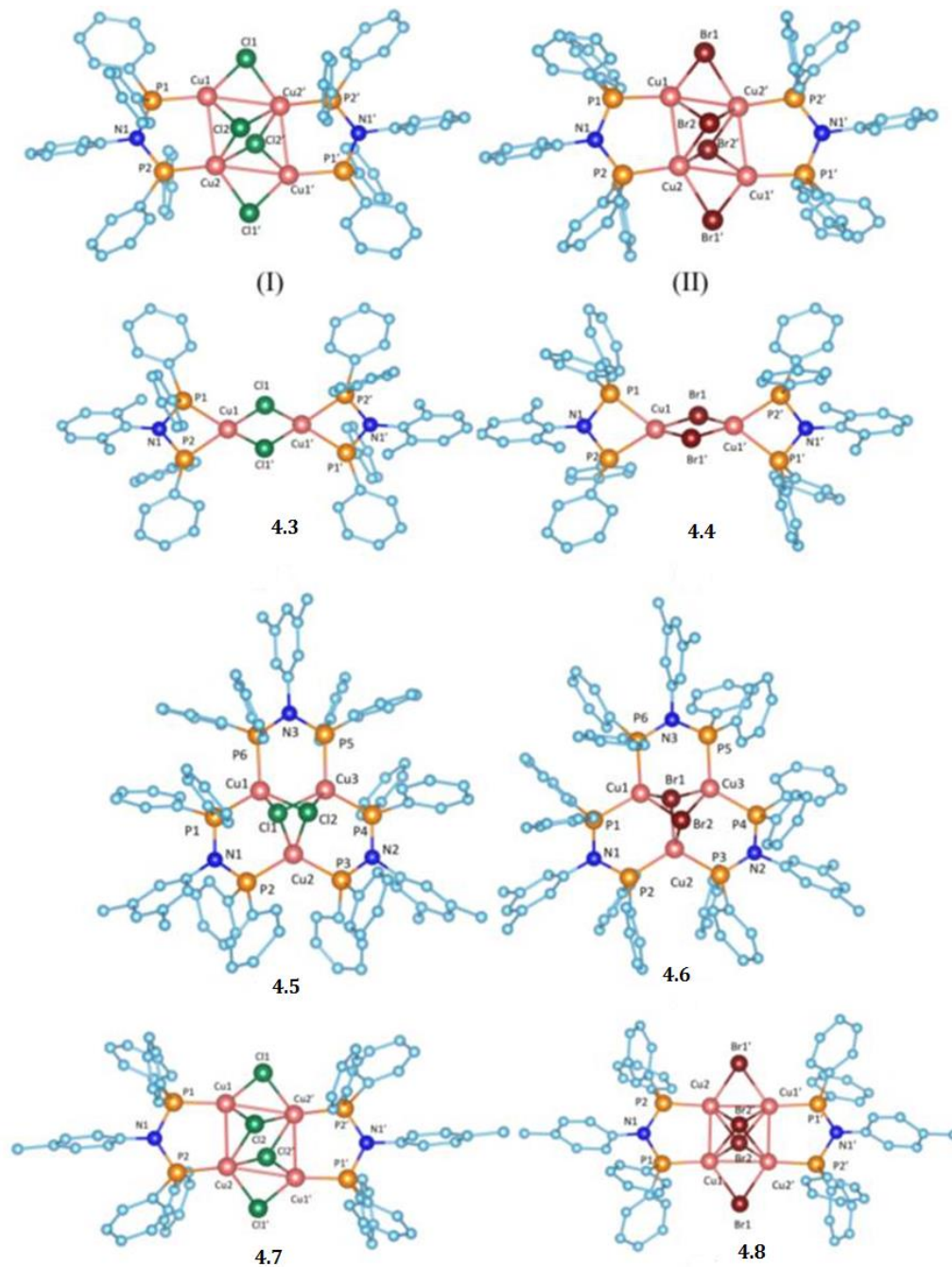
Figure 4.8. *Computed geometrical structures of Copper Complexes **(I)** [Cu$_4$(μ_2-Cl)$_2$(μ_3-Cl)$_2${C$_6$H$_5$N(PPh$_2$)$_2$}$_2$] **(II)** [Cu$_4$(μ_2-Br)$_2$(μ_4-Br)$_2${C$_6$H$_5$N(PPh$_2$)$_2$}$_2$] **(4.3)** [Cu$_2$(μ_2-Cl)$_2${C$_8$H$_9$N(PPh$_2$)$_2$}$_2$] **(4.4)** [Cu$_2$(μ_2-Br)$_2${C$_8$H$_9$N(PPh$_2$)$_2$}$_2$] **(4.5)** [Cu$_3$(μ_3-Cl)$_2${C$_8$H$_9$N(PPh)$_2$}$_3$] **(4.6)** [Cu$_3$(μ_3-Br)$_2${C$_8$H$_9$N(PPh)$_2$}$_3$] **(4.7)** [Cu$_4$(μ_2-Cl)$_2$(μ_3-Cl)$_2${C$_7$H$_7$N(PPh$_2$)$_2$}$_2$] **(4.8)** [Cu$_4$(μ_2-Br)$_2$(μ_4-Br)$_2${C$_7$H$_7$N(PPh$_2$)$_2$}$_2$]. Hydrogen atoms are omitted for clarity. Color code Green Cl, Cayenne Br, Salmon Cu, Tangerine P, Sky C, Blueberry N.*

Cu2-Cu1/ Cu2'-Cu1' bond lengths are smaller (by ~0.073Å) than the experimental values, while the Cu1-Cu2'/ Cu1'-Cu2 distance is larger by ~0.02 Å. All the four calculated Cu-Cu-Cu bond angles in compound **4.7** and **4.8** are found in the range of 77.30 - 102.70°. All the three Cu-Cl-Cu angles in complex **4.7** are (69.01 to 77.19°) corresponds well with the experimental values. The Cu-Br-Cu bond angles in complex **4.8** are in the range of 53.80 to 68.25° (Table 4A.4).

4.4.   Conclusion

In this study, we have shown that the reactions of copper halides with PNP ligands that have the methyl substituent at either the *ortho*, *meta*, and or *para* position led to the formation of complexes with different nuclearities such as dinuclear (**4.3** and **4.4**), trinuclear (**4.5** and **4.6**), and tetranuclear complexes (**4.7**and **4.8**). The formulation of **4.3-4.8** was validated by single-crystal X-ray diffraction studies. Among these complexes, **4.5-4.8** exhibit mechanochromismas well as thermochromism. PXRD patterns reveal that the luminescence properties of complexes **45-4.8** arise from their phase transition from crystalline to microcrystalline/ amorphous nature upon grinding of their solid samples. This study exemplifies the importance of the position of the substituents in the ligand backbone, which may result in novel thermo- and mechanochromic properties of the derived complexes. Similarly, we synthesized DPPA supported Silver (I) triflate complexes (**4.9-4.12**) with Ag-Ag distance ranging from 2.80-3.05 A°. Ag-Ag bond stretching is confirmed by Raman spectra of some of silver complexes. Although these complexes show argentophilic interaction (range 2.7-3.4 A°), they found to be weakly luminescent and nonluminescent.

4.5.   References

1. (a) Yam, V. W.-W; Lo, K. K.-W. *Chem. Soc. Rev.* **1999**, *28,* 323. (b) R. Peng, M. Li, D. Li, Coord. Chem. Rev. **2010**, 254, 1. (c) Y. Takemura, T. Nakajima, T. Tanase, *Dalton Trans.* **2009**, 10231.

2. (a) Pyykkö, P. *Chem. Rev*. **1997**, *97*, 597. (b) Schmidbaur, H.; Schier, A. *Angew. Chem. Int. Ed.* 2015, *54*, 746-784; *Angew. Chem.* **2015**, *127*, 756. (c) Che, C. M. ; Mao, Z.; Miskowski,

V. M.; Tse, M. C.; Chan, C. K.; Cheung, K.-K.; Phillips, D. L.; Leung, K.-H. *Angew. Chem. Int. Ed.* **2000**, *39*, 4084.

3. (a) Bardaji, M.; Laguna, A.; Jones, P. G.; Fischer, A. K. *Inorg. Chem.* **2000**, *39*, 3560. (b) Catalano, V. J.; Horner, S. J. *Inorg. Chem.* **2003**, *42*, 84300. (c) He, X.; Yam, V. W.-W. *Coord. Chem. Rev.* **2011**, *255*, 2111. (d) K. Tsugea, Y. Chishinab, H. Hashiguchib, Y. Sasakib, M. Kato, S. Ishizaka, N. Kitamurab, Coord. Chem. Rev. 2016, 306, 636–651.

4. (a) Guo, X.-X.; Gu, D.-W.; Wu, Z.; Zhang, W. *Chem. Rev.* **2015**, *115*, 1622. (b) Allen, S. E.; Walvoord, R. R.; Padilla-Salinas, R.; M. C. Kozlowski, *Chem. Rev.* **2013**, *113*, 6234.

5. (a) Xu, H.; Chen, R. ; Sun, Q.; Lai, W.; Su, Q. ; Huang, W.; Liu, X. *Chem. Soc. Rev*. **2014**, *43*, 3259. (b) Osawa, M.; Kawata, I.; Ishii, R.; Igawa, S.; Hashimoto, M.; Hoshinoa, M. J. *Mater. Chem. C* **2013**, *1*, 4375. (c) Liu, Z.; Qayyum, M. F.; Wu, C.; Whited, M. T.; Djurovich, P. I.; Hodgson, K. O.; Hedman, B.; Solomon, E. I.; Thompson, M. E. *J. Am. Chem. Soc*. **2011**, *133*, 3700.

6. (a) Kyle, K. R.; Ryu, C. K.; DiBenedetto, J. A.; Ford, P. C. *J. Am. Chem. Soc.* **1991**, *113*, 2954. (b) Rath, N. P.; Holt, E. M. *J. Chem. Soc., Dalton Trans*. **1986**, 2303. (c) N. P. Rath, E. M. Holt, K. Tanimura, *Inorg. Chem*. **1985**, *24*, 3934.

7. (a) Li, D.; Yip, H. K.; Che, C.-M.; Zhou, Z.-Y.; Mak, T. C. W.; Liu, S.-T.; *J. Chem. Soc., Dalton Trans.* **1992**, 2445. (b) Yam, V. W.-W.; Fung, W. K.-M.; Wong, M.- T. *Organometallics* **1997**, *16*, 1772. (c) Roesch, P.; Nitsch, J.; Lutz, M.; Wiecko, J.; Steffen, A.; Müller, C. *Inorg. Chem*. **2014**, *53*, 9855. (d) Zink, D. M.; Baumann, T.; Friedrichs, J.; Nieger, M.; Bräse, S. *Inorg. Chem.* **2013**, *52*, 13509.

8. Harvey, P. D.; Drouin, M.; Zhang, T. *Inorg. Chem*. **1997**, *36*, 4998.

9. (a) Sabin, F.; Ryu, C. K. ; Ford, P. C. ; Vogler, A. *Inorg. Chem*. **1992**, *31*, 1941. (b) Fujisawa, K.; Imai, S.; Kitajima, N.; Moro-oka, Y. *Inorg. Chem*. **1998**, *37*, 168.

10. Pal, S.; Kathewad, N.; Pant, R.; Khan, S. *Inorg. Chem*. **2015**, *54*, 10172.

11. Khan, S.; Ahirwar, S. K.; Pal, S.; Parvin, N.; Kathewad, N. *Organometallics* **2015**, *34*, 5401.

12. Parvin, N.; Dasgupta, R.; Pal, S.; Sen, S. S.; Khan, S. *Dalton Trans*. **2017**, *46*, 6528.

13. (a) Ahuja, R.; Nethaji, M.; Samuelson, A. G. *Inorg. Chim. Acta* **2011**, *372*, 220. (b) Biricik, N.; Durap, F.; Kayan, C.; Gümgüm, B. *Heteroat. Chem*. **2007**, *18*, 613. (c) Naik, S.; Mague, J. T.; Balakrishna, M. S. *Inorg. Chem*. **2014**, *53*, 3864.

14. (a) Pintado-Alba, A.; de la Riva, H.; Nieuwhuyzen, M.; Bautista, D.; Raithby, P. R.; Sparkes, H. A.; Teat, S. J.; López-de-Luzuriagae, J. M.; Lagunas, M. C.; *Dalton Trans*. **2004**, 3459. (b) Zhang, T.-T.; Jia, J.-F.; Ren, Y.; Wu, H.-S. *J. Phys. Chem. A* **2011**, *115*, 3174. (c) Daumann, L. J.; Tatum, D. S.; Andolina, C. M.; Pacold, J. I.; D′Aléo, A.; Law, G.-I.; Xu, J. J.; Raymond, K. N. *Inorg. Chem*. **2016**, *55*, 114.

15. (a) Wang, c.-f.; peng, s.-m. *Polyhrdron* **1996**, *15,* 853. (b) Catalano, V. J.; Horner, S. J. *Inorg. Chem.*, **2003**, *42*, 8430. (c) Crespo, O.; Gimeno, M. C.; Laguna, A.; Larraz, C. *Z. Naturforsch.* 2009, *64b,* 1525. (d) Cui, Y.-Z.; Yuan, Y.; Han, H.-L.; Li, Z.-F.; Liu, M.; Jin, Q.-H.; Yang, Y.-P.; Zhang, Z.-W. *Z. Anorg. Allg. Chem*. **2016**, *642*, 953.

16. (a) Kottke, T.; Stalke, D. J. *Appl. Crystallogr*. **1993**, *26*, 615. (b) Stalke, D. J. *Chem. Soc. Rev.* **1998**, *27*, 171. (c) Sheldrick, G. M. *Acta Crystallogr., Sect. A: Found. Crystallogr*. **2008**, *64*, 112. (d) Schulz, T.; Meindl, K.; Leusser, D.; Stern, D.; Graf, J.; Michaelsen, C.; Ruf, M.; Sheldrick, G. M.; Stalke, D. J. *Appl. Crystallogr*. **2009**, *42*, 885.

17. Trivedi, M.; Singh, G.; Kumar, A.; Rath, N. P. *Dalton Trans*. **2014**, *43*, 13620.

18. a) Kresse, G.; Hafner, J. *J. Phys. Rev. B: Condens. Matter Mater. Phys*. **1993**, *47*, 558. (b) Kresse, G.; Hafner, J. *J. Phys. Rev. B: Condens. Matter Mater. Phys.* **1994**, *49*, 14251. (c) Kresse, G.; Furthmüller, J. *J. Comput. Mater. Sci.* **1996**, *6*, 15. (d) Kresse, G.; Furthmüller, J. *J. Phys. Rev. B: Condens. Matter Mater. Phys.* **1996**, *54*, 11169.

19. (a) Kresse, G.; Joubert, D. *Phys. Rev. B: Condens. Matter Mater. Phys*. **1999**, *59*, 1758. (b) Blöchl, P. E. *Phys. Rev. B: Condens. Matter Mater. Phys*. **1994**, *50*, 17953.

20. Perdew, J. P.; Ruzsinszky, A.; Csonka, G. I.; Vydrov, O. A.; Scuseria, G. E.; Constantin, L. A.; Zhou, X.; Burke, K. *Phys. Rev. Lett*. **2008**, *100*, 136406.

21. (a) Schäfer, A.; Horn, H.; Ahlrichs, R. *J. Chem. Phys.* **1992**, *97*, 2571. (b) Ansgar, S.; Huber, C.; Ahlrichs, R. *J. Chem. Phys.* **1994**, *100*, 5829. (c) Weigend, F.; Ahlrichs, R. *Phys. Chem. Chem. Phys.* **2005**, *7*, 3297.

22. a) Neese, F.; Wennmohs, F. *ORCA (3.0.3)-An ab initio, DFT and semiempirical SCF-MO package, (Max-Planck-Institute for Chemical Energy Conversion Stiftstr. 34-36*, 45470 Mülheim a. d. Ruhr, Germany (b) Neese, F.; Wennmohs, F.; Hansen, A.; Becker, U. *Chem. Phys.* **2009**, *356*, 98. (c) Mingos, D. M. P.; Dahl, J. P. eds. 2. *Springer Science & Business Media*, **2012.** (d) Petrenko, T.; Kossmann, S.; Neese, F. J*. Chem. Phys*. **2011**, *134*, 054116.

23. a) Daly, S.; Haddow, M. F.; Orpen, A. G.; Rolls, G. T. A.; Wass, D. F.; Wingad, R. L.; *Organometallics* **2008**, *27*, 3196. (b) Bera, J. K.; Nethaji, M.; Samuelson, A. G. *Inorg. Chem.* **1999**, *38*, 218.

24. Trivedi, M.; Singh, G.; Kumar, A. ; Rath, N. P. *Dalton Trans*. **2014**, *43*, 13620.

25. (a) Njogu, E. M.; Omondi, B.; Nyamori, V. O. *J. Coord. Chem.* **2015**, 68, 3593. (b) Young, A. G.; Hanton, Lyall R. *Coord. Chem. Rev.* **2008**, *252*, 1346. (c) Yan, C.-F.; Lin, Y.-X. Jiang, F.-L.; Hong, M.-C., *Inorg. Chem. Commun.*, **2014**, *43*, 19.

26. Krishna, H.; Krishnamurthy, S. S.; Nethaji, M., *Polyhedron,* **2006**, *25*, 3189.

27. (a) Krishna, H.; Krishnamurthy, S. S.; Nethaji, M. *Polyhedron*, **2006,** *25,* 3189. (b) Lettko, L; Wood, J. S.; Rausch, M. D. *Inorg. Chim. Acta* **2000**, *308*, 37

28. a) Beyer, M. K.; Clausen-Schaumann, H. *Chem. Rev.* **2005**, *105*, 2921. (b) Wen, T.; Zhang, D.-X.; Liu, J.; Lin, R.; Zhang, J. *Chem. Commun.* **2013**, *49*, 5660. (c) Shan, X.-C.; Jiang, F.-L.; Chen, L.; Wu, M.-Y.; Pan, J.; Wan, X.-Y.; Hong, M.-C. *J. Mater. Chem. C* **2013**, *1*, 4339.

29. (a) Ford, P. C.; Vogler, A. *Acc. Chem. Res.* **1993**, *26*, 220. (b) Vitale, M.; Palke, W. E.; Ford, P. C. *J. Phys. Chem.* **1992**, *96*, 8329. (c) Deshmukh, M. S.; Yadav, A.; Pant, R.; Boomishankar, R. *Inorg. Chem.* **2015**, *54*, 1337.

30. (a) Zhang, J.-X.; He, J.; Yin, Y.-G.; Hu, M.-H.; Li, D.; Huang, X.-C. *Inorg. Chem.* **2008**, *47*, 3471. (b) Dias, H. V. R.; Diyabalanage, H. V. K.; Rawashdeh-Omary, M. A.; Franzman, M. A.; Omary, M. A. *J. Am. Chem. Soc.* **2003**, *125*, 12072.

31. (a) Wong, B. Y.-W.; Wong, H.-L.; Wong, Y.-C.; Au, V. K.-M.; Chan, M.-Y.; Yam, V. W.-W. *Chem. Sci.* **2017**, *8*, 6936. (b) Benito, Q.; Le Goff, X. F; Maron, S.; Fargues, A.; Garcia, A.; Martineau, C.; Taulelle, F.; Kahlal, S.; Gacoin, T. ; Boilot, J.-P. ; Perruchas, S. *J. Am. Chem. Soc.* **2014**, *136*, 11311. (c) Lv, Y.; Liu, Y.; Ye, X.; Liu, G.; Tao, X. *Cryst. Eng. Comm.* **2015**, *17*, 526. (d) Li, Y. G.; Kong, X. Q.; Zhuang, W.; Wang, Y. *J. Mater. Chem. C* **2017**, *5*, 8527.

Chapter 5

Palladium Catalyzed C-N Cross-Coupling of Sterically Hindered Aryl Bromide Using Efficient Diphosphinoamine Ligands

5.1.   Introduction

The discovery of palladium catalyzed C-N cross coupling, namely Buchwald-Hartwig coupling, is a significant breakthrough in organic chemistry due to its importance in the synthesis of pharmaceutical drugs, dyes, polymers, and natural products etc.[1-6] While the Migita and coworkers commenced the Pd catalyzed cross-coupling reactions,[7] the more accessible routes were established by the groups of Buchwald and Hartwig.[8] The most common ligands for the C-N coupling reactions are BINAP,[9] dppf,[10] Xantphos,[11] Josiphos,[12] Xphos,[13] N-heterocyclic carbenes[14], and several phosphines.[15-26] Nevertheless, there are very few ligands available for the coupling of bulky substrates but their substrate scope is very limited, and sometimes the yield of the reactions are also not very high (vide infra).[17,23,26] Moreover, the synthesis of ligand itself is challenging in many cases.[23,26] A further encouragement comes from the recent works by Buchwald and coworkers stating the importance of developing new ligands which can provide a broad substrate scope especially for sterically demanding groups.[8e] Hence, it is deemed desirable to have easily accessible ligands in C-N coupling reactions which can be used for a broad substrate scope for bulky substituents along with high isolated yields of the coupling products. Recently, we have reported diphosphinoamine [(Ph$_2$P)$_2$N(Ar)] based ligands to make luminescent Au(I) and Cu(I) complexes.[27-28] Since bidentate phosphine ligands have already shown their potentials in the C-N coupling reactions, we also got motivated to explore our bidentate PNP ligands [(Ph2P)$_2$N(Ar)] in such catalytic system. These PNP-ligands [(Ph$_2$P)$_2$N(Ar); **5.1** (Ar = C$_6$H$_5$), **5.2** (Ar = 2,6-iPr$_2$C$_6$H$_3$)] (Chart 5.1) are very easy to prepare in bulk scale (90-93% yield). Herein, we report C-N coupling of sterically demanding substrates by using ligands **5.1** and **5.2** in combination with a palladium source by conventional method as well as under microwave assistance (15-30 min). Our ligands **5.1** and **5.2** were found very efficient even in the coupling of very bulky amine Ar*NH$_2$ [Ar*= 2,6-{C(H)Ph$_2$}2-4-MeC$_6$H$_2$][29a] with various bromo substrates (>90% yield), which were obtained in very low yield (~30-65%) with the previously reported ligands (vide infra).[29b] Moreover, -CF$_3$ substituted bromo derivatives also afforded ~90-98% yield of coupled products, which were otherwise obtained in ~28-58% yields respectively.[30]

2.1   **2.3**
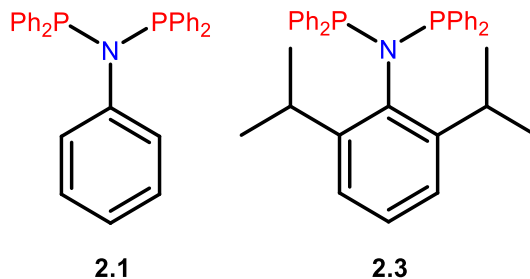
Chart 5.1. *Ligands (**2.1** and **2.3**) used for coupling reactions and selected examples of this work.*

Since bidentate phosphine ligands have already shown their potential in C-N coupling reactions, we also got motivated to explore our bidentate PNP ligands [(Ph$_2$P)$_2$N(Ar)] in such catalytic system. These PNP-ligands [(Ph$_2$P)$_2$N(Ar); **2.1** (Ar = C$_6$H$_5$), **2.3** (Ar = 2,6-iPr$_2$C$_6$H$_3$)] (*Chart 5.1*) are very easy to prepare in bulk scale and cost effective. Herein, we report C-N coupling of sterically demanding substrates by using ligands **2.1** and **2.3** in combination with palladium source by conventional method as well as under microwave assistance. Ligands, **2.1** and **2.3**, were prepared very good yields (90-93%) by literature method.[28]

5.2.   Experimental Section

5.2.1. General Remarks

General: All manipulations were performed under a dry and oxygen-free atmosphere (N$_2$) using standard Schleck techniques and glove box. All solvents were dried over activated molecular sieves after distillation. 200-300 mesh silica gel was employed for column chromatography.^{1}H, ^{13}C, ^{19}F solution NMR spectra were recorded on Jeol and Bruker 400 MHz instrument. Fourier-transform infrared (FT-IR) spectra were taken on a PerkinElmer spectrophotometer.

5.2.2. Synthesis and characterization

Typical procedure for coupling reactions

NaO^{t}Bu (7 eq), Pd (dba)$_2$ (5 mol%), PNP ligand **2.1** (5 mol%) or **2.3** (5 mol%) was taken in 100 mL schlenk flask inside the glove box. To that flask toluene, aromatic amine (1 eq.) and aromatic bromide (1 eq.) was added, and the reaction mixture was subjected to conventional heating (110°C for 5 d). Reaction completion monitored by TLC and NMR and purified using column chromatography using ethyl acetate and *n*-Hexane mixture (2% EA + 98% *n*-Hexane).Required amount of NaOtBu (7 eq), 5 mol% of Pd (dba)$_2$ and 5 mol% PNP ligand (**2.1** or **2.3)** was taken in microwave tube inside the glove box. 4 mL of toluene added to that tube and required amount of aromatic amine and aromatic bromide was added and subjected to microwave heating (184°C for 15-30 min) reaction. Reaction completion monitored by TLC and NMR and some of the compounds purified using column chromatography using ethyl acetate and *n*-Hexane mixture (2% EA + 98% *n*-Hexane).
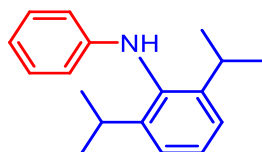
5.3a: Conventional heating method: 2,6-diisopropylaniline 1.88 mL (10 mmol) , bromobenzene 1.05 mL (10 mmol), Yield: **2.1** = 2.18 gm (86%), **2.3** = 2.36 gm (92%). Microwave heating method: 2,6-diisopropylaniline 0.19 mL (1 mmol), bromobenzene 0.11 mL (1mmol), Yield: **2.1** = 0.21 gm (83%), **2.3** = 0.23 gm (90%); ^{1}H NMR (CDCl$_3$, 400 MHz, ppm) : δ 1.17 (*d,* 12H, J= 6.9 Hz, C*H$_3$*), 3.14-3.31 (*m*, 2H, (CH$_3$)$_2$C*H*), 5.14 (*s*, 1H, N*H*), 6.51 (*d*, J = 8.5 Hz, 2H, Ph), 6.74 (*t*, J = 7.3 Hz, 1H, Ph), 7.18 (*dd*, 3H, J=22.2 Hz, Ph), 7.31 (*dd*, *J* = 14.4, 7.7 Hz, 2H, Ph); ^{13}C NMR (CDCl$_3$, 100.613 MHz, ppm) δ 148.1 (Ph), 147.9 (Ph), 147.6 (Ph), 147.6 (Ph), 135.2 (Ph), 135.1 (Ph), 129.2 (Ph), 127.2 (Ph), 123.8 (Ph), 117.7 (Ph), 113.0 (Ph), 28.2 [*C*H(CH$_3$)], 23.8 (*C*H$_3$); IR (cm^{-1}) : 688.62, 742.28, 800.11, 1056.91, 1257.62, 1308.28, 1454.05, 1495.84, 1601.34, 2961.08, 3402.80; HRMS (positive ESI) : 254.1917 (100 % M$^+$ +H)
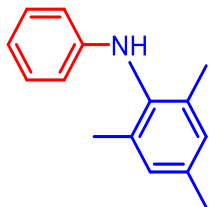
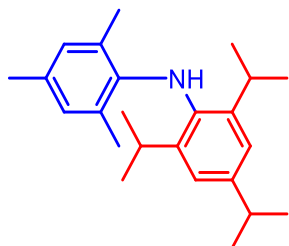**5.3b**: Conventional heating method: 2,4,6-trimethylaniline 0.35 mL (2.5 mmol), bromobenzene 0.26 mL (2.5 mmol), Yield: **2.1** = 0.48 gm (90%), **2.3** = 0.49 gm (92%). Microwave heating method: 2,4,6-trimethylaniline 0.35 mL (1 mmol), bromobenzene 0.26 mL (1mmol) Yield **2.1** = 0.19 gm (91%), **2.3** = 0.19 (90%); ^{1}H NMR (CDCl$_3$, 400 MHz, ppm) δ 2.24 (s, 6H, *o-C*H$_3$) 2.31 (s, 3H, *p-C*H$_3$), 5.10 (s, 1H, N*H*), 6.92 (d, J = 19.4 Hz, 7H, Ph); ^{13}C NMR (CDCl$_3$, 100.613 MHz, ppm) δ 146.7 (Ph), 136.1 (Ph), 135.6 (Ph), 135.5 (Ph), 129.3 (Ph), 118.0 (Ph), 113.3 (Ph), 21.0 (*p-C*H$_3$), 18.4 (*o-C*H$_3$); IR (cm^{-1}) : 685.24, 738.33, 797.04, 1017.62, 1301.56, 1488.69, 1596.67, 2920.95, 3086.04 ; HRMS (positive ESI) : 212.1452 (100 % M$^+$ +H)
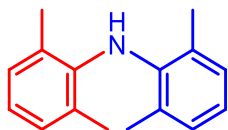
5.3c: Conventional heating method: NaOtBu, 2,6-dimethylaniline 0.31 mL (2.5 mmol), 2,6-dimethylbromobenzene 0.33 mL (2.5 mmol), Yield: **2.1** = 0.51 gm (91%), **2.3** = 0.55 gm (98%). Microwave heating method: 2,6-dimethylaniline 0.12 mL (1 mmol), 2,6-dimethylbromobenzene 0.13 mL (1 mmol), Yield **2.1** = 0.20gm (88%), **2.3** = 0.21 gm (92%); ^{1}H NMR (CDCl$_3$, 400 MHz, ppm) : δ 2.02 (*s,* 12H, C*H*$_3$, Ph), 4.81 (*s*, 1H, N-*H*), 6.79-6.93 (*m*, 2H, Ph), 6.99 (*d*, J = 7.5 Hz, 4H, Ph); ^{13}C NMR (CDCl$_3$, 100.613 MHz, ppm) : δ 141.8 (Ph), 129.7 (Ph), 128.8 (Ph), 121.8 (Ph), 19.2 (*o-C*H$_3$); IR (cm^{-1}) : 791.48, 1011.91, 1087.26, 1259.16, 1433.55, 2922.27, 2961.26; HRMS (positive ESI) : 226.1599 (100 % M$^+$+H)
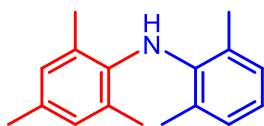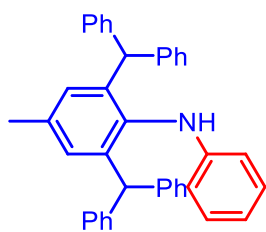

5.3d: Conventional heating method: 2,6-dimethylaniline 0.31 mL (2.5 mmol), 2,4,6-trimethyl-1-bromobenzene 0.38 mL (2.5 mmol), Yield **2.1** = 0.52 gm (87%), **2.3** = 0.56 gm

(94%). Microwave heating method: 2,6-dimethylaniline 0.12 mL (1 mmol), 2,4,6-trimethyl-1-bromobenzene 0.15 mL (1 mmol), Yield **2.1** = 0.21 gm (88%) **2.3** = 0.23 gm (95%); ^{1}H NMR (CDCl$_3$, 400 MHz, ppm) : δ 2.02 (*d*, 12H, J= 2.2 Hz, C*H$_3$*-*o*Ph), 2.28 (*s*, 3H, C*H$_3$*-*p*Ph), 4.74 (*s*, 1H, N*H*), 6.83 (*s*, 3H, Ph), 6.99 (*d*, J = 7.5 Hz, 2H, Ph); ^{13}C NMR (CDCl$_3$, 100.613 MHz, ppm): δ 142.2 (Ph), 139.0 (Ph), 131.6 (Ph), 130.5 (Ph), 129.2 (Ph), 128.8 (Ph), 128.5 (Ph), 121.0 (Ph), 20.6 (*p*-*C*H$_3$), 19.1 (*o*-*C*H$_3$), 19.0 (*o*-*C*H$_3$); IR (cm^{-1}):793.18, 1012.81, 1085.40, 1258.91, 1516.84, 2918.98, 2960.67, 3676.56; HRMS (positive ESI): 240.1760 (100 % M$^+$+H)
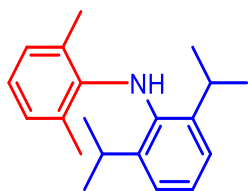
5.3e: Conventional heating method: 2,6-diisopropylaniline 0.47 mL (2.5 mmol), 2,6-dimethyl-1-bromobenzene 0.33 mL (2.5 mmol), Yield: **2.1** = 0.62 gm (88%), **2.3** = 0.65 gm (95%), Microwave heating method: 2,6-diisopropylaniline 0.19 mL (1 mmol), 2,6-dimethyl-1-bromobenzene 0.13 mL (1 mmol), Yield (%)**2.1** = 0.24 gm (87%) **2.3** = 0.26 gm (93%); ^{1}H NMR (CDCl$_3$, 400 MHz, ppm) : δ 1.18 (*d*, J=6.9 Hz,12H, (C*H$_3$*)$_2$CH), 2.04 (*s*, 6H, C*H$_3$*-Ph), 3.22 (dt, 2H, J= 13.7, 6.9 Hz, C*H*(CH$_3$)$_2$), 4.88 (*d,* 1H, J= 20 Hz, N-*H*), 6.78 (*t,* J=7.4 Hz, 1H, Ph), 7.00 (*d*, 2H, J= 7.4 Hz, Ph), 7.15-7.22 (m, 3H, Ph); ^{13}C NMR (CDCl$_3$, 100.613 MHz): δ 144.3 (Ph), 143.3 (Ph), 138.9 (Ph), 129.7 (Ph), 125.8 (Ph), 125.0 (Ph), 123.4 (Ph), 119.8 (Ph), 28.2 [*C*H(CH$_3$)] , 23.6 (*C*H$_3$), 19.5 (*o*-*C*H$_3$); IR (cm^{-1}): 693.14, 930.35, 1427, 1461.85, 1548.47, 1946.42, 2561.63, 3304.84; HRMS (Positive ESI): 282.2229 (100% M$^+$+H)
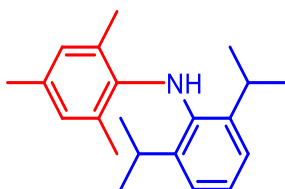
5.3f : Conventional heating method: 2,6-diisopropylaniline 0.94 mL (5 mmol), 2,4,6-trimethyl-1-bromobenzene 0.76 mL (5 mmol) , Yield (%):**2.1** = 1.28 gm (87%), **2.3** = 1.31 gm (89%), Microwave heating method: 2,6-diisopropylaniline 0.19 mL (1 mmol), 2,4,6-trimethyl-1-bromobenzene 0.15 mL (1 mmol), Yield **2.1** = 0.26 gm (88%), **2.3** = 0.26 gm

(88%); ^{1}H NMR (CDCl$_3$, 400 MHz, ppm) : δ 1.16 (*d*, 12H, J = 6.9 Hz,(C*H$_3$*)$_2$CH), 2.01 (*s*, 6H, C*H$_3$*-*o*Ph), 2.28 (*s*, 3H, CH3-*p*-Ph), 3.06-3.28 (*m*, 2H, C*H*(CH)$_3$), 4.72 (*s*, 1H, N*H*), 6.81 (s, 2H, Ph), 7.15 (*s*, 3H, Ph); ^{13}C NMR (CDCl$_3$, 100.613 MHz, ppm) : δ 143.4 (Ph), 140.5 (Ph), 139.2 (Ph), 130.1 (Ph), 126.4 (Ph), 124.2 (Ph), 123.3 (Ph), 28.0 [*C*H(CH$_3$)], 23.5 (*C*H$_3$), 20.5 (*p-C*H$_3$), 19.3 (*o*-CH$_3$).; IR (cm^{-1}) 737.68, 787.59, 852.65, 1017.48, 1265.45, 1334.33, 1480.46, 2959.72 ; HRMS (Positive ESI) : 296.2384 (100% M$^+$+H)
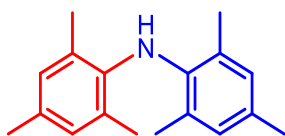
5.3g: Conventional heating method: 2,4,6-trimethylaniline 0.62 mL (5 mmol), 2,4,6-trimethyl-1-bromobenzene 0.77 mL (5 mmol), Yield: **2.1** = 1.12 gm (90%), **2.3** = 1.21 gm (96%). Microwave heating method: 2,4,6-trimethylaniline 0.35 mL (1 mmol), 2,4,6-trimethyl-1-bromobenzene 0.15 mL (1 mmol); Yield **2.1** = 0.23 gm (93%), **2.3** = 0.24 gm (96%); ^{1}H NMR (CDCl$_3$, 400 MHz, ppm) : δ 2.01 (*s*, 12H, C*H$_3$*-*o*-Ph), 2.27 (*s*, 12H, C*H$_3$*-*p*-Ph), 4.64 (*s*, 1H, N*H*), 6.82 (*s*, 4H, Ph); ^{13}C NMR (CDCl$_3$, 100.613 MHz, ppm) : δ 139.5 (Ph), 130.7 (Ph), 129.4 (Ph), 129.3 (Ph), 20.5 (*p-C*H$_3$), 19.0 (*o-C*H$_3$); IR (cm^{-1}): 650.56, 990.36, 1456.56, 1589.36, 1956.56, 2600.25, 3402.25; HRMS (Positive ESI) : 254.1914 (100% M$^+$+H).
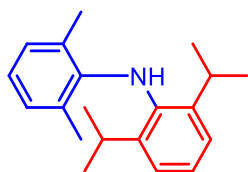
5.3h: Conventional heating method: 2,6-dimethylaniline 1.23 mL (10 mmol), 2,6-diisopropyl-1-bromobenzene 2.06 mL (10 mmol), Yield : **2.1** = 2.33 gm (83%), **2.3** = 2.64 gm (94%). Microwave heating method: 2,6-dimethylaniline, 0.12 mL (1 mmol), 2,6-diisopropyl-1-bromobenzene 0.21 mL (1 mmol); Yield **2.1** = 0.24 gm (87%), **2.3** = 0.26 gm (92%); ^{1}H NMR (CDCl$_3$, 400 MHz, ppm): δ 1.13 (d, 12H, J = 6.9 Hz,(C*H$_3$*)$_2$CH-*o*Ph), 1.99 (s, 6H, C*H$_3$*), 3.15 (*dd*, 2H, J = 13.7, 6.9 Hz, C*H*(CH$_3$)$_2$) 4.80 (s, 1H, N*H*), 6.73 (*t*, J = 7.4 Hz, 1H, Ph), 6.95 (*d*, 2H, J= 7.5 Hz, Ph), 7.13 (t, 3H, J = 4.8 Hz, Ph); ^{13}C NMR (CDCl$_3$, 100.613 MHz, ppm): δ 144.3 (Ph),

143.2 (Ph), 138.9 (Ph) , 129.6 (Ph), 125.7 (Ph), 124.9 (Ph), 123.3 (Ph), 119.7 (Ph), 28.2 [CH(CH$_3$)], 23.6 (CH_3), 19.5 (o-CH_3); IR (cm^{-1}):693.14, 930.35, 142733, 1461.85, 1548.47, 1946.42, 2561, 3304.84; MALDI: 280.98 (M$^+$-H)

5.3i: Conventional heating method: 2,4,6-trimethylaniline 0.62 mL (5 mmol), 2,4,6-triisopropyl-1-bromobenzene 1.26 mL (5 mmol); Yield: **2.1** = 1.52 gm (90%), **2.3** = 1.48 (88%). Microwave heating method: 2,4,6-trimethylaniline 0.35 mL (1 mmol), 2,4,6-triisopropyl-1-bromobenzene 0.24 mL (1 mmol); Yield **2.1** = 0.31 gm (93%), **2.3** = 0.32 gm (95%); ^{1}H NMR (CDCl$_3$, 400 MHz, ppm) : δ 1.14 (d, J= 6.9 Hz, 12H, (CH_3)$_2$CH-oPh), 1.28 (d, J = 6.9 Hz, 6H, (CH_3)$_2$CH-oPh), 1.96 (s, 6H, CH_3-oPh), 2.25 (s, 3H, CH_3-pPh), 2.91 (s, 1H, (CH$_3$)$_2$CH-pPh), 3.17 (dt, J= 13.7, 6.9 Hz, 1H, (CH$_3$)$_2$CH-pPh), 4.63 (s, 1H, NH), 6.77 (s, 2H, Ph), 6.97 (s, 2H, Ph);^{13}C NMR (CDCl$_3$, 100.613MHz, ppm) : δ 144.96 (Ph), 143.91 (Ph), 140.89 (Ph), 136.66 (Ph), 130.08 (Ph), 128.26 (Ph), 125.35 (Ph), 121.03 (Ph), 34.05 [p-CH(CH$_3$)$_2$], 28.11 [o-CH(CH$_3$)$_2$], 24.24 [p-CH(CH$_3$)$_2$], 23.57 [o-CH(CH$_3$)$_2$], 20.40 (p-CH$_3$), 19.23 (o-CH$_3$); IR (cm^{-1}) : 642.38, 698.40, 739.08, 804.43, 853.54, 876.96, 943.02, 1057.25, 1100.89, 1314.17, 1459.07, 1605.03, 1717.71, 2958.62; HRMS (positive ESI) : 338.3423 (100% M$^+$).
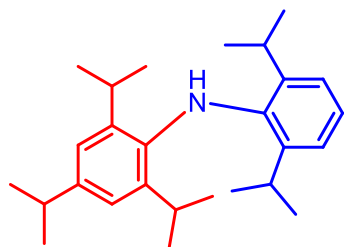
5.3j: Conventional heating method: 2,6-diisopropylaniline, 1.88 mL (10 mmol) 2,4,6-triisopropyl-1-bromobenzene 2.4 mL (10 mmol); Yield: **2.1** = 3.63 gm (96%), **2.3** = 3.71 gm (98%). Microwave heating method: 2,6-diisopropylaniline 0.19 mL (1 mmol), 2,4,6-triisopropyl-1-bromobenzene 0.24 mL (1 mmol); Yield: **2.1** = 0.37 gm (97%), **2.3** = 0.36 gm

(96%); ^{1}H NMR (CDCl$_3$, 400 MHz, ppm) : 1.00-1.24 (*m*, 24H, (C*H$_3$*)$_2$CH-*o*Ph), 1.00-1.24 (*d*, 6H, J = 6.9 Hz,(C*H$_3$*)$_2$CH-*p*Ph), 1.29 (d, J = 6.9 Hz, 5H), 2.90 (*s*, 1H, (CH$_3$)$_2$C*H*-*p*Ph), 3.13 (*ddt*, J=25.9, 13.7, 6.8 Hz, 4H, (CH$_3$)$_2$C*H*-*o*Ph), 4.82 (*s*, 1H, N*H*), 6.90-7.17 (*m*, 5H, Ph); ^{13}C NMR (CDCl$_3$, 100.613 MHz, ppm) : δ 142.57 (Ph), 140.65 (Ph), 139.93 (Ph), 138.81 (Ph), 137.00 (Ph), 122.76 (Ph), 120.88 (Ph), 120.56 (Ph), 32.93 [*p*-C*H*(CH$_3$)$_2$], 26.84 [*o*-C*H*(CH$_3$)$_2$], 26.63 [*p*-CH(C*H$_3$*)$_2$], 23.20 [*o*-CH(C*H$_3$*)$_2$], 22.56 [*o*-CH(C*H$_3$*)$_2$]; IR (cm^{-1}): 729.22, 757.23, 1030.84, 1098.92, 1224.89, 1268.70, 1297.98, 1329.61, 1329.61, 1465.44, 2321.01, 2354.76, 2958.37, 3744.29; HRMS (positive ESI) : 380.3314 (95% M$^+$+H).

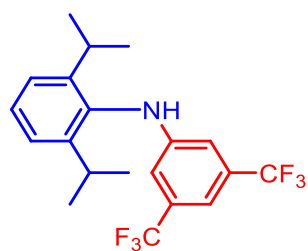**5.3k**: Conventional heating method: 2,6-(CHPh$_2$)-3-methyl-aniline 0.22 gm (5 mmol), bromobenzene 0.52 mL (5 mmol); Yield (%): **2.1** = 2.03 gm (79%), **2.3** = 2.32 gm (90%). Microwave heating method: 2,6-(CHPh$_2$)-3-methyl-aniline 0.44 gm (1 mmol), bromobenzene 0.11 mL (1 mmol); Yield: **2.1** = 0.45 gm (88%), **2.3** = 0.48 gm (94%); ^{1}H NMR (CDCl$_3$, 400 MHz, ppm): δ 2.20 (s, 3H, C*H$_3$*- *p*-Ph), 4.41 (s, 1H, N*H*), 5.65 (s, 2H, C*H*(Ph)$_2$), 6.49 (d, J = 8.5 Hz, 2H, Ph), 6.71 (s, 2H, Ph), 6.79 (s, 1H, Ph), 6.99 (d, J = 7.5 Hz, 8H, Ph), 7.17-7.30 (m,14H, Ph); ^{13}C NMR (CDCl$_3$, 100.613 MHz, ppm) : δ 147.28 (Ph), 144.06, (Ph) 143.53 (Ph), 136.24 (Ph), 135.18 (Ph), 129.79 (Ph), 129.37 (Ph), 128.22 (Ph), 126.19 (Ph), 117.87 (Ph), 112.79 (Ph), 51.71 [*C*H(Ph)$_2$], 21.67 [*C*H(Ph)$_2$]; IR (cm^{-1}) 531.47, 602.17, 996.83, 1218.41, 1442.46, 1722.25, 2311.69, 3396.24, 3850.31; HRMS (positive ESI) : 516.2690 (100% M$^+$+H).
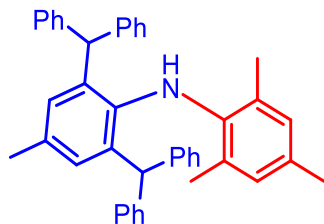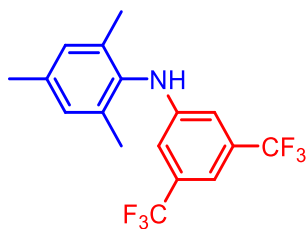
5.3l: Conventional heating method: 2,6-(CHPh2)-3-methyl-aniline 1.1 gm (2.5 mmol), 2,4,6-trimethyl-1-bromobenzene 0.38 mL (2.5 mmol), Yield : **2.1** = 1.29 gm (93%), **2.3** = 1.31 gm (94%), Microwave heating method: 2,6-(CHPh2)-3-methyl-aniline 0.44 gm (1 mmol), 2,4,6-trimethyl-1-bromobenzene 0.15 mL (1 mmol), Yield: **2.1** = 0.55 gm (95%), **2.3** = 0.55 gm (95%). ^{1}H NMR (CDCl$_3$, 400 MHz, ppm) : 1.45 (s, 6H, C*H$_3$-* *o*-Ph),) 2.13 (s, 3H, C*H$_3$-* *p*-Ph), 2.25 (s, 3H, C*H$_3$-* *p*-Ph), 4.12 (s, 1H, N*H*), 5.53 (s, 2H, C*H*(Ph)$_2$), 6.49 (s, 2H, Ph), 6.72 (s, 2H, Ph), 6.85-6.97 (m, 8H, Ph), 7.23 (ddd, J = 8.5, 7.5, 6.0 Hz, 13H, Ph); ^{13}C NMR (CDCl$_3$, 100.61 MHz, ppm): δ 143.66 (Ph), 138.79 (Ph), 138.55 (Ph), 137.58 (Ph), 131.79 (Ph), 129.60 (Ph), 129.10 (Ph), 128.27 (Ph), 126.27 (Ph), 125.95 (Ph), 76.79 (Ph), 52.30 [*C*H(Ph)$_2$], 21.50 (*p*-CH$_3$), 20.55 (*p*-CH$_3$), 18.54 (*o*-CH$_3$); IR (cm^{-1}) : 650.52, 790.25, 905.32, 1056.26, 1300.02 1446.67, 2321.01, 2354.76, 2958.37; HRMS (positive ESI) : 557. 2483 (95% M$^+$).
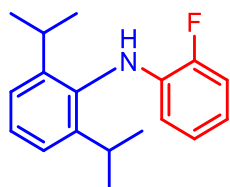
5.3m: Conventional heating method: 2,6-diisopropylaniline 0.47 mL (2.5 mmol), 1-bromo-2-fluorobenzene 0.27 mL (2.5 mmol); Yield: **2.1** = 0.47 gm (70%), **2.3**: 0.53 gm (78%). Microwave heating method: 2,6-diisopropylaniline 0.19 mL (1 mmol), 1-bromo-2-fluorobenzene 0.11 mL (1 mmol); Yield: **2.1** = 0.19 gm (70%), **2.3** = 0.21 gm (79%). ^{1}H NMR (CDCl$_3$, 400 MHz, ppm): δ 1.19 (d, J = 6.9 Hz, 12H, (C*H$_3$*)$_2$CH), 3.22 (m, 2H, (CH$_3$)$_2$C*H*), 5.35 (s, 1H, N*H*), 6.23 (t, J = 8.5 Hz, 1H, Ph), 6.67 (m, 1H, Ph), 6.88 (t, J = 7.6 Hz, 1H, Ph), 7.02-7.18 (m, 1H, Ph), 7.23-7.43 (m, 3H, Ph); ^{13}C NMR (CDCl$_3$, 100.613 MHz): δ 147.79 (Ph), 127.64 (Ph), 124.44 (Ph), 123.95 (Ph), 117.07 (Ph), 114.61 (Ph), 113.19 (Ph), 28.25 [*C*H(CH$_3$)$_2$], 23.88 [CH(*C*H$_3$)$_2$] ppm; ^{19}F NMR : δ -137.33 (s) ppm; IR (cm^{-1}) : 729.22, 808.01, 1035.33,

1102.75, 1446.67, 2321.01, 2354.76, 2958.37; HRMS (positive ESI) : 272.1825 (100% M$^+$+H).
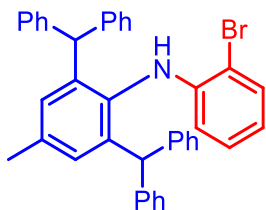
5.3n: Conventional heating method: 2,6-(CHPh$_2$)-3-methyl-aniline 1.1 gm (2.5 mmol), 1,2-dibromobenzene 0.3 mL (2.5 mmol); Yield: **2.1** = 1.3 gm (88%), **2.3** = 1.36 gm (92%). Microwave heating method: 2,6-(CHPh$_2$)-3-methyl-aniline 0.44 gm (1 mmol), 1,2-bromobenzene 0.12 mL (1 mmol); Yield: **2.1** = 0.53 gm (90%), **2.3** = 0.53 gm (90%). ^{1}H NMR (CDCl$_3$, 400 MHz, ppm): δ 2.23 (s, 3H, C*H*$_3$- *p*-Ph),), 5.08 (s, 1H, N*H*), 5.55 (s, 2H, C*H*(Ph)$_2$), 6.30 (s, 2H, Ph), 6.60 (m, 8H, Ph), 6.75-7.43 (m, 16H, Ph); ^{13}C NMR (CDCl$_3$, 100.613 MHz, ppm): δ 144.06 (Ph), 143.73 (Ph), 143.25 (Ph), 143.04 (Ph), 136.63 (Ph), 134.21 (Ph), 132.50 (Ph), 129.69 (Ph), 129.11 (Ph), 128.24 (Ph), 126.21 (Ph), 118.39 (Ph), 112.04 (Ph), 108.73 (Ph), 51.94 (*C*HPh$_2$), 21.70 (*p*-*C*H$_3$); IR (cm^{-1}) : 694.11, 805.01, 1024.36, 1094.77, 1262.88, 1507.67, 1686.49, 2310.40, 2963.36, 3732.30; MALDI: 616.48 (M$^+$+Na)
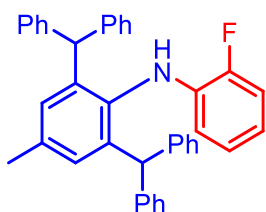
5.3o: Conventional heating method: 2,6-(CHPh$_2$)-3-methyl-aniline 2.2 gm (5 mmol), 1-bromo-2-fluorobenzene 0.54 mL (5 mmol); Yield (%) : **2.1** = 2.52 gm (95%), **2.3** = 2.57 gm (97%). Microwave heating method: 2,6-(CHPh$_2$)-3-methyl-aniline 0.44 gm (1 mmol), 1-bromo-2-fluorobenzene 0.11 mL (1 mmol); Yield: **2.1** = 0.5 gm (96%), **2.3** = 0.5 gm (96%). ^{1}H NMR (CDCl$_3$, 400 MHz, ppm): δ 2.19 (s, 3H, C*H*$_3$- *p*-Ph), 4.73 (s, 1H, N*H*), 5.61 (s, 2H, C*H*(Ph)$_2$), 6.29-6.39 (m, 1H, Ph), 6.73 (s, 9H, Ph), 6.84 (s, 15H, Ph), 6.97 (d, J = 7.1 Hz, 8H), 7.26–7.13 (m, 13H, Ph); ^{13}C NMR (101 MHz, CDCl$_3$, ppm) δ 144.15 (Ph), 143.27 (Ph), 136.55

(Ph), 135.43 (Ph), 134.07 (Ph), 129.82 (Ph), 129.26 (Ph), 128.16 (Ph), 127.79 (Ph), 126.25 (Ph), 124.51 (Ph), 117.29 (Ph), 114.77 (Ph), 112.86 (Ph), 51.77 (CHPh$_2$), 21.68 (*p-C*H$_3$); ^{19}F NMR : δ -136.85 (s) ppm; IR (cm^{-1}) : 565.86, 804.88, 872.06, 997.73, 1092.14, 1217.65, 1378.26, 1734.35, 2311.34, 3739.40; HRMS (positive ESI) : 532.2427 (100% M$^+$+H).
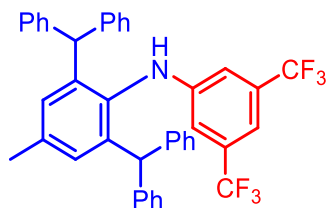
5.3p: Conventional heating method: 2,6-(CHPh$_2$)-3-methyl-aniline 1.1 gm (2.5 mmol), 3,4-trifluoromethyl-1-bromobenzene 0.43 mL (2.5 mmol); Yield: **2.1** = 1.28 gm (79%), **2.3** = 1.3 gm (80%). Microwave heating method: 2,6-(CHPh$_2$)-3-methyl-aniline 1.1 gm (2.5 mmol), 3,4-trifluoromethyl-1-bromobenzene 0.43 mL (2.5 mmol); Yield: **2.1** = 1.27 gm (78), **2.3** = 1.25 gm (77). ^{1}H NMR (CDCl$_3$, 400 MHz, ppm): δ 2.21 (s, 3H, C*H*$_3$- *p*-Ph),), 4.83 (s, 1H, N*H*), 5.48 (s, 2H, C*H*(Ph)$_2$), 6.70 (d, J = 23.4 Hz, 4H, Ph), 6.93 (d, J = 7.5 Hz, 8H, Ph), 7.11-7.33 (m, 13H, Ph); ^{13}C NMR (CDCl$_3$, 100.613 MHz, ppm): δ 148.00 (Ph), 143.96 (Ph), 142.71 (Ph), 137.68 (Ph), 132.93 (Ph), 132.63 (Ph), 132.30 (Ph), 130.18 (Ph), 129.17 (Ph), 128.45 (Ph), 126.50 (Ph), 124.82 (Ph), 122.11 (Ph), 110.92 (Ph), 52.13 (*C*HPh$_2$), 21.74 (*p-C*H$_3$); ^{19}F NMR : δ -63.06 (s) ppm; IR (cm^{-1}): 603.61, 894.42, 894.42, 1432.71, 1689.42, 2313.24, 3562.92, 3736.25; MALDI : 652.13 (M$^+$).

5.3q: Conventional heating method: 2,6-diisopropylaniline 0.47 mL (2.5 mmol), 3,4-trifluoromethyl-1-bromobenzene 0.43 mL (2.5 mmol); Yield: **2.1** = 0.86 gm (89%), **2.3** = 0.89 gm (92%). Microwave heating method: 2,6-diisopropylaniline 0.19 mL (1 mmol), 3,4-trifluoromethyl-1-bromobenzene 0.17 mL (1 mmol); Yield: **2.1** = 0.3 gm (78%), **2.3** = 0.29 gm (77%). ^{1}H NMR (CDCl$_3$, 400 MHz, ppm): δ 1.17 (d, J = 6.9 Hz, 12H, (C*H*$_3$)$_2$CH), 3.01-3.20

(m, 2H, $(CH_3)_2CH$), 5.54 (s, 1H, NH), 6.86 (s, 2H, Ph), 7.20 (s, 1H, Ph), 7.20 (s, 1H, Ph), 7.28 (d, J = 2.1 Hz, 1H, Ph), 7.39 (d, J = 7.8 Hz, 1H, Ph); ^{13}C NMR (CDCl$_3$, 100.613 MHz, ppm): δ 148.95 (Ph), 147.41 (Ph), 133.01 (Ph), 132.70 (Ph), 132.36 (Ph), 132.03 (Ph), 128.50 (Ph), 124.84 (Ph), 124.40 (Ph), 122.13 (Ph), 112.01 (Ph), 111.22–110.02 (CF$_3$), 28.36 [CH(CH$_3$)$_2$], 23.79 [CH(CH$_3$)$_2$]; ^{19}F NMR : δ -63.22 (s) ppm; IR (cm^{-1}) : 535.03, 606.59, 740.76, 999.65, 1125.60, 1273.69, 1381.54, 1485.16, 1619.11, 2920.13, 3369.52; MALDI: 389.0893 (M$^+$).

5.3r: Conventional heating method: 2,4,6-trimethylaniline 0.31 mL (2.5 mmol), 3,4-trifluoromethyl-1-bromobenzene 0.43 mL (2.5 mmol); Yield: **2.1** = 0.78 gm (90%), **2.3** = 0.82 gm (94%). Microwave heating method: 2,4,6-trimethylaniline 0.14 mL (1 mmol), 3,4-trifluoromethyl-1-bromobenzene 0.17 mL (1 mmol), Yield: **2.1** = 0.32 gm (93%), **2.3** = 0.33 gm (95%). ^{1}H NMR (CDCl$_3$, 400 MHz, ppm): δ 2.14 (s, 6H, CH_3- o-Ph), 2.32 (s, 3H, CH_3-p-Ph), 5.46 (s, 1H, NH), 6.80 (s, 2H, Ph), 6.97 (s, 2H, Ph), 7.16 (s, 1H, Ph); ^{13}C NMR (CDCl$_3$, 100.613 MHz, ppm): δ 147.66 (Ph), 136.94 (Ph), 136.03 (Ph), 133.17 (Ph), 132.73 (Ph), 132.41 (Ph), 129.65 (Ph) , 124.86 (Ph), 122.15 (Ph), 112.11 (Ph), 110.80 (CF$_3$), 20.95 (p-CH$_3$), 18.13 (o-CH$_3$); ^{19}F NMR : δ -63.16 (s) ppm; IR (cm^{-1}) : 729.22, 1446.67, 2321.01, 2354.76, 2958.37; HRMS (positive ESI) : 348.1191 (100% M+).

5.2.3.   Computational methodology

Quantum mechanical calculations were carried out for Pd catalyzed Buchwald-Hartwig coupling reaction using Gaussian 09 programme package.[31] All geometries were optimized using the exchange functional of Becke in conjunction with the correlation functional of Perdew (BP86)[32] with def2-SVP basis set.[33] Single-point calculations were done by meta-hybrid GGA functional M06[34] with triple ζ-quality augmented by two set of polarization function (def2-TZVPP). Reaction energy (ΔE) and energy of activation (ΔE‡) were calculated by adding electronic energy at the M06/def2-TZVPP level of theory with zero-point

correction calculated at the BP86/def2-SVP level of theory. Gibbs free energy (ΔG) and Gibbs free energy of activation (ΔG‡) were calculated by adding electronic energy calculated at the M06/def2-TZVPP level of theory with thermal correction to Gibbs free energy calculated at the BP86/def2-SVP level of theory.

5.3.   Result and Discussion

5.3.1. *Optimization of Palladium source and mol %*

Table 5.1*. Optimization of Palladium source and mol %*
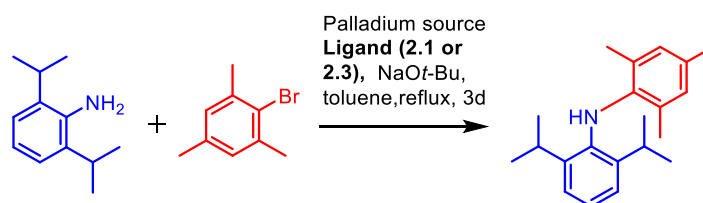
Entry	Palladium source	Ligand	Mol %	Yield [a](%)
1	Pd(dba)$_2$	2.1	1	55
2	Pd(dba)$_2$	2.1	2.5	65
3	Pd(dba)$_2$	2.1	3	65
4	**Pd(dba)$_2$**	**2.1**	**5**	**87**
5	Pd(OAc)$_2$	2.1	5	75
6	Pd$_2$(dba)$_3$	2.1	5	93
7	Pd(dba)$_2$	2.3	1	60
8	Pd(dba)$_2$	2.3	2.5	65
9	**Pd(dba)$_2$**	**2.3**	**5**	**88**
8	Pd(OAc)$_2$	2.3	5	78
9	Pd$_2$(dba)$_3$	2.3	5	90
10	Pd(dba)$_2$	-	5	>10

For the optimization of reaction conditions for the C-N cross-coupling, 2,4,6-trimethyl bromobenzene, and 2,6-diisopropyl aniline are taken as substrate. This reaction involves the use of NaO-tBu as a base and toluene as solvent whereas the palladium source has been optimized (Table 5.1).

It was observed that yields of cross-coupling products in case of $Pd(dba)_2$ and $Pd_2(dba)_3$ are higher compared to $Pd(OAc)_2$. Blank reaction with only palladium source, without ligands **2.1** or **2.3**, afforded less than 10 % of the product. Mole percentage of $Pd(dba)_2$ has been optimized, and it was observed that low catalyst loading (1, 2.5 and 3 mol%) gives low yield (50-65%) of coupling products, whereas 5 mol% leads >85 % yield. The reaction conditions for the conventional route involves 1:1 palladium /ligand ratio and 3-4 days reaction time.

To evaluate the effectiveness of our ligands, **2.1** and **2.3**, we performed a model coupling reaction of bulky 1-Bromo 2,4,6-triisopropyl benzene with 2,6-diisopropyl aniline (Scheme 1)[17,23,29] and compared with the reported ligands. A range of phosphine ligands (Chart 5.2) were used in the coupling of 1-Bromo-2,4,6-triisopropyl benzene with 2,6-diisopropylaniline (Scheme 5.1), and few of them found efficient.
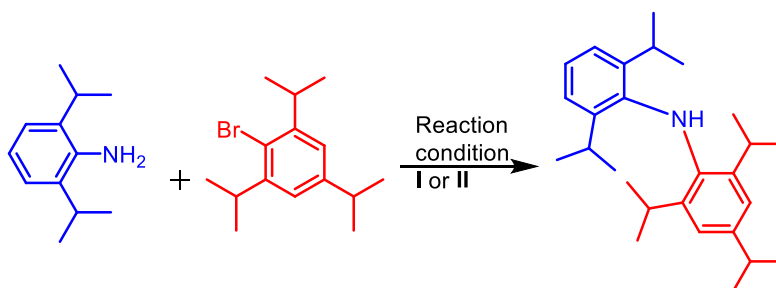
Scheme 5.1. *Coupling of 1-bromo-2,4,6-triisopropylbenzene with 2,6-diisopropyl aniline*

Reaction condition

I Pd(dba)2 (5mol%) 2.1 or 2.3 (5mol%) NaOt-Bu, toluene, reflux, 3d

II : Pd(dba)2 (5mol%) 2.1 or 2.3 (5mol%) NaOt-Bu, toluene, MW, 15-30 min

The reaction conditions are same as that of conventional, but the reaction completion time gets reduced drastically to 15-30 min. Subsequently, we accessed the substrate scope for a broad variety of sterically demanding aryl halides and amines. We investigated the variation of aryl bromides including the one with electron withdrawing groups like fluorine and CF_3, to check the activeness of the catalyst (Table 5.3). Nonetheless, our ligands were found very efficient and give excellent isolated yields for such sterically hindered substrates (Entry 20 and 21). Other than **2.1** and **2.3**, ligands A[17] and C[17] (Table 5.2, Entry 1 and 2) also reported to give excellent isolated yields with very low catalyst loading. However, upon comparison, it can be seen that access to our ligand is very easy. In order to reduce the reaction time, compared to conventional route, we also performed microwave assisted synthetic route. It was observed that aryl bromides with alkyl substituents lead to very good isolated yields (83-98%) of coupling products **5.3a-5.3j**.

R_1 = 2,6-OMePh, R_2= CH_3 (**A**[17])
R_1 = 2,6-OMePh, R_2= Ph (**B**[17])
R_1= 2,6-OMePh, R_2 = H (**C**[17])
R_1 = Ph, R_2= H (**D**[17])
R_1= OMe, R_2= 2-OMePh (**E**[17])
R_1 = OMe, R_2= Ph (**F**[17])
R_1 = 2-NMe_2Ph, R_2= H (**G**[17])

R_1= R_2 = R_3 = t-Bu (**H**[23,29])
R_1= R_2 = t-Bu, R_3= CH_2t-Bu (**I**[23,29])
R_1= R_2 = CH_2t-Bu, R_3= CH_2t-Bu (**J**[23,29])
R_1= R_2 = R_3= CH_2t-Bu (**K**[23,29])
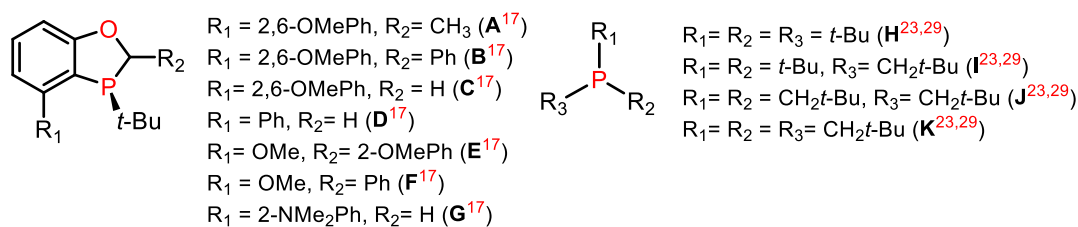
Chart 5.2. *Some P-based ligands used for the cross coupling of 1-Br-2,4,6-iPr_3C_6H_2 and 2,6-iPr_2C_6H_3NH_2.*

However, fluorine substituted aryl bromides give low to moderate yield of coupling products (65-80%). It is noteworthy to mention that CF_3 substituted aryl bromides (**5.3p-5.3r**) were found to give very good isolated yield (~77-95%). We also probed very bulky amine Ar*NH_2 [Ar*= (C_6H_2{C(H)Ph_2}_2Me-2,6,4)][30] as a substrate and found when it is coupled with bromide like 1,2-di-bromobenzene, gives selectively mono-substituted coupling product, 3n in 88-92% yield. Moreover, the coupling of this very bulky amine Ar*NH_2 with other halides was also found very effective (**5.3k**, **5.3i**, **5.3n-p**; ~88-94% isolated yield).
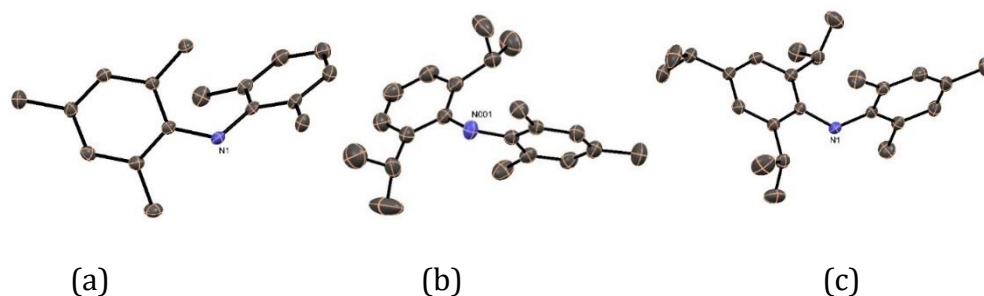
Figure 5.1 *Molecular structure of (a)* **5.3d** *(b)* **5.3f** *and (c)* **5.3i** *with anisotropic displacement parameters depicted at the 50% probability level. All hydrogen atoms and lattice solvent have been omitted   for   clarity.*

Table 5.2. *Screening of various ligands for the coupling of 1-Bromo-2,4,6-triisopropyl benzene and 2,6-diisopropylaniline*

Entry	Ligand	Conversion Yield (%)[a]	Entry	Ligand	Conversion Yield (%)[a]
1	A[b,17]	100 (96)[e]	12	t-Bu$_2$PMe[c,29]	83
2	B[b,17]	24	13	P (o-tol)$_3$[c,29]	29
3	C[b,17]	100 (98)[e]	14	BINAP[c,17]	0
4	D[b,17]	72	15	Xanthphos[c,17]	46
5	E[b,17]	61	16	PCy$_3$[c,29]	100
6	F[b,17]	24	17	Johnphos[c,17]	0
7	G[b,17]	70	18	SPhos[c,17]	18
8	H[c,29]	36	19	XPhos[c,17]	5
9	I[c,29]	0	20	I.HBF$_4$[d,23]	- (75)[e]
10	J[c,29]	4	21	**2.1**	- (96[I]/97[II])[e]
11	K[c,29]	100	22	**2.2**	-(98[I]/96[II])[e]

[a]*Determined by GC and HPLC analysis,* [b]*Conditions: aryl bromide (1.0 equiv.), amine (1.2 equiv.), Pd$_2$(dba)$_3$ (0.05 mol%)/Ligand (0.3 mol%) 1:3, NaOt-Bu (1.5 equiv.), toluene, 110°C, 20 h.* [c]*Reaction conditions: 1-bromo-2,4,6-triisopropylbenzene (1.0 mmol), 2,6-diisopropylaniline (1.2 mmol), Pd$_2$(dba)$_3$ (0.5 mol %), Ligand (1.0 mol %), NaOt-Bu (1.5 mmol), toluene (2 mL), 80 °C, 1 h.* [d]*Aryl bromide (0.8 mmol), aniline (1.0 mmol), NaOt-Bu (0.85 mmol), Pd (2 mol %), DTBNpP.HBF$_4$ (2 mol %), toluene (2*

mL), 50ᵒC, 3-4 hrs. I, II: Reaction condition I (Conventional heating), II (Microwave heating); ᵉIsolated yield is given in bracket.

Crystal structures of some of the coupling products are given. All the cross-coupling reactions led to good to excellent isolated yields (Table 5.3). Higher yields were observed in the case of ligand **2.3**, compared to that of ligand **2.1** for cross-coupling product and the reason behind such behavior might be the steric bulk on the backbone of ligand **2.3**.[9a,24,25] All the coupling reactions were performed by microwave route too and the yields are given as reaction condition II in Table 5.3.

5.3.2. Catalysis using ligand **2.1** and **2.3**

Table 5.3 *Pd(dba)₂/***2.1** *or ***2.2***-Catalyzed coupling of aryl bromides with aryl amines and substrate scope*

5.3a (86%[1], 92%[2])[I]
(83%[1], 90%[2])[II]

5.3b (90%[1], 92%[2])[I]
(91%[1], 90%[2])[II]

5.3c (91%[1], 98%[2])[I]
(88%[1], 92%[2])[II]

5.3d (87%[1], 94%[2])[I]
(88%[1], 95%[2])[II]

5.3e (88%[1], 95%[2])[I]
(87%[1], 93%[2])[II]

5.3f (87%[1], 89%[2])[I]
(88%[1], 88%[2])[II]
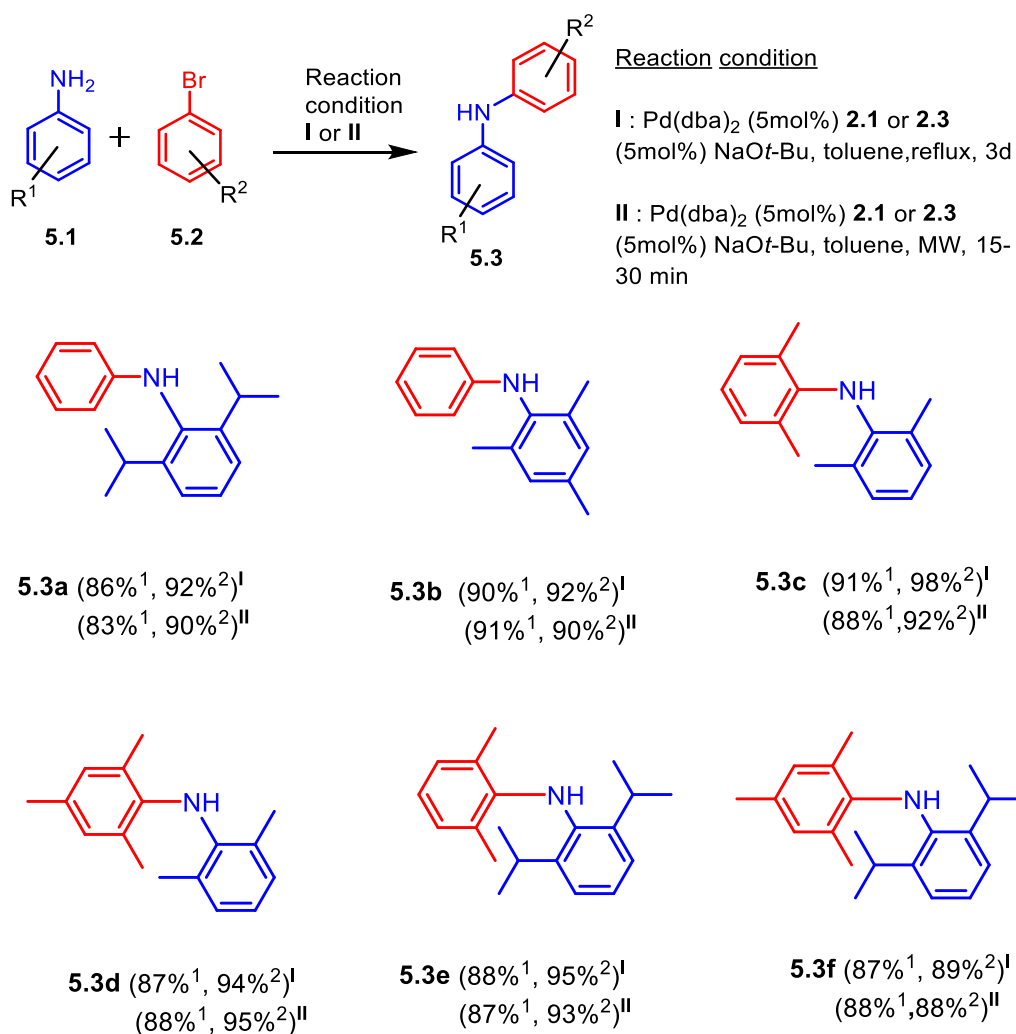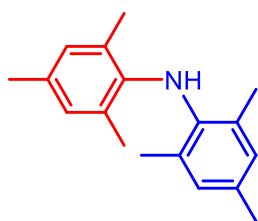
5.3g (90%[1], 88%[2])[I]
(93%[1], 95%[2])[II]
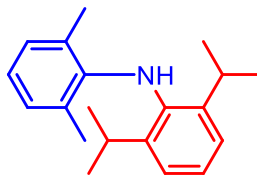
5.3h (83%[1], 94%[2])[I]
(87%[1], 92%[2])[II]
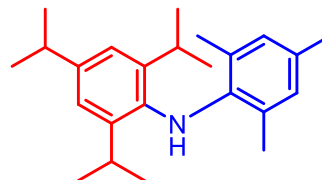
5.3i (90%[1], 88%[2])[I]
(93%[1], 95%[2])[II]
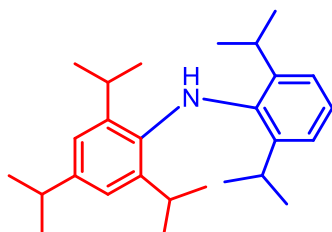
5.3j (96%[1], 98%[2])[I]
(97%[1], 96%[2])[II]
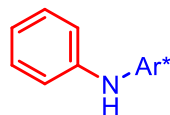
5.3k (79%[1], 90%[2])[I]
(88%[1], 94%[2])[II]
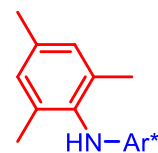
5.3l (93%[1], 98%[2])[I]
(97%[1], 96%[2])[II]
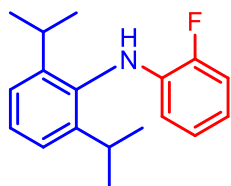
5.3m (70%[1], 78%[2])[I]
(70%[1], 79%[2])[II]
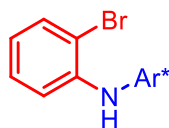
5.3n (88%[1], 92%[2])[I]
(90%[1], 90%[2])[II]
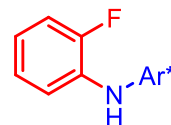
5.3o (95%[1], 97%[2])[I]
(96%[1], 96%[2])[II]
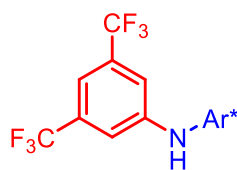
5.3p (79%[1], 80%[2])[I]
(78%[1], 77%[2])[II]
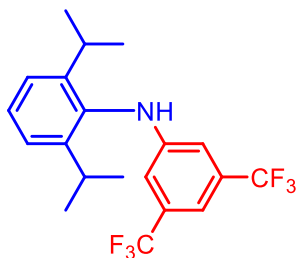
5.3q (89%[1], 92%[2])[I]
(78%[1], 77%[2])[II]
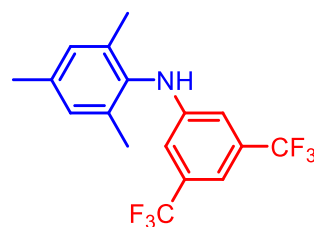
5.3r (90%[1], 94%[2])[I]
(93%[1], 95%[2])[II]

Ar* =

115
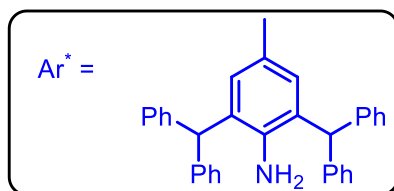
*Isolated yields using ^{1} : Ligand **2.1** and ^{2}: Ligand **2.3** (average of two runs), Reaction conditions: Aryl bromide (1 mmol), Aryl amine (1 mmol), NaOt-Bu (2.8 mmol) dba = dibenzylideneacetone, Palladium source (5 mol%), ligand (5 mol%), Reaction condition **I** : Conventional heating, Reaction condition **II** : Microwave heating.*

5.4.   Theoretical calculation

Pd complexes with an ancillary ligand are the active catalyst involved in coupling reactions. Hence, we have considered Pd_2 {**2.3** = [(PPh$_2$)$_2$N(CH(CH$_3$)$_2$)$_2$Ph]} as an active catalyst. Since variation in the reaction energetics is found to be minimal in presence of solvent toluene (Scheme 5.2), we considered gas reaction energetics for further discussion.

The first step of the reaction can be considered as the formation of tri-coordinated planar complex **Int1** by coordinating the lone pair on bromine atom of aryl bromide with the catalyst Pd2 (Scheme 5.2). This step of reaction is thermodynamically favorable (ΔE= -18.0 kcal/mol and ΔG = -6.6 kcal/mol). The C-Br bond in **Int1** (1.971 Å) is significantly elongated as compared to that in free aryl bromide (1.912 Å, Figure S1), which facilitates its oxidative addition to Pd(0) center resulting in the square planar Pd(II) complex **Int2**.
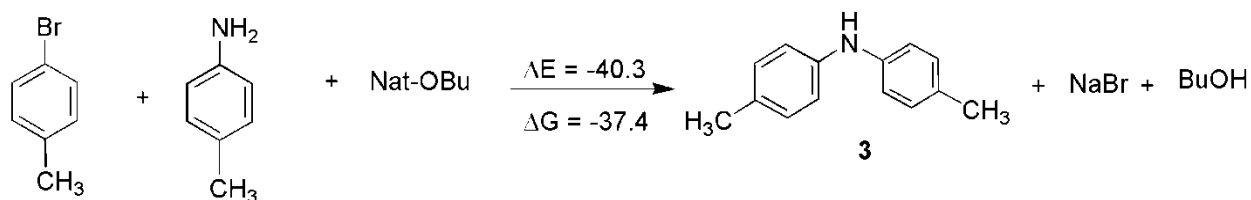
Scheme 5.2. *Total reaction energy and Gibbs free energy (ΔE, ΔG in kcal/mol) for the formation of **3** with solvent as toluene calculated at the M06/Def2-TZVPP//BP86/Def2-SVP level of theory.*

The reaction energy for this step is highly favorable (ΔE= -22.9 kcal/mol and ΔG = -21.3 kcal/mol) and the corresponding energy barrier is also very low ($\Delta E^{\ddagger}$= 2.4 kcal/mol and $\Delta G^{\ddagger}$ = 3.3 kcal/mol). The next step is the formation of complex **Int3** by the coordination of the lone pair of electron of amino group of p-amino toluene with concomitant Pd-Br bond

breakage, which is assisted by the hydrogen bond formation between the formally Br- anion (NBO charge = -0.78 e) with positively charged hydrogen atom of the amino group (NBO charge = 0.45 e). Note that the Pd-Br distance in **Int3** is 3.859 Å and the Br---H distance is within the hydrogen bond distance (2.114 Å). The hydrogen bonded N-H bond length (1.07 Å) in **Int3** is elongated as compared to the non-hydrogen bonded N-H bond length (1.02 Å).
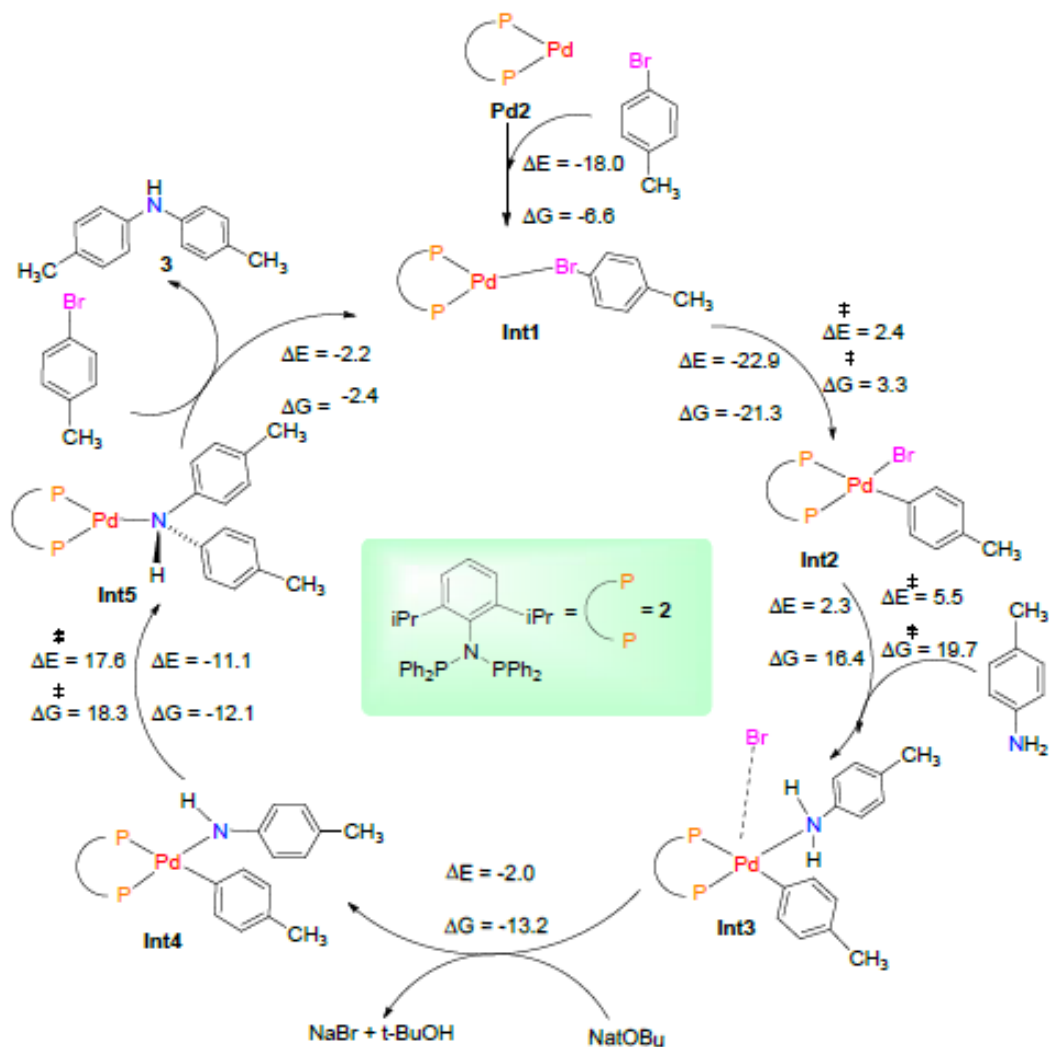
Scheme 5.3. *Catalytic cycle for the formation of **3** from p-bromo toluene and p-toluidine calculated at the M06/Def2- TZVPP//BP86/Def2-SVP level of theory. ΔE and ΔG (in kcal/mol) represent the reaction energy and Gibb's free energy. ΔE‡ and ΔG‡ (in kcal/mol) represent activation energy and Gibb's free energy of activation respectively.*

This step is slightly endothermic (ΔE=2.3kcal/mol) and endergonic (ΔG = 16.4kcal/mol) and involves a low activation energy barrier ($\Delta E^{\ddagger}$= 5.5kcal/mol and $\Delta G^{\ddagger}$ =19.7kcal/mol). The hydrogen bonded acidic proton can be easily removed by the base sodium tert-butoxide resulting Pd(II) complex **Int4**, t-BuOH and NaBr, which is thermodynamically favorable. The next step is the coupling between the N-atom of NH-C_6H_4-CH_3 group with a phenylic carbon atom of C_6H_4-CH_3 group resulting tri-coordinated planar Pd(0) complex **Int5**. This step is thermodynamically (ΔE= -11.1 kcal/mol and ΔG = -12.1 kcal/mol) as well as kinetic favorable ($\Delta E^{\ddagger}$ = 17.6 kcal/mol and $\Delta G^{\ddagger}$ = 18.3 kcal/mol) at reaction condition. The elimination of the C-N coupled product from Int5 followed by the addition of aryl bromide (ΔE= -2.2 kcal/mol and ΔG = -2.4 kcal/mol)) carry forward the catalytic cycle further.

Note that the reaction pathway which involves the oxidative addition of N-H bond to palladium is highly energy demanding (Scheme 5.3; ΔE= 15.5 kcal/mol, ΔG= 18.1 kcal/mol) and hence did not consider further.

5.5.   Conclusion

In summary, we have studied the easily accessible, cost effective phosphinoamine ligands, **2.1** and **2.3** in the C-N cross-coupling of sterically demanding aryl bromides and aryl amines, by conventional as well as microwave-assisted organic synthesis (MAOS) technique. All the coupling products are obtained in multigram scale with good to excellent yields. MAOS method drastically reduces the reaction completion time up to 15-30 min when compared to the conventional heating and thereby rendering facile access to the C-N cross-coupled products, especially for the bulky substrates.

5.6.   References

1. Bariwal, J.; Der Eycken, E.V. *Chem. Soc. Rev.* **2013**, *42*, 9283.

2. Castillo, P. R.; Buchwald, S. L. *Chem. Rev.* **2016**, *116*, 12564.

3. Yang, B. H.; Buchwald, S. L. *J. Organomet. Chem.* **1999**, *576*, 125.

4. Wolfe, J. P.; Wagaw, S.; Marcoux, J.-F.; Buchwald, S. L. *Acc. Chem. Res.* **1998**, *31*, 805.

5. Hartwig, J. F. *Angew. Chem., Int. Ed.* **1998**, *37*, 2046.

6. (a) Hong, J. B.; Davidson, J. P.; Jin, Q.; Lee, G. R.; Matchett, M.; O'Brien, E.; Welch, M.; Bingenheimer, B.; Sarma, K. *Org. Process Res. Dev.* **2014**, *18*. (b) Liu, Y.; Prashad, M.; Shieh, W.-C. *Org. Process Res. Dev.*, **2014**, *18*.

7. Kousagi, M.; Kameyama, M.; Migita, T. *Chem. Lett.* **1983**, 927.

8. (a) Muci, A. R.; Buchwald, S. L. *Top. Curr. Chem.* **2002**, 219,131. (b) Sato, S.; Sakamoto, T.; Miyazawa, E.; Kikugawa, Y. *Tetrahedron* **2004**, *60*, 7899. (c) Ji, P.; Atherton, J. H.; Page, M. I. *J. Org. Chem.* **2012**, *77*, 7471. (d) Kwong, F. Y. Buchwald, S. L. *Org. lett.* **2003**, *5*, 793-796. (e) Castillo, P. R.; Blackmond, D. G.; Buchwald, S. L. *J. Am. Chem. Soc.* **2015**, *137*, 3085. (f) Maiti, D.; Fors, B. P.; Henderson, J. L.; Buchwald, S. L. *Chem. Sci.* **2011**, *2*, 57.

9. (a) Wolfe, J. P.; Wagaw, S.; Marcoux, J.-F.; Buchwald, S. L. *Acc. Chem. Res.* **1998**, *31*, 805. (b) Heravi, M. M.; Kheilkordi, Z.; Zadsirjan, V.; Heydari, M.; Malmir, M. *J. Organomet. Chem.* **2018**, *104*, 861.

10. (a) Wolfe, J.P.; Wagaw, S.; Buchwald, S. L. *J. Am. Chem. Soc.*1**996**, *118*, 7215. (b) J. P. Wolfe and S. L. Buchwald, *J. Org. Chem.*, **2000**, *65*, 1144.

11. Driver, M. S; Hartwig, J. F. *J. Am. Chem. Soc.* **1996**, *118*, 7217.

12. Guari, Y.; Van Es, D. S.; Reek, J. N.H.; Kamer, P. C. J.; Van Leeuwen, P.W. N.M. *Tetrahedron. Lett.* **1999**, *40*, 3789.

13. Hamann, B. C.; Hartwig, J. F. *J. Am. Chem. Soc.* **1998**, *120*, 7369.

14. Huang, X.; Anderson, K. W.; Zim, D.; Jiang, L.; Klapars, A.; Buchwald, S. L. *J. Am. Chem. Soc.* **2003**, *125*, 6653.

15. (a) Fortman, G. C.; Nolan, S. P. *Chem. Soc. Rev.* **2011**, *40*, 5151. (b) Li, Y.-J.; Zhang, J.-L.; Li, X.-J.; Geng, Y.; Xu, X.-H.; Jin, Z. *J. Org. Chem.* **2013**, *737*, 12. (c) Fortman, G. C.; Nolan, S. P. *Chem. Soc. Rev.* **2011**, *40*, 5151.

16. Li, G. Y.; Zheng, G.; Noonan, A. F. *J. Org. Chem.* **2001**, *66*, 8677.

17. Rodriguez, S.; Qu, B.; Haddad, N.; Reeves, D. C.; Tang, W.; Lee, H.; Krishnamurthy, D.; Senanayake, C. H. *Adv. Synth. Catal.* **2011**, *353*, 533.

18. Liu, D.; Gao, W.; Dai, Q.; Zhang, X. *Org. lett.* **2005**, *7*, 4907.

19. Rataboul, F.; Zapf, A.; Jackstell, R.; Harkal, S.; Riermeier, T.; Monsees, A.; Dingerdissen, U.; Beller, M. *Chem. Eur. J.* **2004**, *10*, 2983.

20. Suresh, R. R.; Swamy, K. C. K. *Tetrahedron Lett.* **2009**, *50*, 6004.

21. Ackermann, L.; Born, R. *Angew. Chem., Int. Ed.* **2005**, *44*, 2444.

22. Chen, G.; Lam, W. H.; Fok, W. S.; Lee, H. W.; Kwong, F. Y. *Chem. Asian J.* **2007**, *2*, 306.

23. Hill, L. L.; Moore, L. R.; Huang, R.; Craciun, R.; Vincent, A. J.; Dixon, D.A.; Chou, J.; Woltermann, C. J.; Shaughnessy, K. H. *J. Org. Chem.* **2006**, *71*, 5117.

24. Surry, D. S.; Buchwald, S. L. *Chem. Sci.* **2011**, *2*, 27.

25. Hartwig, J. F. *Inorg. Chem.* **2007**, *46*, 1936.

26. Raders, S. M.; Moore, J. N.; Parks, J. K.; Miller, A. D.; Leising, T. M.; Kelley, S. P.; Rogers, R. D.; Shaughnessy, K. H. *J. Org. Chem.* **2013**, *78*, 4649.

27. Pal, S.; Kathewad, N.; Pant, R.; Khan, S. *Inorg. Chem.* **2015**, *54*, 10172.-10183.

28. Kathewad, N.; Pal, S.; Kumawat, R. L.; Ali, E.; Khan, S. *Eur. J. Inorg. Chem.*, **2018**, *22*, 2518.

29. (a) Berthon-Gelloz, G.; Siegler, M. A.; Spek, A. L.; Tinant, B.; Reek, J. N. H.; Marko, I. E. *Dalton Trans.* **2010**, *39*, 1444. (b) Hadlington, T. J.; Li, J.; Jones, C. *Can. J. Chem.* **2014**, *92*, 427.

30. Wild, C. T.; Zhu, Y.; Na, Y.; Mei, F.; Ynalvez, M. A.; Chen, H.; Cheng, X.; Zhou, J. *ACS Med. Chem. Lett.* **2016**, *7*, 460.

31. Gaussian 09, Revision A.01, Frisch, M. J.; Trucks, G. W.; Schlegel, H. B.; Scuseria, G. E.;Robb, M. A.; Cheeseman, J.R.; Scalmani, G.; Barone, V.; Mennucci, B.; Petersson, G. A.;Nakatsuji, H.; Caricato, M.; Li, X.; Hratchian, H. P.; Izmaylov, A. F.; Bloino, J.; Zheng, G.;Sonnenberg, J. L.; Hada, M.; Ehara, M.; Toyota, K.; Fukuda, R.; Hasegawa, J.; Ishida, M.;Nakajima, T.; Honda, Y.; Kitao, O.; Nakai, H.; Vreven, T.; Montgomery, J. J. A.; Peralta, J. E.;Ogliaro, F.; Bearpark, M.; Heyd, J. J.; Brothers, E.; Kudin, K. N.; Staroverov, V. N.; Kobayashi,R.; Normand, J.; Raghavachari, K.; Rendell, A.; Burant, J. C.; Iyengar, S. S.; Tomasi, J.; Cossi,M.; Rega, N.; Millam, J. M.; Klene, M.; Knox, J. E.; Cross, J. B.; Bakken, V.; Adamo, C.;Jaramillo, J.; Gomperts, R.; Stratmann, R. E.; Yazyev, O.; Austin, A. J.; Cammi, R.; Pomelli,C.; Ochterski, J. W.; Martin, R. L.;Morokuma, K.; Zakrzewski, V. G.; Voth, G. A.; Salvador, P.;Dannenberg, J. J.;Dapprich, S.; Daniels, A. D.; Farkas, O.; Foresman, J. B.; Ortiz, J. V.;Cioslowski, J.; Fox, D. J., *Gaussian Inc., Wallingford CT*, **2009**

32. (a) Becke A. D. Phys. Rev. A **1988**, *38*, 3098. (b) Perdew, J. P., *Phys. Rev. B*, **1986**, *33*, 8822. (c) Perdew, J. P., *Phys. Rev. B*, **1986**, 34, 7406.

33. Weigend, F.; Ahlrichs, R. *Phys. Chem. Chem. Phys.*, **2005**, 7, 3297.

34. Zhao, Y.; Truhlar, D. G. *Theor. Chem. Acc,* **2008**, *120*, 215.

Summary

In summary, the thesis presents the synthesis, characterization and application of diphosphinoamine ligands (DPPA). In chapter 2, differently N-functionalized DPPA ligand supported Au(I) complexes (neutral and cationic) are synthesized and characterized using routine NMR, Mass spectra analysis. DPPA supported mononuclear and dinuclear Au(I) complexes do not show any intermolecular aurophillic interaction while the dinuclear Au(I) complexes possess intramolecular aurophillic interaction which ranges from 2.794-3.005 Å.

In chapter 3, we discussed the photophysical and theoretical investigation of DPPA supported Au(I) complexes. It is observed that the complexes having intramolecular aurophillic interaction show luminescent behaviour, while those are devoid of aurophillic interaction are found to be non-luminescent. Theoretical investigation show that transition responsible for luminescent behavior of cationic gold complexes are of mixed in nature *i. e.* mixture of ligand to metal transition (LMCT) and intra-ligand charge transfer (ILCT) whereas for neutral gold complex, mixture of metal to ligand charge transfer (MLCT) and halide to ligand charge transfer (XLCT) transitions are observed. It is observed that subtle change of substituent leads to the different colour of emission which could be very useful in designing new luminescent material of selective colour.

In chapter 4, we synthesized the differently N-functionalized DPPA supported copper (I) complexes and their photophysical properties are investigated. Copper complexes with different nuclearity i.e. dinuclear, trinuclear and tetranuclear clusters were obtained by reaction of DPPA ligand and copper halide in 1:1 ratio. It was observed that those complexes possess Cu$\cdots$Cu distances >2.8 Å shows mechanochromic and thermochromic luminescencent behaviour. PXRD patterns reveals that the luminescence properties of these copper complexes arise from their phase transition from crystalline to microcrystalline/ amorphous nature upon grinding of their solid samples.

In chapter 5, we employed these DPPA ligands for catalytic application in C-N coupling using palladium metal salt. Easily accessible, cost effective DPPA ligands, **2.1** and **2.3** in the C-N cross-coupling of sterically demanding aryl bromides and aryl amines, by conventional as

well as microwave-assisted organic synthesis (MAOS) technique. All the coupling products are obtained in multigram scale with good to excellent yields. MAOS method drastically reduces the reaction completion time up to 15-30 min when compared to the conventional heating and thereby rendering facile access to the C-N cross-coupled products, especially for the bulky substrates.

Appendix

Table 2A.1 Crystallographic data for **2.6-2.8**

	2.6	2.7	2.8
Chemical formula	$C_{60}H_{50}Au_2Cl_2N_2P_4$	$C_{60}H_{50}Au_2F_{12}N_2P_4Sb_2$	$C_{32}H_{29}AuCl\ N\ P_2$
Formula weight	1387.73	1788.33	721.92
Temperature	150 (2)	150 (2)	150 (2)
Wavelength (Å)	0.71073	0.71073	0.71073
Crystal system	Triclinic	Orthorhombic	Triclinic
Space group	*P -1*	P c a 21	*P -1*
Unit cell dimensions	a = 9.8734(10) Å	a = 21.2744(19) Å	a = 10.7487(19) Å
	b = 11.6662(12) Å	b = 16.6689(15) Å	b = 13.558(2) Å
	c = 12.3849(12) Å	c = 19.4149(18) Å	c = 19.785(4) Å
	α= 70.703(3)^o	α= 90o	α= 96.481(4)^o
	β= 81.836(3)^o	β= 90°	β= 99.229(4)^o
	γ= 74.313(3)^o	γ= 90°	γ= 96.747(4)^o
Volume (Å^3)	1294.1(2)	6884.9(11)	2800.6(9)
Z	1	4	4
Density (calculated) (g/cm^3)	1.781	1.794	1.712
Absorption coefficient (mm^{-1})	5.931	5.265	5.485
F(000)	676	3544	1416
Theta range for data collection (^{o})	2.153 to 25.248	2.183 to 25.249	2.297 to 28.313
Index ranges	-11<=h<=11 -13<=k<=13 -14<=l<=14	-25<=h<=25 -20<=k<=20 -23<=l<=23	-14<=h<=14 -18<=k<=18 -26<=l<=26
Reflections collected	49442	216082	53758
Independent reflections	6411 [R(int) = 0.0613]	12392 [R(int)= 0.0578]	13788 [R(int) = 0.0890]
Coverage of independent reflections (%)	98.5	99.9	99.4
Function minimized	$\Sigma\ w(Fo^2 - Fc^2)^2$	$\Sigma\ w(Fo2 - Fc2)2$	$\Sigma\ w(Fo^2 - Fc^2)^2$
Data/ restraints/ parameters	6411/ 0/ 316	12392/ 7/ 740	13788/ 0/ 671

Goodness-of-fit on F2	0.613	1.041	0.748
Δ/ σ max	0.003	0.003	0.003
Final R indices	5827 data; [I>2σ(I)] R1= 0.0186, wR2= 0.0613	12055 data; [I>2σ(I)] R1= 0.0220, wR2= 0.0578	11255 data; [I>2σ(I)] R1= 0.0311, wR2= 0.0890
	all data, R1= 0.0259, wR2= 0.0720	all data, R1= 0.0229, wR2= 0.0582	all data, R1= 0.0464, wR2= 0.1029
Largest diff. peak and hole (eÅ^{-3})	1.192 and -1.197	0.711 and -0.558	0.858 and -1.706
R. M. S deviation from mean (eÅ^{-3})	0.155	0.095	0.156

Table 2A.2 Crystallographic data for **2.9-2.11**

	2.9	2.10	2.11
Chemical formula	$C_{66}H_{62}Au_2Cl_4F_{12}N_2P_4Sb_2$	$C_{37} H_{39} Au Cl_3 N P_2$	$C_{72} H_{74} Au_2 N_2 P_4, F_{12} Sb_2$
Formula weight	2014.29	862.95	1956.64
Temperature	150 (2)	100(2)	100(2)
Wavelength (Å)	0.71073	Colourless niddle	Colourless plate
Crystal system	Monoclinic	monoclinic	orthorhombic
Space group	*P 21/n*	*C 2/c*	*C c c a*
Unit cell dimentions	a = 13.516(4) Å	a = 30.781(4)	a = 14.313(4)
	b = 13.530(4) Å	b = 10.6267(14)	b = 19.807(6)
	c = 18.730(6) Å	c = 43.893(6)	c = 25.416(8)
	α= 90º	α = 90°	α = 90°
	β= 95.971(8)º	β= 99.789(5)°	β= 90º
	γ= 90º	γ= 90º	γ= 90º
Volume (Å^3)	3406.5(17)	14148(3)	7205(4)
Z	2	16	4

Density (calculated) (g/cm³)	1.964	1.620	1.804
Absorption coefficient (mm⁻¹)	5.404	4.503	4.964
F(000)	1936	6848	3792
Theta range for data collection (⁰)	2.135 to 28.367	1.766 to 25.243	2.377 to 25.247
Index ranges	-18<=h<=17 -17<=k<=18 -24<=l<=25	-36<=h<=30 -12<=k<=10 -52<=l<=52	-17<=h<=17 -23<=k<=23 -30<=l<=30
Reflections collected	77882	82928	66170
Independent reflections	8541 [R(int) = 0.0716]	12756 [R(int) = 0.1098]	3276 [R(int) = 0.1717]
Coverage of independent reflections (%)	99.0	99.6	99.9
Function minimized	$\Sigma\, w(Fo2 - Fc2)2$	$\Sigma\, w(Fo2 - Fc2)2$	$\Sigma\, w(Fo2 - Fc2)2$
Data/ restraints/ parameters	8541/ 0/ 417	12756/ 0/ 803	3276/ 7/ 194
Goodness-of-fit on F2	1.987	0.923	1.211
Δ/ σ max	0.003	0.003	0.001
Final R indices	7883 data, [I>2σ(I)] R1= 0.0292, wR2= 0.0716	11438 data, [I>2σ(I)] R1= 0.0319, wR2= 0.1098	1897data, [I>2σ(I)] R1= 0.0856, wR2= 0.1717
	all data, R1= 0.0327, wR2= 0.0724	all data, R1= 0.0373, wR2= 0.1152	all data, R1= 0.1552, wR2= 0.2074
Largest diff. peak and hole (eÅ⁻³)	2.213 and -1.321	1.076 and -1.53	3.183 and -1.593
R. M. S deviation from mean (eÅ⁻³)	0.147	0.134	0.207

Table 2A.3 Crystallographic data for **2.12-2.13**

	2.12	2.13
Chemical formula	$C_{60} H_{58} Au_2 F_{14} N_2 P_4 Sb_2$	$C_{62} H_{58} Au_2 Cl_2 F_{12} N_2 O P_4 Sb_2$
Formula weight	1834.39	1907.31
Temperature	150 (2)	150 (2)
Wavelength (Å)	0.71073	0.71073
Crystal system	triclinic	Monoclinic
Space group	*P -1*	P 21/n
Unit cell dimensions	a = 10.838(16)	a = 12.427(2)Å
	b = 10.94(2) Å	b = 17.067(3)Å
	c = 15.43(3) Å	c = 17.350(3)Å
	α= 103.01(6)°	α= 90°
	β= 98.45(6)°	β= 91.086(5)°
	γ= 116.91(6)°	γ= 90°
Volume (Å³)	1523(5)	3679.3(11)
Z	1	2
Density (calculated) (g/cm³)	2.000	1.722
Absorption coefficient (mm⁻¹)	5.867	4.929
F(000)	878	1828
Theta range for data collection (°)	2.196 to 20.974	2.327 to 25.242
Index ranges	-14<=h<=14 -20<=k<=20 -20<=l<=19	-14<=h<=14 -20<=k<=20 -20<=l<=19
Reflections collected	3219	30137
Independent reflections	3219 [R(int) = 0.1361]	6396 [R(int) = 0.0704]
Coverage of independent reflections (%)	98.9	96
Function minimized	Σ w(Fo2 - Fc2)2	Σ w(Fo2 - Fc2)2
Data/ restraints/ parameters	3219/0/412	6396/ 0/ 416
Goodness-of-fit on F2	1.050	1.064
Δ/ σ max	1.507	0.001
Final R indices	1715 data, [I>2σ(I)] R1= 0.1361, wR2= 0. 3001	5797 data, [I>2σ(I)] R1= 0.0704, wR2= 0.1932

	all data, R1= 0.2264, wR2= 0.3465	all data, R1= 0.0772, wR2= 0.2009
Largest diff. peak and hole (eÅ^{-3})	2.245 and -3.107	14.612 and -1.785
R. M. S deviation from mean (eÅ^{-3})	0.415	0.327
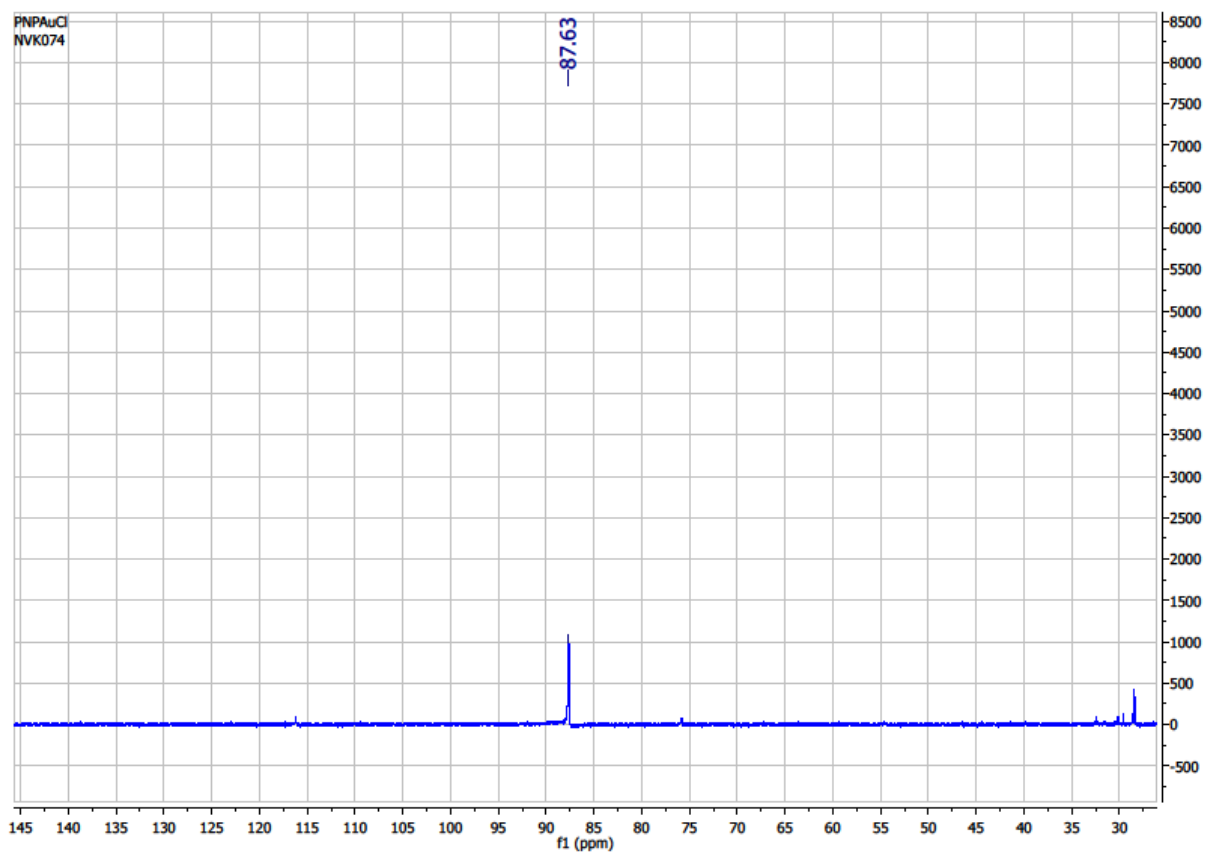
Figure 2A.1 ^{31}P NMR (CDCl$_3$) of **2.6**
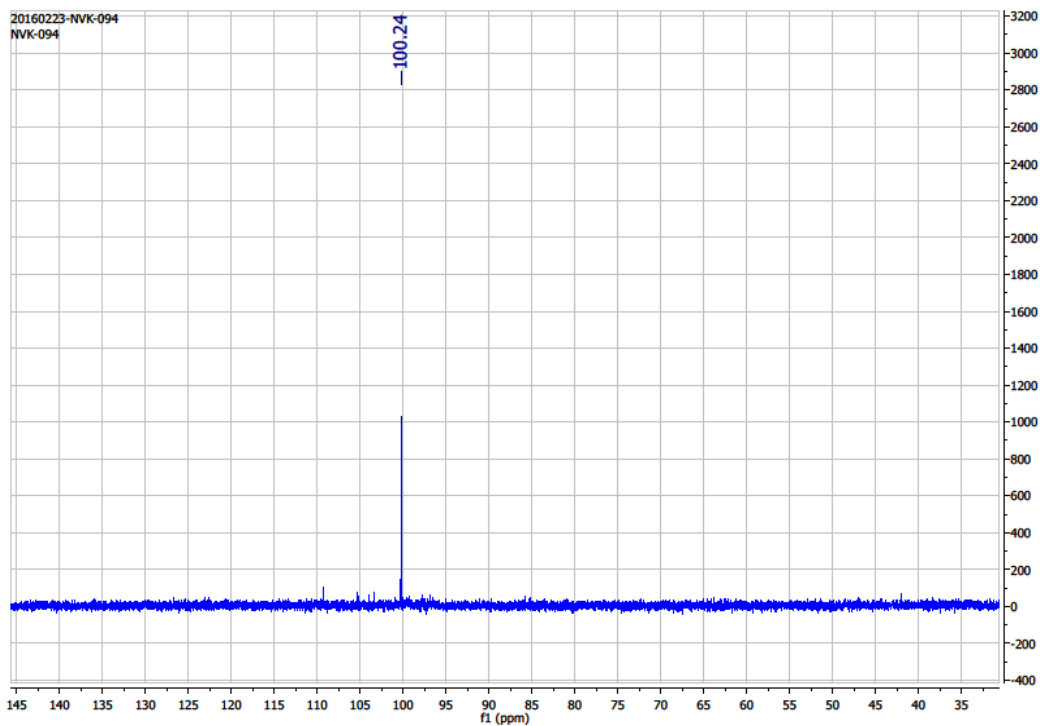
Figure 2A.2 *³¹P NMR (CDCl₃) of **2.7***
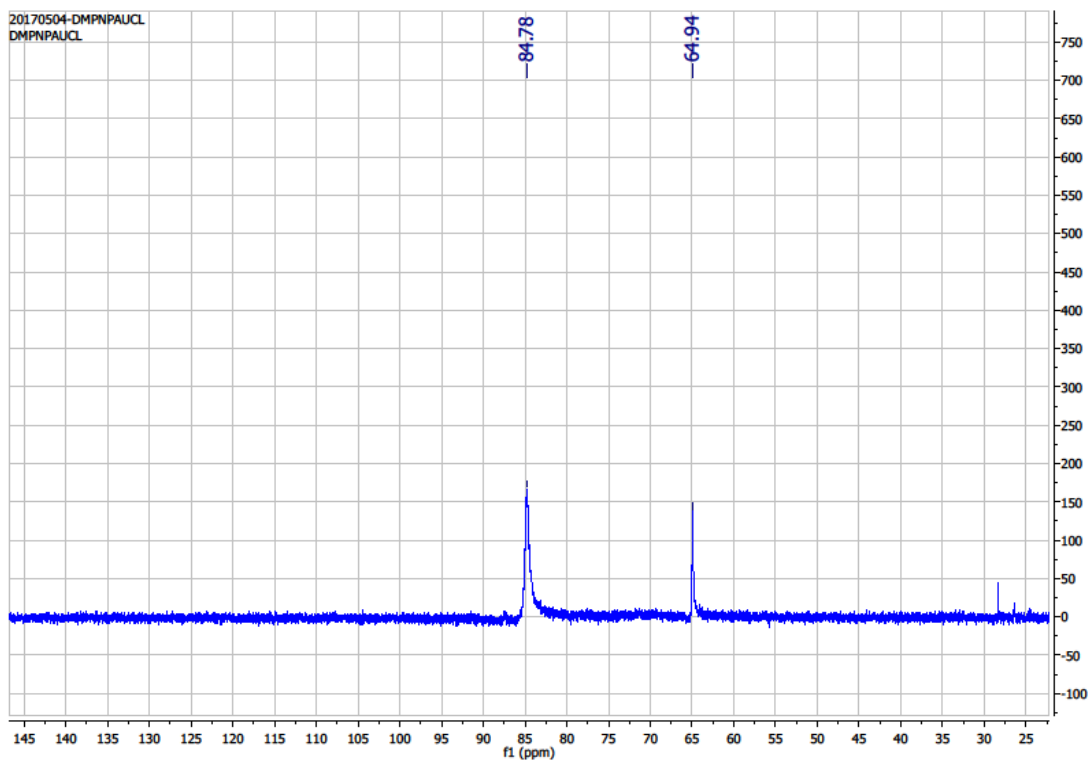
Figure 2A.3 *³¹P NMR (CDCl₃) of **2.8***
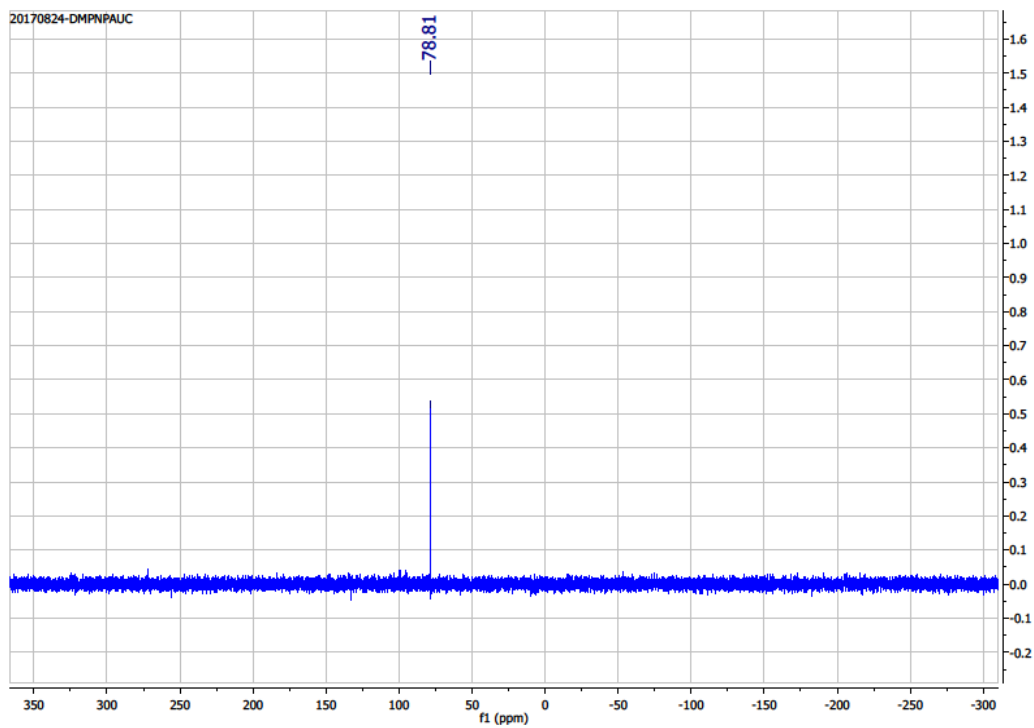
Figure 2A.4 ^{31}P *NMR (CDCl$_3$) of* **2.9**
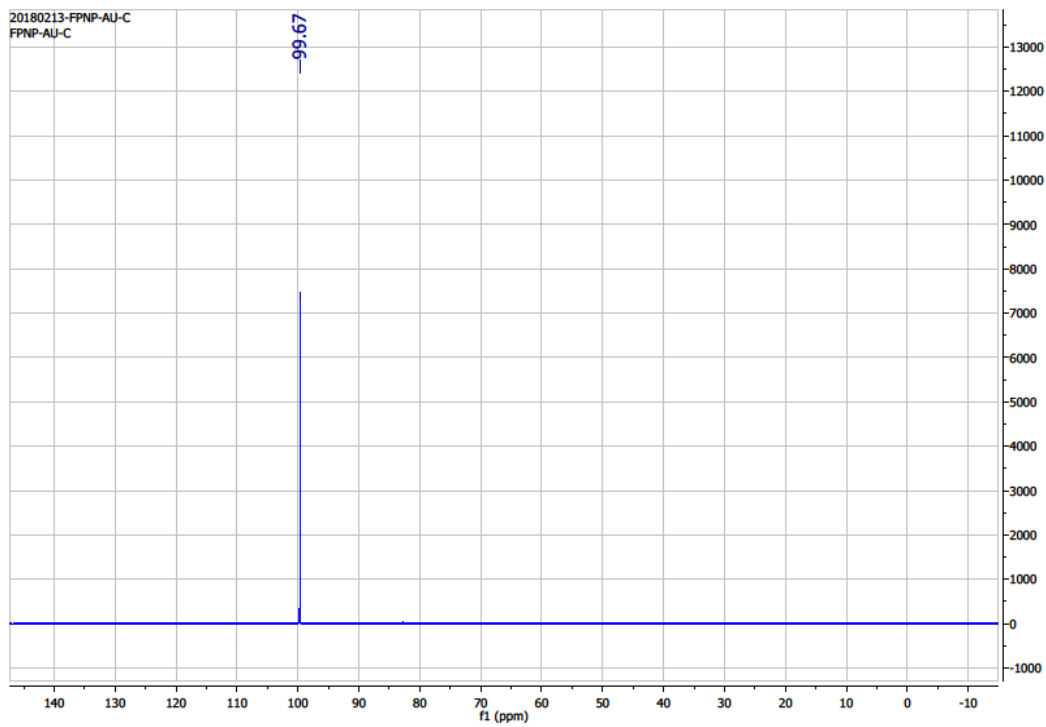
Figure 2A.7 ^{31}P *NMR (CDCl$_3$) of* **2.12**
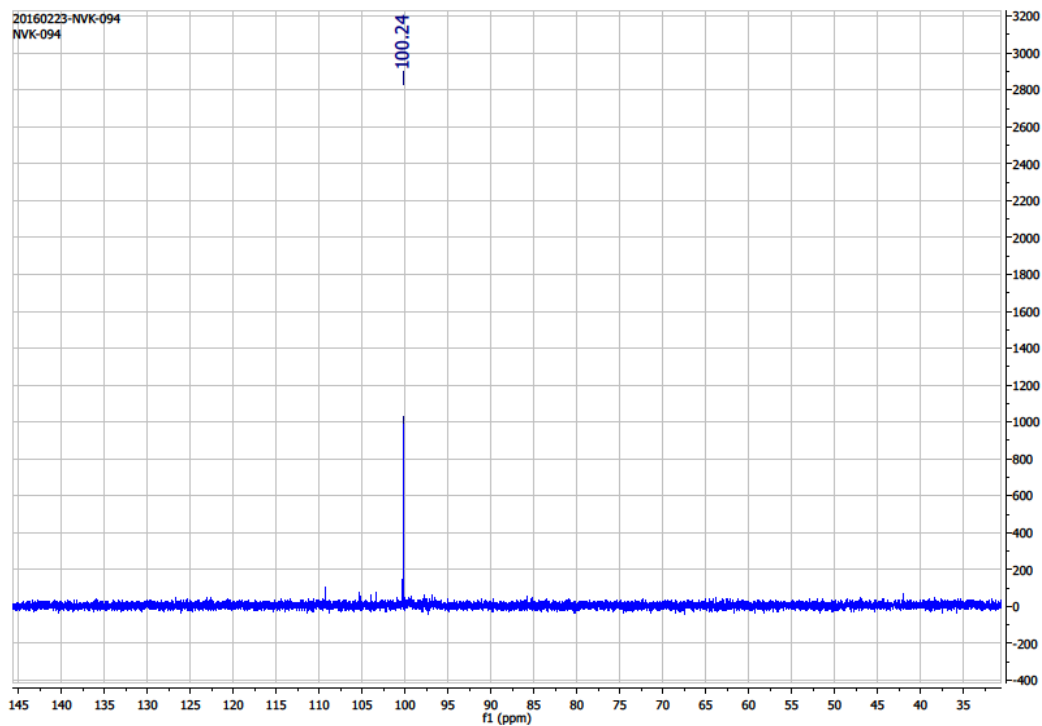
Figure 2A.8 *31P NMR (CDCl₃) of* **2.13**
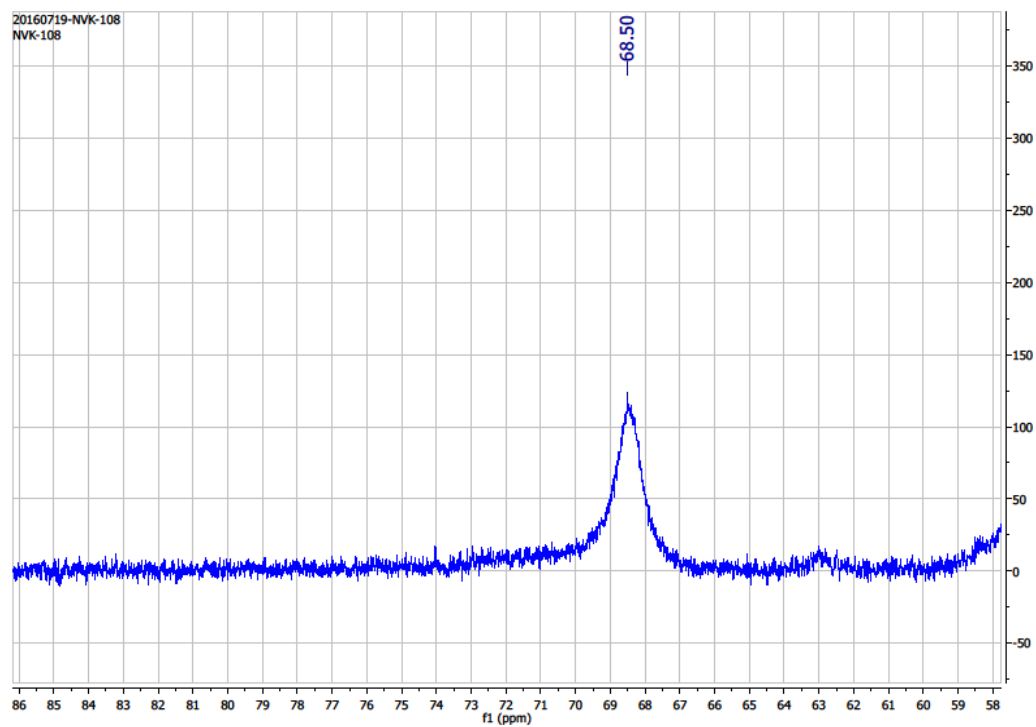
Figure 4A.1 *31P NMR (CDCl₃) of* **4.3**

—73.62
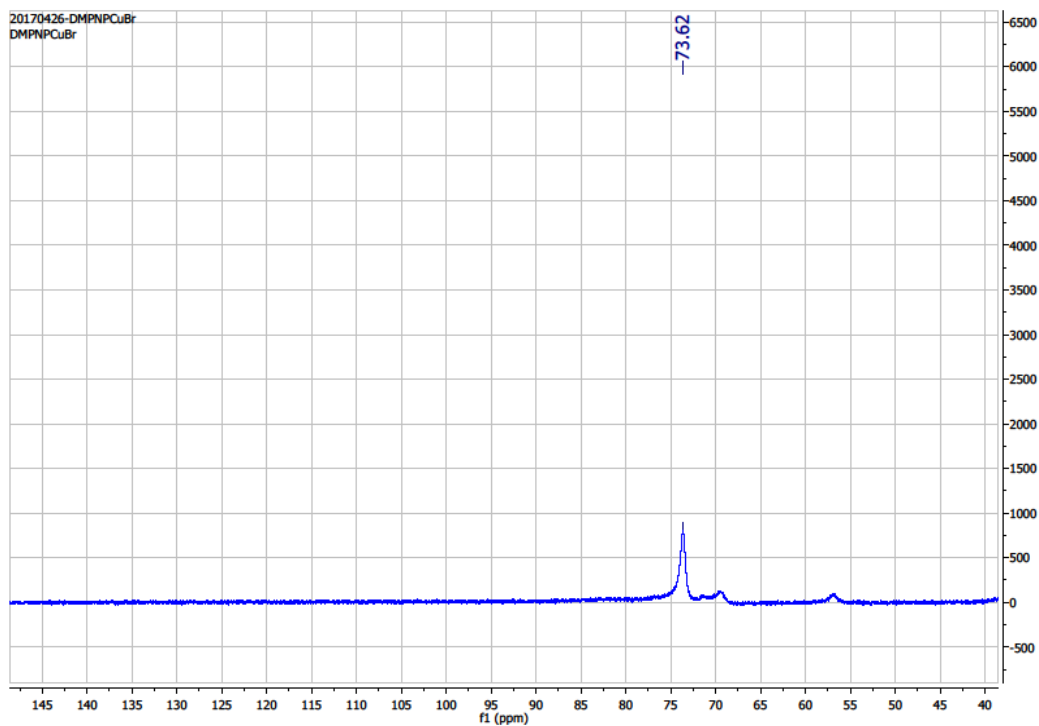
Figure 4A.2 ^{31}P *NMR (CDCl$_3$) of* *4.4*

—59.11
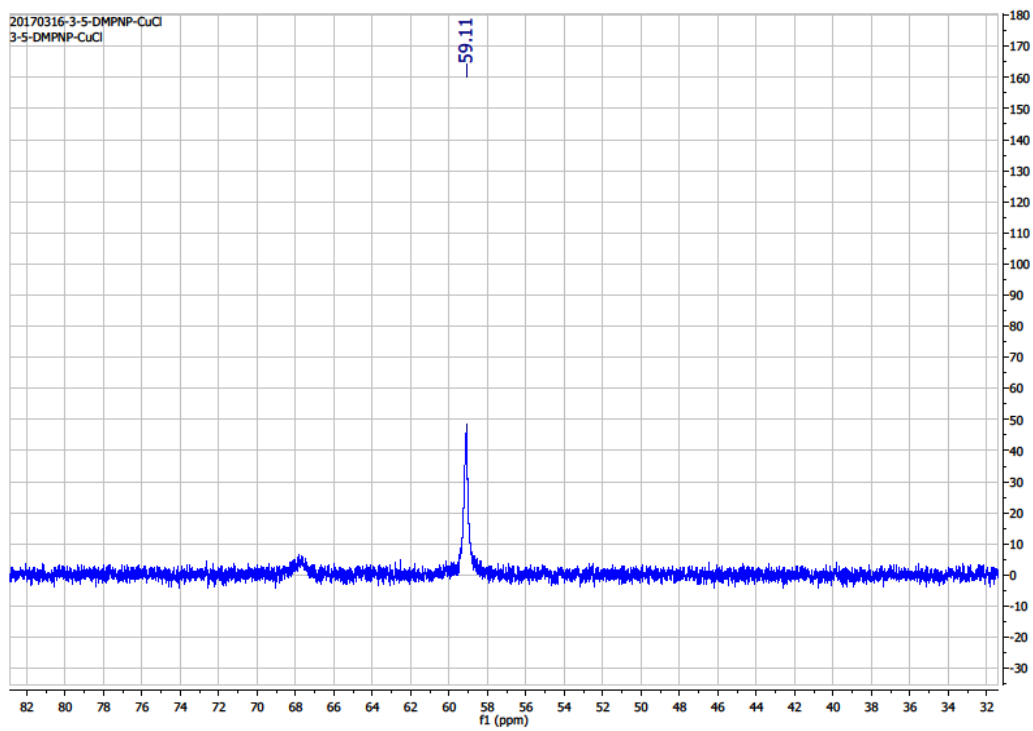
Figure 4A.3 ^{31}P *NMR (CDCl$_3$) of* *4.5*
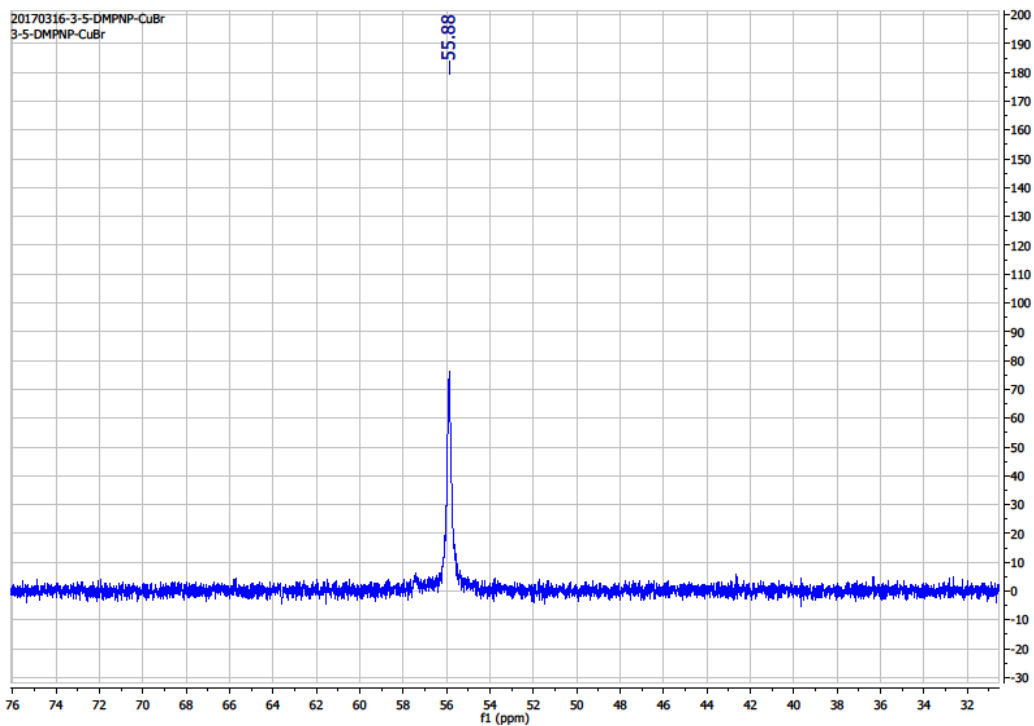
Figure 4A.4 ^{31}P *NMR (CDCl$_3$) of* **4.6**
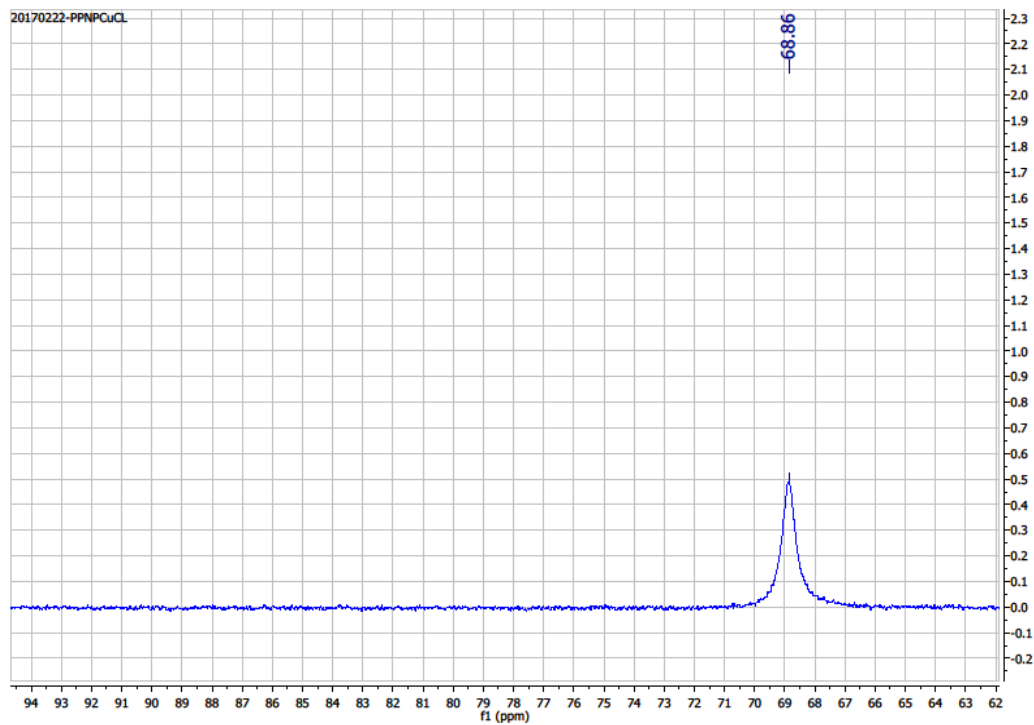
Figure 4A.5 ^{31}P *NMR (CDCl$_3$) of* **4.7**
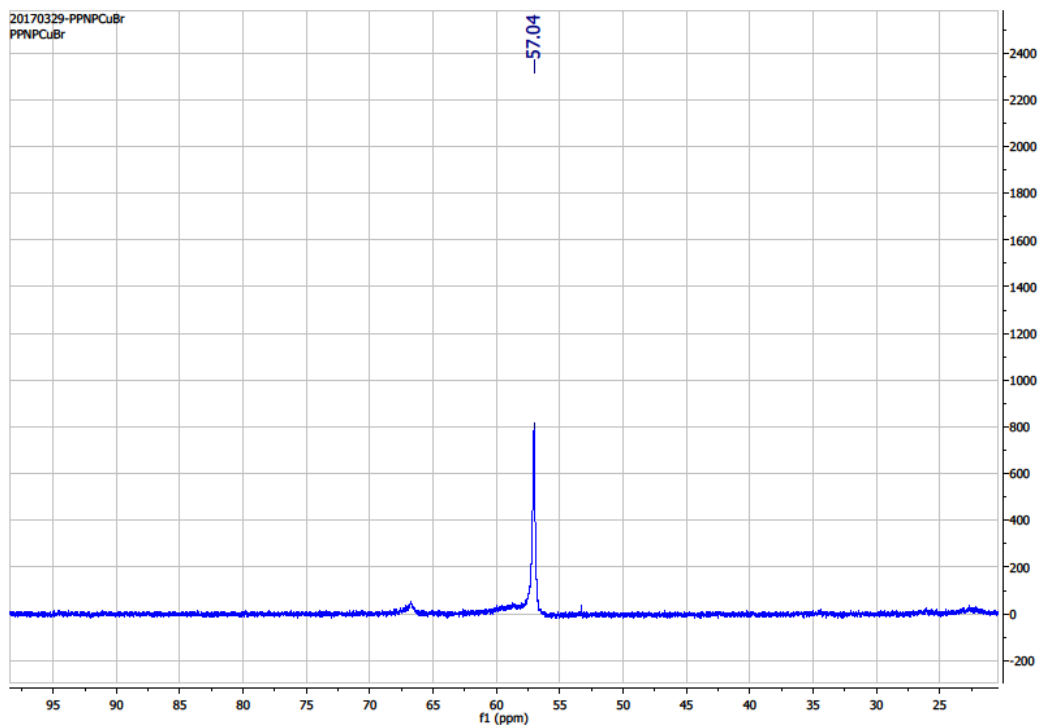
Figure 4A.6 ^{31}P *NMR (CDCl$_3$) of* **4.8**
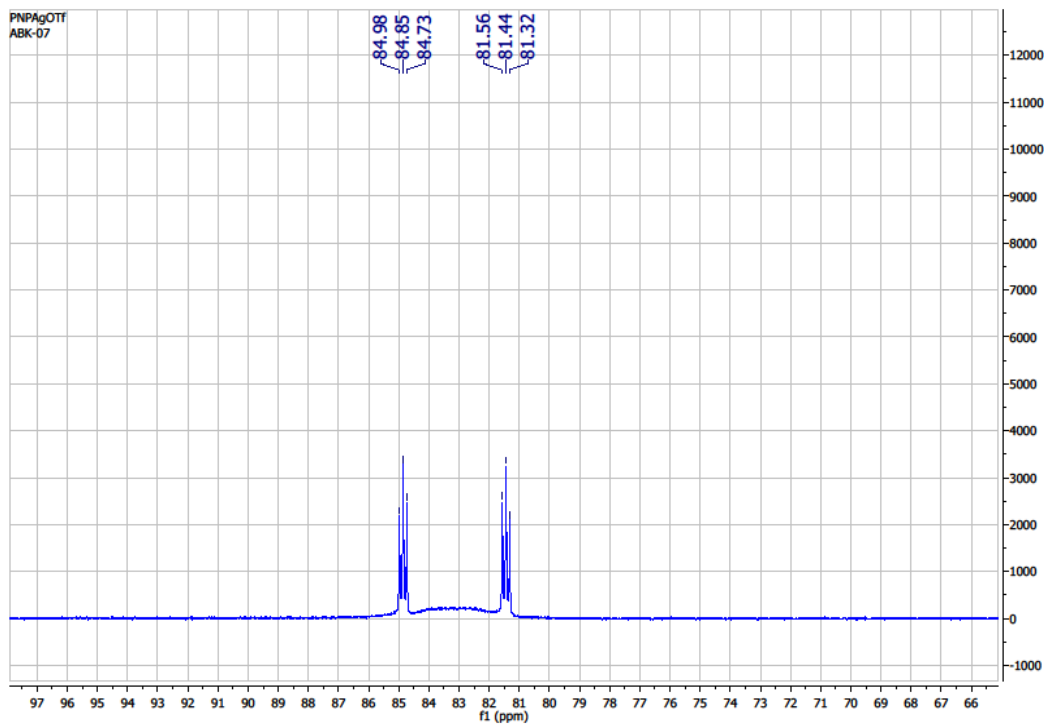
Figure 4A.7 ^{31}P *NMR (CDCl$_3$) of* **4.9**
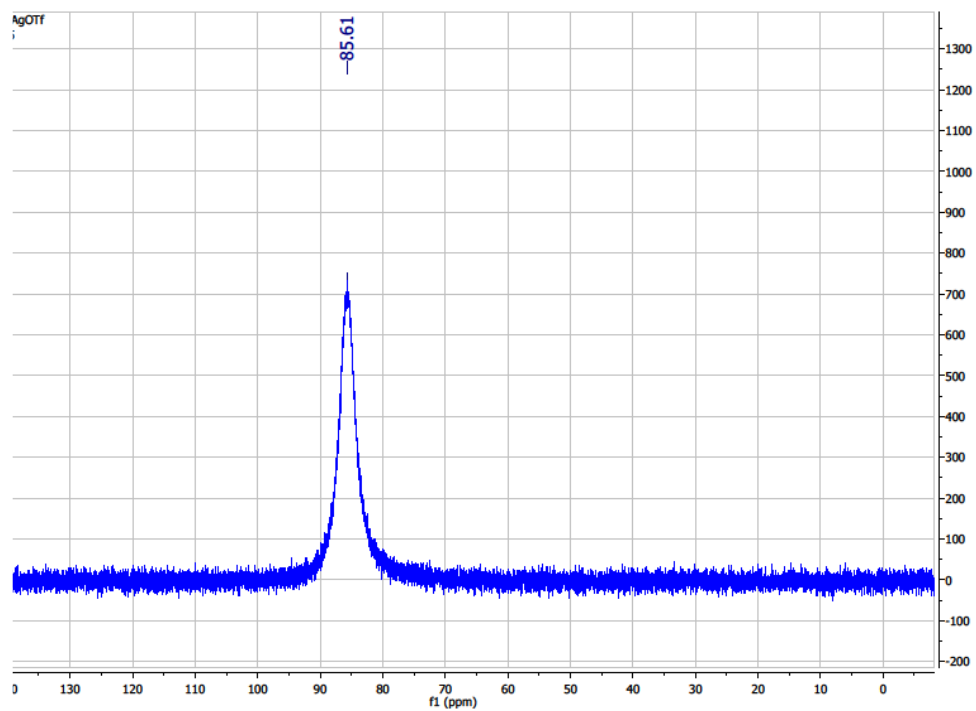
Figure 4A.8. ^{31}P NMR (CDCl$_3$) of **4.10**
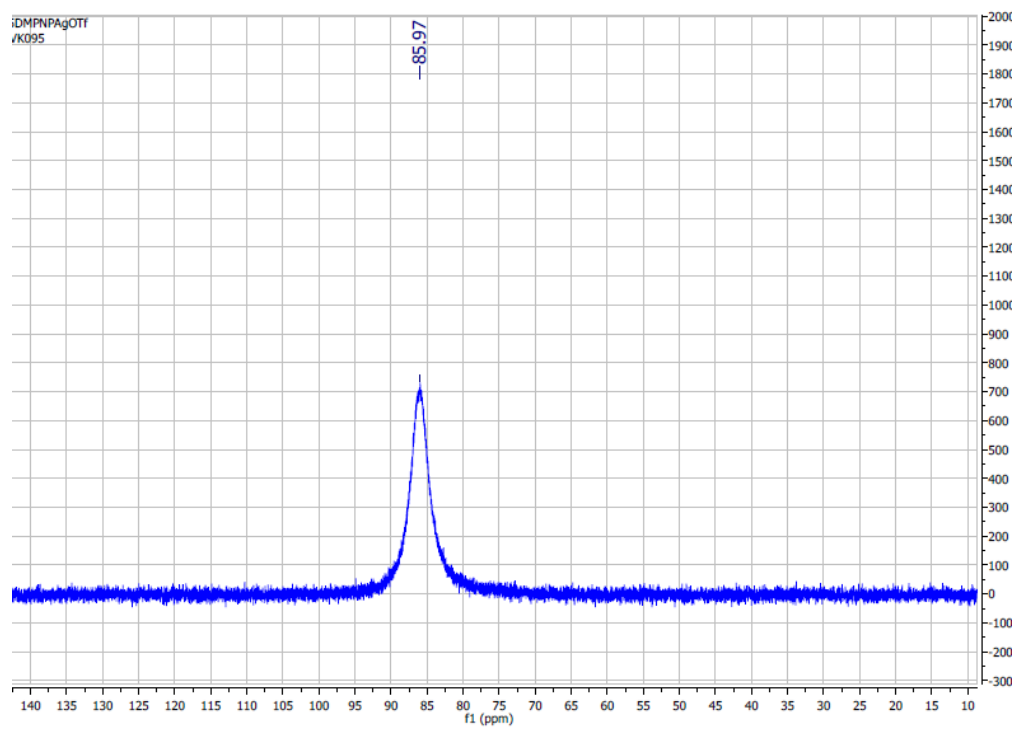
Figure 4A.9. ^{31}P NMR (CDCl$_3$) of **4.11**

86.14
86.02
85.90
82.75
82.62
82.51

-11000

-10000

-9000

-8000

-7000

-6000

-5000

-4000

-3000

-2000

-1000

-0

--1000

101 99 98 97 96 95 94 93 92 91 90 89 88 87 86 85 84 83 82 81 80 79 78 77 76 75 74 73 72 71 70 69
f1 (ppm)
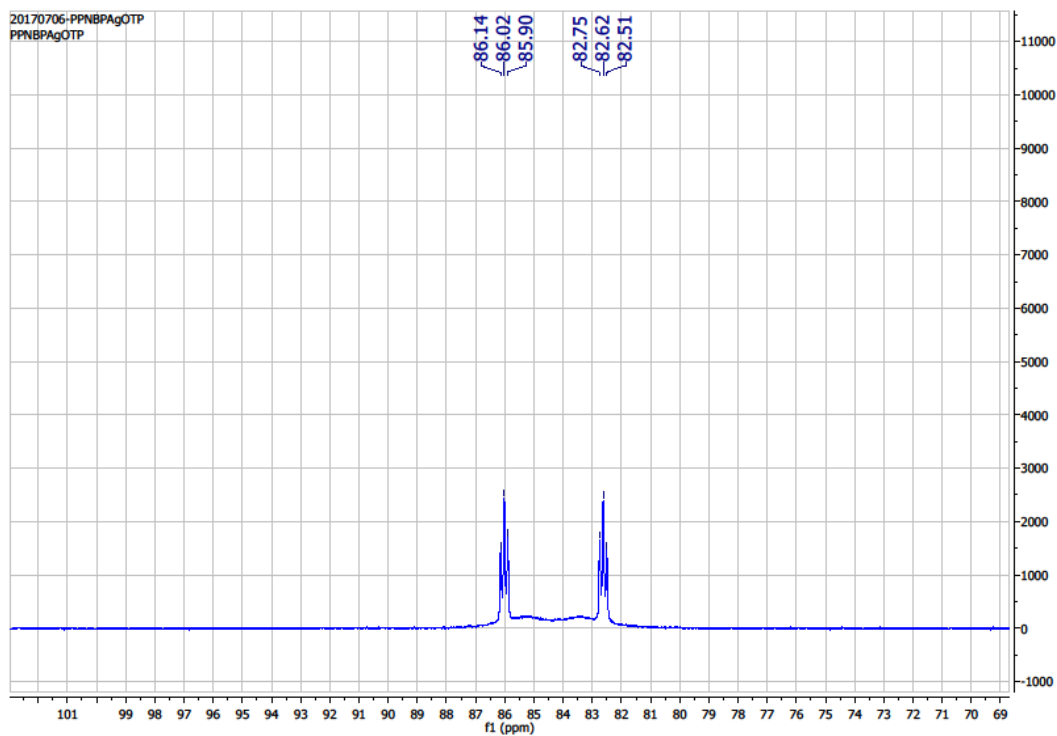
Figure 4A.10. ^{31}P *NMR (CDCl$_3$) of*

88.93 Ag-Ag

4.9

Intensity (normalized)

Raman Shift, cm^{-1}
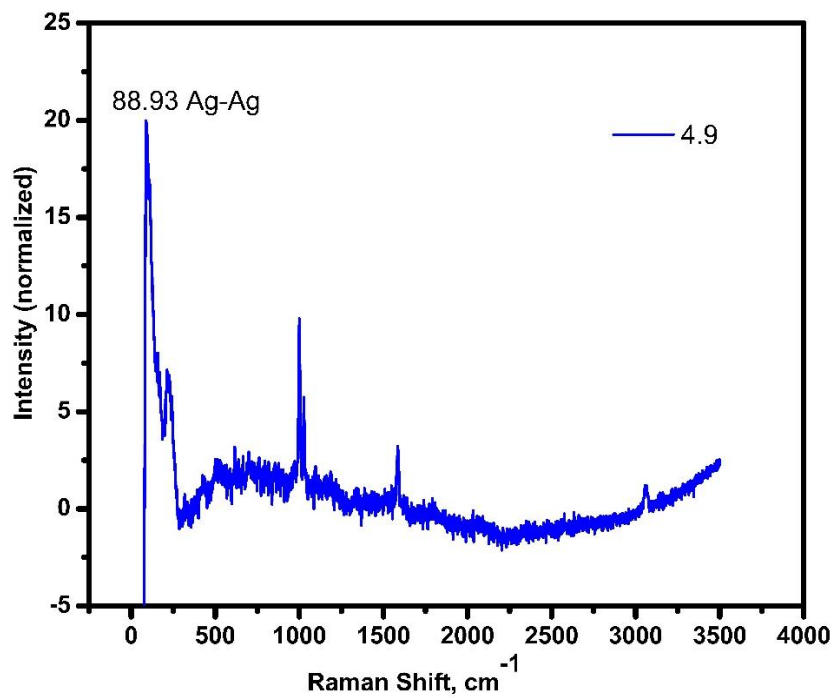
Figure 4A.11. Raman spectra of 4.9
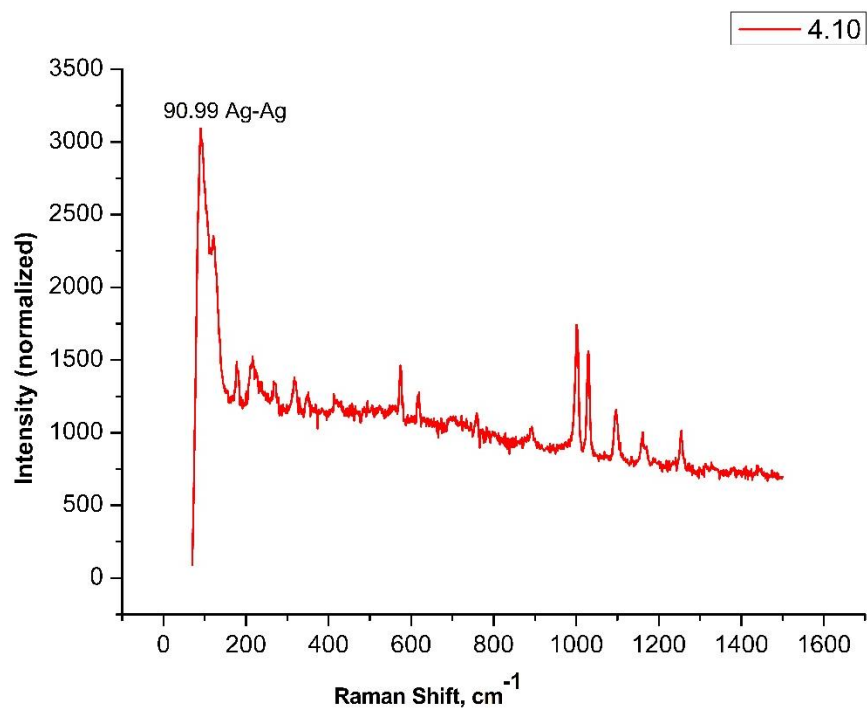
Figure 4A.12. *Raman spectra of* **4.10**

Table 4A.1 *Crystallographic data for* **4.3-4.5**

	4.3	4.4	4.5
Formula	$C_{64}H_{58}Cl_2Cu_2N_2P_4$	$C_{128}H_{104}Br_4Cu_4N_4P_8$	$C_{103}H_{95}Cl_4Cu_4N_3P_6$
Formula weight	1176.98	2519.71	1956.59
***T*, K**	150 (2)	150 (2)	150 (2)
color, habit	Pale yellow, block	Yellow, block	Colorless, block
crystal system	Monoclinic	Monoclinic	Orthorhombic
Space group	P21/c	P21/c	Pbca
Unit cell dimensions	a = 9.891(4) Aº	a = 9.9192(7)	a = 25.523(3)
	b = 16.678(6) Aº	b = 16.7083(13) Aº	b = 22.815(3) Aº
	c = 17.378(6) Aº	b = 17.4691(13) Aº	b = 34.364(5) Aº
	α = 90º	α = 90º	α = 90o

	β = 102.441(10)°	β =102.762(5)°	β = 90°
	γ = 90°	γ = 90°	γ = 90°
V, Å³	2799.5(18)	2823.7(4)	20010(5)
Z	2	1	8
d_{calcd}, g cm⁻³	1.396	1.482	1.299
Absorption coefficient (mm⁻¹)	1.012	3.980	3.197
F(000)	1936	1276	8064
Theta range for data collection (°)	2.135 to 28.367	3.705 to 67.964	2.572 to 67.479
Index ranges	-11<=h<=11 -20<=k<=20 -20<=k<=20	-11<=h<=11 -19<=k<=19 -20<=k<=20	-30<=h<=30 -27<=k<=23 -41<=k<=40
Reflections collected	35190	47655	347179
Independent reflections	5053 [R(int) = 0.0790]	5045 [R(int) = 0.1691]	17905 [R(int) = 0.1970]
Coverage of independent reflections (%)	99.0	98.3	99.4
Function minimized	Σ w(Fo2 - Fc2)2	Σ w(Fo2 - Fc2)2	Σ w(Fo2 - Fc2)2
Data/ restraints/ parameters	5053/ 0/ 336	5045/ 0/ 336	17905 / 72/ 1112
Goodness-of-fit on F2	1.023	1.056	1.079
Δ/σ max	0.001	0.000	0.069
Final R indices	3894 data, [I>2σ(I)] R1= 0.0389, wR2= 0.0790	2789 data, [I>2σ(I)] R1= 0.0795, wR2= 0.1691	12339 data, [I>2σ(I)] R1= 0.1059, wR2= 0.1970
	all data, R1= 0.0624, wR2= 0.0877	all data, R1= 0.1657, wR2= 0.2115	all data, R1= 0.1613, wR2= 0.2218
Largest diff. peak and hole (eÅ⁻³)	0.485 and -0.349	0.703 and -0.846	0.674 and -1.404
R. M. S deviation from mean (eÅ⁻³)	0.068	0.142	0.109

Table 4A.2. Crystallographic data for **4.6-4.8**

	4.6	4.7	4.8
Formula	$C_{96}H_{87}Br_4Cu_4N_3P_6$	$C_{32}H_{29}Cl_4Cu_2NP_2$	$C_{62}H_{54}Br_4Cu_4N_2P_4$
Formula weight	2042.30	758.38	1524.75
T, K	150 (2)	150 (2)	150 (2)
color, habit	Colourless, block	Yellow, Needle	Colorless, block
crystal system	orthorhombic	Monoclinic	Monoclinic
Space group	Pbca	P21/c	P 21/n
Unit cell dimensions	a = 25.764(3) A°	a = 9.776(19) A°	a = 14.344(3) A°
	b = 22.909(3) A°	b = 22.94(4) A°	b = 16.175(3) A°
	c = 34.509(4) A°	C = 16.07(3) A°	c = 14.823(3) A°
	$\alpha = 90°$	$\alpha = 90°$	$\alpha = 90°$
	$\beta = 90°$	$\beta = 91.19(7)°$	$\beta = 111.997(5)°$
	$\gamma = 90°$	$\gamma = 90°$	$\gamma = 90°$
V, Å³	20368(4)	3604(12)	3189.1(10)
Z	8	4	2
d_{calcd}, g cm^{-3}	1.332	1.398	1.588
Absorption coefficient (mm^{-1})	3.989	1.587	3.960
F(000)	8240	1536	1512
Theta range for data collection (°)	2.561 to 68.187	2.181 to 25.246	2.498 to 25.248
Index ranges	-30<=h<=30 -26<=k<=27 -41<=k<=41	-11<=h<=11 -19<=k<=19 -27<=k<=27	-17<=h<=17 -19<=k<=19 -17<=k<=17
Reflections collected	423156	76565	28184
Independent reflections	18423 [R(int) = 0.1650]	6527 [R(int) = 0.1981]	5770 [R(int) = 0.0963]

Coverage of independent reflections (%)	98.9	100	99.8
Function minimized	Σ w(Fo2 - Fc2)2	Σ w(Fo2 - Fc2)2	Σ w(Fo2 - Fc2)2
Data/ restraints/ parameters	18423/1698/ 1024	6527/ 0/ 371	5770/ 0/ 344
Goodness-of-fit on F2	1.020	1.166	1.012
Δ/ σ max	0.001	0.000	0.003
Final R indices	12529 data, [I>2σ(I)] R1= 0.0660, wR2= 0.1650	2855 data, [I>2σ(I)] R1= 0.0840, wR2= 0.1981	4104 data, [I>2σ(I)] R1= 0.0442, wR2= 0.0963
	all data, R1= 0.1070, wR2= 0.1926	all data, R1= 0.2135, wR2= 0.2525	all data, R1= 0.0780, wR2= 0.1088
Largest diff. peak and hole (eÅ-3)	1.657and -1.705	0.808 and -0.825	0.696 and -0.578
R. M. S deviation from mean (eÅ^{-3})	0.138	0.123	0.114

Table 4A.3. *Crystallographic data for* **4.9-4.10**

	4.9	4.10
Formula	$C_{64} H_{54} Ag_2 Cl_4 F_6 N_2 O_6 P_4 S_2$	$C_{140} H_{132} Ag_4 F_{12} N_8 O_{12} P_8 S_4$
Formula weight	1606.63	3154.01
T, K	150 (2)	150 (2)
color, habit	Colourless, Needle	Colourless, block
crystal system	orthorhombic	Monoclinic
Space group	P n a 21	P 21/n
Unit cell dimensions	a = 25.662(4) Aº	a = 13.6191(9) Aº
	b = 21.397(4) Aº	b = 13.0833(10) Aº
	c = 11.9939(18) Aº	C = 18.4322(15) Aº

	$\alpha = 90^o$	$\alpha = 90^o$
	$\beta = 90^o$	$\beta = 97.486(2)^o$
	$\gamma = 90^o$	$\gamma = 90^o$
V, Å³	6585.7(18)	3256.3(4)
Z	4	1
d_{calcd}, g cm⁻³	1.620	1.608
Absorption coefficient (mm⁻¹)	3.989	0.839
F(000)	8240	1604
Theta range for data collection (°)	2.324 to 25.249	2.167 to 28.362
Index ranges	-30<=h<=30 -25<=k<=25 -14<=k<=14	-17<=h<=18 -17<=k<=17 -24<=k<=24
Reflections collected	264647	162494
Independent reflections	11926 [R(int) = 0.1002]	8148 [R(int) = 0.0649]
Coverage of independent reflections (%)	99.9	99.9
Function minimized	Σ w(Fo2 - Fc2)2	Σ w(Fo2 - Fc2)2
Data/ restraints/ parameters	11926/73/ 812	8148 / 0/ 427
Goodness-of-fit on F2	1.031	0.977
Δ/ σ max	0.023	0.005
Final R indices	11247 data, [I>2σ(I)] R1= 0.0400, wR2= 0.1002	6346 data, [I>2σ(I)] R1= 0.0315, wR2= 0.0649
	all data, R1= 0.0437, wR2= 0.1033	all data, R1= 0.0315, wR2= 0.0649
Largest diff. peak and hole (eÅ-3)	1.979 and -1.464	0.533 and -0.997
R. M. S deviation from mean (eÅ⁻³)	0.106	0.093

Table 4A.4. *Crystallographic data for* **4.11-4.12**

	4.11	4.12
Formula	$C_{69} H_{64} Ag_2 Cl_6 F_6 N_2 O_6 P_4 S_2$	$C_{64} H_{54} Ag_2 F_6 N_2 O_6 P_4 S_2$
Formula weight	1747.66	1464.83
T, K	150 (2)	150 (2)
color, habit	Colourless, block	Colourless, block
crystal system	triclinic	Monoclinic
Space group	P -1	C 2/c
Unit cell dimentions	a = 14.276(14) A^o	a = 20.297(8) A^o
	b = 15.177(19)A^o	b = 15.800(6) A^o
	c = 19.090(18) A^o	C = 19.955(8) A^o
	α = 84.04(6)^o	α = 90°
	β = 82.53(6)^o	β = 101.272(12) ^{o}
	γ = 64.19(5)^o	γ = 90°
V, Å^3	3687(7)	6276(4)
Z	2	4
d_{calcd}, g cm^{-3}	1.574	1.550
Absorption coefficient (mm^{-1})	0.958	0.863
F(000)	1764	2960
Theta range for data collection (^{o})	2.155 to 25.250	2.492 to 28.254
Index ranges	-17<=h<=17	-27<=h<=26
	-18<=k<=18	-21<=k<=20
	-22<=k<=22	-26<=k<=26
Reflections collected	86134	133472

Independent reflections	13323 [R(int) = 0.1376]	7741 [R(int) = 0.0755]
Coverage of independent reflections (%)	99.9	99.7
Function minimized	Σ w(Fo2 - Fc2)2	Σ w(Fo2 - Fc2)2
Data/ restraints/ parameters	18423/1698/ 1024	7741 / 0/ 389
Goodness-of-fit on F2	1.020	1.000
Δ/ σ max	0.001	0.004
Final R indices	7523 data, [I>2σ(I)] R1= 0.0642, wR2= 0.1376	5363 data, [I>2σ(I)] R1= 0.0467, wR2= 0.0755
	all data, R1= 0.1504, wR2= 0.1793	all data, R1= 0.0943, wR2= 0.0878
Largest diff. peak and hole (eÅ-3)	1.717 and -0.832	0.751 and -0.557
R. M. S deviation from mean (eÅ-3)	0.133	0.113

Table 4A.5. *Selected experimental and calculated bond lengths (Å) and bon angles angles (°) of complex **I** and **II**.*

Complex I			Complex II		
Bonds	Exp	Cal	Bonds	Exp	Cal
Cu2-Cu1/ Cu2'-Cu1'	2.776	2.722	Cu2-Cu1/ Cu2'-Cu1'	2.685	2.641
Cu1-Cu2'/ Cu1'-Cu2	2.903	2.881	Cu1-Cu2'/ Cu1'-Cu2	2.711	2.719
Cu2'-Cl1/ Cl1'-Cu2	2.351	2.351	Cu2'-Br1/ Br1-Cu2'	2.440	2.460
Cu1-Cl1/ Cu1'-Cl1'	2.264	2.266	Cu1-Br1/ Cu1'-Br1'	2.398	2.415
Cu1-Cl2/ Cl2'-Cu1'	2.368	2.331	Cu1-Br2/ Br2'-Cu1'	2.448	2.454
Cu2-Cl2/ Cu2'-Cl2'	2.380	2.371	Cu2-Br2/ Cu2'-Br2	2.441	2.447
Cl2-Cu2'/ Cl2'-Cu2	2.534	2.620	Br2-Cu2'/ Br2'-Cu2	2.810	2.905

P2-Cu2/ P2'-Cu2'	2.172	2.156	P2-Cu2/ P2'-Cu2'	2.187	2.189
P1-Cu1/ P1'-Cu1'	2.181	2.178	P1-Cu1/ P1'-Cu1'	2.196	2.198
Cu1-Cu2-Cu1'/Cu1-Cu2'-Cu1'	104.52	106.10	Cu1-Cu2-Cu1'/Cu1-Cu2'-Cu1'	103.21	104.27
Cu2-Cu1-Cu2'/Cu2-Cu1'-Cu2'	75.48	73.90	Cu2-Cu1-Cu2'/Cu2-Cu1'-Cu2'	76.79	75.73
P1-Cu1-Cu2/ P1-Cu1-Cu2	92.55	94.25	P1-Cu1-Cu2/ P1-Cu1-Cu2	96.18	96.58
P2-Cu2-Cu1/ P2'-Cu2'-Cu1'	90.03	90.42	P2-Cu2-Cu1/ P2'-Cu2'-Cu1'	90.94	92.12
Cu2-Cl1'-Cu1'/Cu1-Cl1-Cu2'	77.93	77.19	Cu2-Cl1'-Cu1'/Cu1-Cl1-Cu2'	68.15	67.81
Cu1-Cl2-Cu2/ Cu1'-Cl2'-Cu2'	71.56	70.75	Cu1-Cl2-Cu2/ Cu1'-Cl2'-Cu2'	66.62	64.75
Cu1-Cl2-Cu2'/ Cu1'-Cl2'-Cu2	72.55	70.89	Cu1-Cl2-Cu2'/ Cu1'-Cl2'-Cu2	61.62	60.29

Table 4A.6. *Selected experimental and calculated Bond lengths (Å) and angles (°) of complex **4.3** and **4.4**.*

Complex 4.3			Complex 4.4		
Bonds	Exp	Cal	Bonds	Exp	Cal
Cu1-Cl1/Cu1'-Cl1'	2.304(1)	2.335	Cu1-Br1/Cu1'-Br1'	2.472 (2)	2.495
Cu1-Cl1'/Cu1'-Cl1	2.3508 (9)	2.352	Cu1-Br1'/Cu1'-Br1	2.442 (4)	2.461
P1-Cu1/P1'-Cu1'	2.290 (1)	2.280	P1-Cu1/P1'-Cu1'	2.354 (5)	2.293
P2-Cu1/P2'-Cu1'	2.320 (1)	2.286	P2-Cu1/P2'-Cu1'	2.299 (7)	2.287
P1-N1/P1'-N1'	1.728 (2)	1.747	P1-N1/P1'-N1'	1.693 (9)	1.749
P2-N1/P2'-N1'	1.722 (2)	1.749	P2-N1/P2'-N1'	1.761 (8)	1.753

Cl1-Cu1-Cl1'/Cl1-Cu1'-Cl1'	96.41 (3)	97.66	Br1-Cu1-Br1'/Br1-Cu1'-Br1'	100.44 (5)	97.64
Cu1-Cl1-Cu1'/Cu1-Cl1'-Cu1'	83.59 (3)	82.34	Cu1-Br1-Cu1'/Cu1-Br1'-Cu1'	79.56 (5)	82.41
P1-Cu1-P2/P1'-Cu1'-P2'	73.82 (3)	74.43	P1-Cu1-P2/P1'-Cu1'-P2'	73.09 (9)	74.16

Table 4A.7*. Selected experimental and calculated Bond lengths (Å) and angles (°) of complex **4.5** and **4.6***.

Complex 4.6			Complex 4.7		
Bonds	Exp	Cal	Bonds	Exp	Cal
Cu1-Cu2	2.809 (1)	2.841	Cu1-Cu2	2.923 (1)	2.906
Cu2-Cu3	2.922 (1)	2.939	Cu2-Cu3	2.801 (1)	2.828
Cu3-Cu1	2.934 (1)	2.971	Cu3-Cu1	2.934 (1)	2.930
Cu1-Cl1	2.434 (2)	2.516	Cu1-Br1	2.565 (1)	2.648
Cu1-Cl2	2.466 (2)	2.467	Cu1-Br2	2.546 (1)	2.609
Cu2-Cl1	2.416 (2)	2.551	Cu2-Br1	2.534 (1)	2.596
Cu2-Cl2	2.475 (2)	2.587	Cu2-Br2	2.590 (1)	2.664
Cu3-Cl1	2.469 (2)	2.489	Cu3-Br1	2.553(1)	2.627
Cu3-Cl2	2.431 (2)	2.495	Cu3-Br2	2.585(1)	2.630
Cl3-Cu4/ Cl3-Cu4	2.081 (5)	2.164	Cu4-Br3/ Cu4-Br4	2.210 (2)	2.296
P1-Cu1	2.243 (2)	2.252	P1-Cu1/ P2-Cu2	2.240 (2)	2.257
P2-Cu2	2.238 (2)	2.249	P3-Cu2/ P6-Cu1	2.241 (2)	2.264
P3-Cu2	2.230 (2)	2.244	P4-Cu3	2.252 (2)	2.254
P4-Cu3	2.241 (2)	2.248	P5-Cu3	2.244 (2)	2.256
P5-Cu3	2.240 (2)	2.248			
P6-Cu1	2.242 (2)	2.249			

Cu1-Cu2-Cu3	61.54 (3)	61.83	Cu1-Cu2-Cu3	61.62 (3)	61.45
Cu2-Cu3-Cu1	57.33 (3)	57.45	Cu2-Cu3-Cu1	61.23 (3)	60.60
Cu3-Cu1-Cu2	61.13 (3)	60.72	Cu3-Cu1-Cu2	57.15 (3)	57.95
Cu1-P1-N1	117.7 (2)	118.23	Cu1-P1-N1	117.29 (2)	117.69
Cu2-P2-N1	117.1 (2)	117.33	Cu2-P2-N1	118.0 (2)	118.56
Cu2-P3-N2	118.3 (2)	118.84	Cu2-P3-N2	117.5 (2)	117.52
Cu1-P6-N3/ Cu3-P4-N2	117.6 (2)	118.40	Cu1-P6-N3	117.0 (2)	118.69
Cu3-P5-N3	117.5 (2)	117.89	Cu3-P4-N2/Cu3-P5-N3	117.4 (2)	117.83
Cl3-Cu4-Cl4	176.8 (2)	179.1	Br3-Cu3-Br4	178.23 (9)	173.1
P1-N1-P2	120.5 (3)	120.12	P1-N1-P2	121.8 (3)	119.98
P3-N2-P4	121.3 (3)	120.08	P3-N2-P4	120.4 (3)	119.59
P5-N3-P6	120.7 (3)	119.37	P5-N3-P6	121.4 (3)	119.80

Table 4A.8. *Selected experimental and calculated Bond lengths (Å) and angles (°) of complex **4.7** and **4.8***.

Complex 4.7			Complex 4.8		
Bonds	Exp.	Cal.	Bonds	Exp.	Cal.
Cu2-Cu1/ Cu2'-Cu1'	2.748(4)	2.675	Cu2-Cu1/ Cu2'-Cu1'	2.650(1)	2.646
Cu1-Cu2'/ Cu1'-Cu2	2.858(5)	2.879	Cu1-Cu2'/ Cu1'-Cu2	2.701(1)	2.742
Cu2'-Cl1/ Cl1'-Cu2	2.344(4)	2.348	Cu2-Br1'/ Br1-Cu2'	2.424(1)	2.447
Cu1-Cl1/ Cu1'-Cl1'	2.235(4)	2.267	Cu1-Br1/ Cu1'-Br1'	2.417(8)	2.439
Cu1-Cl2/ Cl2'-Cu1'	2.381(4)	2.334	Cu1-Br2/ Br2'-Cu1'	2.786(1)	2.927/2.886

Cu2-Cl2/ Cu2'-Cl2'	2.411(4)	2.386	Cu2-Br2/ Cu2'-Br2'	2.865(9)	2.922
Cl2-Cu2'/ Cl2'-Cu2	2.569(4)	2.639	Cu2-Br2'/ Cu2'-Br2	2.560(9)	2.531
P2-Cu2/ P2'-Cu2'	2.185(4)	1.181	Cu1-Br2'/ Cu1'-Br2	2.580(1)	2.505
P1-Cu1/ P1'-Cu1'	2.163(4)	2.159	P2-Cu2/ P2'-Cu2'	2.192(1)	2.189
			P1-Cu1/ P1'-Cu1'	2.186(2)	2.177
Cu1-Cu2-Cu1'/Cu1-Cu2'-Cu1'	99.60(5)	102.70	Cu1-Cu2-Cu1'/Cu1'-Cu2'-Cu1	87.53(3)	89.17
Cu2-Cu1-Cu2'/Cu2-Cu1'-Cu2'	80.40(5)	77.30	Cu2-Cu1-Cu2'/Cu2'-Cu1'-Cu2	92.47(3)	90.81
P1-Cu1-Cu2/ P1-Cu1-Cu2	92.02(8)	93.81	P1-Cu1-Cu2/ P1'-Cu1'-Cu2'	93.67(4)	93.19
P2-Cu2-Cu1/ P2'-Cu2'-Cu1'	90.92(7)	92.48	P2-Cu2-Cu1/ P2'-Cu2'-Cu1'	93.62(4)	95.09
Cu2-Cl1'-Cu1'/Cu1-Cl1-Cu2'	77.20(9)	77.19	P1-N1-P2/ P1'-N1'-P2'	117.1(2)	116.80
Cu1-Cl2-Cu2/ Cu1'-Cl2'-Cu2'	69.97(7)	69.01	Cu2-Br1'-Cu1'/Cu1-Br1-Cu2'	67.84(3)	68.25
Cu1-Cl2-Cu2'/ Cu1'-Cl2'-Cu2	70.42(7)	70.46	Cu1-Br2-Cu2/ Cu1'-Br2'-Cu2'	56.43(2)	53.80
			Cu1-Br2-Cu2'/ Cu1'-Br2'-Cu2	59.22(2)	60.53
			Cu1-Br2'-Cu2/Cu1'-Br2-Cu2'	62.09(2)	63.40
			Cu1-Br2'-Cu2'/ Cu2-Br2-Cu1'	61.24(2)	60.31

Table 4A.9. *Computed frontier molecular orbital energy difference in eV obtained using the B3LYP/def2-TZVP(P) level.*

Compound	E_{HOMO}	E_{LUMO}	$\Delta E_{HOMO-LUMO}$
I	-4.9047	-1.2664	3.6383
II	-4.8421	-1.249	3.5931
1	-4.5895	-1.1480	3.4415
2	-4.6744	-1.2066	3.4678
3	-6.9857	-3.1876	3.7981
4	-7.1535	-3.1898	3.9637
5	-4.8514	-1.1280	3.7234
6	-4.7527	-1.2836	3.4691

** = Grease; * = Toluene; # =H₂O
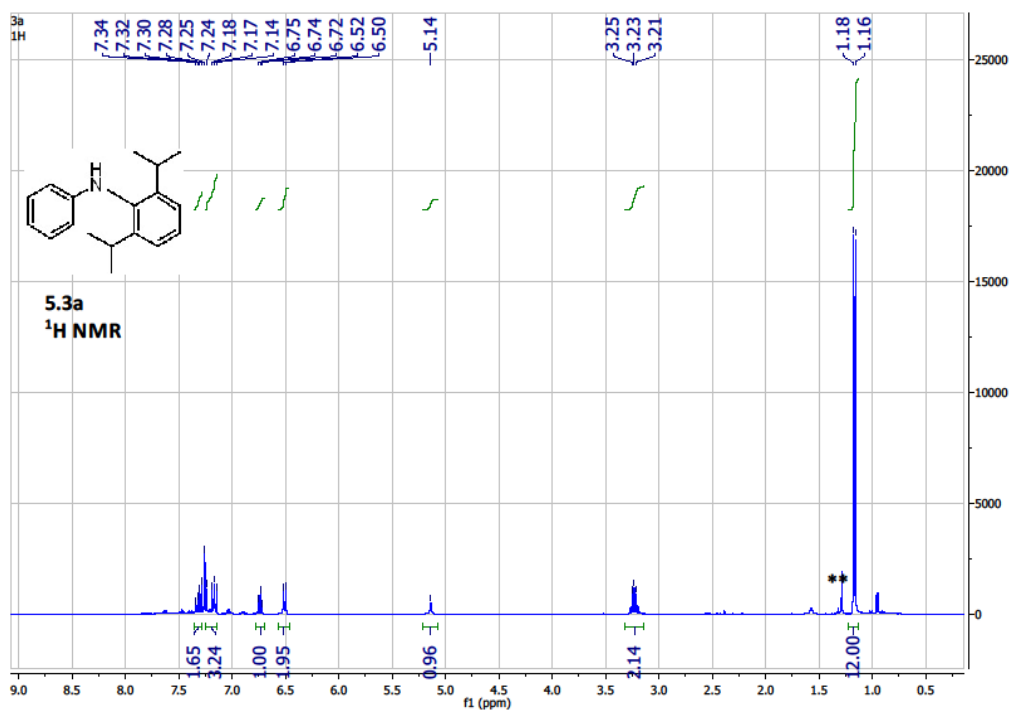
Figure 5A.1 ¹H NMR (CDCl₃) of **5.3a**
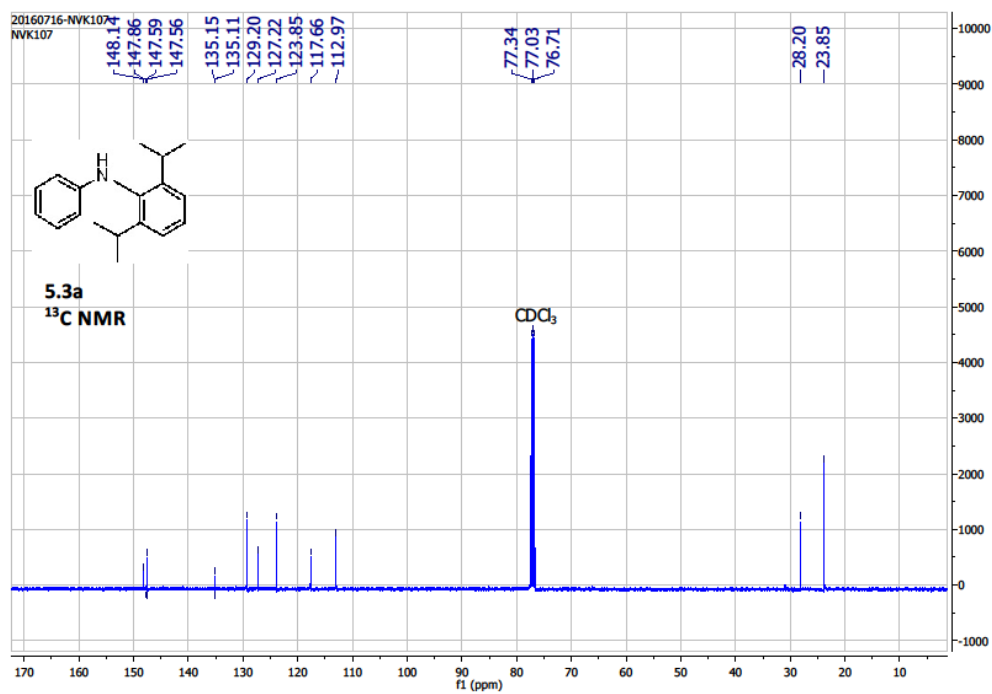
Figure 5A.2 ¹³C NMR (CDCl₃) of **5.3a**
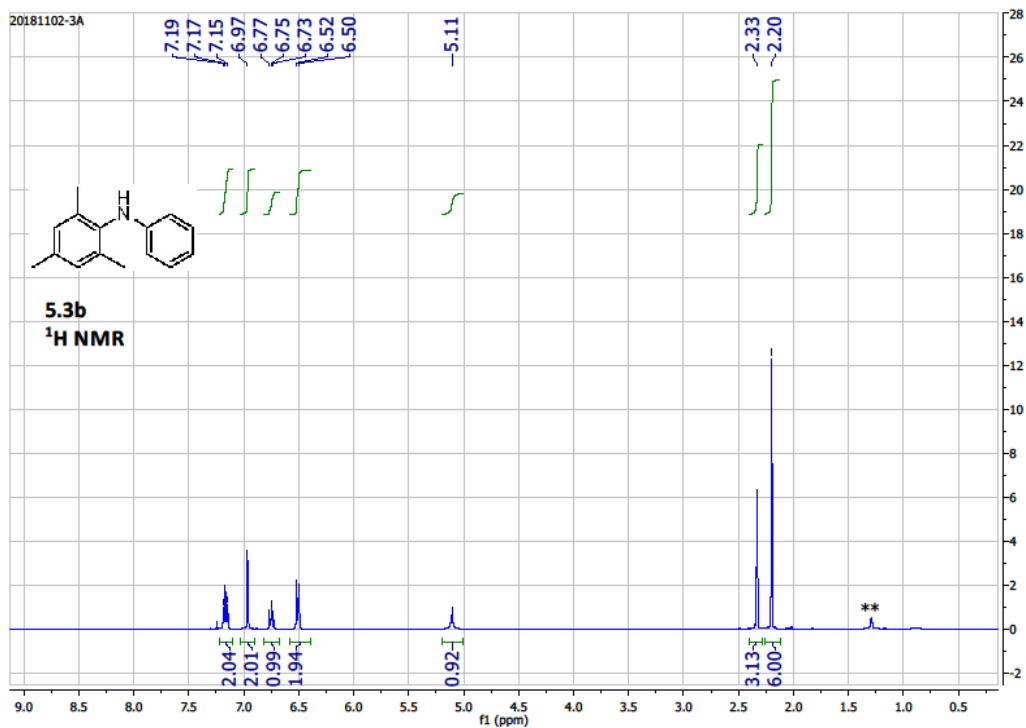
Figure 5A.3 ^{1}*H NMR (CDCl$_3$) of **5.3b***
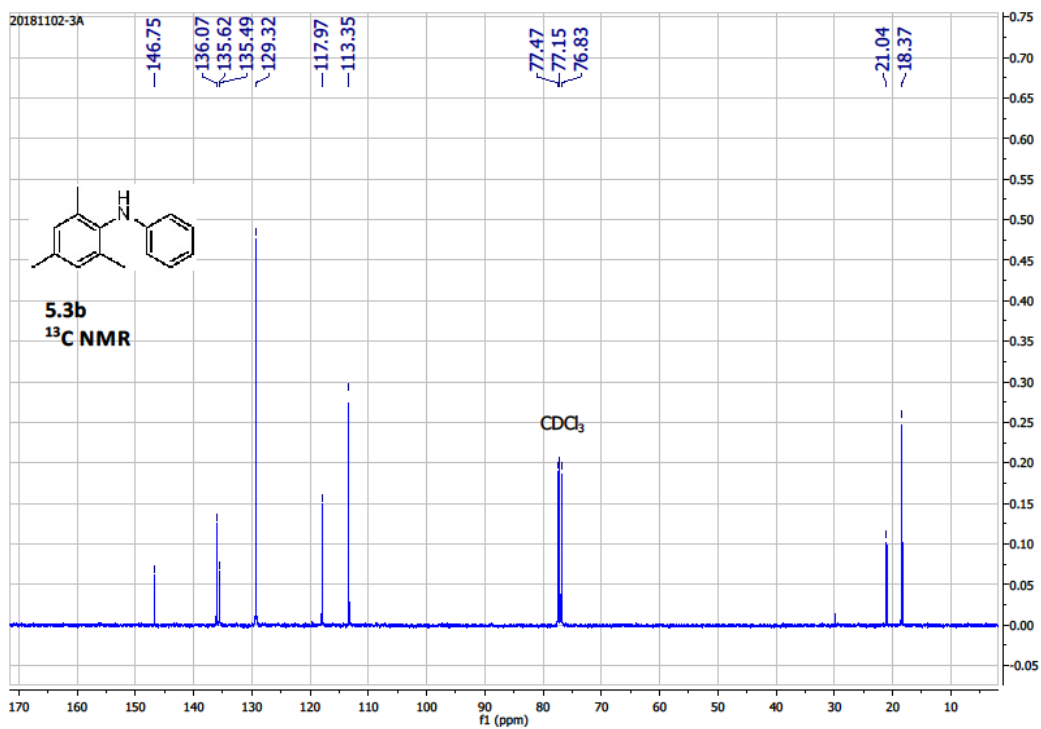
Figure 5A.4 ^{13}*C NMR (CDCl$_3$) of **5.3b***
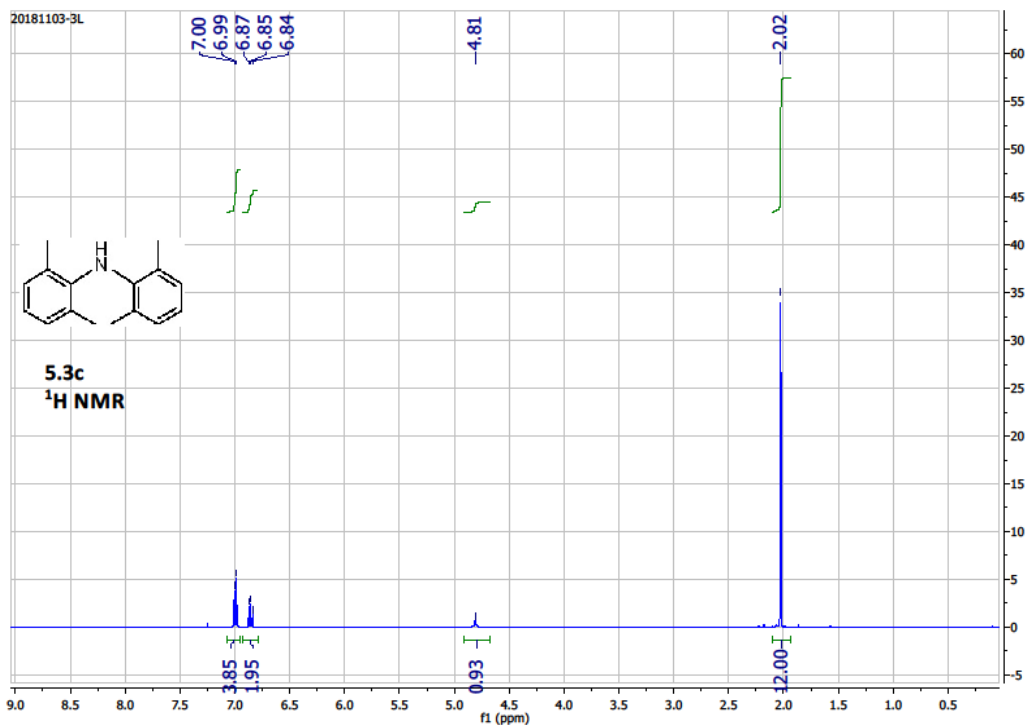
Figure 5A.5 ^1H NMR (CDCl$_3$) of **5.3c**
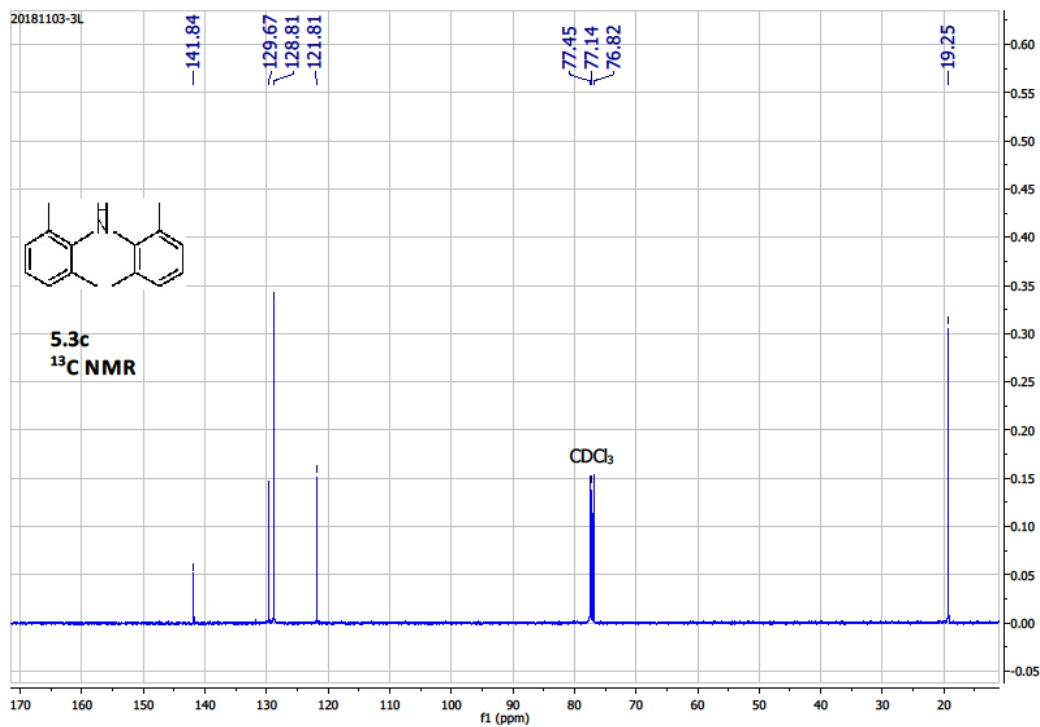
Figure 5A.6 ^{13}C NMR (CDCl$_3$) of **5.3c**
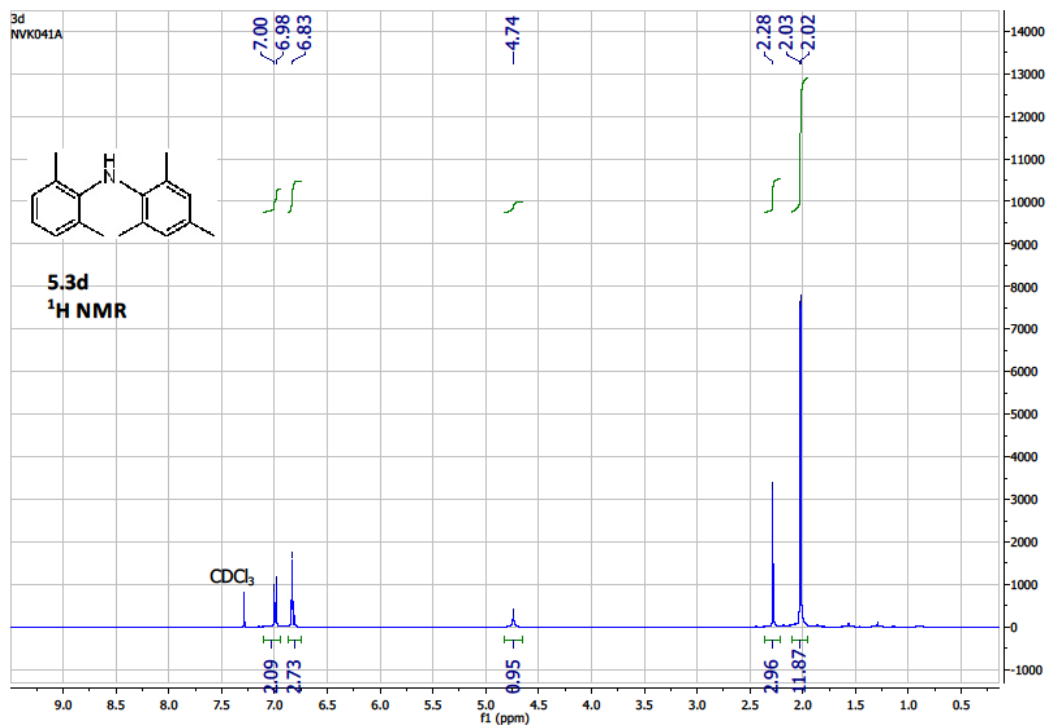
Figure 5A.7 ¹H NMR (CDCl₃) of **5.3d**
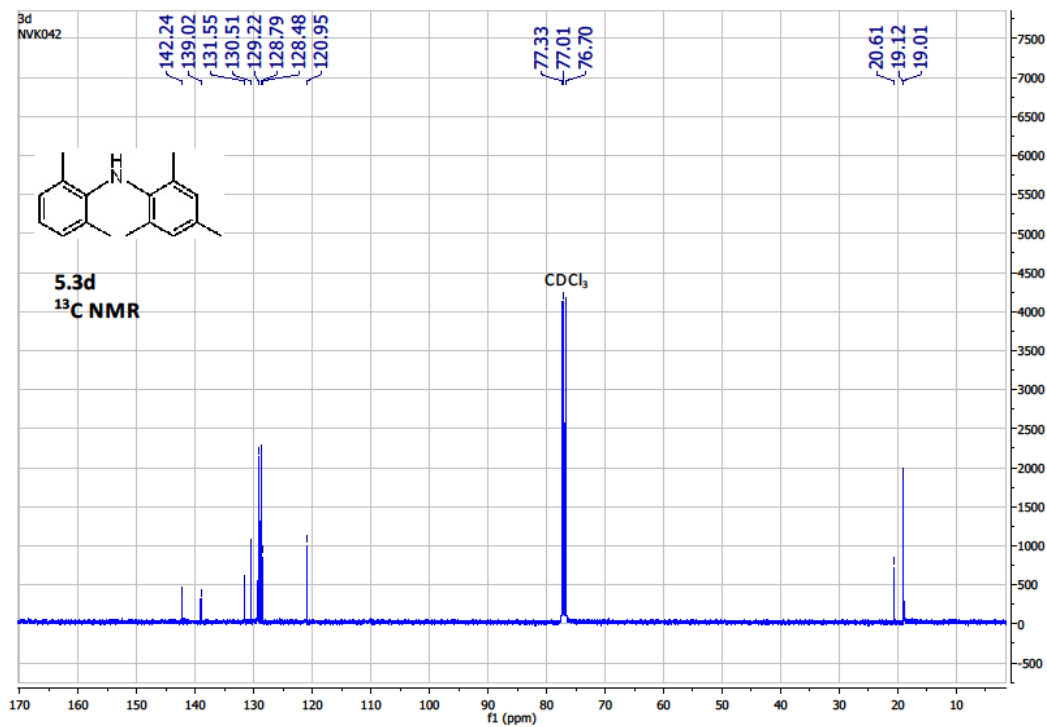
Figure 5A.8 ¹³C NMR (CDCl₃) of **5.3d**
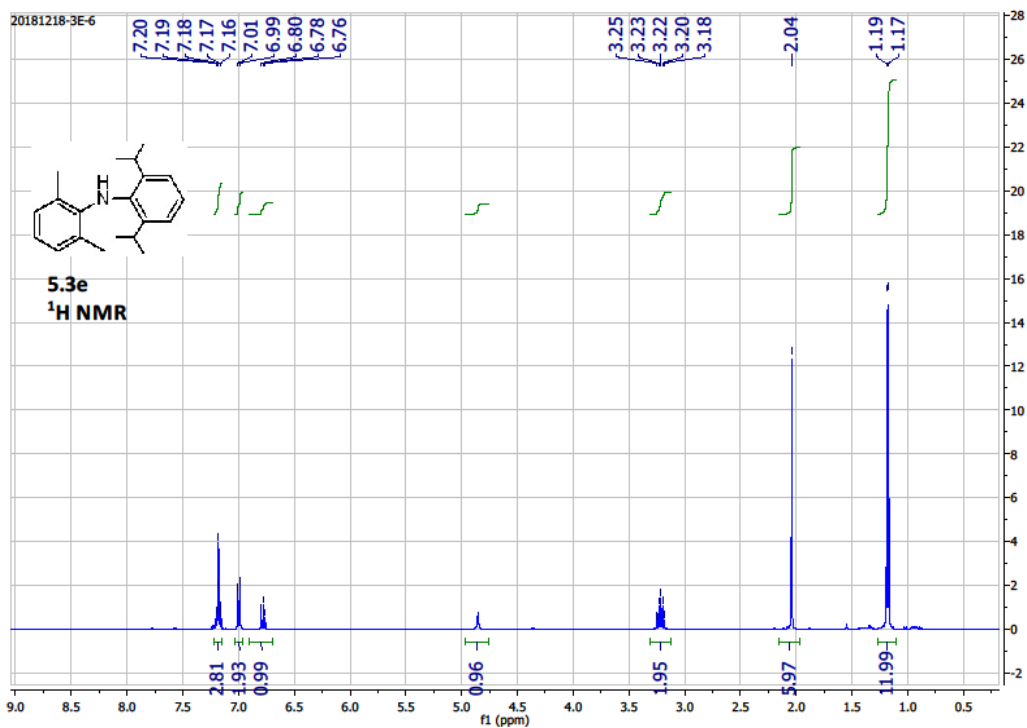
Figure 5A.9 ^1H NMR (CDCl$_3$) of **5.3e**
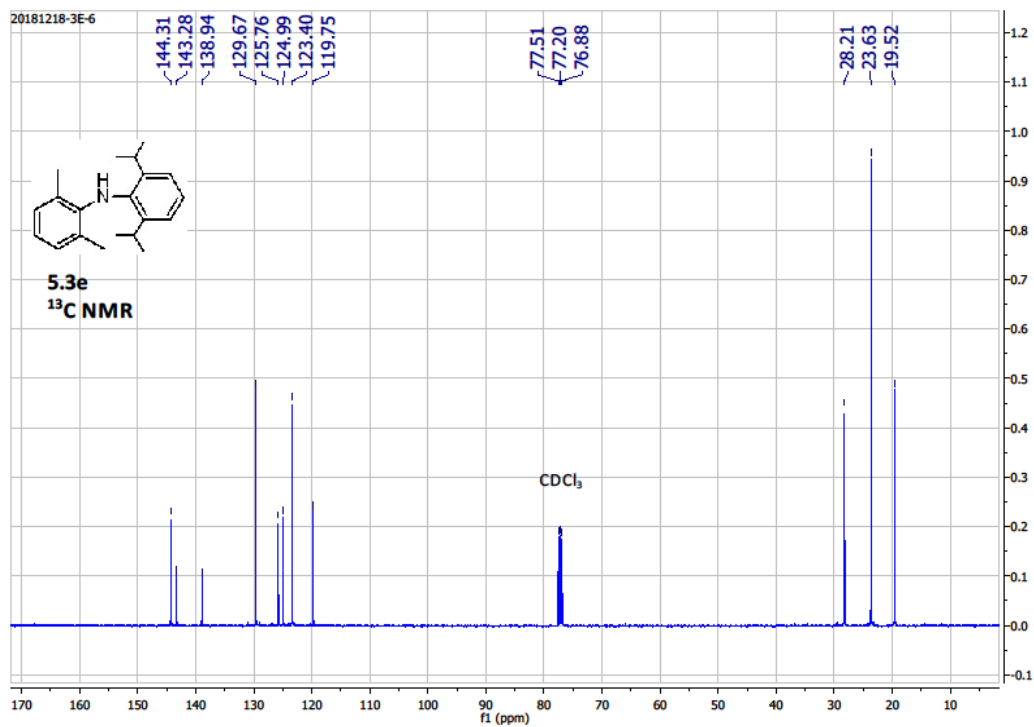
Figure 5A.10 ^{13}C NMR (CDCl$_3$) of **5.3e**
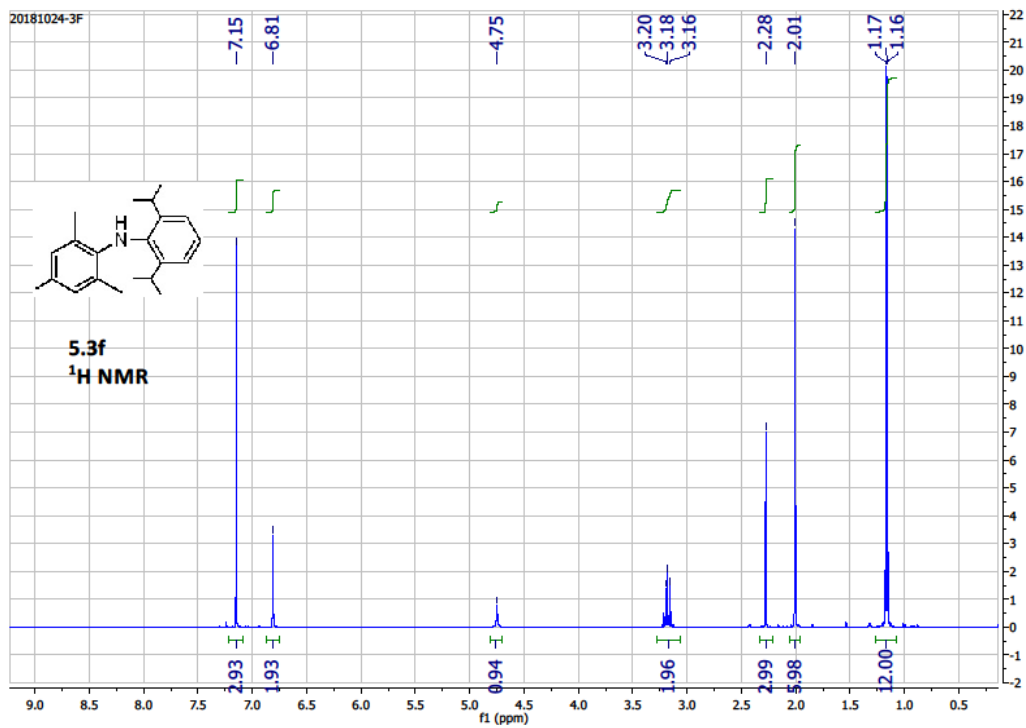
Figure 5A.11 ^{1}H NMR (CDCl$_3$) of **5.3f**
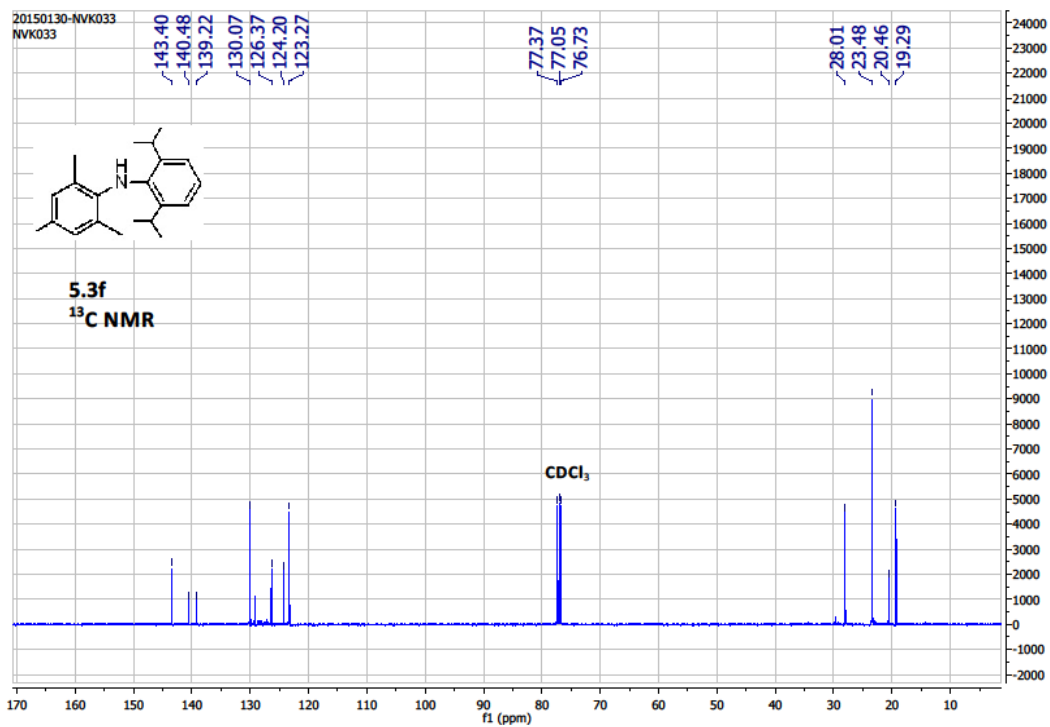
Figure 5A.12 ^{13}C NMR (CDCl$_3$) of **5.3f**
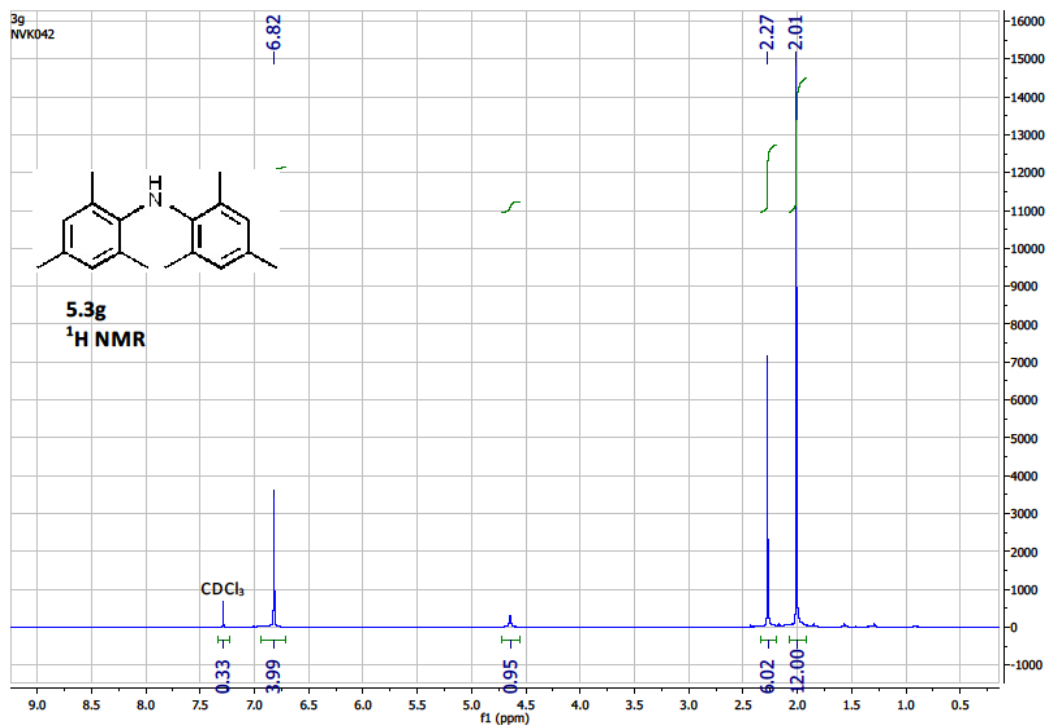
Figure 5A.13 ^{1}*H NMR (CDCl₃) of* **5.3g**
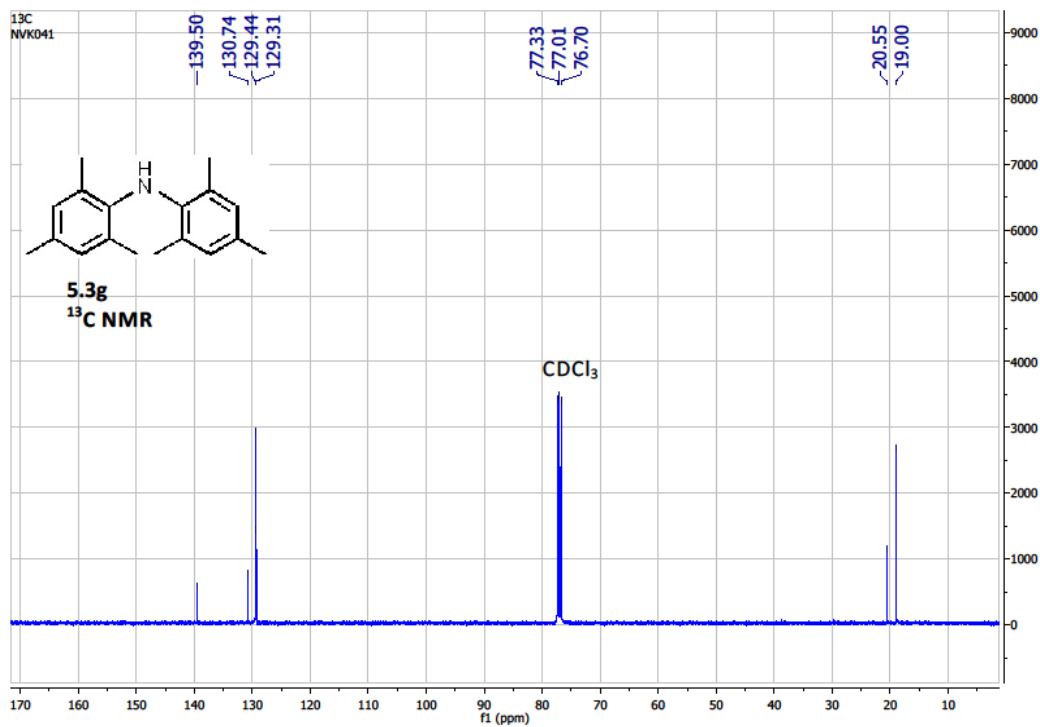
Figure 5A.14 ^{13}*C NMR (CDCl₃) of* **5.3g**
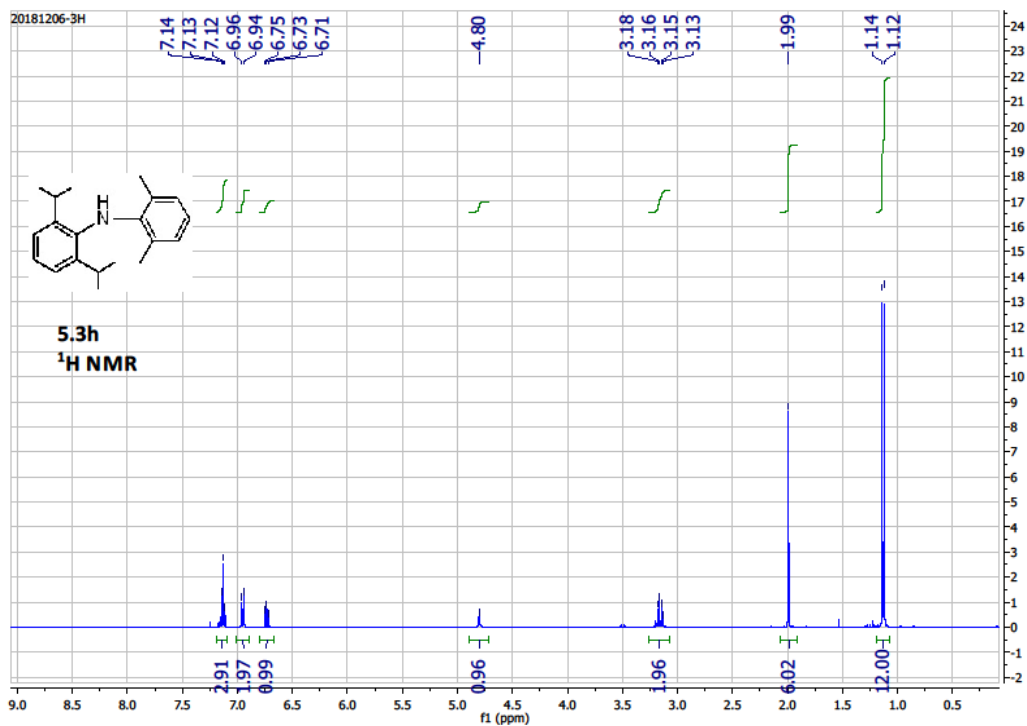
Figure 5A.15 *^1H NMR (CDCl$_3$) of* **5.3h**
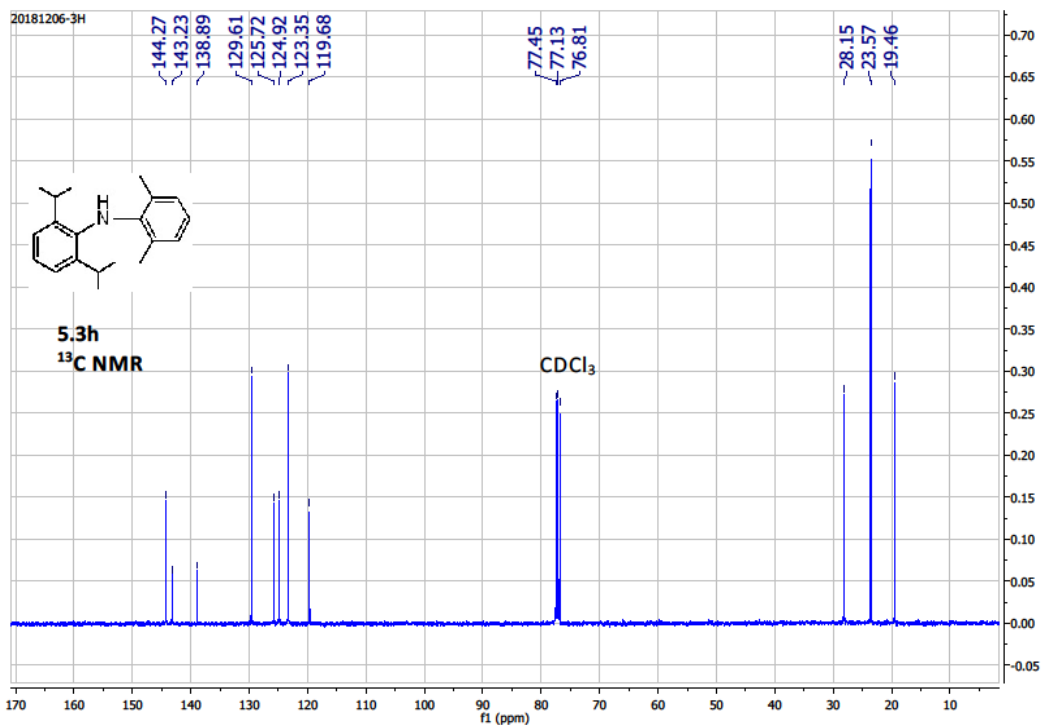
Figure 5A.16 *^{13}C NMR (CDCl$_3$) of* **5.3h**
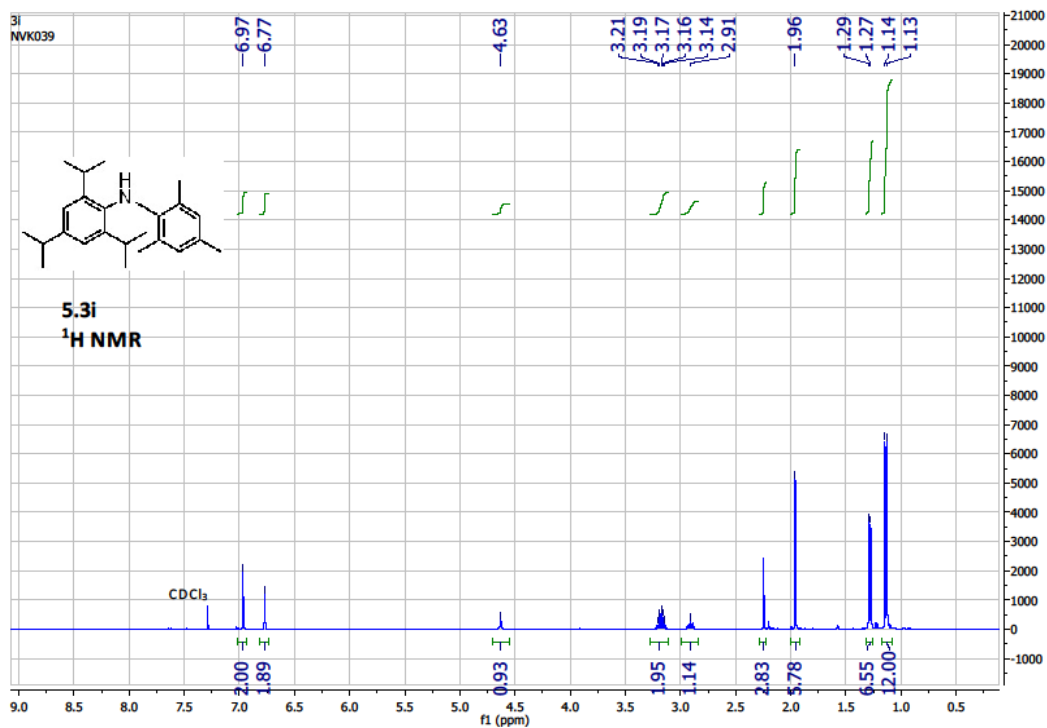
Figure 5A.17 *1H NMR (CDCl3) of* **5.3i**
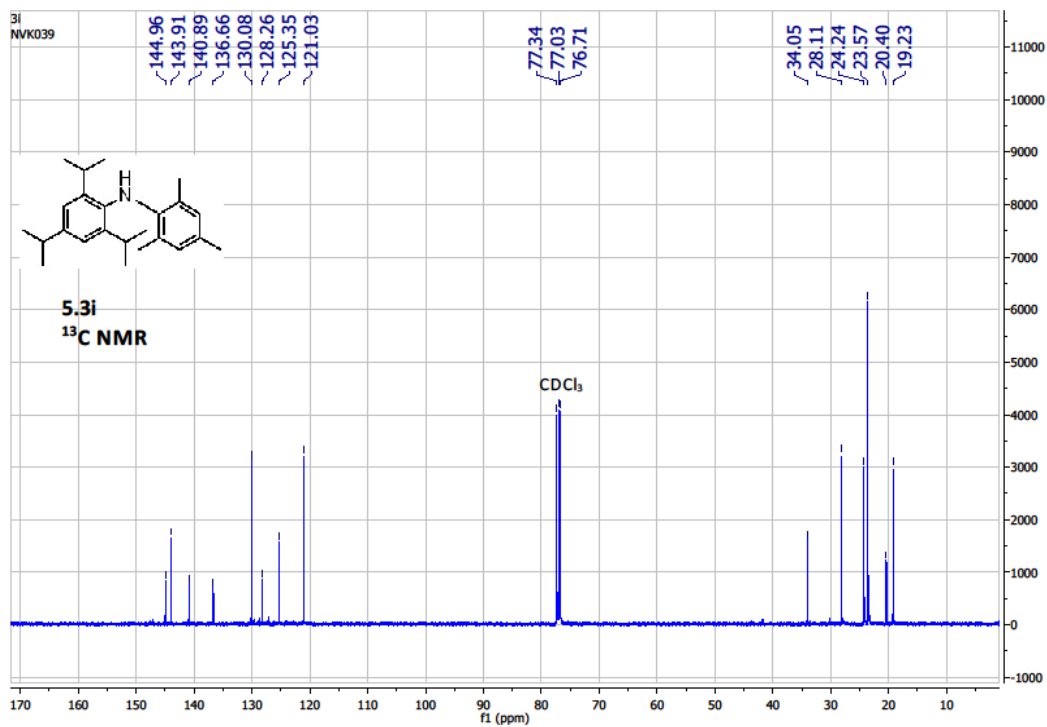
Figure 5A.18 *13C NMR (CDCl3) of* **5.3i**
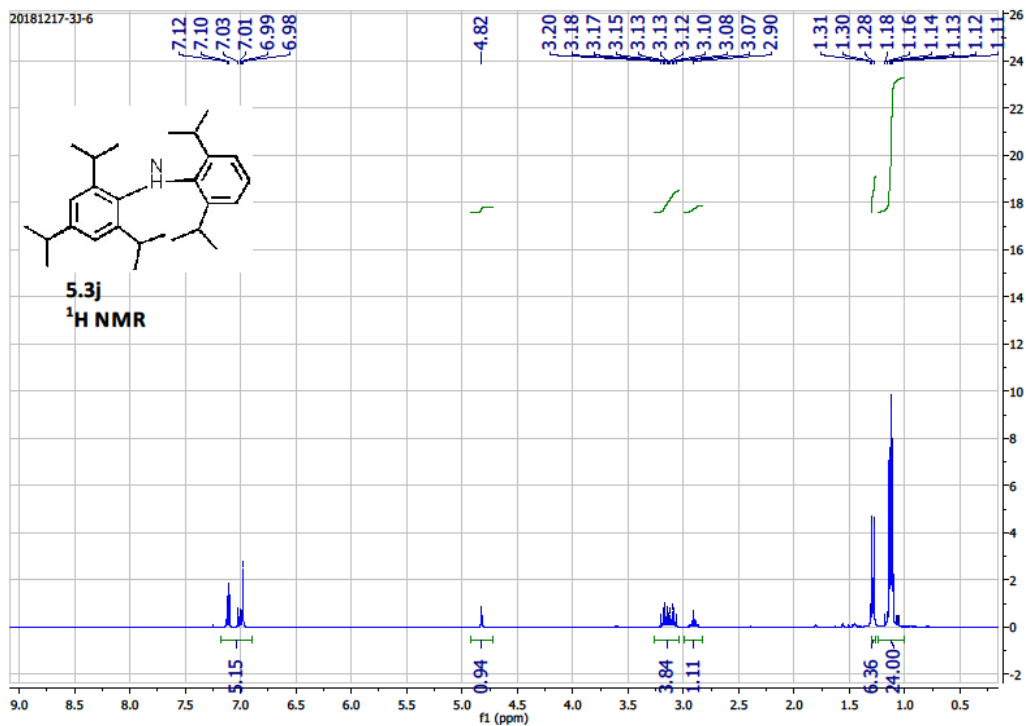
Figure 5A.19 ^{1}H NMR (CDCl$_3$) of 5.3j
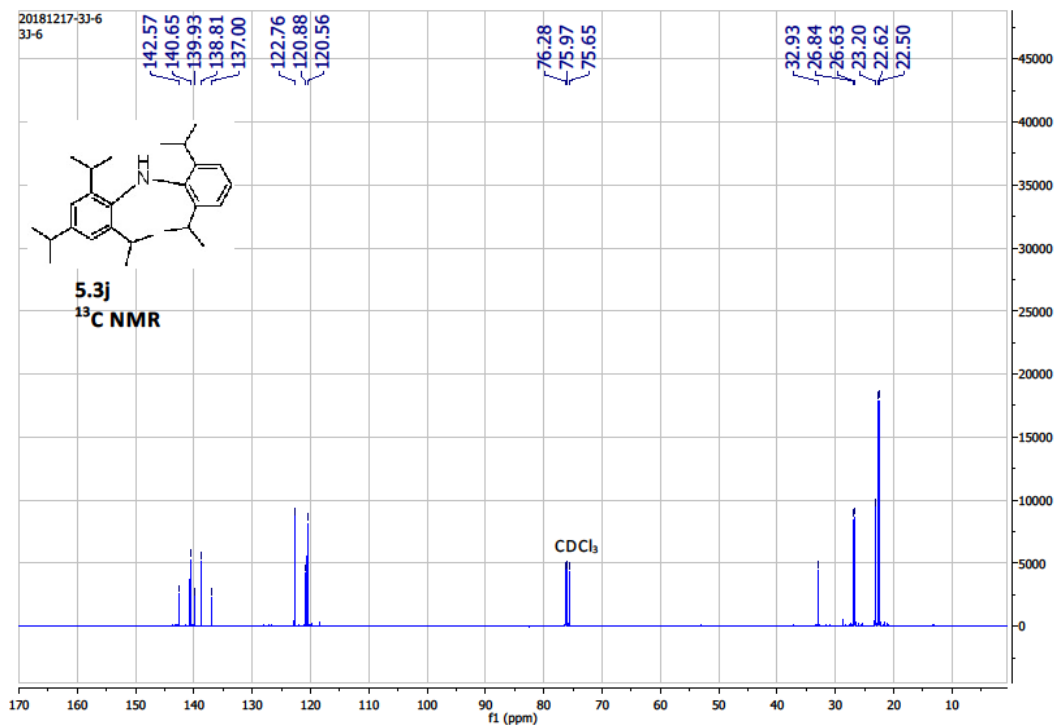
Figure 5A.20 ^{13}C NMR (CDCl$_3$) of 5.3j
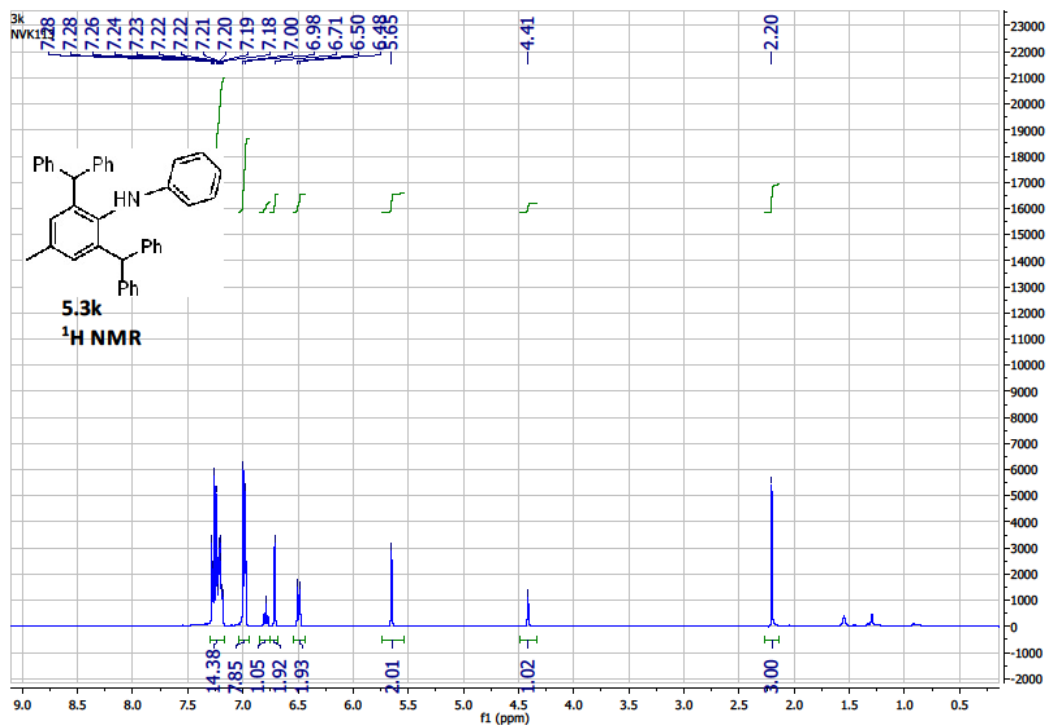
Figure 5A.21 ^1H *NMR (CDCl$_3$) of* **5.3k**
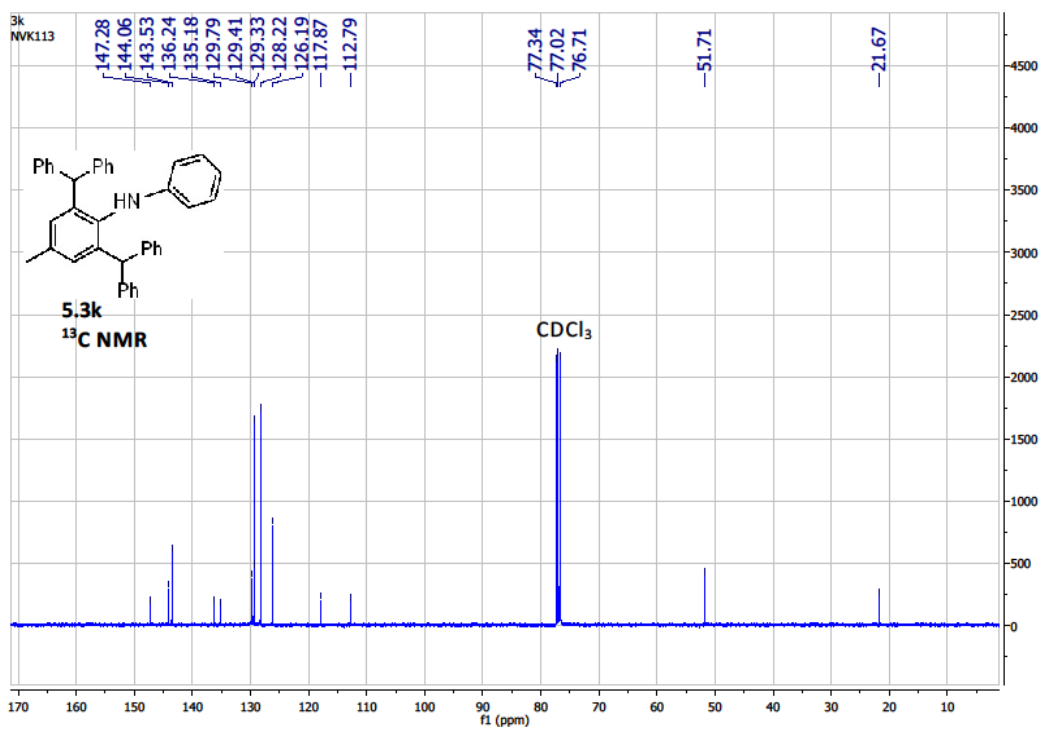
Figure 5A.22 ^{13}C *NMR (CDCl$_3$) of* **5.3k**
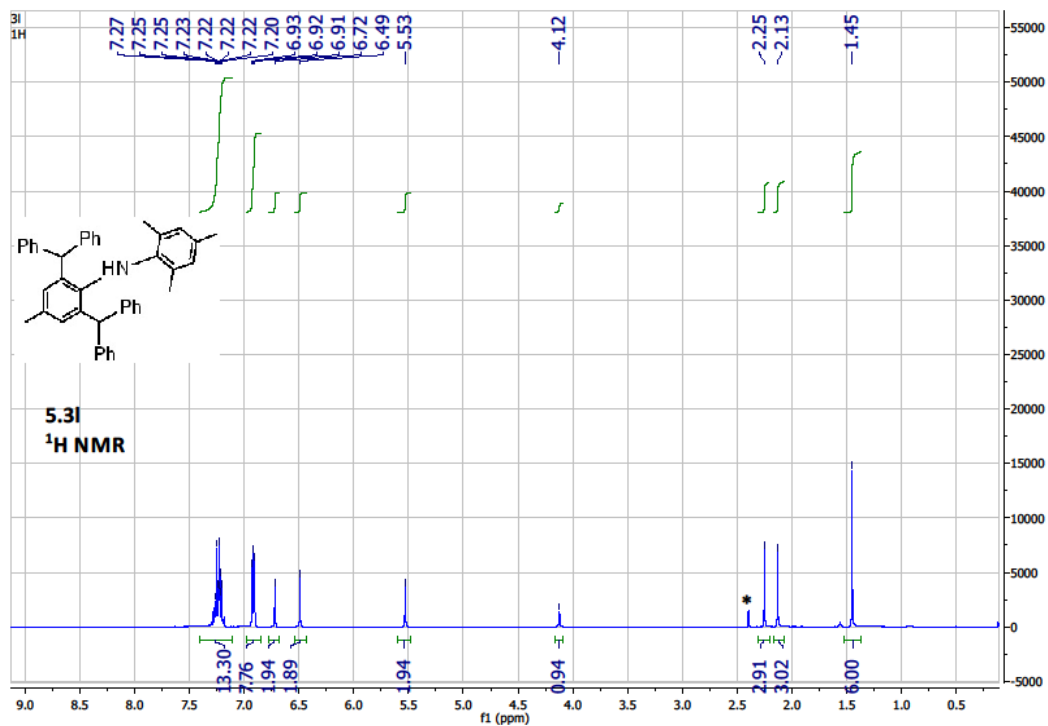
Figure 5A.23 ^{1}H NMR (CDCl$_3$) of 5.3l
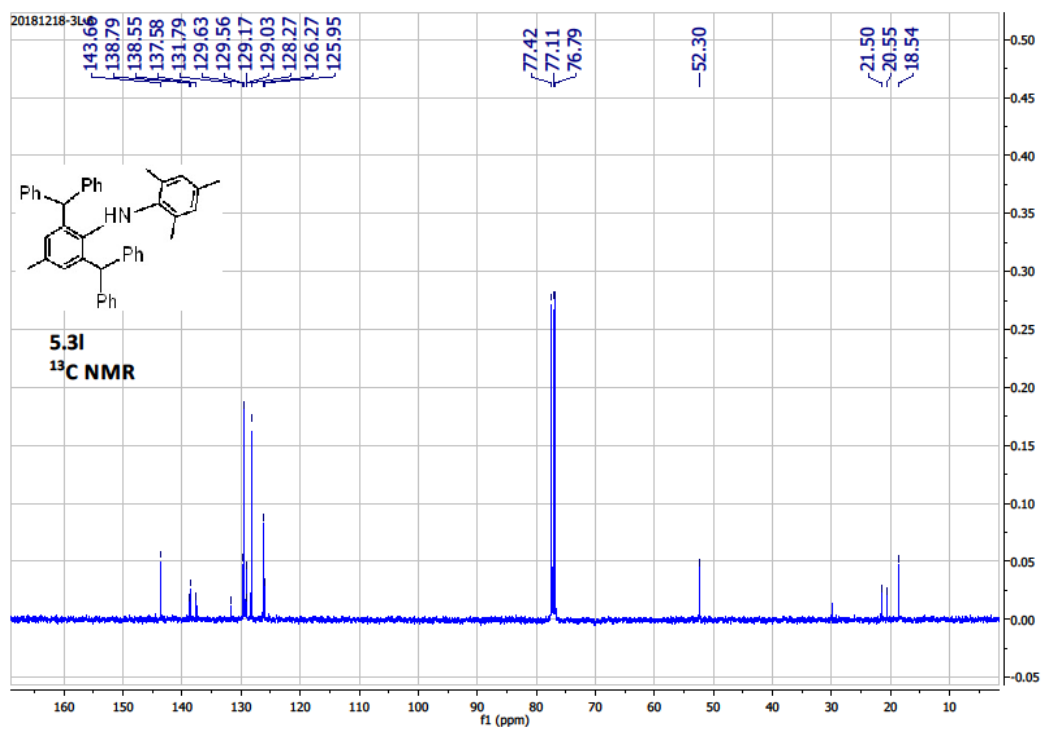
Figure 5A.24 ^{13}C NMR (CDCl$_3$) of 5.3l
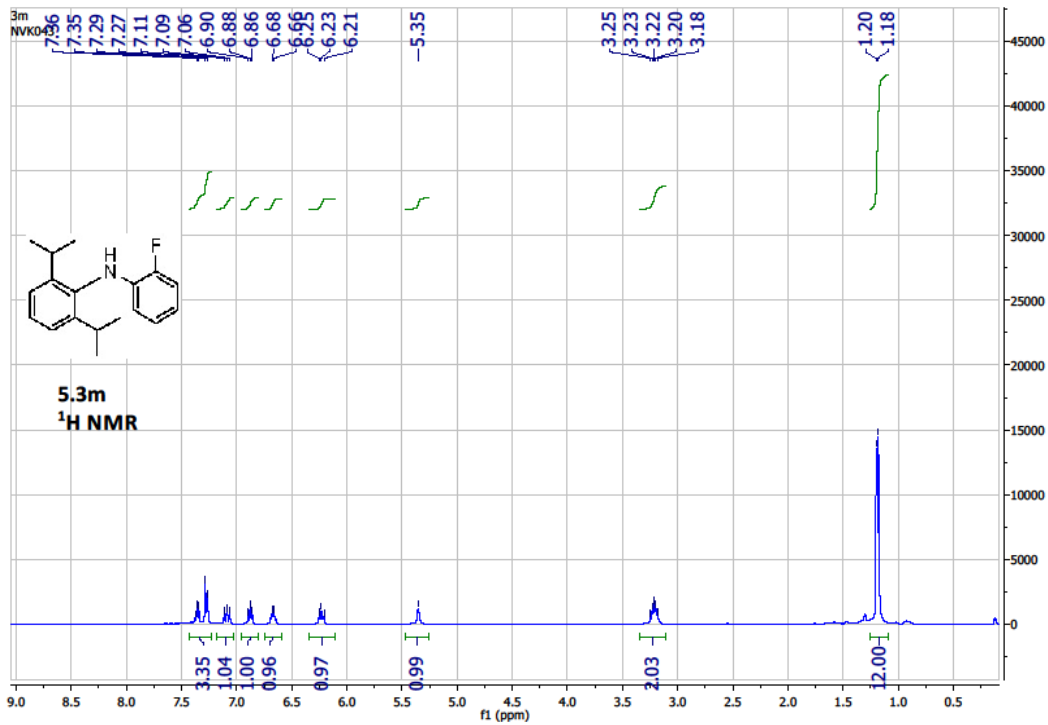
Figure 5A.25 *¹H NMR (CDCl₃) of **5.3m***
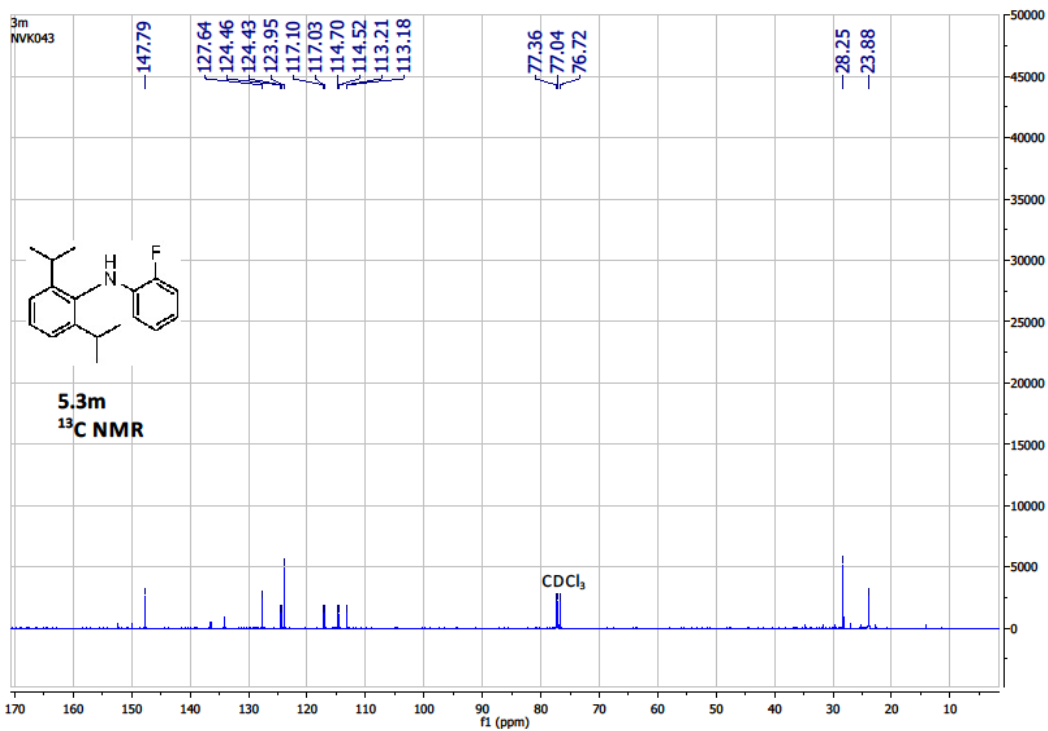
Figure 5A.26 *¹³C NMR (CDCl₃) of **5.3m***
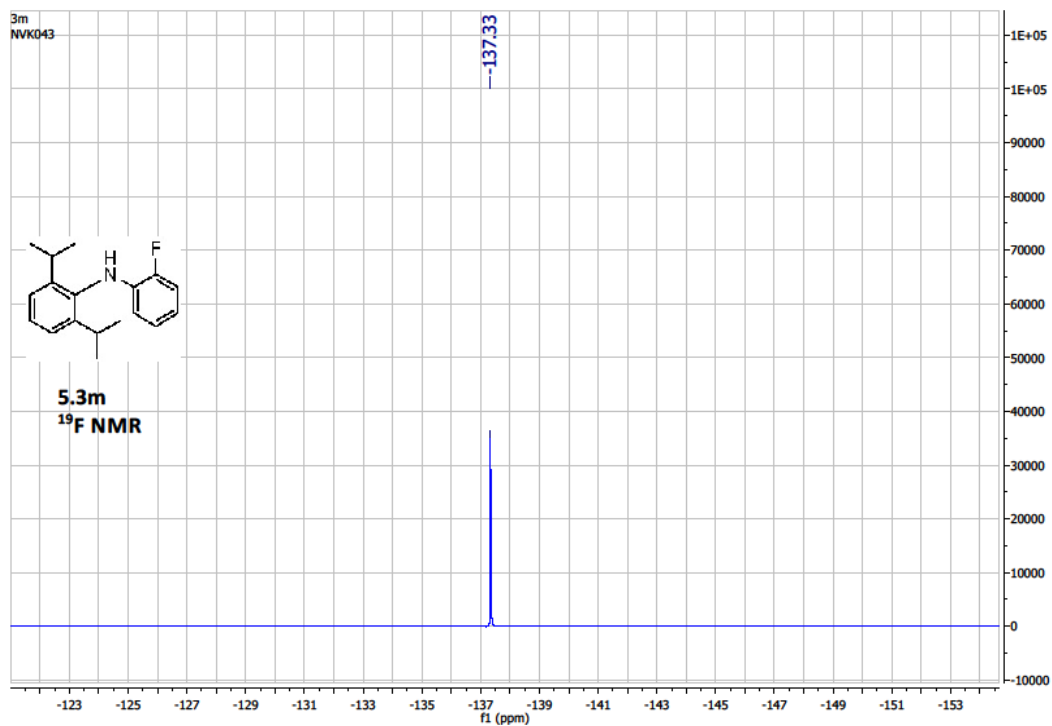
Figure 5A.27 ^{19}F NMR (CDCl₃) of **5.3m**
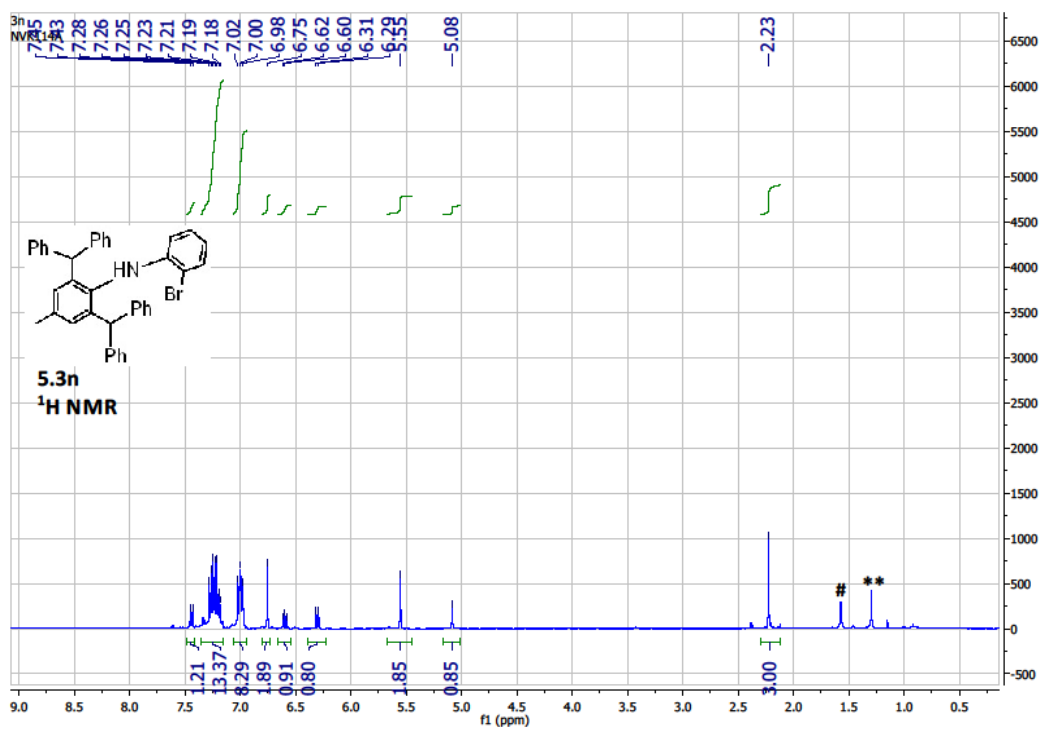
Figure 5A.28 ^{1}H NMR (CDCl₃) of **5.3n**
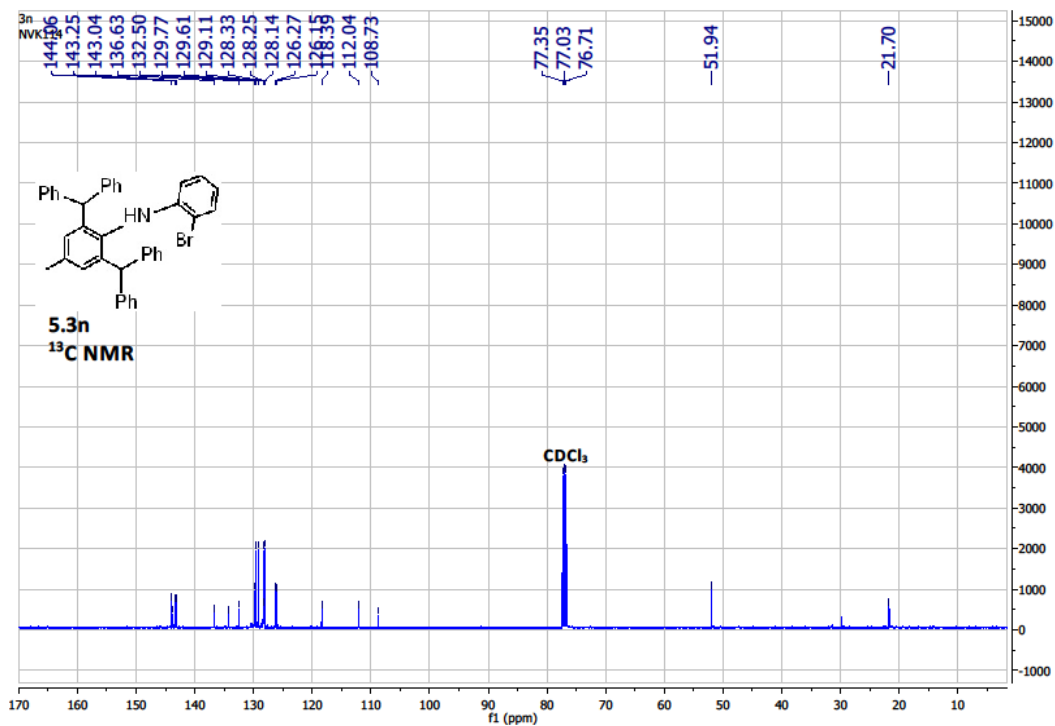
Figure 5A.29 ^{13}C *NMR (CDCl₃) of 5.3n*
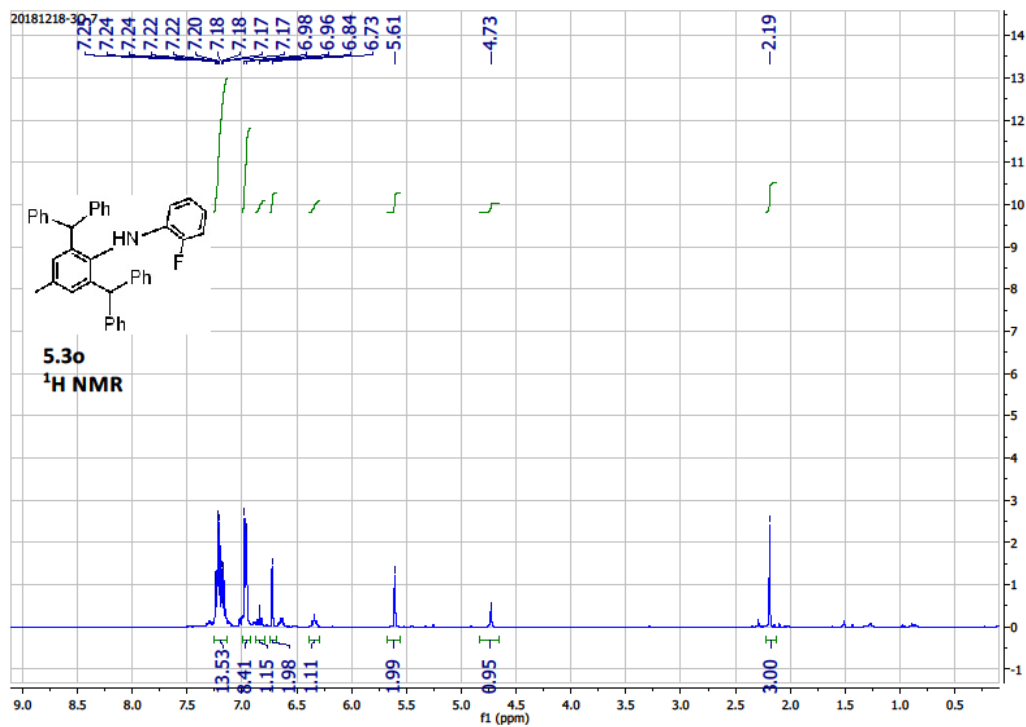
Figure 5A.30 ^{1}H *NMR (CDCl₃) of 5.3o*
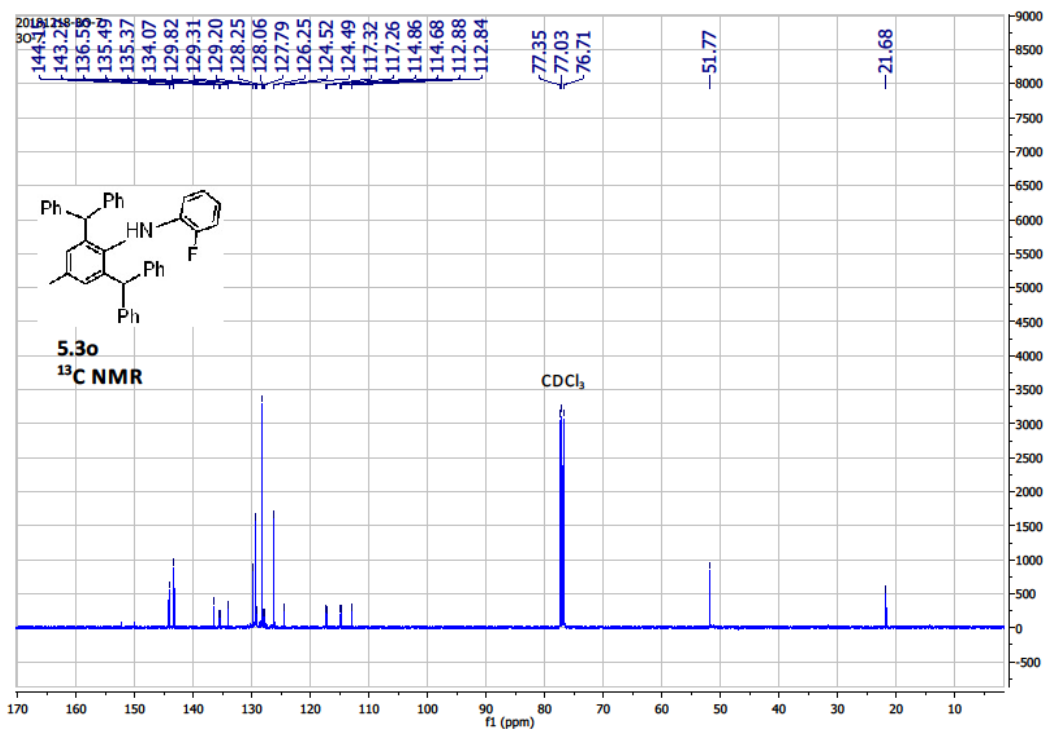
Figure 5A.31 *13C NMR (CDCl3) of **5.3o***
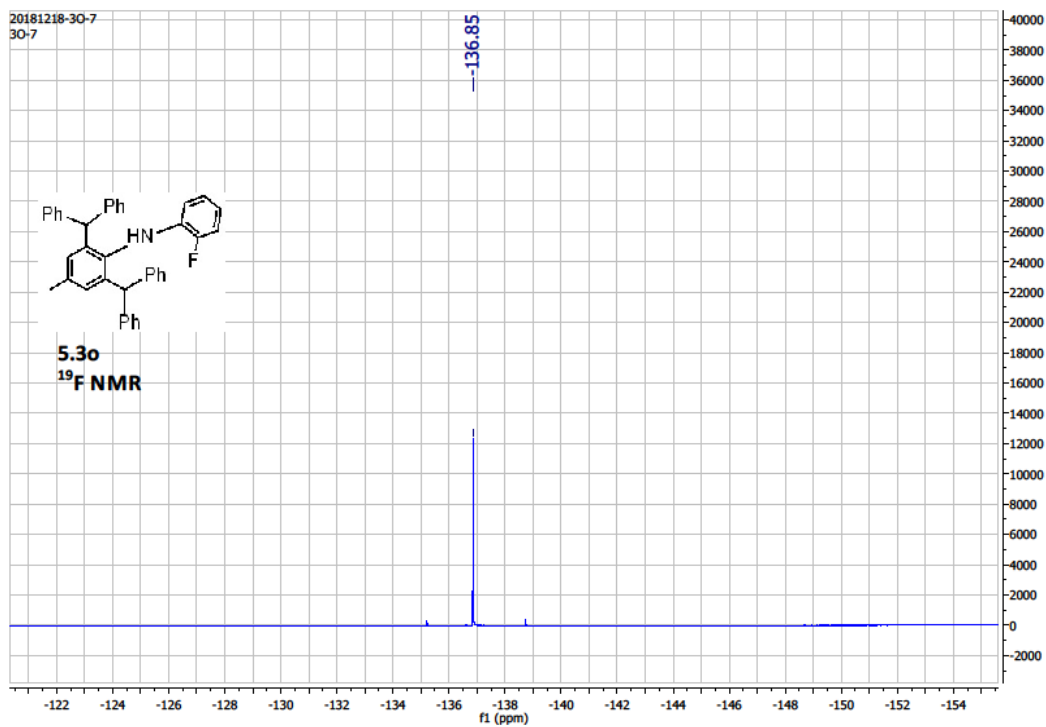
Figure 5A.32 *19F NMR (CDCl3) of **5.3o***
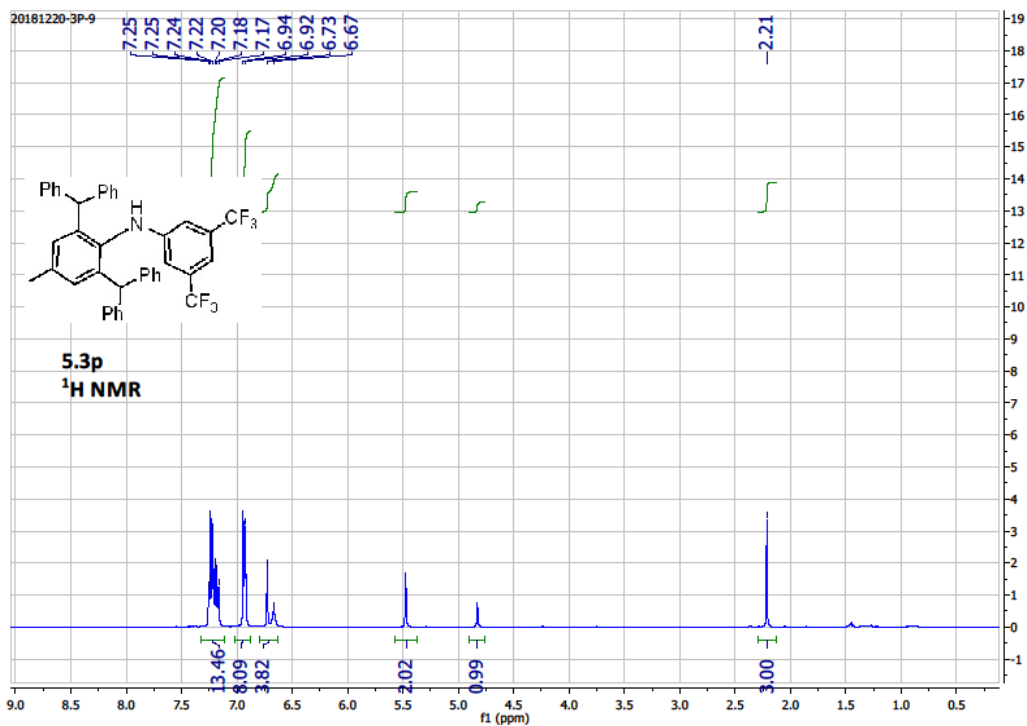
Figure 5A.33 *1H NMR (CDCl₃) of* **5.3p**
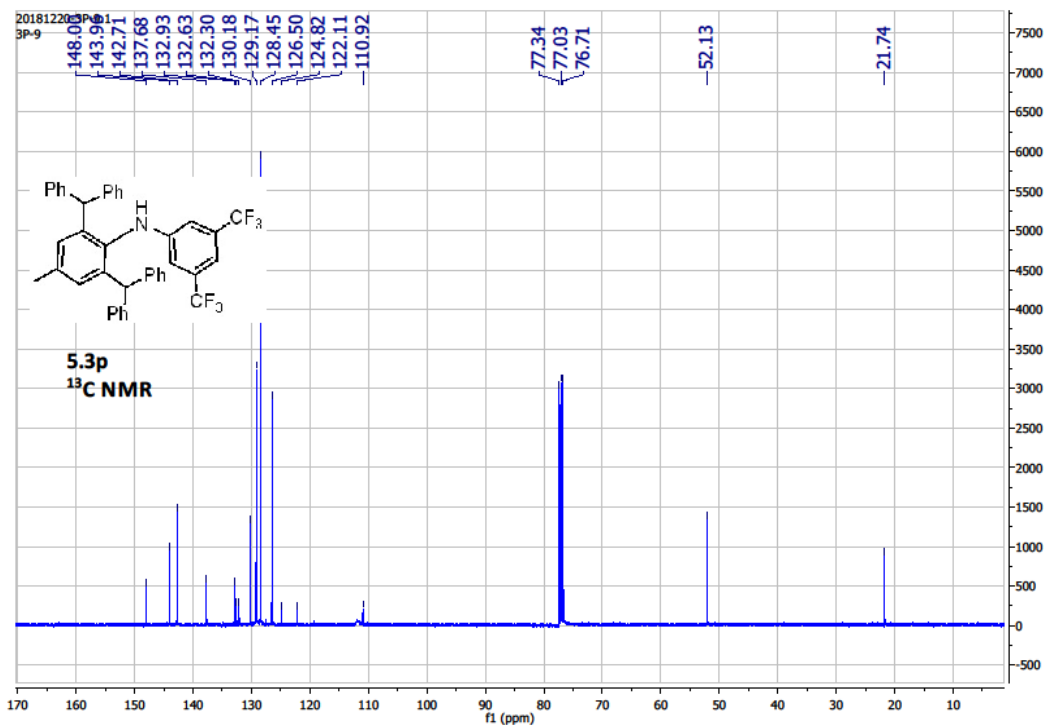
Figure 5A.34 *13C NMR (CDCl₃) of* **5.3p**
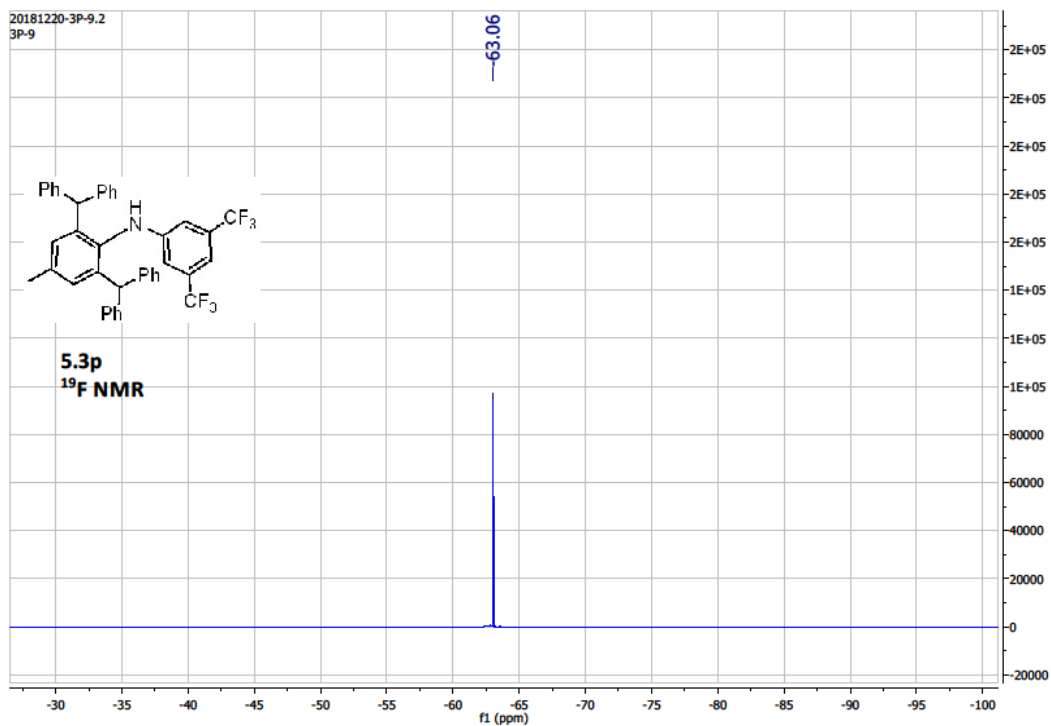
Figure 5A.35 ^{19}F NMR (CDCl$_3$) of **5.3p**
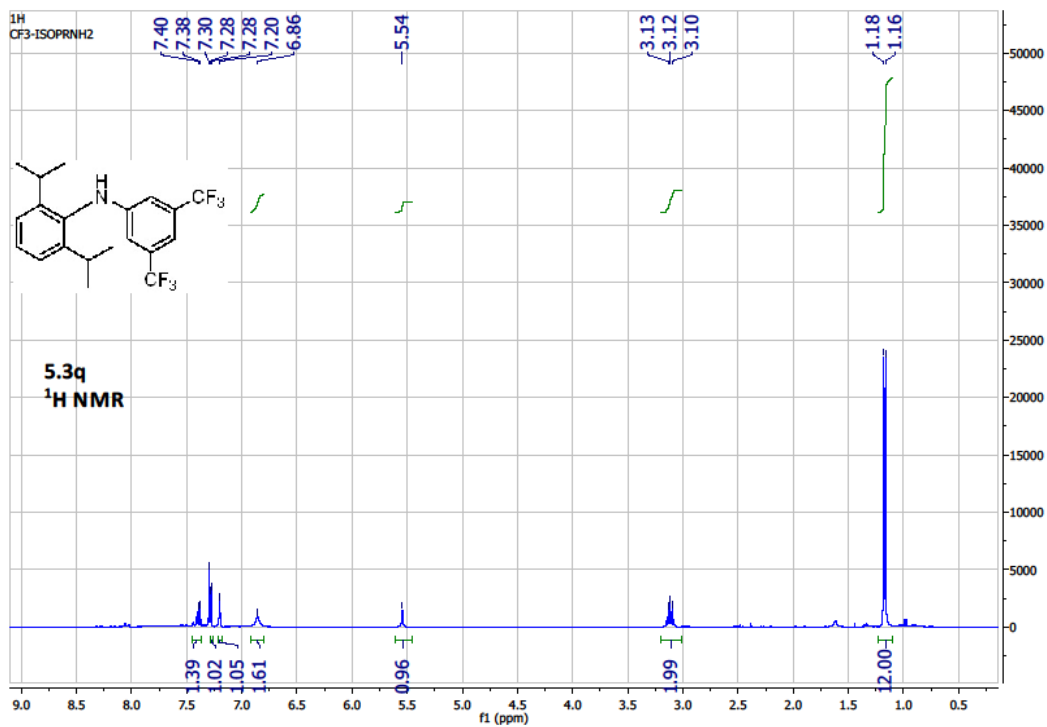
Figure 5A.36 ^{1}H NMR (CDCl$_3$) of **5.3q**
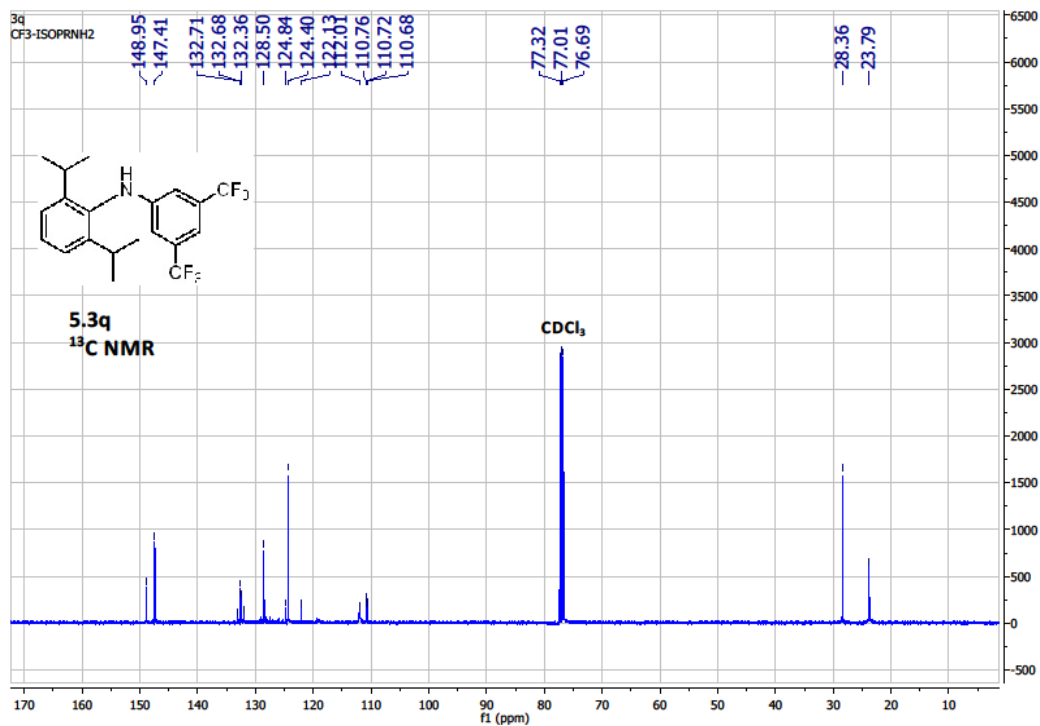
Figure 5A.37 *¹³C NMR (CDCl₃) of* **5.3q**
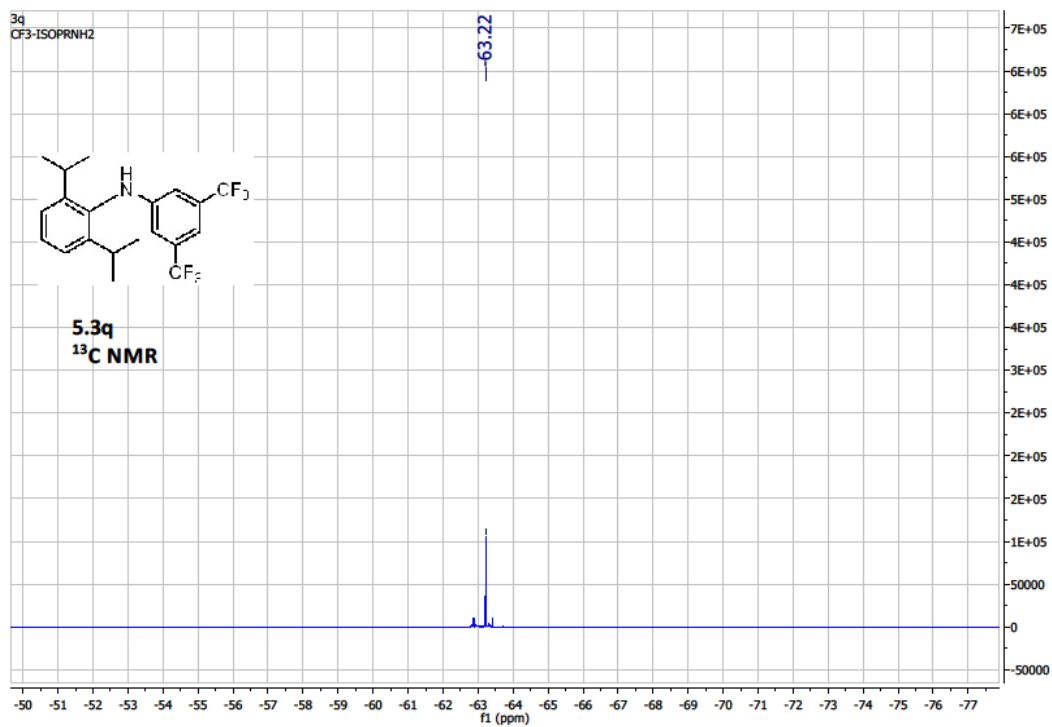
Figure 5A.38 *¹⁹F NMR (CDCl₃) of* **5.3q**
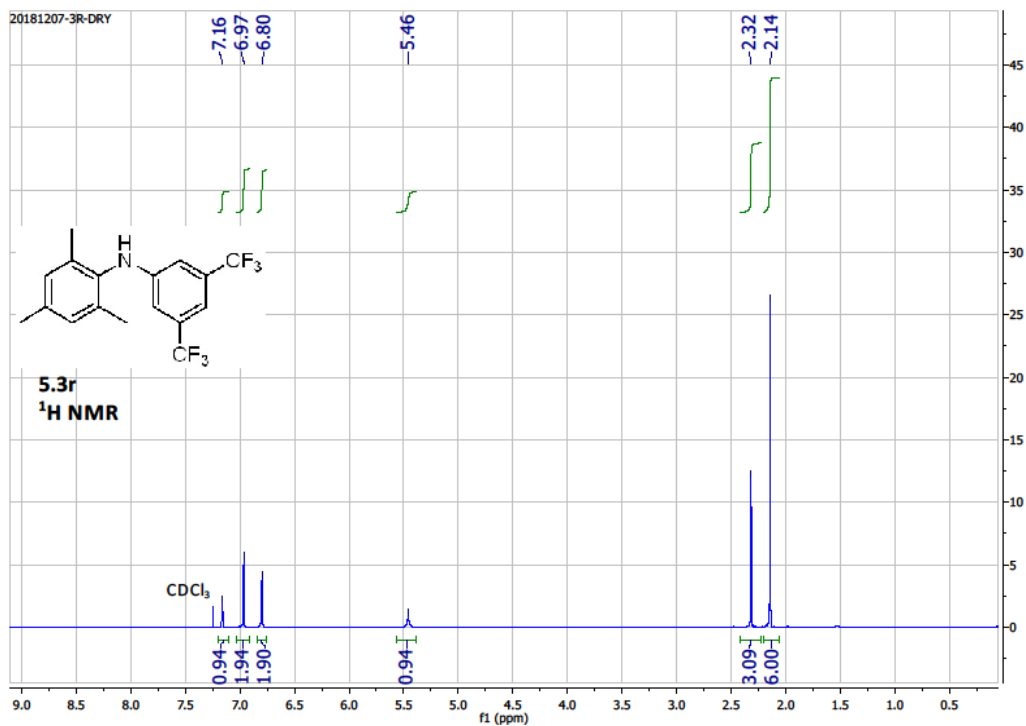
Figure 5A.39 ^1H *NMR (CDCl$_3$) of* **5.3r**
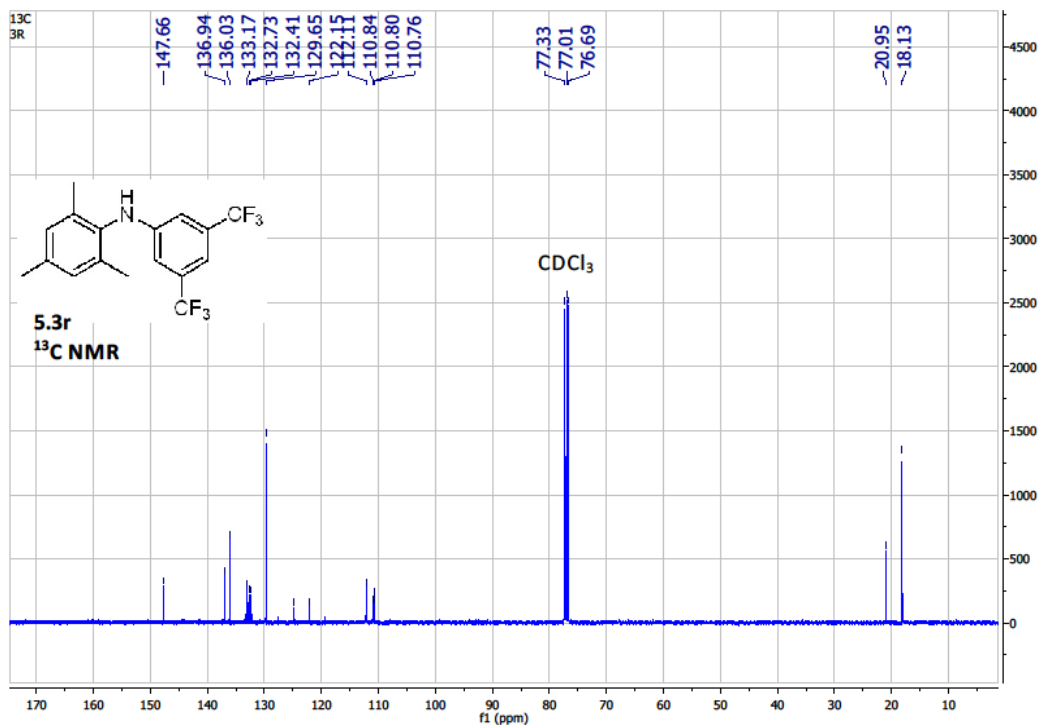
Figure 5A.40 ^{13}C *NMR (CDCl$_3$) of* **5.3r**
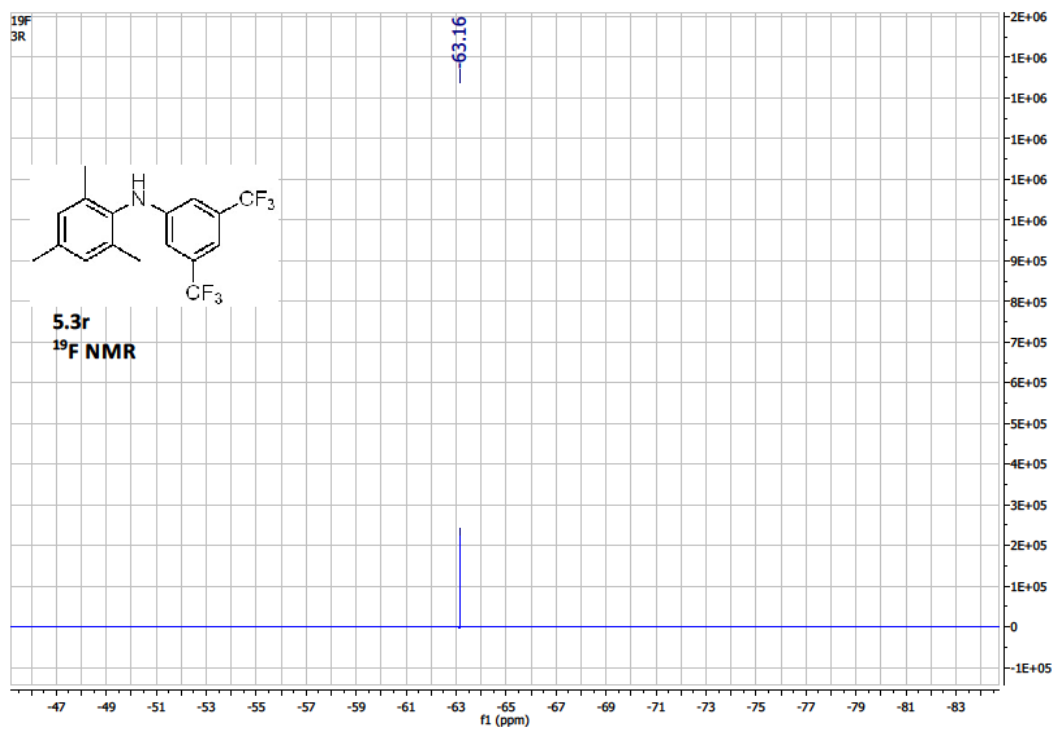
Figure 5A.41 *19F NMR (CDCl3) of* **5.3r**

Rights and Permission

Copyright Clearance Center

RightsLink®

Home | Account Info | Help

Title:	Synthetic Diversity and Luminescence Properties of ArN(PPh2)2-Based Copper(I) Complexes
Author:	Neha Kathewad, Shiv Pal, Rameshwar L. Kumawat, et al
Publication:	European Journal of Inorganic Chemistry
Publisher:	John Wiley and Sons
Date:	May 29, 2018

Copyright © 2018, John Wiley and Sons

Logged in as:
Neha Kathewad

LOGOUT

Order Completed

Thank you for your order.

This Agreement between Ms. Neha Kathewad ("You") and John Wiley and Sons ("John Wiley and Sons") consists of your license details and the terms and conditions provided by John Wiley and Sons and Copyright Clearance Center.

Your confirmation email will contain your order number for future reference.

printable details

License Number	4432540681566
License date	Sep 19, 2018
Licensed Content Publisher	John Wiley and Sons
Licensed Content Publication	European Journal of Inorganic Chemistry
Licensed Content Title	Synthetic Diversity and Luminescence Properties of ArN(PPh2)2-Based Copper(I) Complexes
Licensed Content Author	Neha Kathewad, Shiv Pal, Rameshwar L. Kumawat, et al
Licensed Content Date	May 29, 2018
Licensed Content Volume	2018
Licensed Content Issue	22
Licensed Content Pages	6
Type of use	Dissertation/Thesis
Requestor type	Author of this Wiley article
Format	Print and electronic
Portion	Full article
Will you be translating?	No
Title of your thesis / dissertation	Synthesis, Characterization and Application of Diphosphinoamine (PNP) Ligand
Expected completion date	Jan 2019
Expected size (number of pages)	150
Requestor Location	Ms. Neha Kathewad Hostel-2, IISER hostel, IISER Pune Pashan, Pune Pune, Maharashtra 411008 India

Copyright Clearance Center

RightsLink®

Home | Create Account | Help | ✉

ACS Publications
Most Trusted. Most Cited. Most Read.

Title: Synthesis, Characterization, and Luminescence Studies of Gold(I) Complexes with PNP- and PNB-Based Ligand Systems

Author: Shiv Pal, Neha Kathewad, Rakesh Pant, et al

Publication: Inorganic Chemistry

Publisher: American Chemical Society

Date: Nov 1, 2015

Copyright © 2015, American Chemical Society

PERMISSION/LICENSE IS GRANTED FOR YOUR ORDER AT NO CHARGE

BACK | CLOSE WINDOW